Natural Resources Canada | Ressources naturelles Canada

GEOLOGICAL SURVEY OF CANADA
OPEN FILE 7725

Temperature measurements and thermal gradient estimates on the slope and shelf-edge region of the Beaufort Sea, Canada

M. Riedel, H. Villinger, K. Asshoff, N. Kaul, S.R. Dallimore

2015

Canada

GEOLOGICAL SURVEY OF CANADA
OPEN FILE 7725

Temperature measurements and thermal gradient estimates on the slope and shelf-edge region of the Beaufort Sea, Canada

M. Riedel[1], H. Villinger[2], K. Asshoff[2], N. Kaul[2], S.R. Dallimore[1]

[1] Natural Resources Canada, Geological Survey of Canada, 9860 West Saanich Road, Sidney, British Columbia
[2] University Bremen, FB Geowissenschaften, D-28334 Bremen, Germany

2015

doi:10.4095/296570

This publication is available for free download through GEOSCAN (http://geoscan.nrcan.gc.ca/).

Recommended citation
Riedel, M., Villinger, H., Asshoff, K., Kaul, N., and Dallimore, S.R., 2015. Temperature measurements and thermal gradient estimates on the slope and shelf edge region of the Beaufort Sea, Canada; Geological Survey of Canada, Open File 7725, 143p. doi:10.4095/296570

Publications in this series have not been edited; they are released as submitted by the author.

Table of Contents

Abstract

In situ temperature measurements were conducted at 63 gravity-core stations during the 2013 expedition with the *CCGS Sir Wilfrid Laurier* in the Canadian Beaufort Sea. Outriggers attached to the outside of the gravity core-barrel were used to mount portable miniature temperature loggers (MTL) for down-core in situ temperature measurements. Several sub-regions were investigated during the expedition including two shelf-slope crossings, three mud volcano-type expulsion features, as well as two canyon sites. The last site visited was at the Gary Knolls, just east of the Mackenzie Trough at water depths of less than 100 m.

Overall, temperature data obtained from the MTLs were of high quality at most stations and the data acquisition technique was proven to be robust and easy to adapt in the Arctic. However, depth determination for each logger position remains the largest challenge as no additional pressure sensor was used with the MTLs. Instead, depths were estimated based on the apparent core penetration and the geometry of the outriggers.

The most significant result from this work is the discovery of the very large apparent geothermal gradients associated with the two expulsion features (EF) Coke Cap and the mud volcano at 420 m water depth. Temperatures measured within the top 2.5 meter below seafloor suggest geothermal gradients of up to 2.94ºC/m (Station 96, 420m EF) and 1.37 ºC/m (Station 58, Coke Cap EF). Away from the centre of the EFs, thermal gradients decrease to values of 0.5ºC/m for Station 99 at the 420 m EF, and 0.92ºC/m at Station 21 at the Coke Cap EF.

Temperature data across the slope-shelf transect and the two transects across the canyon heads did not reveal considerable geothermal gradients, but show a water-depth dependent trend in temperature. From deep to shallow water, temperature appear to decrease until the most negative temperature values are found on the shelf itself at water depths of ~100 m (-1.2 to -1.4ºC).

Overall, data from the top 1.0 to 1.5 meter below seafloor are likely affected by seasonal variations in the water column temperature and may not be used to define geothermal gradients. With an optimal full penetration of the core barrel, the deepest temperature data are from ~2.3 mbsf, which limits the accuracy of the estimated geothermal gradients as only few data points (2 – 4) can be used in the calculations.

1 Introduction

Arctic continental shelf areas that are less than 100 m deep comprise more than 3.2 million km^2, which is ~30% of the total area of the Arctic Ocean. Throughout the past two million years these shallow water environments experienced a dynamic geologic history. During periods of low sea level stand, many of the marine shelf areas were exposed to mean annual air temperatures that were -20ºC or colder (e.g. Brigham and Miller, 1983). These cold temperatures caused the formation of a substantial permafrost layer, which in the Canadian Beaufort Sea is up to 700 m thick (e.g. Judge. 1982; Smith and Judge, 1983). In contrast, interglacial periods associated with sea level rises resulted in transgressions that inundated coastal areas with warmer seawater that causes the degradation of offshore permafrost. Because of the slow diffusion of heat, it will take considerable amount of time, in the order of thousands of years, to fully melt the subsurface permafrost.

The repeated changes between permafrost formation during terrestrial exposure, and warming and permafrost degradation during marine transgression in the Quaternary has had profound impact on the geology of Arctic shelve regions. Unique geologic and hydro-geologic processes are likely to occur as a consequence of transgression with the associated melting of the offshore permafrost, such (fresh) water and gas release. Paull et al. (2007) suggested that large conical features on the Beaufort shelf termed “pingo-like features” (PLFs) may be due to methane-generated overpressure in subsurface sediments causing sediment extrusion. Similar processes may cause methane releases associated with geomorphic features at that shelf edge transition including PLFs, pockmarks and landslides (Paull et al., 2011).

Despite the fact that large parts of the Canadian Beaufort shelf have been submerged for more than 7000 years, the offshore permafrost is currently still responding to the thermal change because of slow rates of heat diffusion and latent heat effects (e.g. Taylor et al., 1996, 2013). The shelf edge, where the permafrost layer pinches out, is a critical zone where pressurized fluids are expected to migrate vertically and horizontally. Key to the understanding of these processes is an improved knowledge of the timing and rate of sediment deposition, subaerial exposure and transgression of the permafrost-affected sediments. Because permafrost degradation is ongoing, it is also important to

evaluate the effects of ocean temperature variability, including potential warming of bottom water, on the geothermal regime controlling the degradation.

The expedition to the Canadian Beaufort Sea on the Canadian Coast Guard vessel *Sir Wilfrid Laurier* conducted in the fall of 2013 had several objectives to address the above mentioned processes (Melling, 2013) and include:

- Sediment coring to obtain samples for stratigraphic interpretation, age-dating, as well as pore-water geochemical studies,
- Measurement of temperatures in the sediments,
- Measurement of sediment geotechnical properties with a free-fall cone penetrometer,
- Oceanographic water-column measurements,
- Acquisition of high-resolution bathymetric and sub-bottom profiler data with an autonomous underwater vehicle (AUV),
- Use of a remotely operated vehicle (ROV) for detailed seabed sampling and video observations.

Regional distributions in geothermal gradients, and heat flow values derived from these gradients, are typically used to understand surficial process within sediments. Local variations are useful to unravel surficial process such as fluid expulsion from deeper sediments into the ocean and detection of ice within sediments. Determining the geothermal gradients is also important to estimate the extent of the local gas hydrate stability zone, especially around the three known expulsion features in the survey area: 'Coke-Cap' (~280 m water depth), the '420-Expulsion feature' (~420 m water depth), and a 'Triple mound feature' (~760 m water depth). Previous regional thermal modeling conducted by Taylor et al., 2013 estimates that the classical marine (no underlying permafrost) gas hydrate stability zone (GHSZ) of pure methane occurs along the shelf edge starting at water depths of ~300 m. This estimate of the GHSZ puts all three expulsion features near the edge or within the GHSZ and as such, gas hydrate could be stable at all these three sites.

In order to verify and fine-tune the calculations of the GHSZ by Taylor et al. (2013), temperature profiles in the sediments were measured by attaching temperature

data loggers to the outside of a gravity core barrel during the CCGS *Sir Wilfrid Laurier* expedition in 2013. The equipment for these measurements was provided by the University of Bremen (Germany). Similar additional temperature measurements were conducted during Expedition ARA04C on the Korean icebreaker Araon in 2013 (Jin et al., 2015). Here we report on the data acquisition process, data analysis, and estimation of thermal gradients based on the data from the CCGS *Sir Wilfrid Laurier* expedition in 2013. The study region is centered on the shelf-edge and slope region of the Canadian Beaufort Sea (Figure 1), where previous studies have also been conducted (see summary in Blasco et al., 2013). At 63 locations temperature profiles in the surficial sediments were measured and a gravity core was recovered at 52 of the stations. Sediments were washed out of the barrel at the other 11 stations to gain operational time at locations that were previously occupied during the expedition.

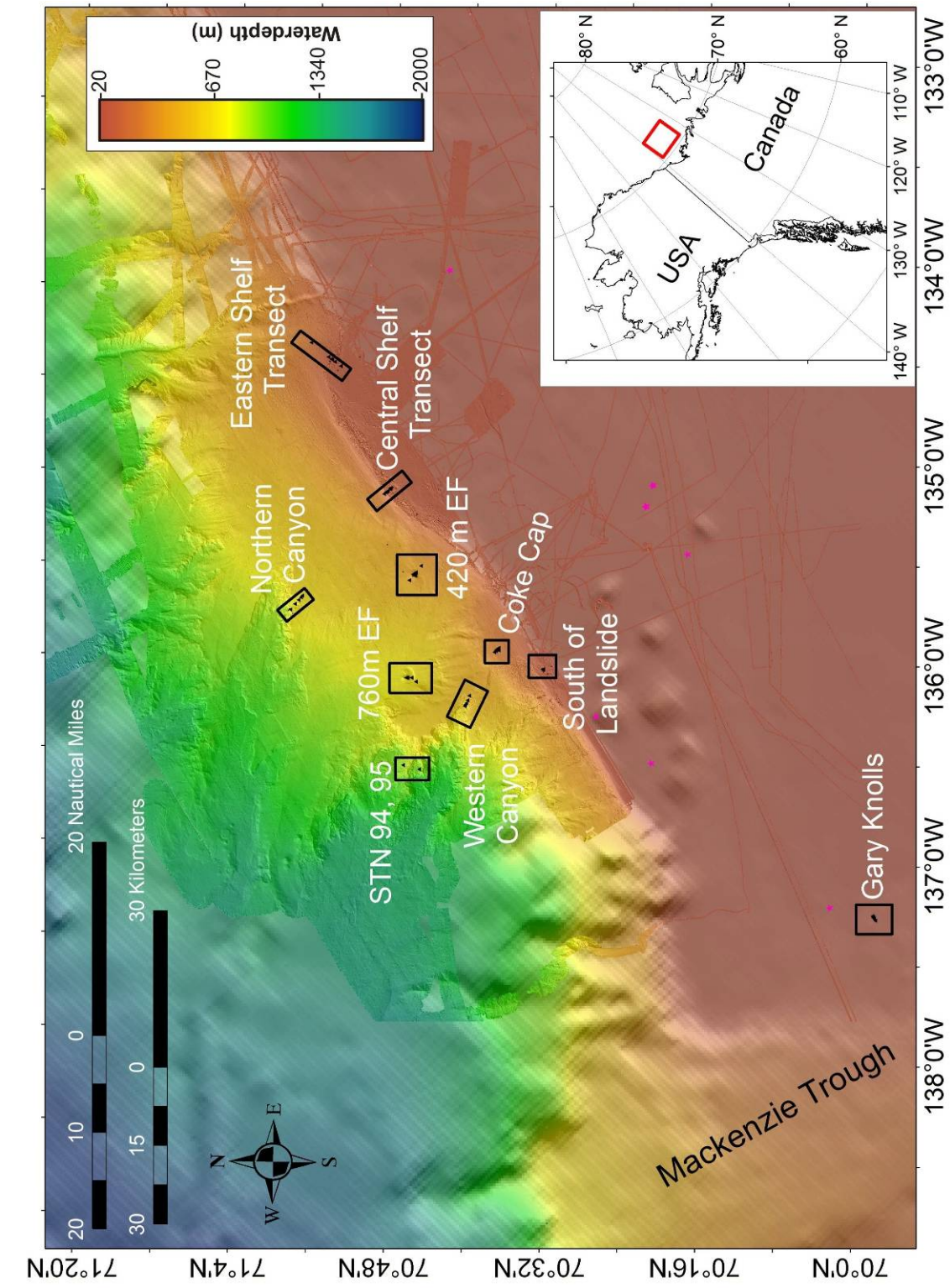

Figure 1. Map showing research area of the CCGS Sir Wilfrid Laurier 2013 expedition and sub-regions where temperature measurements were taken at gravity core sites. Also shown are industry wells (purple symbols). [EF: Expulsion Feature]

2 Data and Methods

During the expedition on CCGS Sir Wilfrid Laurier, temperature measurements were carried out by mounting Miniaturised Temperature Data Loggers (MTLs) with outriggers to the outside of the gravity-core barrels. The range of temperature measurement is from -4.5ºC to +60ºC with a maximum resolution of 1 mK (for details see Pfender and Villinger, 2002). The temperature loggers were calibrated in August 2013 at the University Bremen laboratories. No additional calibration was made on the ship. The loggers were time-synchronized at sea with standard PC-time (local time in the Northwest Territories, Canada, UTC-8 hours).

For the majority of the program, a fixed deployment configuration was used (Figure 2), with 5 outriggers and loggers, located at 20 cm, 45 cm, 70 cm, 120 cm, and 170 cm measured from the bottom of the core barrel. The MTLs were attached with clamps (outriggers) to the outside of the core-barrel (Figure 3).

For the first and second measurement-transect, the loggers deployed were kept attached throughout the entire coring sequence (Stations 3 - 13, eastern shelf-crossing; Stations 17 - 27, Coke-Cap expulsion feature). For deployments at the third region, Western Canyon (Stations 31 - 35), the loggers were exchanged once during the 5-core transect. After Station 41, the temperature loggers were exchanged after each core deployment. Throughout the entire program, several loggers froze while exposed on deck to temperatures below -4.5ºC for too long a period. Although the logger continued to run, a constant, minimum temperature of ~ -4.5ºC was recorded throughout the deployment.

The weight of the gravity corer allows the core and the loggers to penetrate into the sediment; however, no pressure sensors were used to monitor the penetration of the core barrel and to verify actual depth of total penetration of each logger. Therefore, only approximate depth information relative to sea floor is available for each position of the MTLs. During the core-recovery, apparent penetration was measured using the height of sediment (mud) attached to the core-barrel as indicator for how deep the tool likely entered into the sediment. A complete penetration is equivalent to 2.5 meter below seafloor (mbsf). However, if the core did not penetrate completely, some of the loggers may not enter the sediment and remain in the water column.

Due to the uncertainly in penetration we report both depths: nominal depth assuming full penetration (2.5 m), and apparent depth using the recorded information from the core-logging sheets-. The estimation of a geothermal gradient is, however, less affected by the actual total depth of the loggers, as long as the differential distance between individual loggers did not change. The temperature record of each deployment was used to verify the apparent penetration depth by determining if a friction heating pulse was recorded at the loggers indicating that the logger did physically penetrate into the sediment. However, this was not always unambiguously possible (as noted later in the Results section), particularly for sediments with temperatures below 0ºC.

After the gravity core penetrated into the sediment, it remained in the sediments for several minutes to equilibrate to in situ temperatures before being extracted. On average, the tool remained in the sediment for 7 minutes. To avoid disturbances of the temperature measurement, the vessel must be kept on-station for the measurement period to avoid moving the core up or side-ways. Overall, we did not identify any disturbances of the temperature measurements that would suggest movement of the core while in the sediments.

The temperature equilibration process is, as a first approximation, linearly depended on the inverse of time (1/t) (Villinger and Davis, 1987). The extrapolation to infinite time (1/t = 0) provides the undisturbed in situ temperature. For this, the later portion of the temperature record of the logger in situ (e.g. last 2 – 3 minutes of the total 7 minute record) was plotted against the inverse of time (1/t) and linear regression was applied to estimate equilibrium temperature. For approximately half the measurements such linear regression was applied (Table 2). In all other cases, equilibrium was reached after 7 minutes, and the average temperature was determined from the final 20 seconds of recorded values.

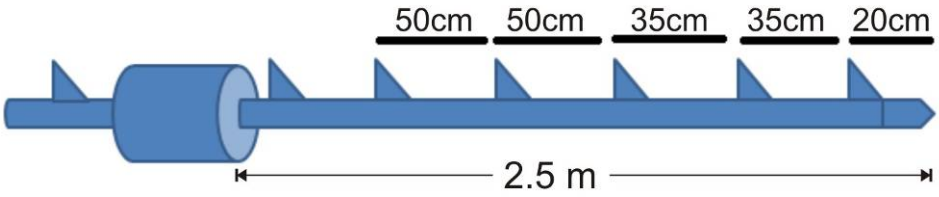

Figure 2. Schematic diagram of the gravity core with location of the outriggers holding the MTL. The distances shown are representative for the deployments of Stations 56 to 129.

Figure 3. Image of the gravity core recovered on deck, showing outriggers used for the MTL loggers. Note the amount of sediment on the outside of the core-barrel which was used to identify the apparent penetration of the tool.

3 Results

In this section we present the down-core temperature profiles measured at all 63 stations occupied during the *Sir Wilfrid Laurier* expedition (Melling, 2013), grouped by region and target. The main research area is at the central Beaufort Sea slope and shelf transition area, where high-resolution multibeam data were acquired as part of the Arctic-Net project (Figure 4). None sub-regions were investigated: two shelf-crossings (eastern and central transect), three expulsion features (Coke Cap, 420 m, and 760 m water depth), as well as two Canyon Sites (northern and western). Two additional sites were visited slightly north of the western Canyon (Stations 94, and 95) as well as south of the landslide region. The 10th site visited was at Gary Knolls, just east of the Mackenzie Trough in water depths of less than 100 m. The individual temperature records of each logger are shown in the Appendix, together with the temperature-fit analysis and linear regressions. All data shown in this section are also listed in Table 2.

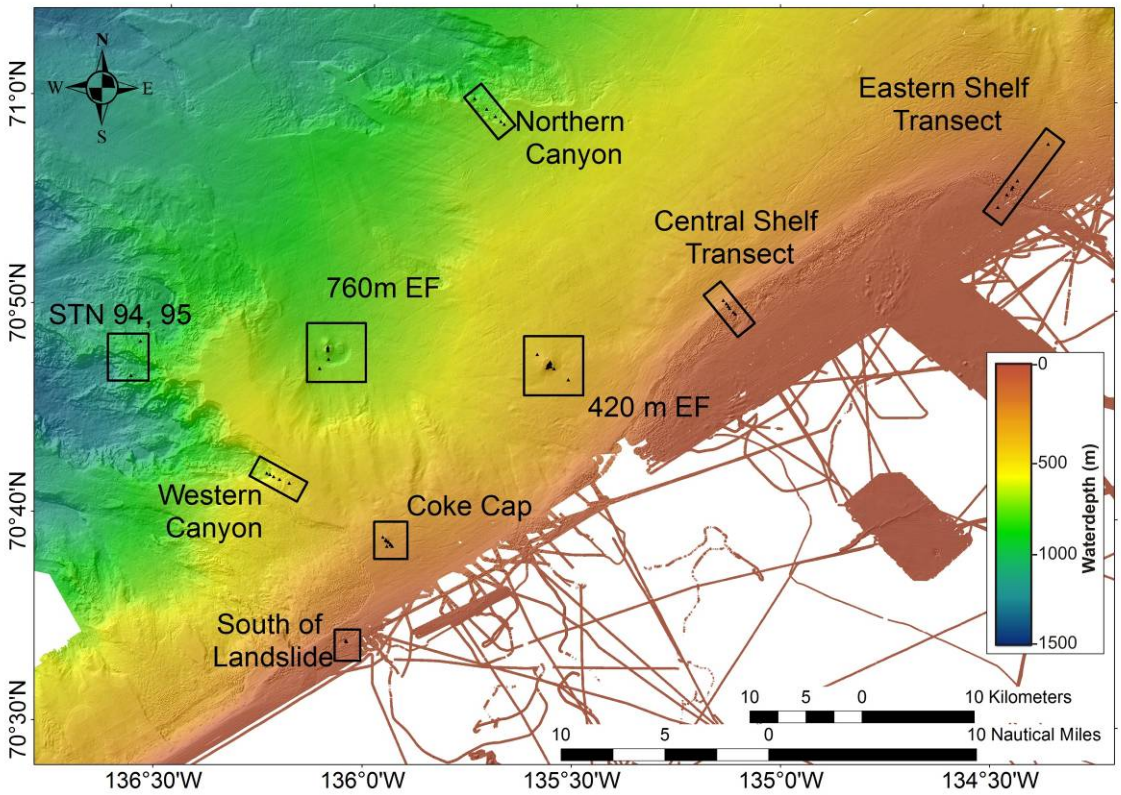

Figure 4. Map showing the location of nine sub-regions where temperature measurements at cores sites were recorded. The base map is from the Arctic-Net high-resolution multibeam data coverage (Blasco et al., 2013).

3.1 Eastern Shelf Transect, (Stations 3, 5, 7, 9, 11, 13)

The first set of thermal measurements were conducted along a transect of six stations at the eastern shelf region (Figure 5). The shelf edge is marked by a characteristic seafloor morphology made up of numerous small-scale pingo-like features (PLFs). Three stations of the transect are within this PLF region (Stations 7, 9, 11). Station 3 is in deepest water (see profile in Figure 6) and temperatures are accordingly the highest at this stations (see Figure 7). Stations 5 and 7 are slightly warmer than all remaining stations across the PLF morphology and on the shelf itself, which appear almost isothermal at around -1.4 ºC.

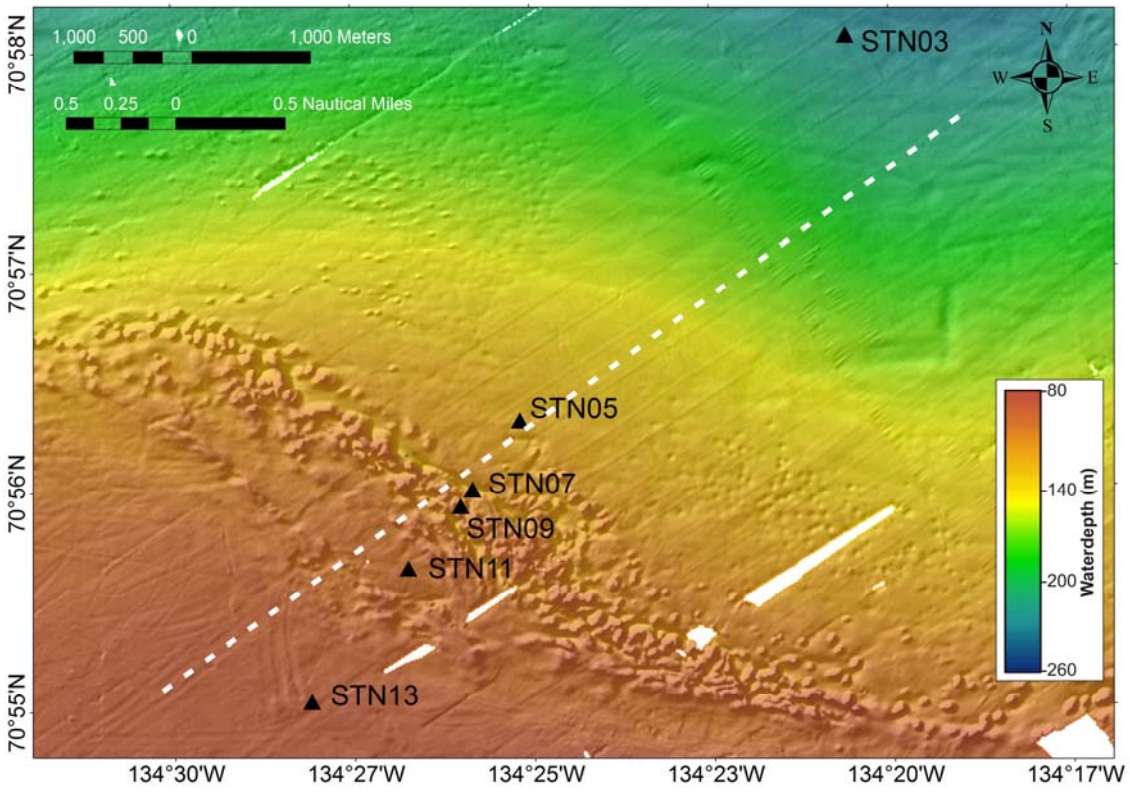

Figure 5. Map showing location of Stations 3, 5, 7, 9, 11, and 13 along the Eastern Shelf transect. The white dashed line represents the seismic transect shown in Figure 7.

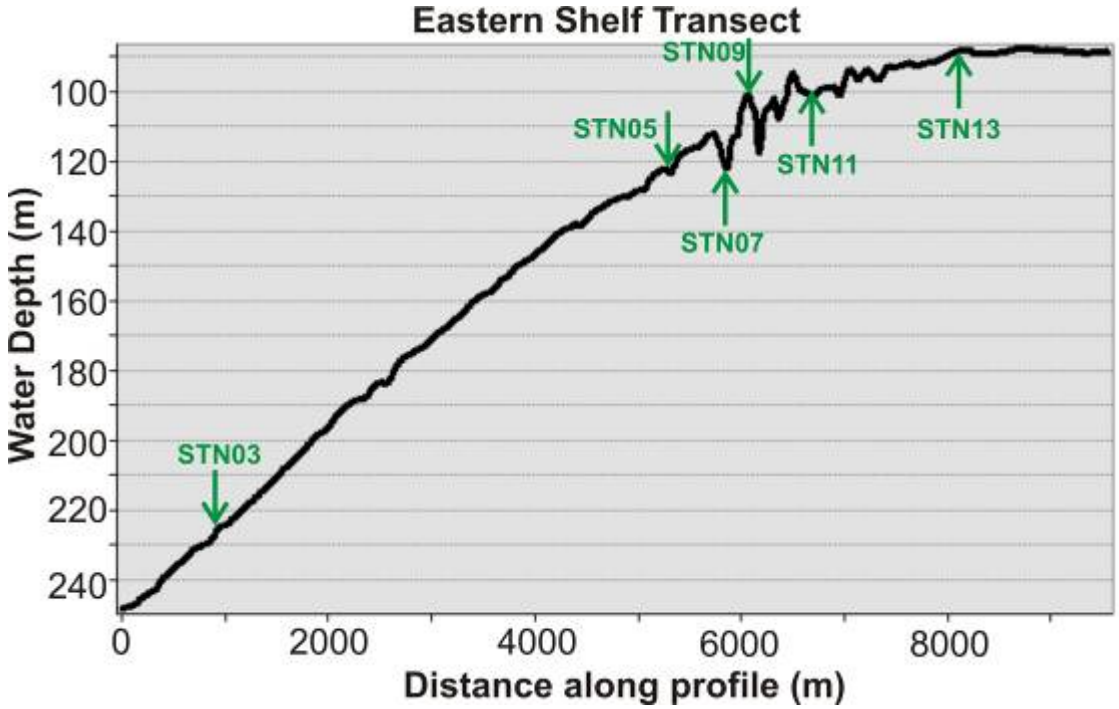

Figure 6. Depth profile along the Eastern Shelf Transect. Each core station with temperature measurements is shown by a green arrow.

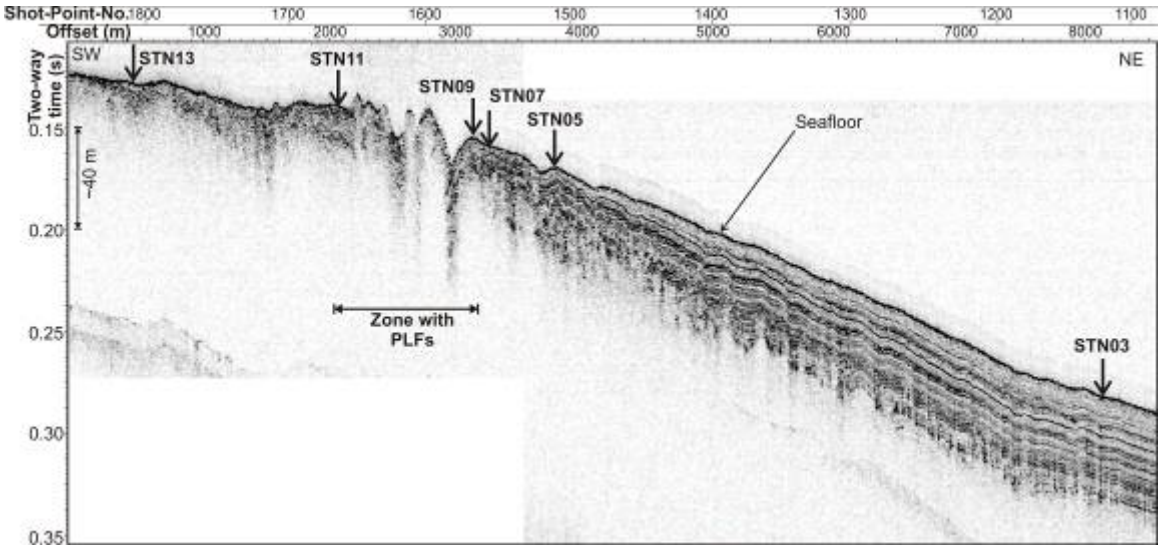

Figure 7. Seismic section of 3.5 kHz sub-bottom profiler data (shown is envelop of recorded amplitude) across the eastern shelf region representative of the transect of temperature measurements. Station locations are projected identified with arrows (see location of line in Figure 5).

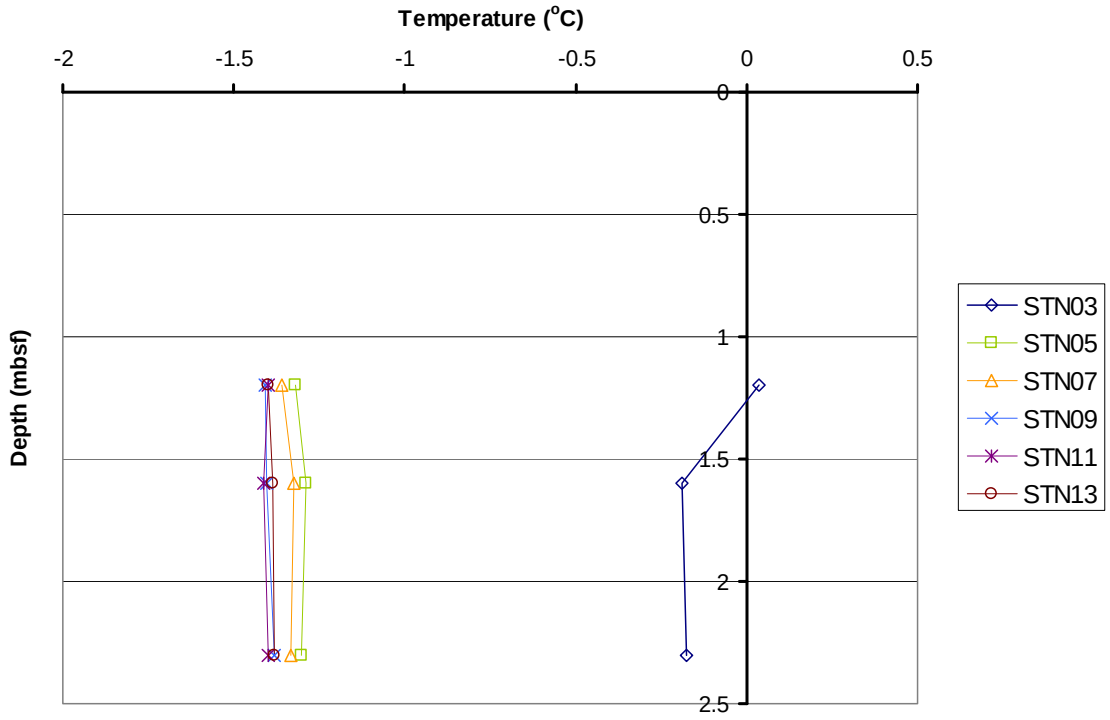

Figure 8a. Down-core temperature profiles for Eastern Shelf crossing. Three temperature loggers were used at all six stations of this transect.

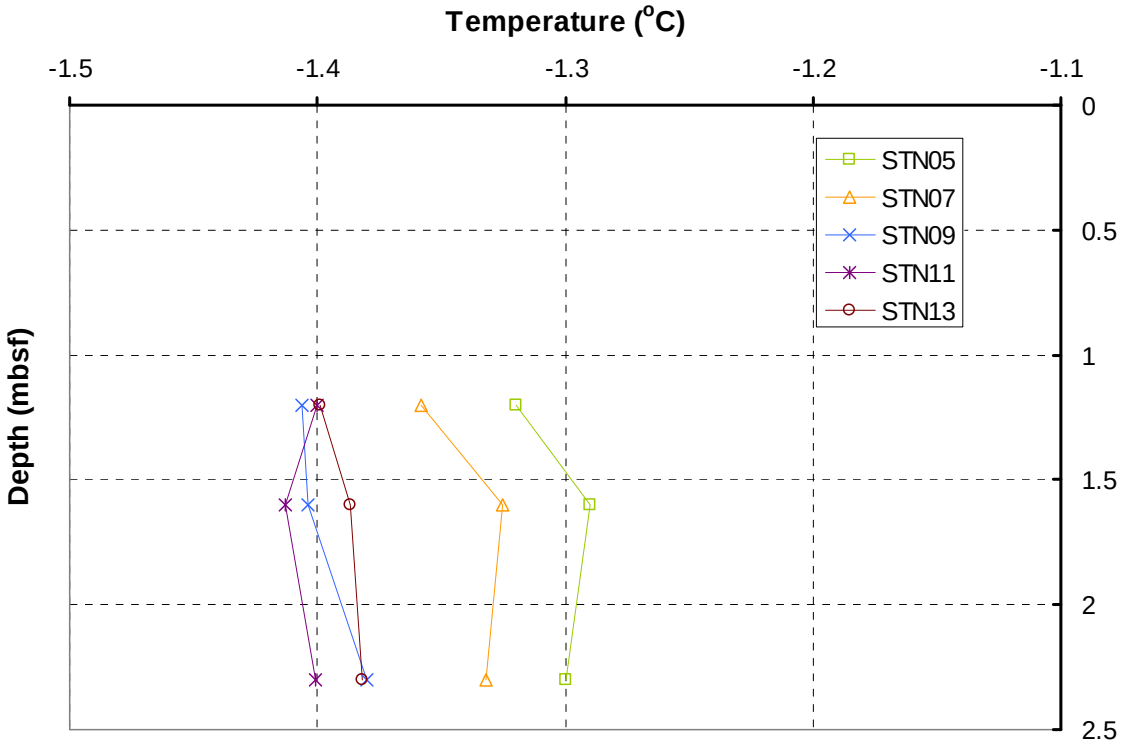

Figure 8b. Down-core temperature profiles for Eastern Shelf crossing without Station 3 to augment details in the temperature records.

3.2 Coke-Cap, (Stations 17, 19, 21, 23, 25, 27, and 56, 58, 60, 62, 64)

The Coke-Cap expulsion feature was visited twice during the expedition (Figure 9). The first set of measurements were made at Stations 17 to 27 and consisted of a single temperature logger attached to the gravity core barrel. The second visit consisted of five additional measurements (Stations 56 to 64) with five temperature loggers. No core was recovered at the second set of stations.

Four stations are within the main circular expulsion zone (Stations 23, 25, 58 and 60), two are on the rim of the feature (Stations 21, 62) and all other stations are outside the expulsion feature. During the 2012 *Sir Wilfrid Laurier* expedition (Melling et al., 2012) a seismic line crossing through all but one of the stations was acquired using the deep-tow Huntec system (Figure 10). The centre of the expulsion feature is marked by gas-rich sediments creating a blanking effect. The layered regular pelagic sedimentation

is disrupted by individual mud flows, imaged as more bright reflections than the regular pelagic sediments, particularly to the NW into the deeper water.

Within the centre of the expulsion feature (gas rich sediments) the temperatures measured are higher compared to the values obtained outside or at the rim of the feature (Figure 11). Data from Stations 58 and 60 suggest relatively steep, but nearly linear thermal gradients (Figure 12) of 1.37 ºC and 0.92ºC per meter, respectively. Although only one temperature logger was used for the other two centre-stations (25, 23), their values seem to agree well with those from Stations 58 and 60.

Data from Station 56 appears to disagree with the regional pattern emerging from all other stations. Although five loggers were deployed, only two reliable data points were obtained. Two loggers froze on deck during the pre-deployment period, and one logger showed an unusual shift in temperature approximately 2.5 minutes prior to the gravity core hitting bottom. This time difference of 2.5 minutes prior to the core hitting the bottom is equivalent to the expected time for the gravity core to be lowered to the seafloor at a winch-speed of 1 m/s, given the water depth of ~260 meter at this station. It is speculated that the logger's internal electronics were damaged during the gravity core deployment. The temperature recordings are reasonable if the temperature jump is ignored. Removing the offset in temperature (17.76ºC) results in an estimated equilibrium temperature value of 3.17ºC for this logger at a depth of 1.7 mbsf.

The two reliable temperature values obtained were the two highest values measured around Coke Cap and agree to the thermal gradient from Station 58. However, the coordinates of this station suggest it is located ~480 m SSW of the centre of the Coke Cap feature. As the temperature measurements were often twinned with the deployment of the free-fall cone penetrometer (FFCP), comparing station coordinates show that the twin FFCP-station 57 for thermal Station 56 is indeed in the centre of the expulsion feature (Figure 9). We therefore suggest a new coordinate for thermal Station 56 in the centre of the expulsion feature.

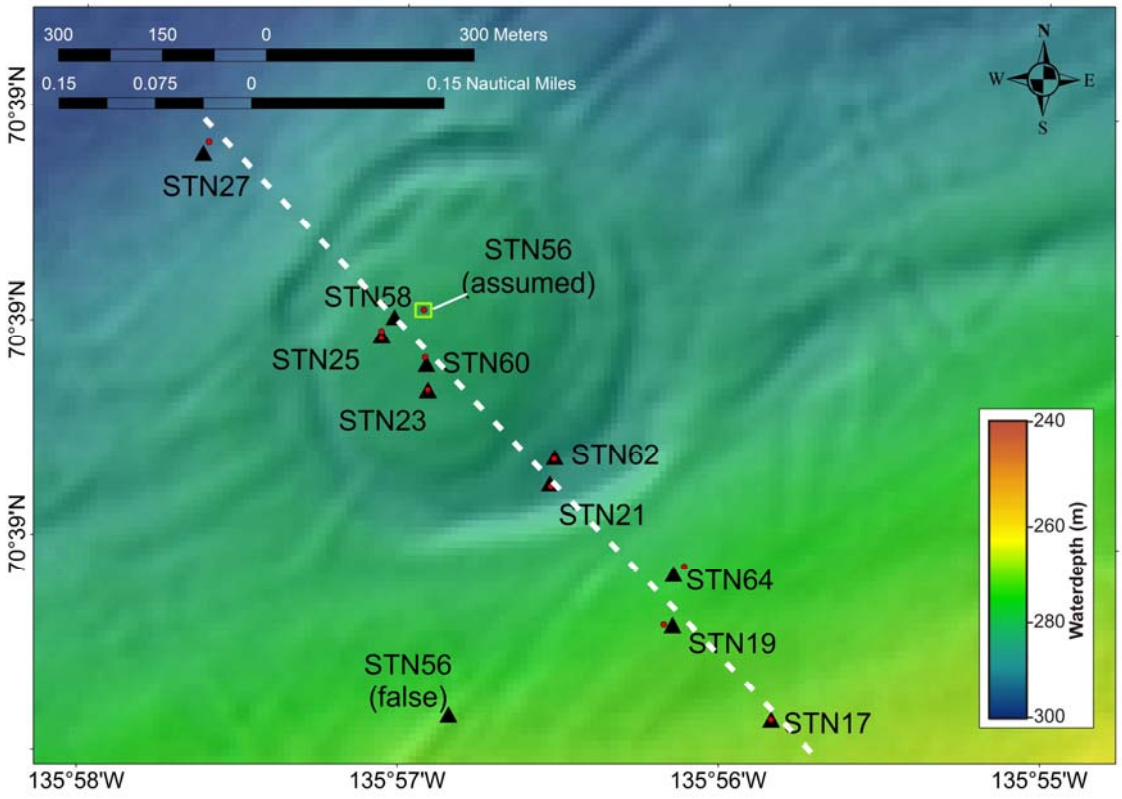

Figure 9. Map showing location of Stations 17, 19, 21, 23, 25, 27, 56, 58, 60, 62, and 64 around the Coke Cap expulsion feature. The white dashed line represents the seismic transect shown in Figure 10. Also shown are the twinned stations using the free-fall cone penetrometer (FFCP) as red circles. The twinned stations are usually very close to each other, with the exception of Station 57 (FFCP) and 56 (thermal). It can thus be assumed, that Station 56 is also in the centre of the expulsion feature as suggested by the measured temperatures, and hand-written field notes (S.R. Dallimore, pers. comm., 2014).

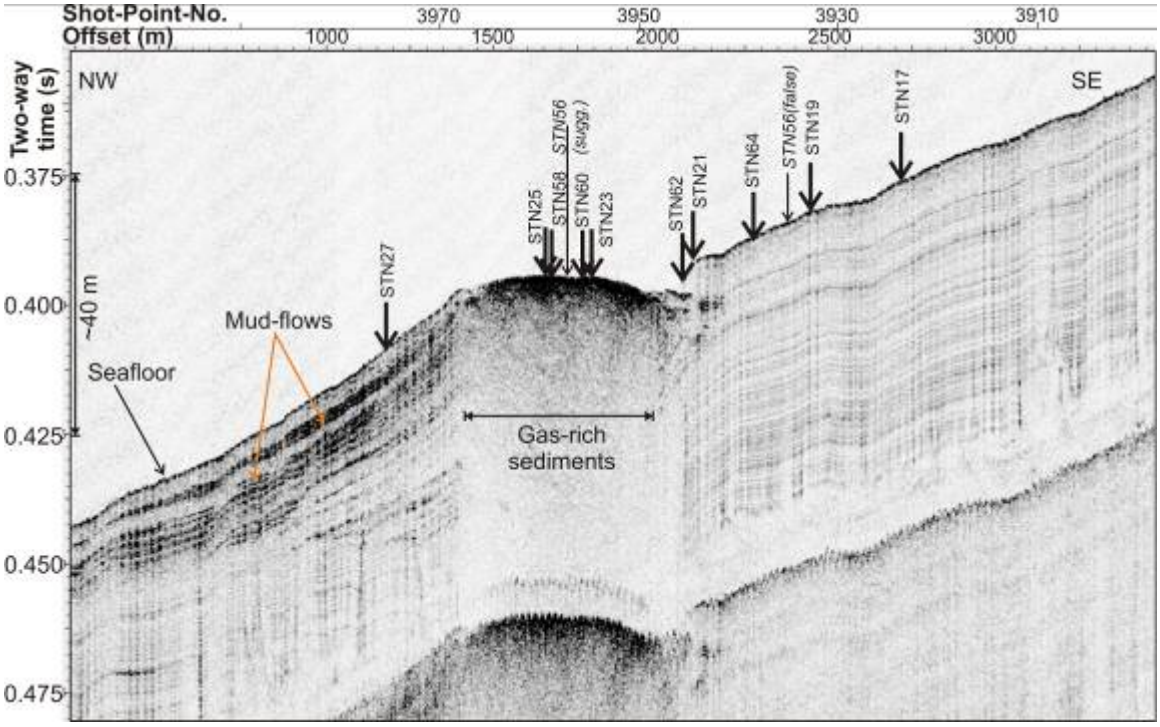

Figure 10. Seismic section acquired in 2012 with the deep-towed Huntec sub-bottom profiler system (shown is the envelope of the recorded amplitude after band-pass filtering to remove tow-noise) across Coke Cap. Stations are projected onto this seismic line (compare to map shown in Figure 9).

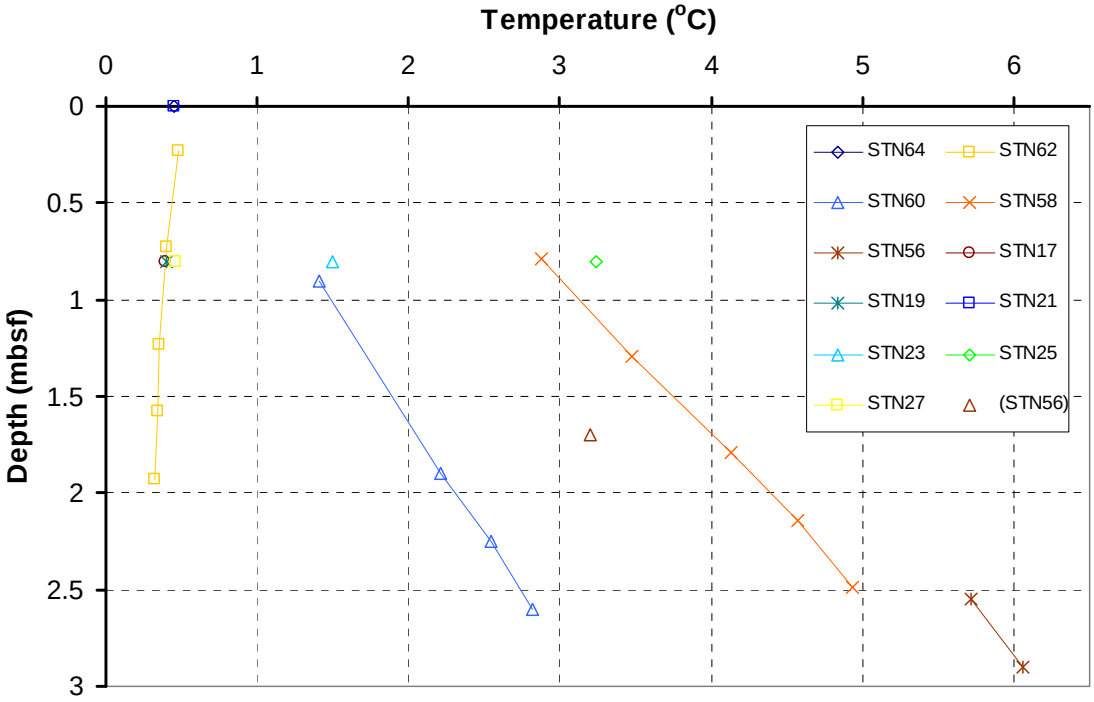

Figure 11. Down-core temperature profiles for the Coke-Cap expulsion feature. Data from Stations 58 and 60 were used to define a geothermal gradient. Both these stations are in the centre of the expulsion feature (see Figure 12). A single data point from Station 56 at 1.7 mbsf was defined after correction of an artificial temperature-jump seen in the data. However, the value is likely unreliable and is not used for an estimation of a thermal gradient at Station 56.

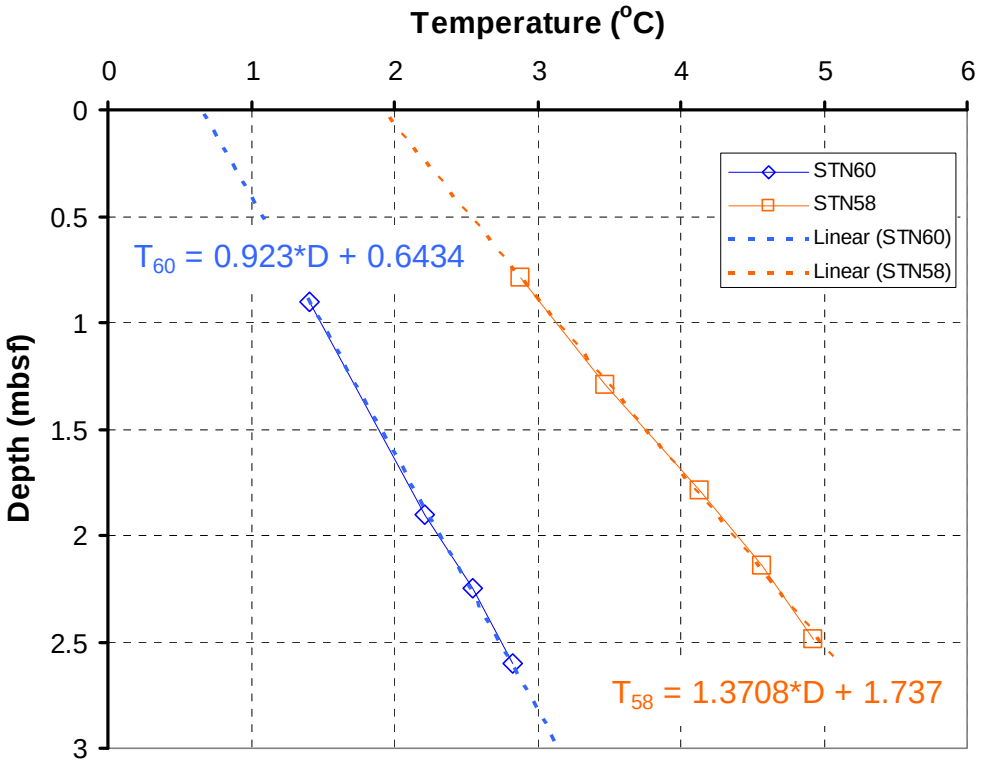

Figure 12. Definition of thermal gradients for Stations 58 and 60 at the centre of the Coke Cap expulsion feature.

3.3 420 m water depth expulsion feature, (Stations 41, 43, 45, 47, 49, 51, 96, 97, 99, 101, 103, 105)

12 stations were visited at the 420 m water depth expulsion feature for temperature measurements (Figure 13). Three stations were outside the elevated plateau area (Stations 41, 49, 51) and all other stations were on the south-eastern half of the plateau. Seismically, the 420 m expulsion feature appears similar to Coke Cap, as the centre of the feature is dominated by gas-rich sediments, creating a blanking effect in the seismic data (Figure 14, 15). The features appear to be almost circular, rising 20-30 m above the surrounding seafloor. Mud flows can be seen on either side of the expulsion feature, but are more dominant towards the NW, in a down-slope direction. Temperature data from all 12 stations are of high quality (Figure 16) resulting in the calculation of reliable geothermal gradients (Figure 17a, b). Overall, the three background stations

outside the expulsion feature show, as expected, no significant change of temperature with depth (Figure 16). Within the plateau of the expulsion feature, temperatures as high as 9.2ºC were measured at depth of ~2.5 mbsf (Station 96). Thermal gradients range from ~0.5 ºC/m at Station 99 to 2.9 ºC/m at Station 96. Significant gas plumes in the water column were detected during the ARA04C expedition at this site. Also, gas hydrate was recovered at one core site during the Araon expedition ARA05C in September 2014 (Jin et al., 2014). All these observation support the presence of a vigorous fluid flow system that expels warm fluid at the seafloor in a highly localized manner.

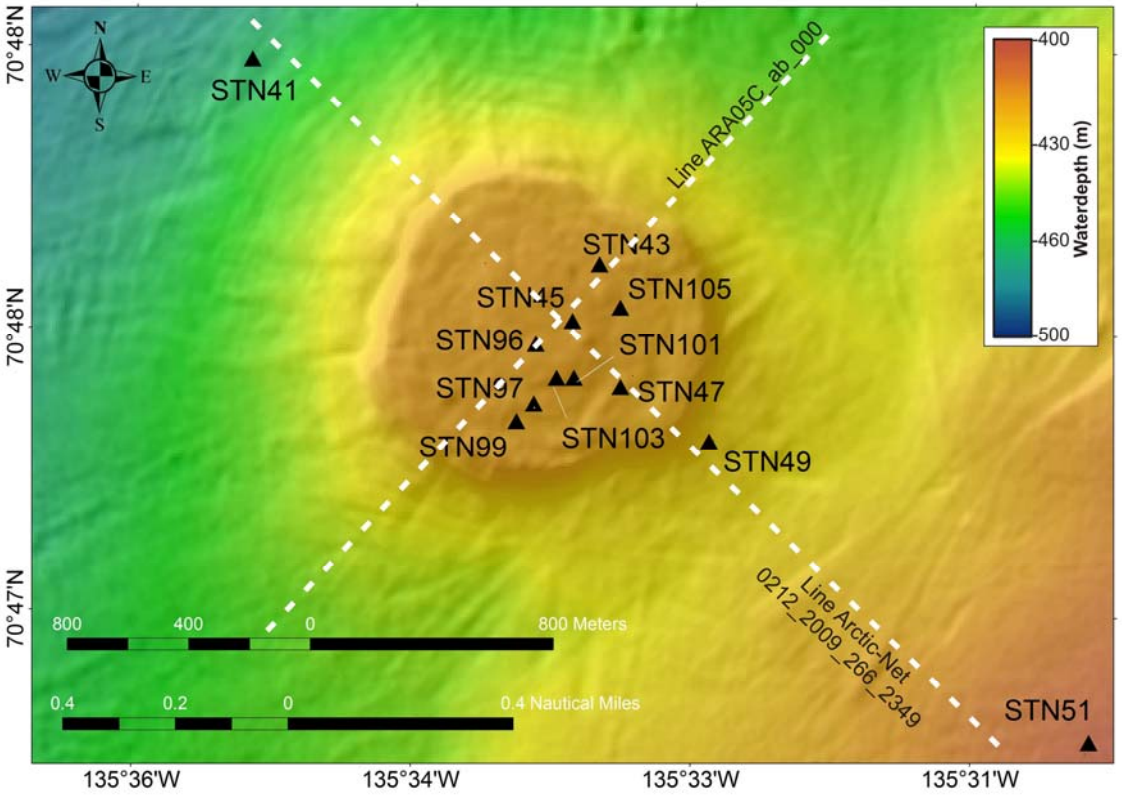

Figure 13. Map showing location of Stations 41, 45, 47, 49, 59, and 96, 97, 99, 101, 103, and 105 around the 420 m water depth expulsion feature. Two seismic sections crossing this feature (shown by the dashed grey lines) are shown in Figure 14, and 15.

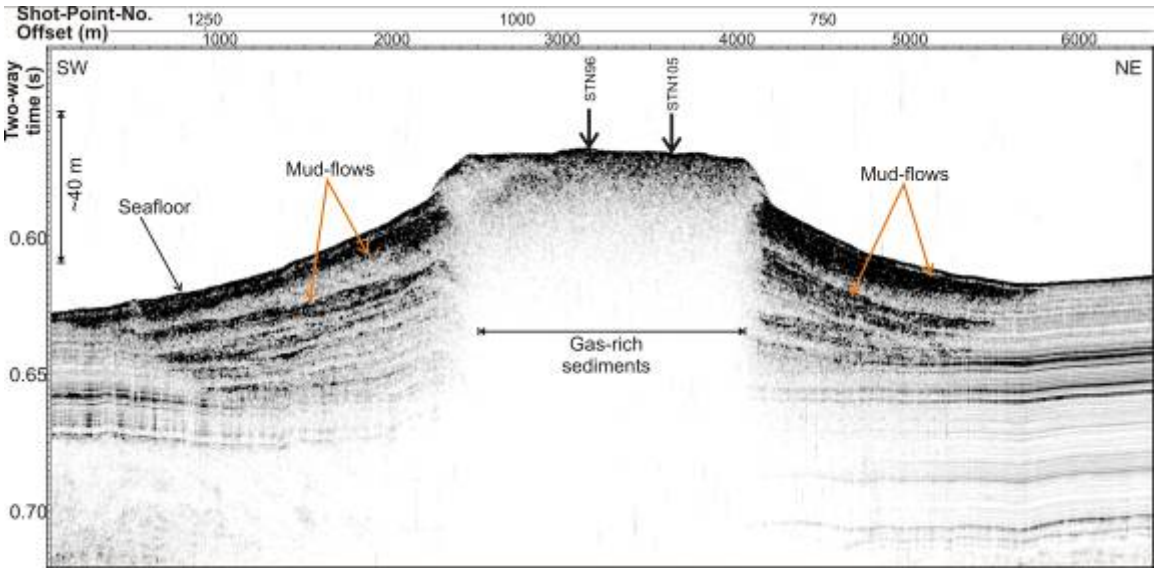

Figure 14. Seismic section of 3.5 kHz sub-bottom profiler data (shown is envelop of recorded amplitude) of line ARA05C_ab_000 (SW to NE) across the 420 m water depth expulsion feature. Stations are projected onto this seismic line.

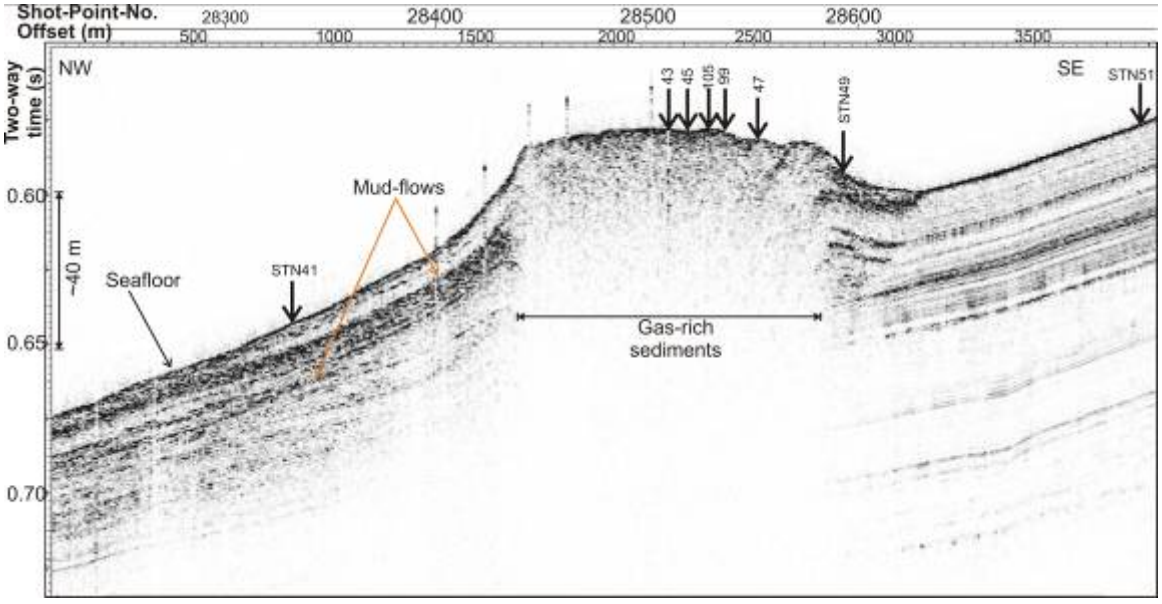

Figure 15. Seismic section of 3.5 kHz sub-bottom profiler data (shown is envelop of recorded amplitude) of Arctic-Net line 0212_2009_266_2349 (SE to NW) across the 420 m water depth expulsion feature. Selected stations are projected onto this seismic line.

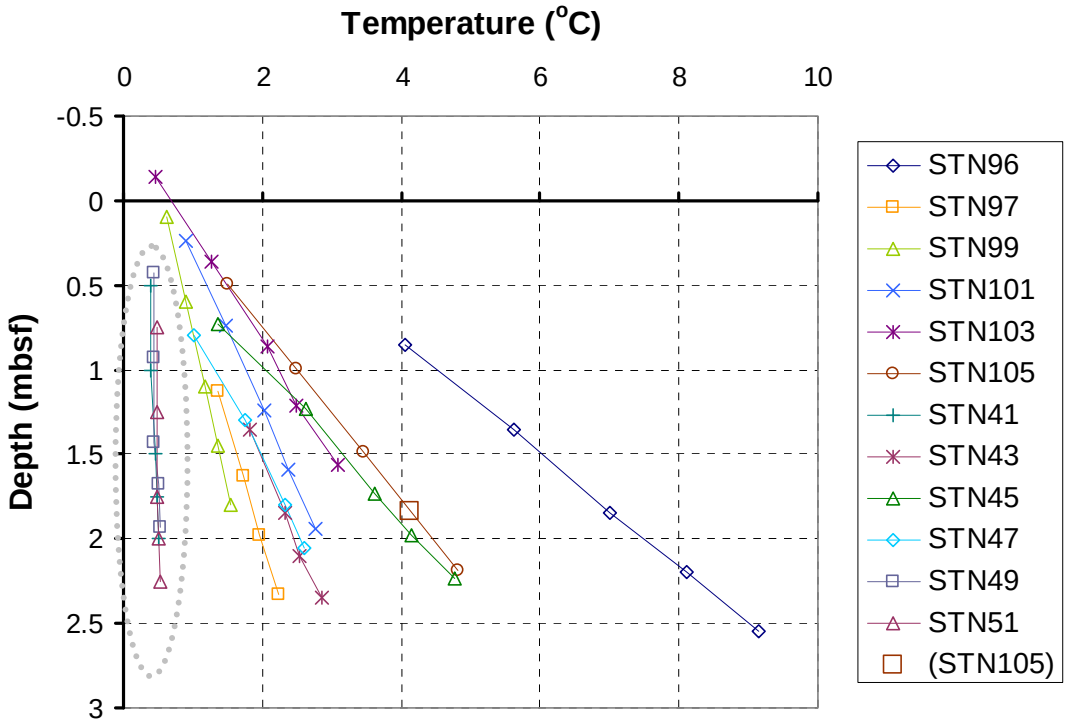

Figure 16a. Down-core temperature profiles for the 420 m water depth expulsion feature. Note the three almost constant temperature profiles highlighted by the gray oval (Stations 41, 49, 51), which are all outside the expulsion feature. Negative depth values were assigned, where water temperature was measured.

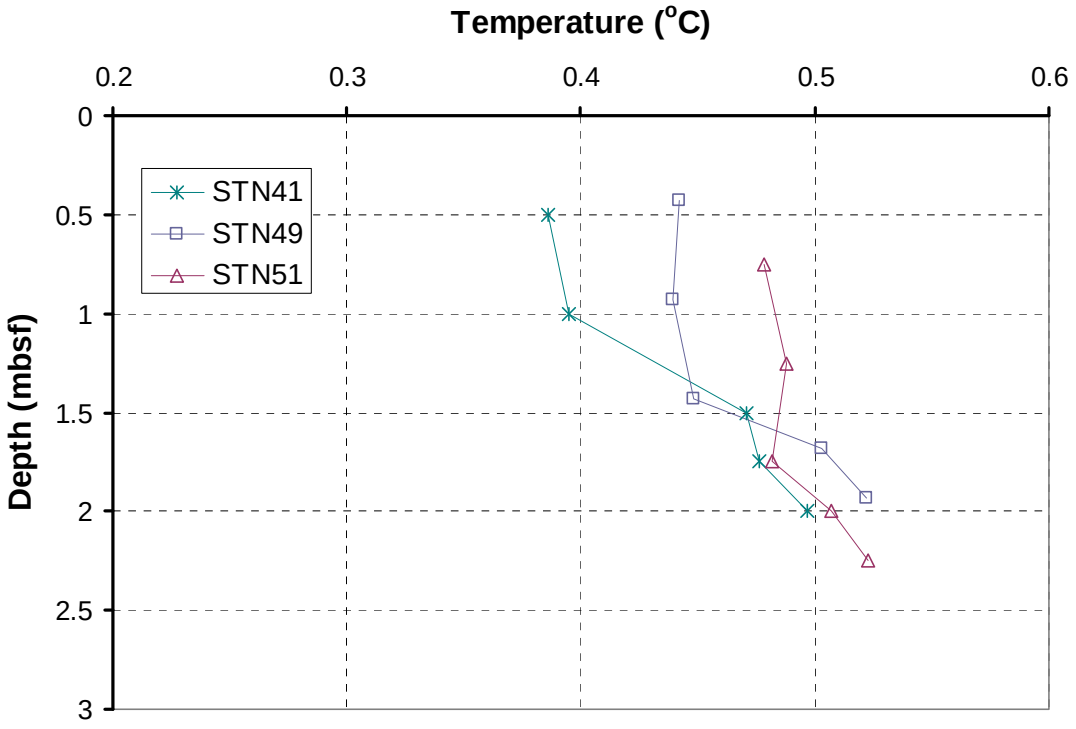

Figure 16b. Down-core temperature profiles for the 420 m water depth expulsion feature for Stations 41, 49, and 51, which are all outside the expulsion feature.

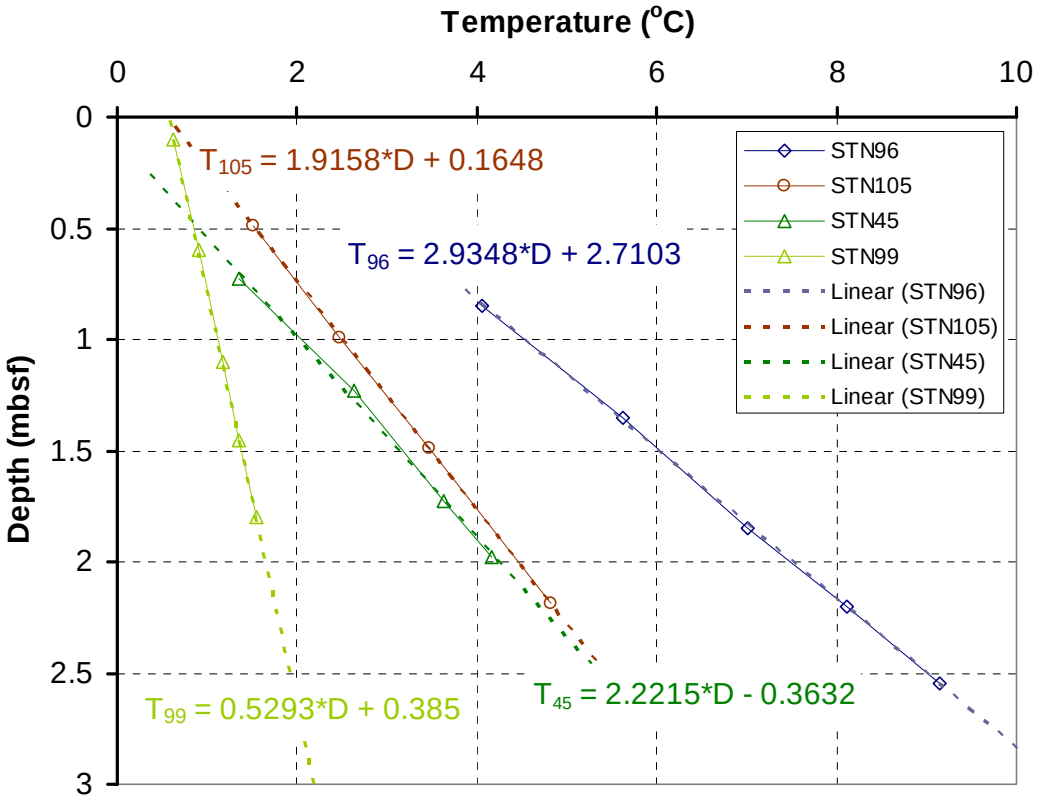

Figure 17a. Definition of thermal gradients for Stations 45, 96, 99, and 105 at the 420 m water depth expulsion feature.

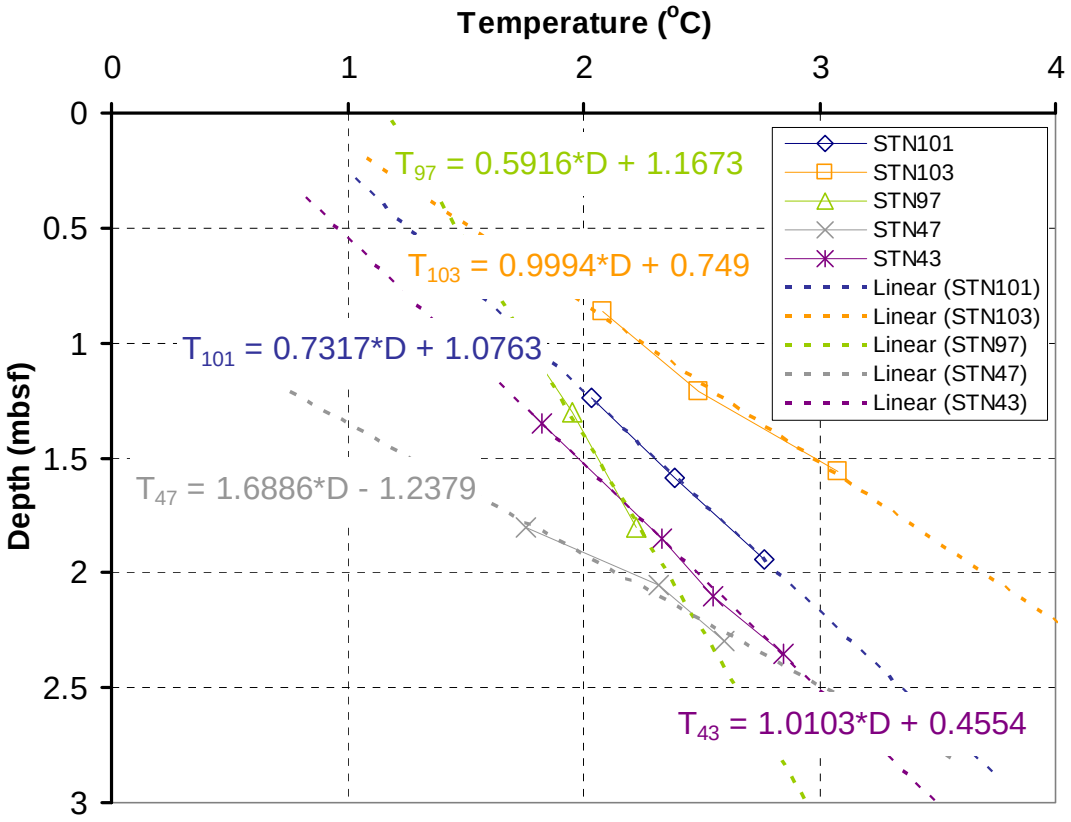

Figure 17b. Definition of thermal gradients for Stations 43, 47, 97, 101, and 103 at the 420 m water depth expulsion feature.

3.4 760 m water depth expulsion feature, (Stations 75, 76, 77, 78, 79, 80)

Six stations with temperature measurements were occupied at the 760 m water depth expulsion feature (also referred to as triple mound, Figure 18) that consists of three mounds and a near-circular moat. At the southern end of the structure, extensional faulting can be seen (Figure 19), where the seafloor dips into the moat in a step-wise pattern. One station is positioned outside of the expulsion zone and surrounding moat (Station 77), one station is within the moat itself (Station 80) and the remaining four stations are across the plateau-like southern mound of the three apparent expulsion centres.

Temperature data were generally of good quality (Figure 20), but all stations appear thermally similar with an average temperature of 0.15ºC, with small variations with depth (< 0.2 ºC). Some of the measured temperature depth profiles appear disturbed by outliers. Data from Stations 75, 76, and 77 suggest similar gradients of 0.1 ºC/m if outliers are omitted. Apparent core recovery was shorter than the spread of outriggers attached to the core barrel on two deployments, resulting in negative depth values assigned to the loggers (Station 78, 80).

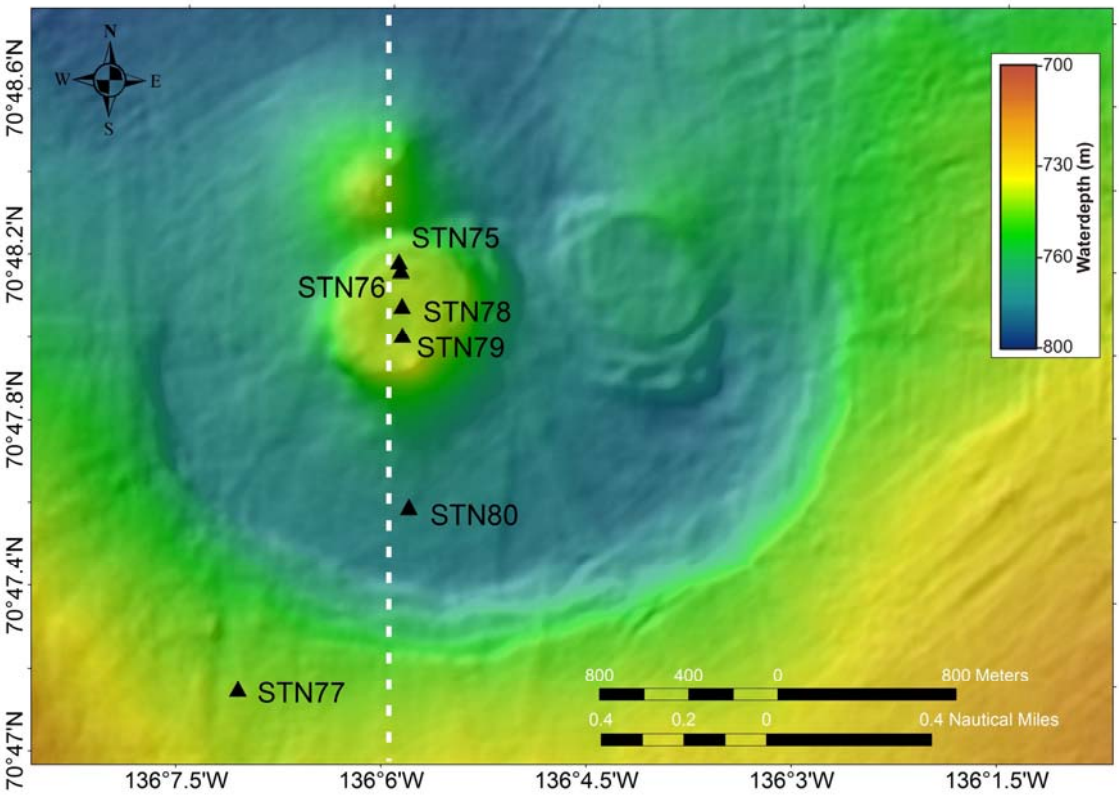

Figure 18. Map showing location of Stations 75, 76, 77, 78, 79, and 80 around the 760 m water depth expulsion feature (triple mound) with three mound structures. The white dashed line represents the seismic transect of Arctic-Net line 0012_2009_257_1858 shown in Figure 19.

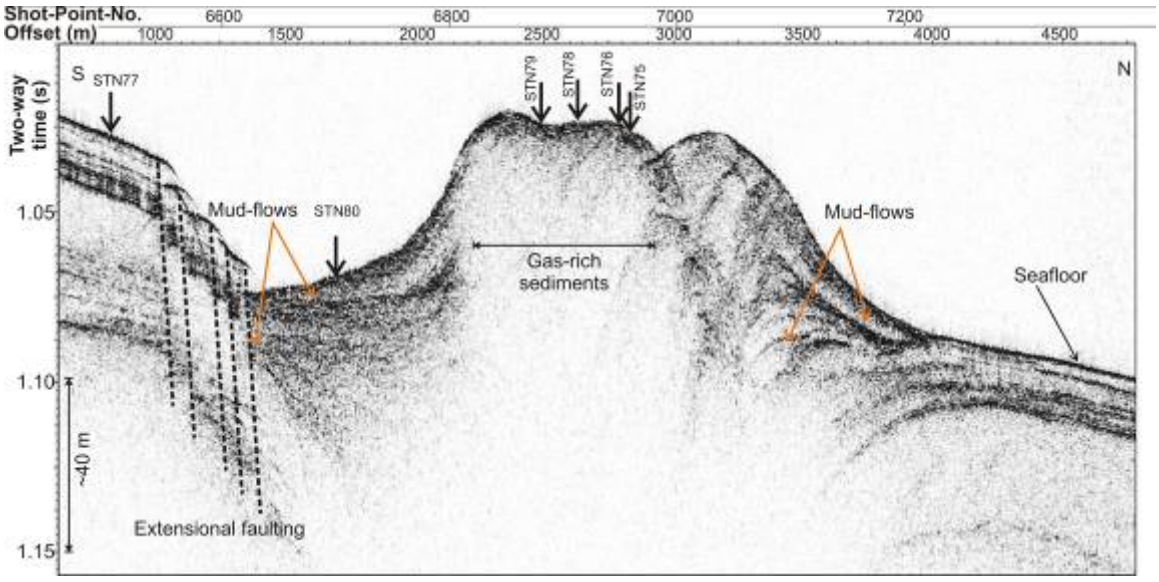

Figure 19. Seismic section of 3.5 kHz sub-bottom profiler data (shown is envelop of recorded amplitude) of Arctic-Net line 0012_2009_257_1858 (S to N) across the 760 m water depth expulsion feature. Stations are projected onto this seismic line.

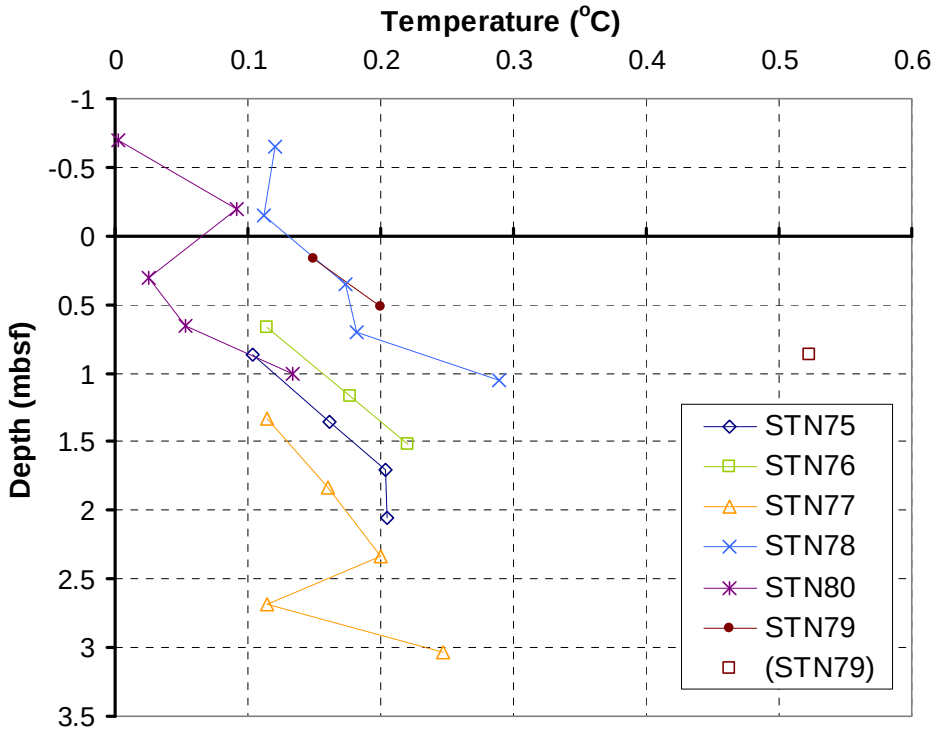

Figure 20. Down-core temperature profiles for the 760 m water depth expulsion feature (triple mound). Negative depth values were assigned, where water temperature was measured.

3.5 Western Canyon, (Stations 31, 32, 33, 34, 35, 94, 95)

Several large canyon systems dominate the topography in the NW portion of the research area (Figure 2). The canyon heads appear to be slope-failures and a series of gravity cores were taken across the features accompanied with FFCP deployments. One transect was made at the western Canyon (Figure 21). The seismic section (slightly further to the west than the line of stations) shows the general structure of the canyon, revealing the canyon-head as a series of blocks failing in a step-wise fashion (Figure 22). Station 35 is on the southern end of the transect in stable terrain, Stations 34, and 33 are within the blocky slope failed section, and Stations 32 and 31 are at the toe and floor of the canyon head.

Two additional cores with temperature data measurements were conducted slightly further north of this canyon transect in the vicinity of a ROV dive site (Figure 23).

These two core locations belong to the same general western-canyon structure. However, topography across these sites is very rough and seismic imaging is degraded.

Temperature values from the five stations of the canyon-head transect (Figure 24) vary slightly between 0.2ºC and 0.4ºC and show a slightly positive geothermal gradient. However, data above 1.0 mbsf are likely influenced by seasonal variations in the water-temperatures and thus may not contribute to a reliable geothermal gradient. A general warming trend in the top-most measured temperature values from the deepest water (Station 31) to Station 35 in shallowest water can be identified. The two deepest data points were used to define an approximate geothermal gradient at Stations 34, 35, and 95, which yields values of 0.056ºC/m, 0.046ºC/m, and 0.074ºC/m, respectively. These values are two orders of magnitude smaller than those gradients defined at the centres of the Coke-Cap and 420 m water depth expulsion features.

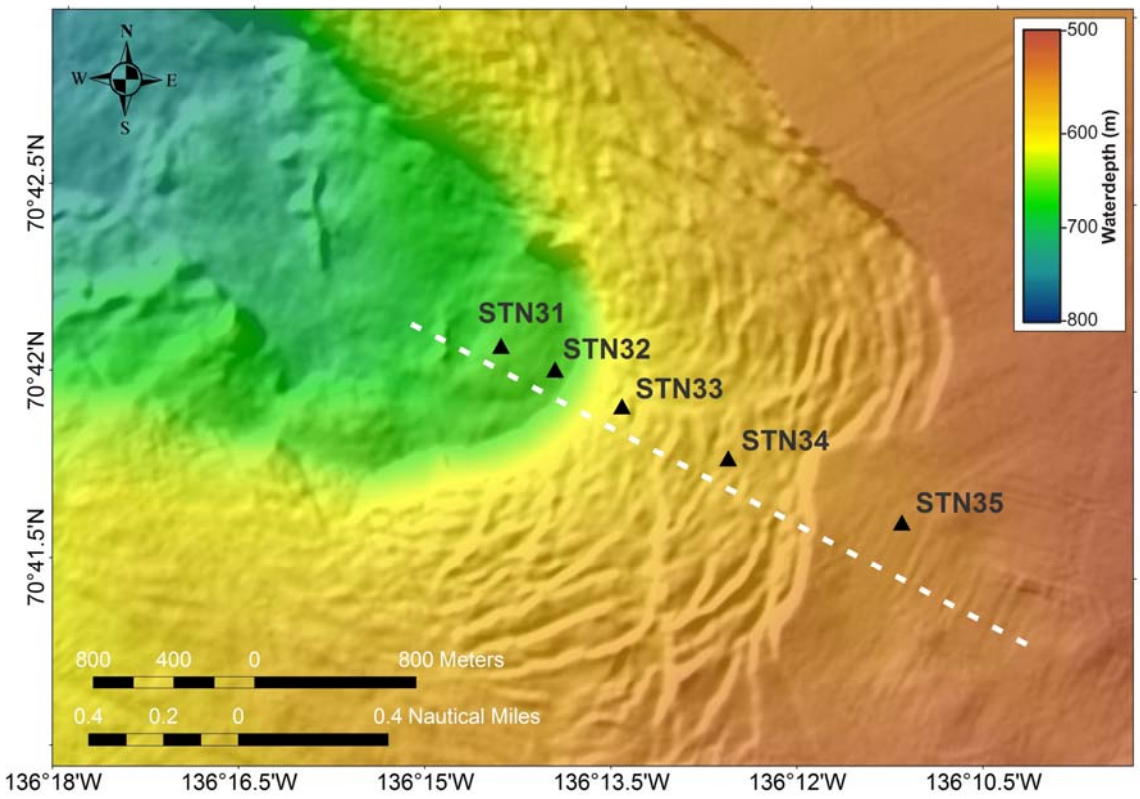

Figure 21. Map showing location of Stations 31 to 34 along a transect across the western canyon site. The white dashed line represents the seismic transect of Arctic-Net line 0130_2009_264_0224 shown in Figure 22.

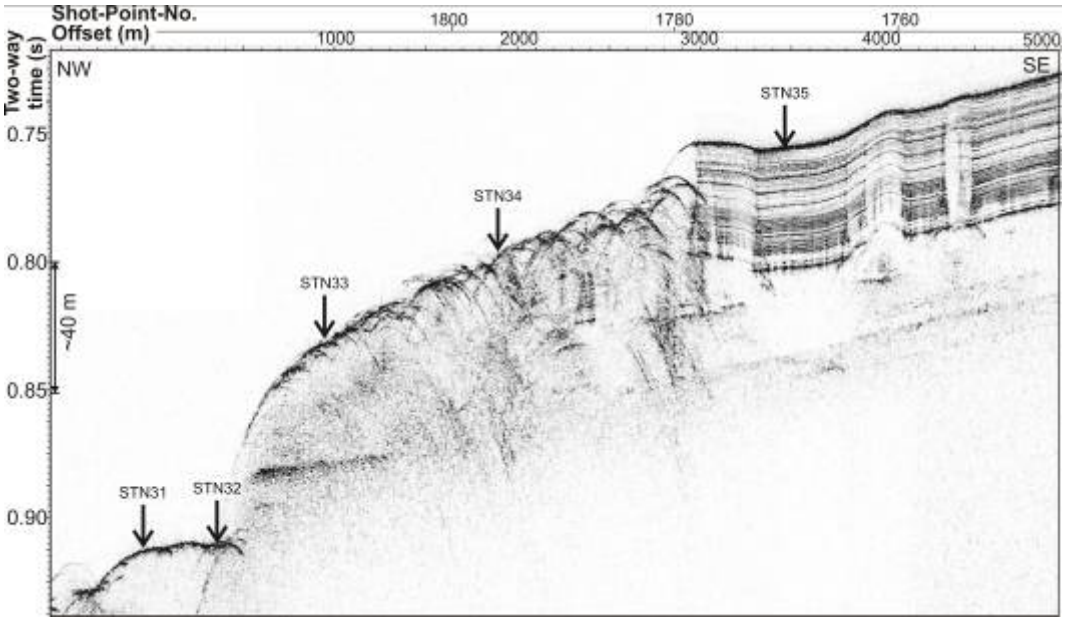

Figure 22. Seismic section of 3.5 kHz sub-bottom profiler data (shown is envelop of recorded amplitude) of Arctic-Net line 0130_2009_264_0224 across the western canyon site. Stations are projected onto this seismic line.

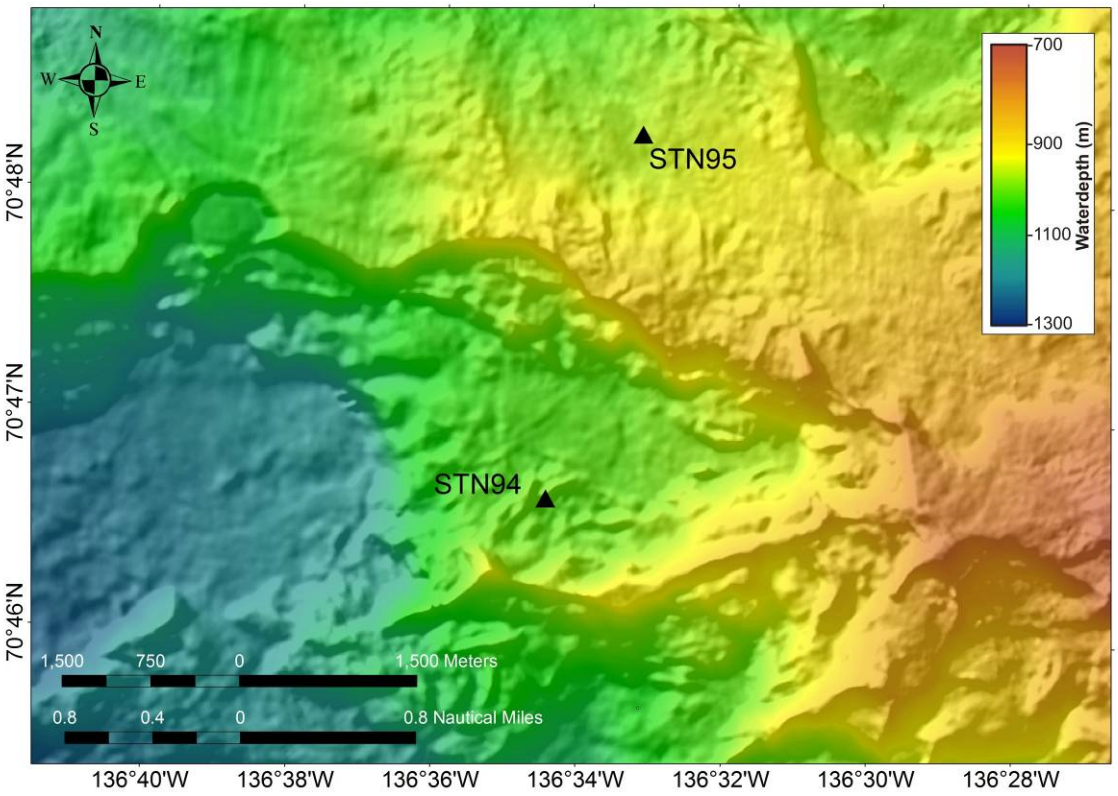

Figure 23. Map showing location of Stations 94 and 95.

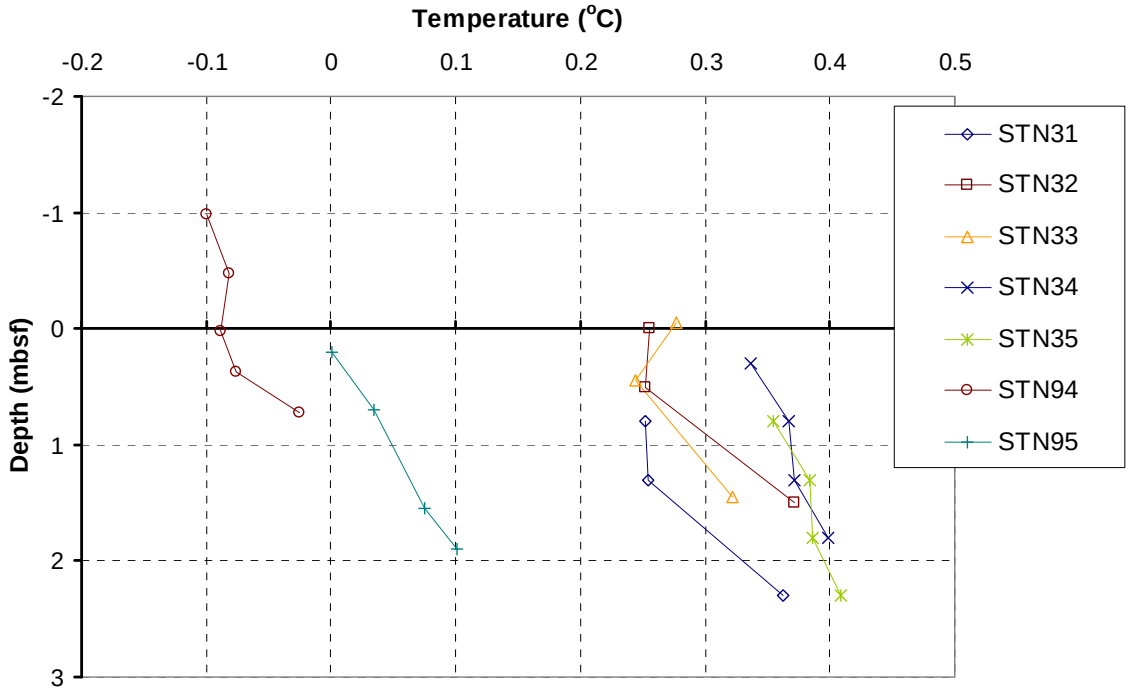

Figure 24. Down-core temperature profiles for the western canyon transect sites, as well as Stations 94, and 95.

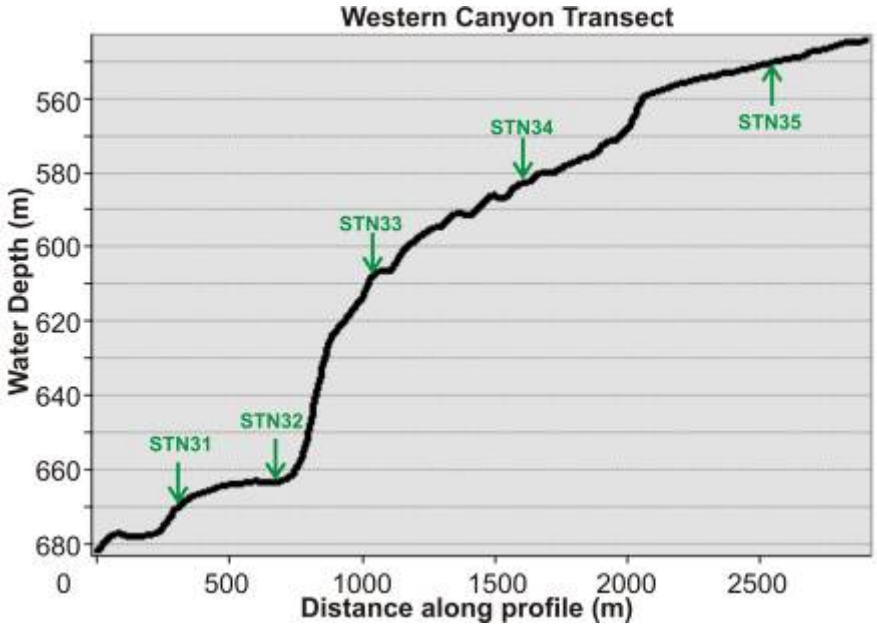

Figure 25. Depth profile along the western canyon transect. Each core station with temperature measurements is shown by a green arrow.

3.6 Northern Canyon (Stations 67, 68, 69, 70, 71)

As described in section 3.5, several large canyon systems occur in the NW portion of the research area. The second canyon-head transect, consisting of five gravity cores with temperature measurements twinned with FFCP deployments, was made at a northern Canyon site (Figure 26). The seismic section (slightly oblique to the line of stations) shows the general structure of the canyon, revealing the canyon-head as a series of blocks failing in a step-wise fashion (Figure 27), similar to the western Canyon site. Station 67 is on the southern end of the transect in stable terrain, Stations 68, and 69 are within the blocky slope failed section, and Stations 70 and 71 are within the outrunner material at the floor of the canyon.

Temperature values from all depths at the five stations of the northern canyon transect (Figure 28a) vary slightly between 0.05ºC and 0.2ºC and show a slightly positive geothermal gradient (Figure 28b). However, data above 1.0 mbsf are likely influenced by seasonal variations in the water-temperatures and thus may not contribute to a reliable geothermal gradient. No significant temperature-trend across the transect from Station 71 in deepest water to Station 67 in shallowest water can be identified.

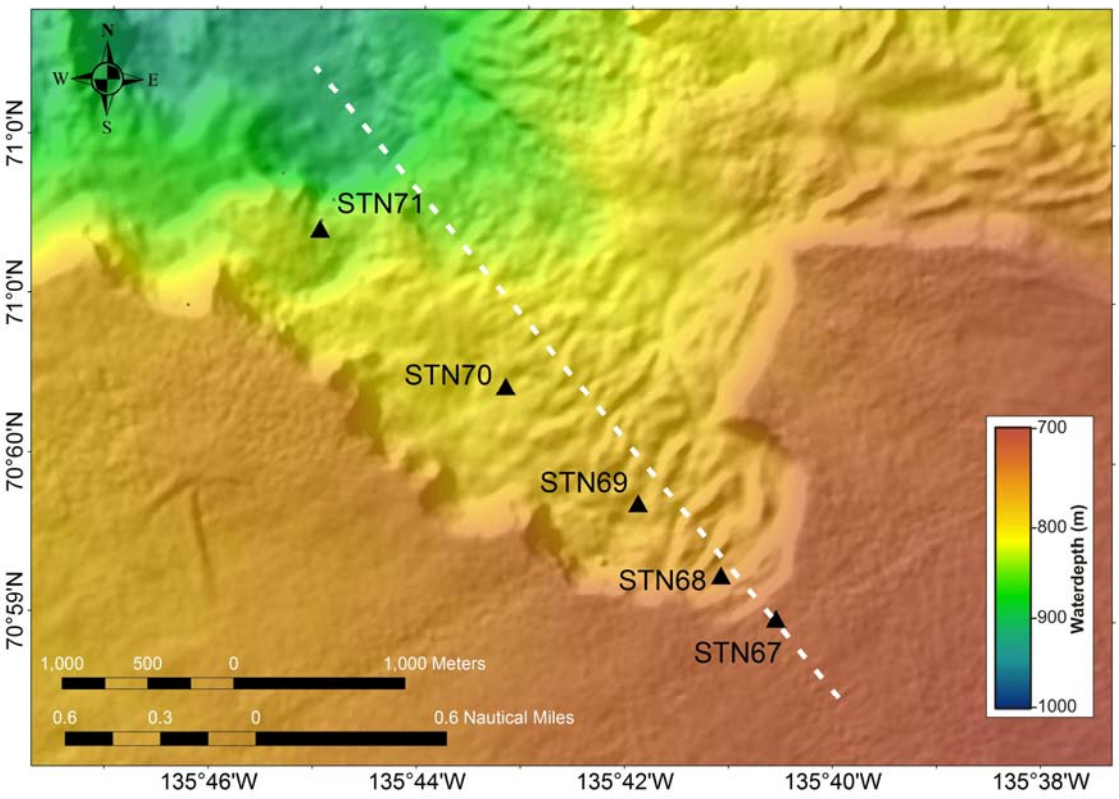

Figure 26. Map showing location of Stations 67, 68, 69, 70, 71, and 72 along a transect across the northern canyon site. The white dashed line represents the seismic transect of Arctic-Net line 0032_2010_248_1030 shown in Figure 27.

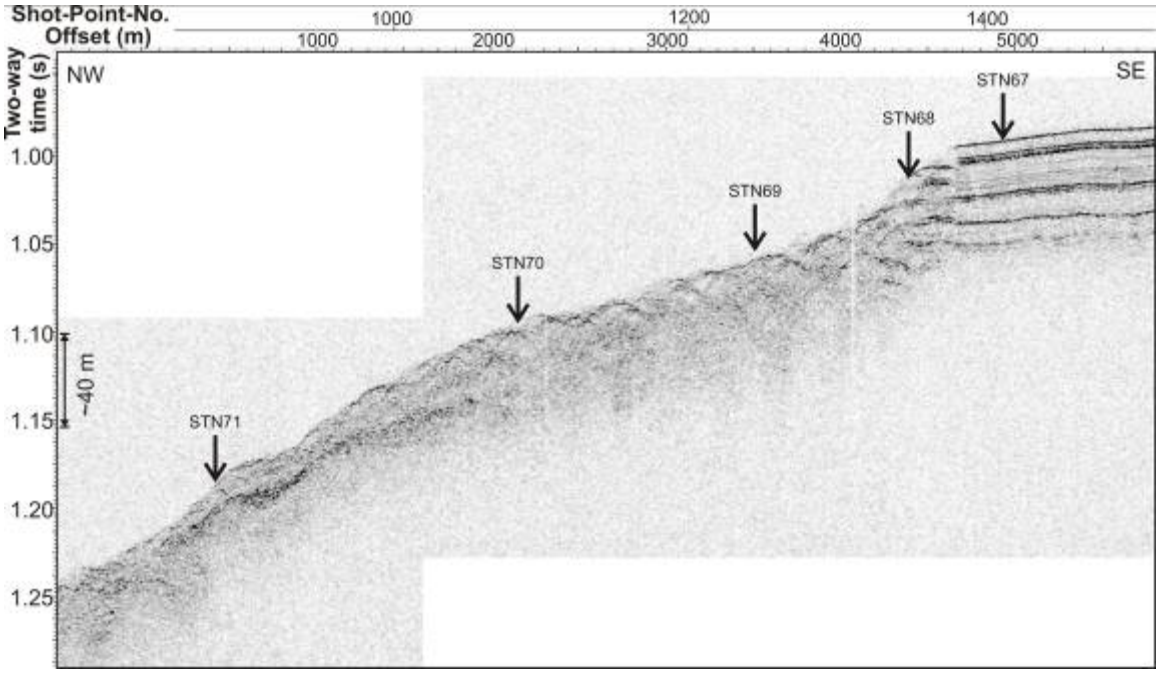

Figure 27. Seismic section of 3.5 kHz sub-bottom profiler data (shown is envelop of recorded amplitude) of Arctic-Net line 0032_2010_248_1030 across the northern canyon site. Stations are projected onto this seismic line.

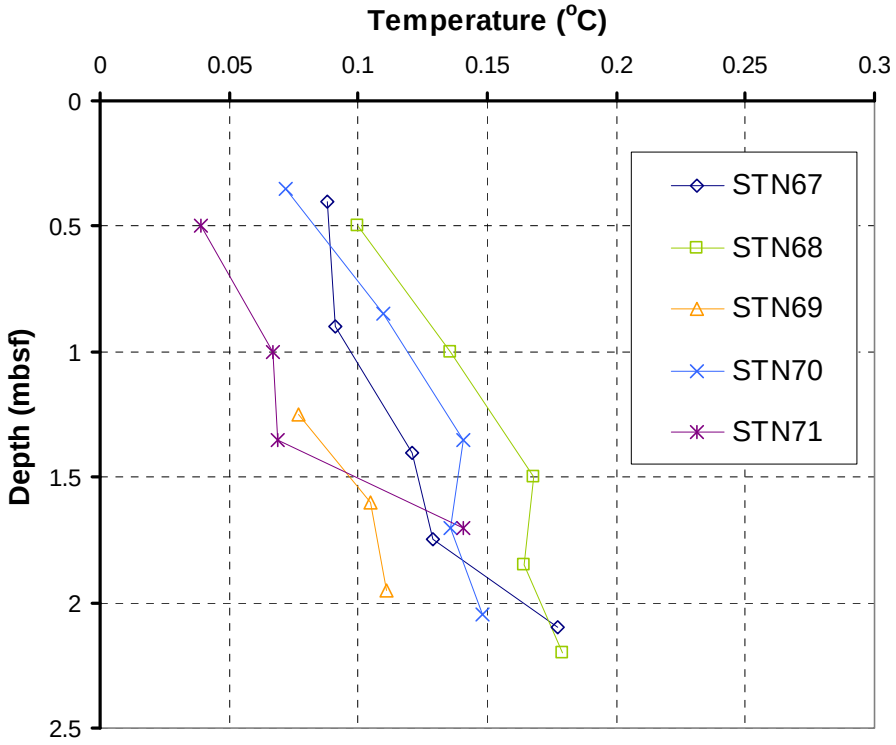

Figure 28a. Down-core temperature profiles for Stations 67, 68, 69, 70, and 71 across the northern canyon.

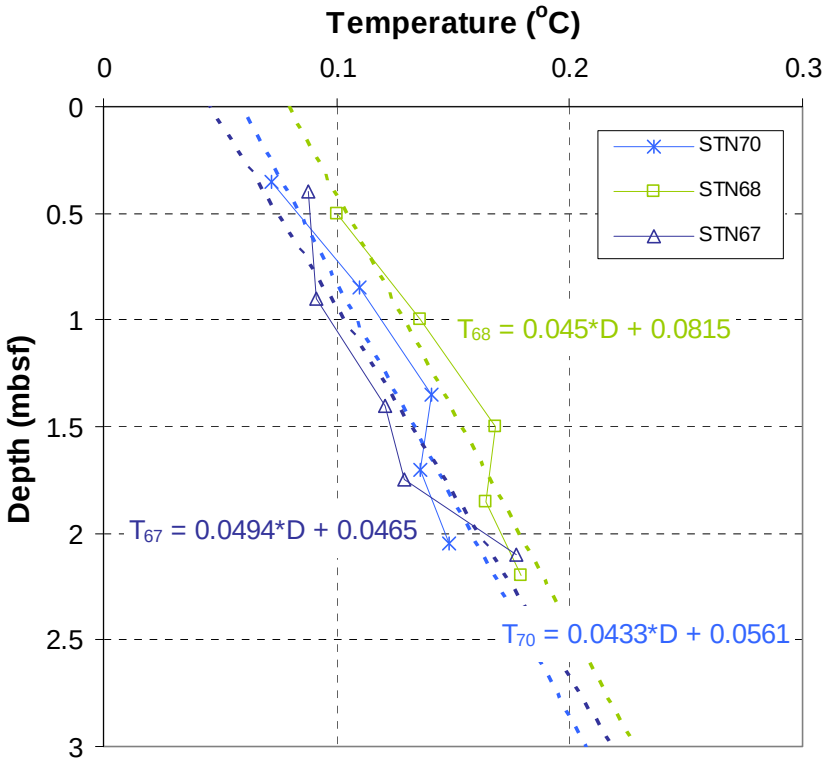

Figure 28b. Definition of thermal gradients for stations 67, 68, and 70 at the northern canyon site. Gradients are all very similar and average 0.046ºC/m.

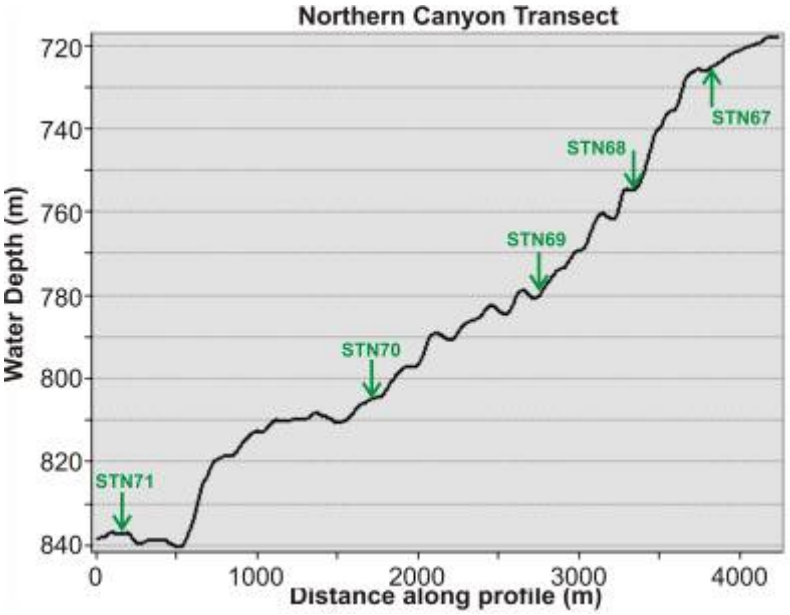

Figure 29. Depth profile along the northern canyon transect site. Each core station with temperature measurements is shown by a green arrow.

3.7 South of Landslide (Stations 111, 113, 115)

Three stations were visited around elongated ridges on the shelf region (Figure 30), just south of the main submarine slope failure complex (compare to Figure 2). The temperature data from these sites were overall sparse, as the apparent penetration was less than the length of the core barrel and several temperature loggers did not penetrate into the sediments. No thermal gradients can be defined from the few data points; overall, temperatures are colder than -1.3ºC, typical for the shelf stations visited during the expedition.

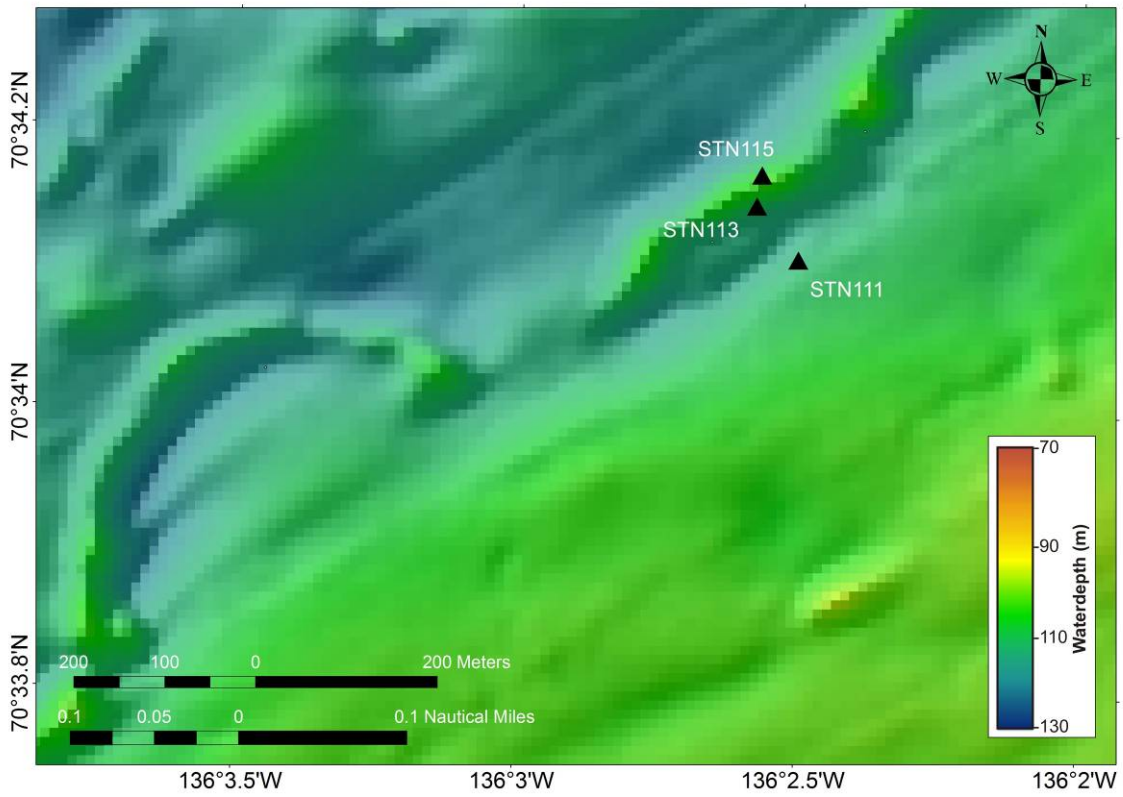

Figure 30. Map showing location of Stations 111, 113, and 115 south of the landslide at suspected elongated glacial moraine deposits.

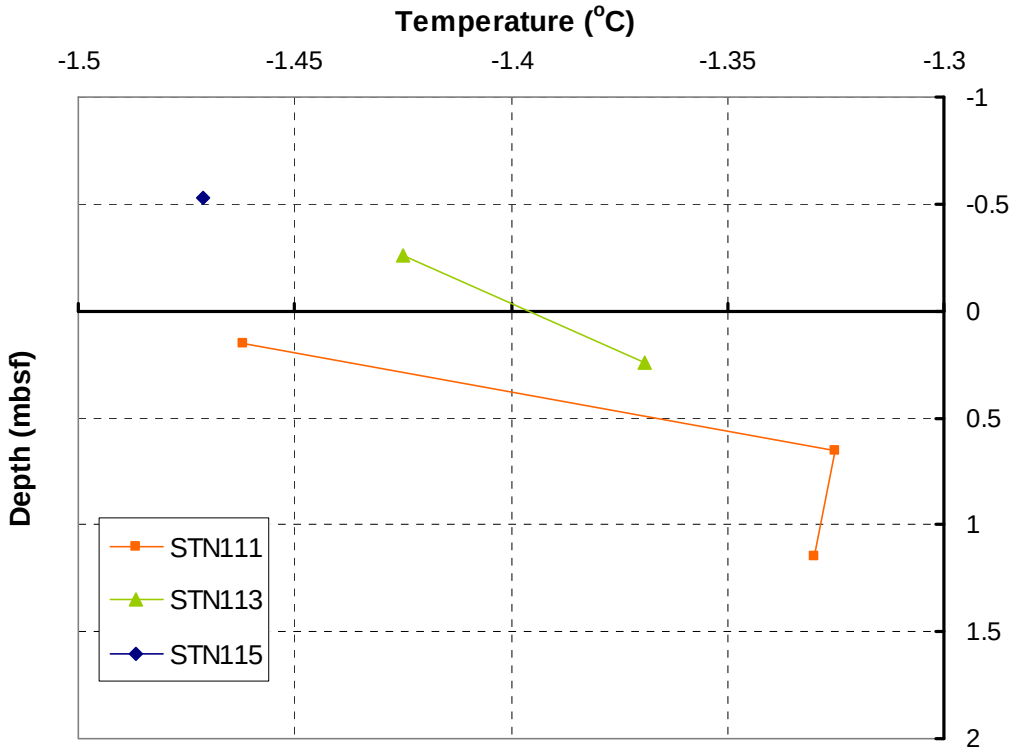

Figure 31. Down-core temperature profiles for Stations 111, 113, and 115, across an apparent glacial landform south of the main landslide feature. Negative depth values were assigned where water temperature was measured.

3.8 Central shelf transect (Stations 81, 83, 85, 87, 89, 91)

A second crossing of the slope-shelf region was established approximately in the centre of the study region with the PLF-dominating seafloor morphology (Figure 32). The six stations with temperature measurements were positioned along line 0027 of the AUV deployment (Figure 33). At these six stations apparent core penetrations were always less than the nominal 2.5 m long core barrel, resulting in data points mostly above 1.5 mbsf (Figure 34). Using the top-most temperature value determined at each station, a clear decrease of temperature from deep (Station 81 with +0.15ºC) to shallow water (Station 91 with -1.01ºC) is seen. Temperatures determined below seafloor at all stations (including the deepest Station 81) are below 0ºC, typical for the shelf-environment in this study region. No geothermal gradients were determined at these sites.

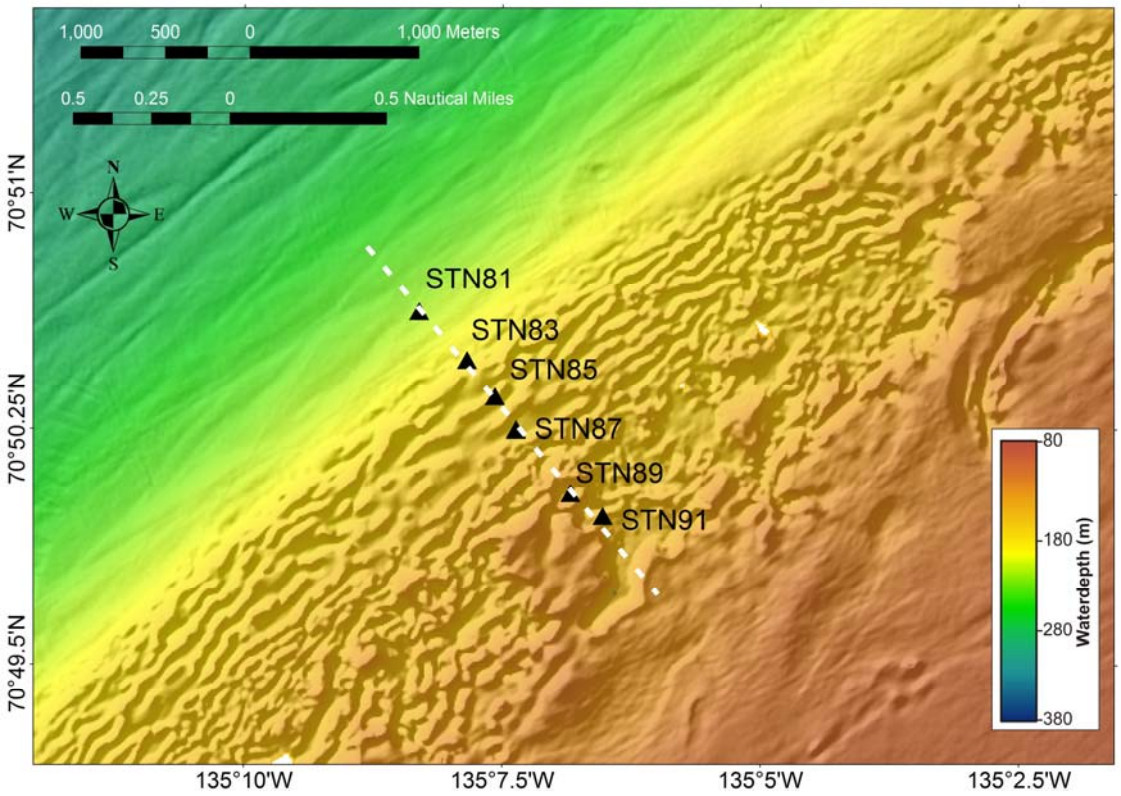

Figure 32. Map showing location of Stations 81, 83, 85, 87, 89, and 91 along the central shelf transect. The white dashed line represents the seismic transect of AUV CHIRP data (line 0027 of AUV Dive-3) shown in Figure 33. A depth section across this profile is also shown in Figure 35.

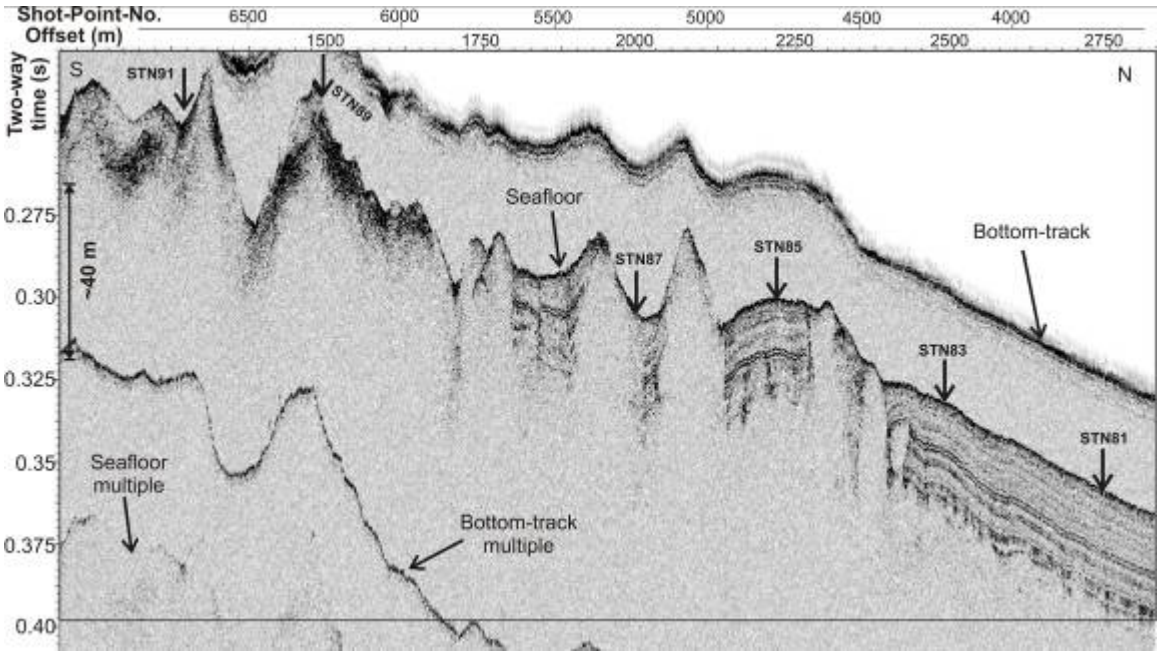

Figure 33. Seismic section of AUV 3.5 kHz CHIRP data (shown is envelop of recorded amplitude) of line 0027 from AUV Dive-3 across the central shelf transect. The actual stations location matches that of the line so that no projection is required.

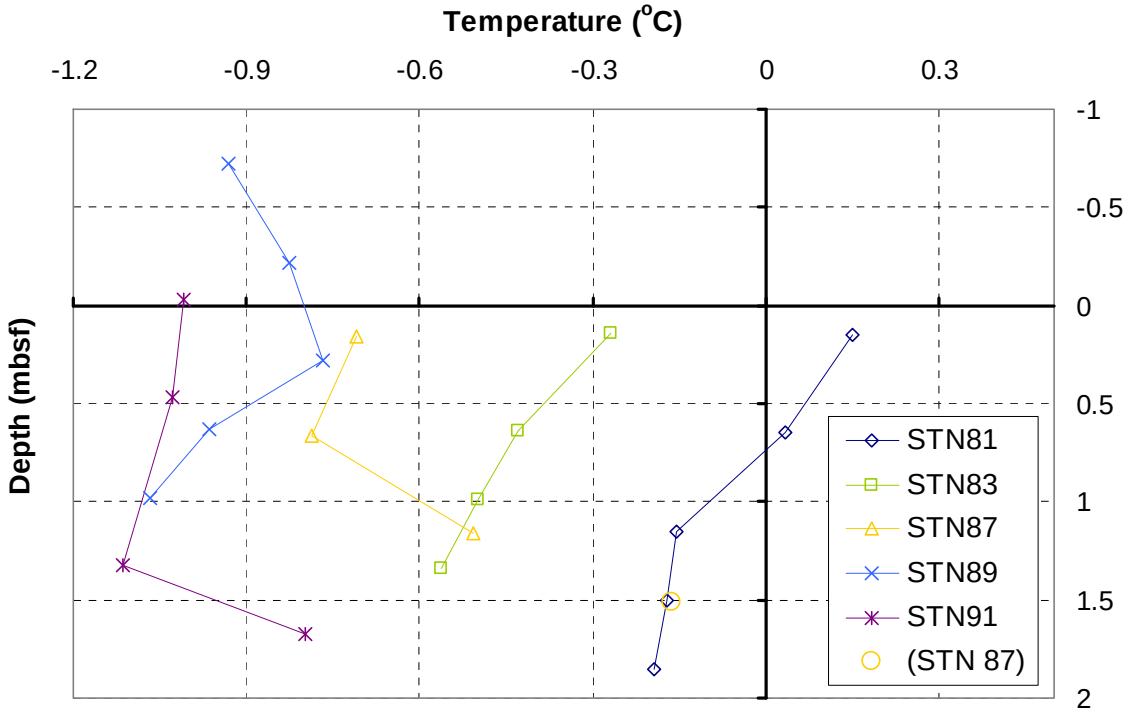

Figure 34. Down-core temperature profiles for the central shelf transect (compare to map in Figure 32). Negative depth values were assigned, where water temperature was measured.

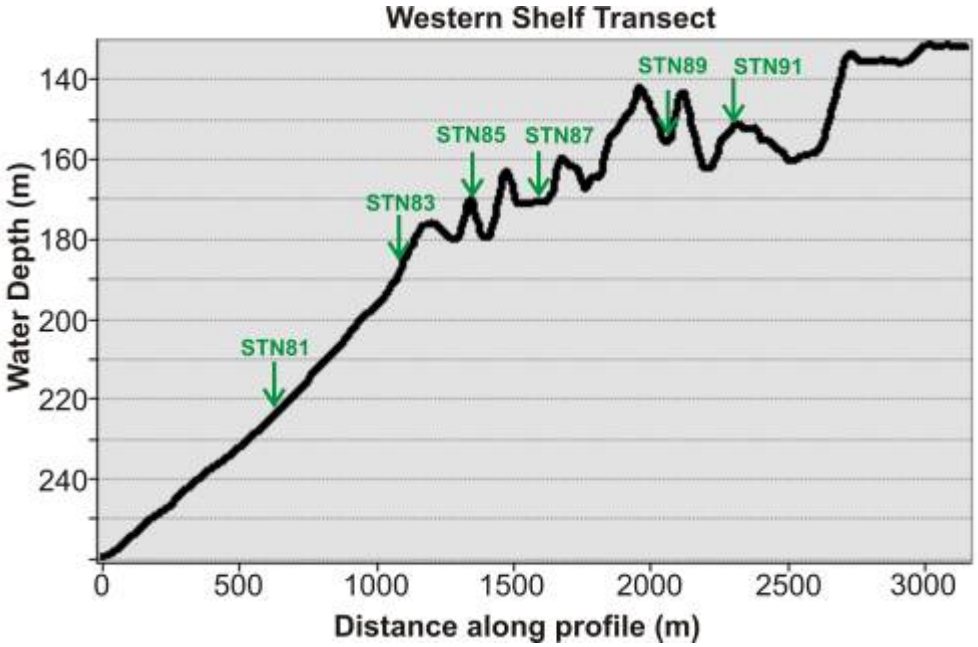

Figure 35. Depth profile along the central shelf transect. Each core station with temperature measurements is shown by a green arrow.

3.9 Gary Knolls (Stations 119, 121, 123, 125, 127, 129)

The last set of temperature measurements were made in the region known as Gary Knolls. The seafloor is marked with small, isolated PLFs (Figure 36). Some of these features extending several meter to 10's of meter above the seafloor develop moats, which are filled with striated sediments. No seismic record exists along the actual transect of measurements taken. Instead we show a typical section of 3.5 kHz CHIRP data across the Gary Knolls area (Figure 37) from the Araon expedition ARA04C (Jin et al., 2013). Temperature values obtained from all stations are below -1.25ºC (Figure 38), typical for a shelf-setting like the Gary Knolls area. No consistent temperature-depth trend is seen in the data and no thermal gradients were determined.

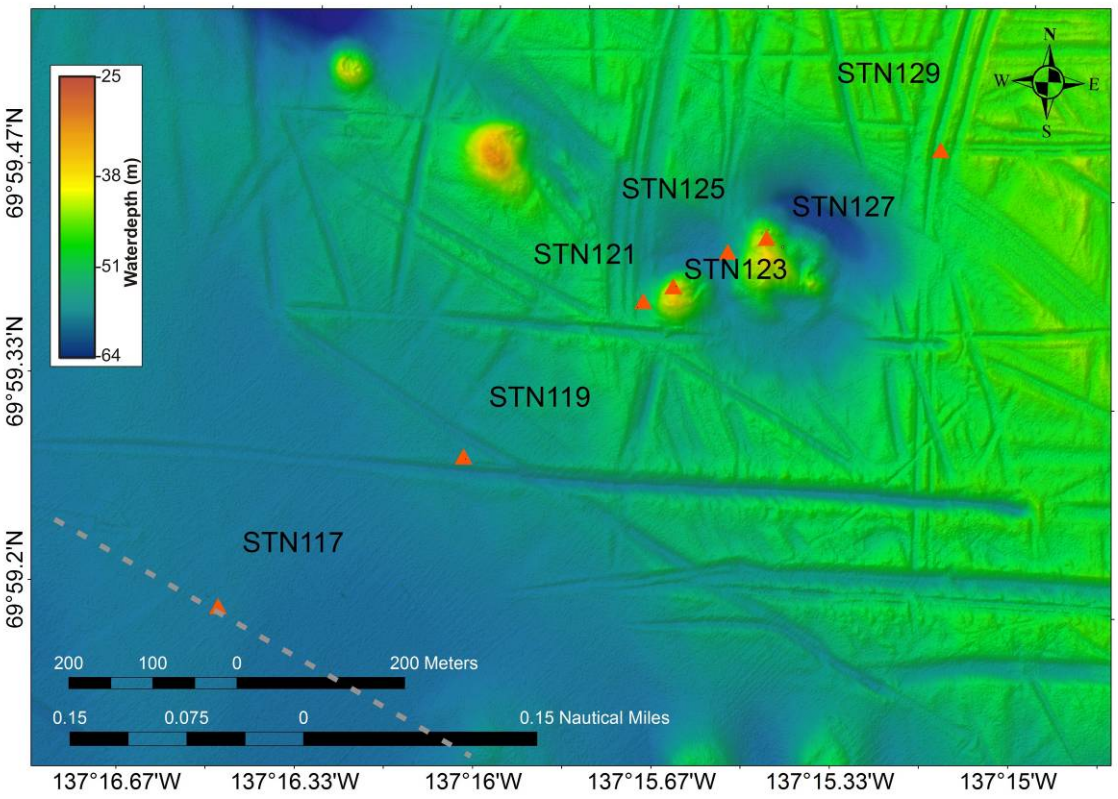

Figure 36. Map showing location of Stations 119, 121, 123, 125, 127, and 129 along the transect at the Gary Knolls area. A typical seismic section across the Gary Knolls is shown in Figure 37 from the ARA04C expedition in 2013 (Jin et al., 2013).

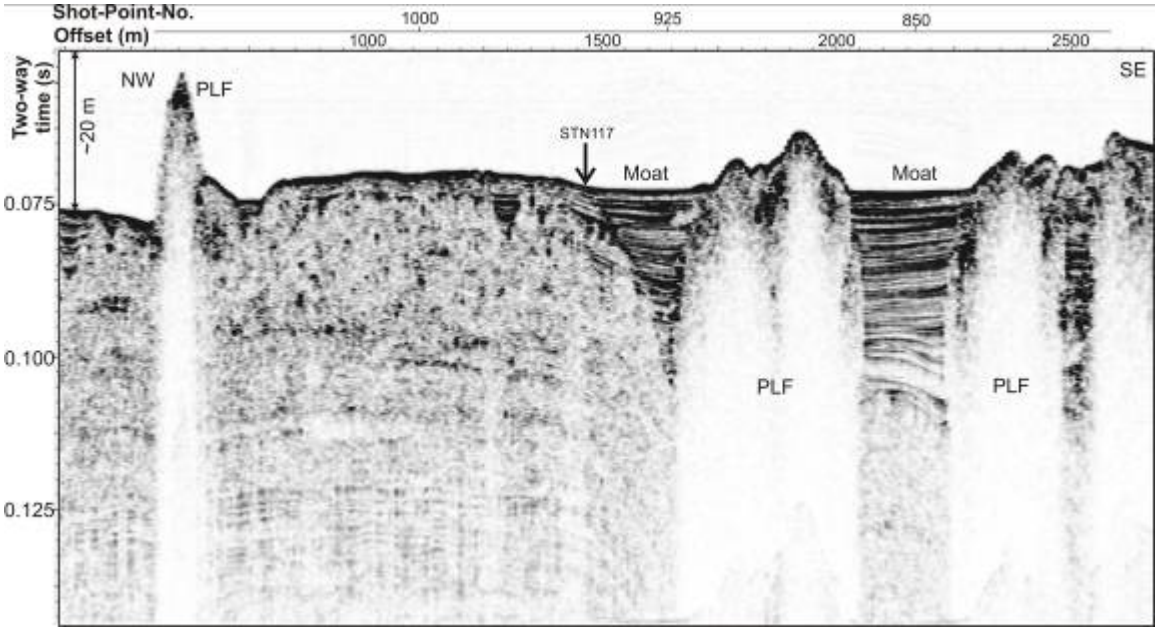

Figure 37. Typical seismic section of 3.5 kHz sub-bottom profiler data (shown is envelop of recorded amplitude) of line ARA04C across the Gary Knolls region crossing Station 117. The PLF structures show a shadow of low seismic reflectivity, likely from the ice-content inside the PLF. Moats developing around individual PLF structures are filled with laminated sediments.

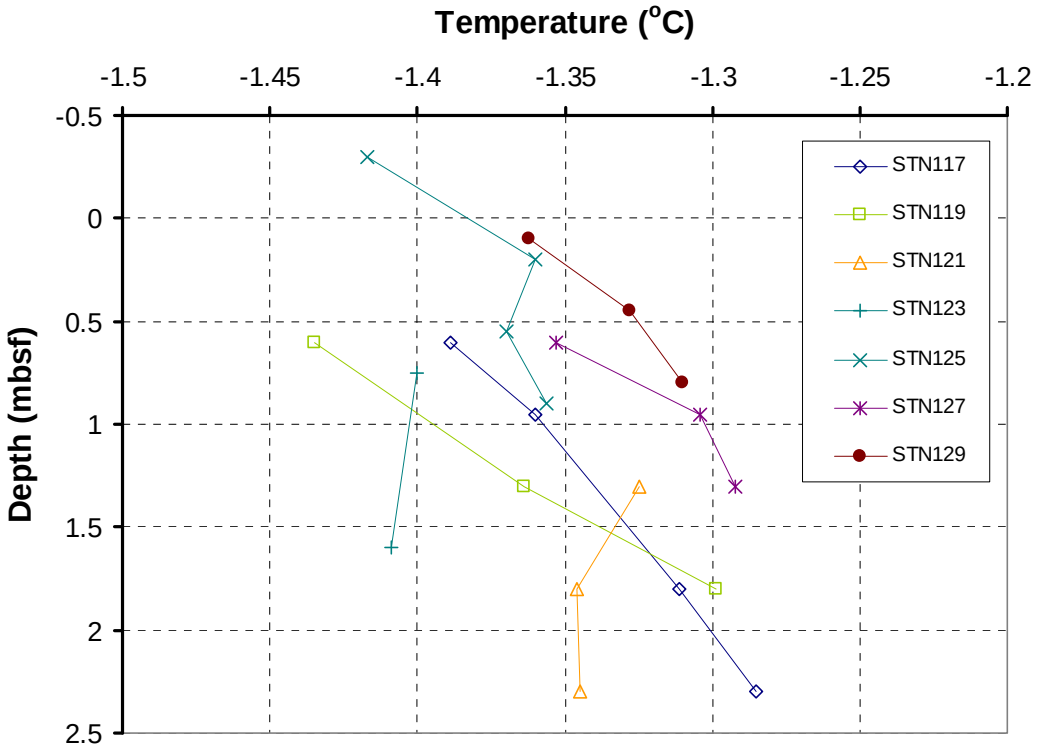

Figure 38. Down-core temperature profiles for the Gary Knolls transect. Negative depth values were assigned, where water temperature was measured.

4 Recommendations for future studies

The technique to use outriggers mounted to gravity core barrels is an efficient way to obtain simultaneous information on the temperature of the sediment. MTLs are easy and sufficiently robust to use in Arctic environments. However, exposure to temperatures below instrument capacity (-4.5 ºC) should be avoided and loggers should be inserted into the outriggers just prior to the core deployment. While the MTLs are efficient in storage (up to 18 hours), the data should be recovered after each deployment and checked for completeness of recording and overall quality to determine if a re-run of measurements at the station is required.

The greatest problem with the use of MTL in outriggers is determining the depth of penetration which can only be estimated from the apparent penetration of the gravity core. Ideally, a high resolution pressure sensor should be attached to the core barrel to monitor the penetration of the core barrel. An additional MTL mounted on the core head would have provided high resolution bottom water temperatures which are very helpful when interpreting the temperature profiles. If one mounts the outriggers equipped with MTLs on a solid lance (i.e. not a core barrel) one could make measurements in a pogo-style fashion and acquire data along profiles with smaller spacing between individual stations to obtain a better idea of local variations in the subsurface temperature field.

With less than maximum apparent penetrations (< 2.5 m), reliable geothermal gradients could not be determined at stations where loggers remained in the water-layer above the sediment. In these cases, the loggers that penetrated into the sediment are recording temperatures that are within the seasonally affected upper layer and are not suitable for calculation of geothermal gradients. However, the temperatures recorded by the loggers in the water column above the sediment provide a record of the near-seafloor temperatures, which typically are not determined with common surface-deployed CTD tools, which stop at a safe distance from bottom to avoid touching the sediment.

5 Summary and Conclusions

A total of 63 stations with temperature measurements were visited during the 2013 expedition with the *CCGS Sir Wilfrid Laurier*. Outriggers attached to the outside of the gravity core-barrel were used to mount portable miniature temperature loggers (MTL) for down-core in situ temperature measurements. The main research area is at the central Beaufort Sea slope and shelf transition area, where high-resolution multibeam data were acquired as part of the Arctic-Net project. Ten sub-regions were investigated: two shelf-slope crossings (eastern and central transect), three expulsion features (Coke-Cap, 420 m and 760 m water depth), as well as two Canyon Sites (northern, western). Two additional sites were visited slightly north of the western Canyon (Stations 94 and 95) as well as south of a landslide region. The last site visited was at the Gary Knolls, just east of the Mackenzie Trough, at water depths of less than 100 m.

Overall, temperature data obtained from the loggers at most stations were of high quality and the data acquisition technique is robust and easy to adapt in the Arctic. However, depth determination for each logger position remains challenging as no additional pressure sensor was used. Instead depths were estimated based on the apparent core penetration. The most significant results are the very large geothermal gradients associated with the two expulsion features (EF), Coke Cap and the 420 m water depth mud volcano. Temperatures measured within the top 2.5 mbsf suggest geothermal gradients of up to 2.94ºC/m (Station 96, 420 m EF) and 1.37 ºC/m (Station 58, Coke Cap EF). Away from the centre of these two EFs, geothermal gradients decrease to around 0.5ºC/m for Station 99 at the 420 m EF, and 0.92ºC/m at Station 21 at the Coke Cap EF. Temperature data across the slope-shelf transect (eastern and central region as well as at Gary Knolls) as well as the two transects across the Canyon head did not reveal considerable geothermal gradients, but show a water-depth dependent trend in temperature. From deep to shallow water, temperature appears to decrease until the most negative temperature values are found on the shelf itself (-1.2 to -1.4ºC).

Acknowledgments

The authors would like to thank the crew onboard CCGS Sir Wilfrid Laurier for their support and help during the expedition, as well as staff at the Pacific Geoscience Centre for numerous support in travel and shipping arrangements. We would like to thank B. Heesemann at the University of Bremen for helping in setting up the experiment and for the pre-field calibration of the MTLs. We also like to thank M. Côté for useful comments and critical review.

References

Blasco, S., Bennett, R., Brent, T., Burton, M., Campbell, P., Carr, E., Covill, R., Dallimore, S., Davies, E., Hughes-Clarke, J., Issler, D., Leonard, L., MacKillop, K., Mazzotti, S., Patton, E., Rogers, G., Shearer, J. and White, M., 2013. 2010 State of Knowledge: Beaufort Sea Seabed Geohazards Associated with Offshore Hydrocarbon Development; Geological Survey of Canada, Open File 6989, 340 p. doi:10.4095/292616

Brigham, J.K., Miller, G.H., 1983. Paleo-temperature estimates of the Alaskan Arctic Coastal Plain during the last 125,000 years, Proceedings of the 4th International Conference on Permafrost, Fairbanks, Alaska, p. 80-85.

Jin, Y.K., Riedel, M., Hong, J.K., Nam, S.I., Jung, J.Y., Ha, S.Y., Lee, J.Y., Conway, K.W., Kim, G.Y., Standen, G., Yoo, J., Kim, G., Ulmi, M., Neelands, P.J., Dallimore, S.R., 2015. Overview of field operations during a 2013 research expedition to the southern Beaufort Sea on the RV Araon, Geological Survey of Canada, Open File 7754, 180p., doi: 10.4095/295856

Melling, H., 2013. Beaufort Marine Hazards, 2013 Field Expedition Report, Sir Wilfrid Laurier, September 25 – October 16, 2013. Department of Fisheries and Ocean unpublished report, 38 pp.

Melling, H., Dallimore, S.R., Paull, C.K., 2012. Beaufort Sea cruise examines geohazards and geologic processes near the continental shelf edge, NETL Fire in the ice newsletter, Vol. 12, Issue 2, 16 – 17, available online at: http://www.netl.doe.gov/research/oil-and-gas/methane-hydrates/fire-in-the-ice (last visited April 16, 2015)

Pfender, M., and Villinger, H., 2002. Miniaturized data loggers for deep sea sediment temperature gradient measurements, Marine Geology, 186, 557 - 570.

Taylor, A. E., S. R. Dallimore, P. R. Hill, D. R. Issler, S. Blasco, and F. Wright, 2013. Numerical model of the geothermal regime on the Beaufort Shelf, arctic Canada since the Last Interglacial, Journal of Geophysical Research, Earth Surface, 118, doi:10.1002/2013JF002859.

Villinger, H., Davis, E. E., 1987. A new reduction algorithm for marine heat flow measurements, Journal of Geophysical Research, 92 (B12), 846-856.

Judge, A.S., 1982. Natural gas hydrates in Canada, *in* French, H.M., ed. Proceedings, Fourth Canadian Permafrost Conference: Ottawa, National Research Council of Canada, p. 320-328.

Smith, S.L., Judge, A.S., 1993. Gas hydrate database for Canadian Arctic and selected East Coast wells, Geological Survey of Canada, Open File Report, 2746, 120 p.

Paull, C.K., Ussler, W., Dallimore, S.R., Blasco, S.M., Lorenson, T.D., Melling, H., Medioli B.E,, Nixon, F.M., McLaughlin F.A., 2007. Origin of pingo-like features on the Beaufort Sea shelf and their possible relationship to decomposing methane gas hydrates Geophysical Research Letters, v. 34, no. 1, doi:10.1029/2006GL02797.

Paull, C. K., Dallimore, S.R., Hughes-Clarke, J., Blasco, S.M., Lundsten, E., Ussler, W. III, Graves, D., Sherman, A., Conway, K., Melling, H., Vagle, S., Collett, T.S., 2011. Proceedings of the 7th International Conference on Gas Hydrates, Edinburg, Scotland, July 2011.

Taylor, A.E., Dallimore, S.R., Outcalt, S.I., 1996. Late Quaternary history of the Mackenzie-Beaufort region, Arctic Canada, from modelling of permafrost temperatures. 1. The onshore-offshore transition. Canadian Journal of Earth Sciences, v. 33, p. 52-61.

Taylor, A.E., Dallimore, S.R., Hill, P.R., Issler, D.R., Blasco, S., Wright F., 2013. Numerical model of the geothermal regime on the Beaufort Shelf, Arctic Canada since the Last Interglacial, Journal of Geophysical Research, Earth Surface, Vol. 118(4), 2365-2379.

Table 1

Information on all Stations visited, number of MTL loggers used, apparent penetration, core recovery, and geometry of MTLs used.

Station No.	Gravity Core No.	Sub-region	No. of loggers	Time in sediment (min)	Apparent penetration (m)	Core recovery (m)	Logger spacing (cm) (top to bottom)	Logger ID (top to bottom)
3	1	East shelf	3	7	2.5	1.6	50-60-50-20	190-159-203-194
5	2	East shelf	3	7	2.5	1.74	50-60-50-20	190-159-203-194
7	3	East shelf	3	7	2	1.6	50-60-50-20	190-159-203-194
9	4	East shelf	3	7	1	0.3	50-60-50-20	190-159-203-194
11	5	East shelf	3	7	1	0.6	50-60-50-20	190-159-203-194
13	6	East shelf	3	7	1.5	0.28	50-60-50-20	190-159-203-194
17	7	Coke cap	1	7.5	2.5	1.72	50-50-50-20	194-203-157-159
19	8	Coke cap	1	7	2.5	1.73	50-50-50-20	194-203-157-159
21	9	Coke cap	1	7.25	1.7	1.3	50-50-50-20	194-203-157-159
23	10	Coke cap	1	7.3	2.5	0.3	50-50-50-20	194-203-157-159
25	11	Coke cap	1	7.5	2.5	0.75	50-50-50-20	194-203-157-159
27	12	Coke cap	1	7.25	2.5	1.45	50-50-50-20	194-203-157-159
31	13	Canyon West	3	8	2.5	1.55	50-50-50-20	344-216-194-261
32	14	Canyon West	3	6.5	1.7	1.54	50-50-50-20	344-216-194-261
33	15	Canyon West	3	9	1.65	1.34	50-50-50-20	344-216-194-261
34	16	Canyon West	4	8.5	2	1.86	50-50-50-20	493-406-346-407
35	17	Canyon West	4	8.5	2.5	1.94	50-50-50-20	493-406-346-407
41	washed	420 MV	5	7	2.2	0	50-50-25-25-20	407-494-493-495-406
43	washed	420 MV	4	7.55	2.55	0	50-50-25-25-20	203-261-159-376-344
45	washed	420 MV	5	7.7	2.43	0	50-50-25-25-20	407-494-493-495-406
47	washed	420 MV	5	7.15	2.5	0	50-50-25-25-20	203-261-159-376-344
49	washed	420 MV	5	8.1	2.13	0	50-50-25-25-20	406-407-494-495-493
51	washed	420 MV	5	7.15	2.45	0	50-50-25-25-20	157-203-376-261-159
56	washed	Coke cap	5	7.6	3.1	0	50-50-35-35-20	346-190-261-493-157
58	washed	Coke cap	5	7.5	2.69	0	50-50-35-35-20	406-407-376-494-216
60	washed	Coke cap	4	9.5	2.8	0	50-50-35-35-20	346-190-261-493-157

Station No.	Gravity Core No.	Sub-region	No. of loggers	Time in sediment (min)	Apparent penetration (m)	Core recovery (m)	Logger spacing (cm) (top to bottom)	Logger ID (top to bottom)
62	washed	Coke cap	5	7.9	2.13	0	50-50-35-35-20	406-407-376-494-216
64	washed	Coke cap	4	8.3	2.4	0	50-50-35-35-20	346-190-261-493-157
67	18	Canyon North	5	8.15	2.3	1.43	50-50-35-35-20	407-376-494-216-346
68	19	Canyon North	5	7.7	2.4	1.6	50-50-35-35-20	194-493-406-203-159
69	20	Canyon North	4	7.3	2.15	1.15	50-50-35-35-20	407-376-494-216-346
70	21	Canyon North	5	7.5	2.25	1.05	50-50-35-35-20	194-493-406-203-159
71	22	Canyon North	4	7.5	1.9	0.92	50-50-35-35-20	407-376-494-216-495
75	23	760 MV	4	7.75	2.26	1.22	50-50-35-35-20	190-494-407-495-261
76	24	760 MV	4	9.15	2.07	1.22	50-50-35-35-20	190-494-407-495-261
77	25	760 MV	5	8.1	3.23	1.78	50-50-35-35-20	203-194-157-216-406
78	26	760 MV	5	7.6	1.25	1.04	50-50-35-35-20	406-194-203-216-157
79	27	760 MV	3	7.35	1.07	0.97	50-50-35-35-20	407-195-376-494-159
80	28	760 MV	5	6.5	1.2	0.8	50-50-35-35-20	203-157-406-216-194
81	29	Central Shelf	5	8.1	2.05	1.27	50-50-35-35-20	194-406-216-203-157
83	30	Central Shelf	4	7	1.54	1.22	50-50-35-35-20	346-159-376-190-494
85	31	Central Shelf	5	6.6	1.37	n/a	50-50-35-35-20	406-157-216-194-203
87	32	Central Shelf	3	6.8	2.06	1.4	50-50-35-35-20	494-376-261-159-190
89	33	Central Shelf	5	6.7	1.18	n/a	50-50-35-35-20	216-406-194-203-157
91	34	Central Shelf	4	6.5	1.87	n/a	50-50-35-35-20	159-201-190-376-494
94	35	Canyon West	5	8.2	0.92	0.53	50-50-35-35-20	494-261-376-216-203
95	36	Canyon West	4	7.3	2.1	1.08	50-50-35-35-20	493-406-346-194-157
96	37	420 MV	5	6.9	2.75	0.56	50-50-35-35-20	261-494-216-203-376
97	38	420 MV	4	7.05	2.53	0.76	50-50-35-35-20	199-346-157-406-493
99	39	420 MV	5	7.15	2	0.91	50-50-35-35-20	216-494-376-261-203
101	40	420 MV	5	6.6	2.14	1.24	50-50-35-35-20	190-157-346-406-493
103	41	420 MV	5	6.9	1.76	0.6	50-50-35-35-20	261-376-203-216-494
105	42	420 MV	4	7.4	2.39	1	50-50-35-35-20	493-346-157-190-406
111	43	S. of landslide	3	7.15	2.05	1.2	50-50-35-35-20	216-203-261-376-194
113	44	S. of landslide	2	6.6	1.64	1.13	50-50-35-35-20	493-406-494-157-346

Station No.	Gravity Core No.	Sub-region	No. of loggers	Time in sediment (min)	Apparent penetration (m)	Core recovery (m)	Logger spacing (cm) (top to bottom)	Logger ID (top to bottom)
115	45	S. of landslide	1	6.8	1.37	0.35	50-50-35-35-20	376-199-261-293-216
117	46	Gary Knolls	4	6.7	2.2	1.6	50-50-35-35-20	376-261-159-203-157
119	47	Gary Knolls	3	7.15	1.8	1.42	50-50-35-35-20	216-190-494-406-261
121	48	Gary Knolls	3	6	1.7	0.68	50-50-35-35-20	493-159-157-203-376
123	49	Gary Knolls	2	6.7	2.15	0.3	50-50-35-35-20	190-261-494-406-216
125	50	Gary Knolls	4	6.5	1.1	0.65	50-50-35-35-20	493-376-159-203-157
127	21	Gary Knolls	3	7.5	1.5	0.28	50-50-35-35-20	190-494-216-406-261
129	52	Gary Knolls	3	7.1	1	0.54	50-50-35-35-20	493-157-376-159-203

Table 2 Detailed information on each logger and station

STN	Logger ID	T-fit required	Temperature (ºC)	Nominal Depth (mbsf)	Corrected Depth (mbsf)	Apparent penetration (mbsf)	Location
3	159	yes	0.035	0.7	1.2	2.50	East shelf
3	194	no	-0.175	1.2	2.3	2.50	East shelf
3	203	no	-0.188	2.3	1.6	2.50	East shelf
5	159	no	-1.320	0.7	1.2	2.50	East shelf
5	194	no	-1.300	1.2	2.3	2.50	East shelf
5	203	no	-1.290	2.3	1.6	2.50	East shelf
7	159	no	-1.358	0.7	1.2	2.00	East shelf
7	194	no	-1.332	1.2	2.3	2.00	East shelf
7	203	no	-1.325	2.3	1.6	2.00	East shelf
9	159	no	-1.406	0.7	1.2	1.00	East shelf
9	194	no	-1.380	1.2	2.3	1.00	East shelf
9	203	no	-1.404	2.3	1.6	1.00	East shelf
11	159	no	-1.400	0.7	1.2	1.00	East shelf
11	194	no	-1.401	1.2	2.3	1.00	East shelf
11	203	no	-1.413	2.3	1.6	1.00	East shelf
13	159	no	-1.399	0.7	1.2	1.50	East shelf
13	194	no	-1.382	1.2	2.3	1.50	East shelf
13	203	no	-1.387	2.3	1.6	1.50	East shelf
17	194	no	0.388	0.8	0.8	2.50	Coke-Cap
19	194	no	0.402	0.8	0.8	2.50	Coke-Cap
21	194	no	0.449	0.8	0	1.70	Coke-Cap
23	194	yes	1.496	0.8	0.8	2.50	Coke-Cap
25	194	yes	3.242	0.8	0.8	2.50	Coke-Cap
27	194	no	0.460	0.8	0.8	2.50	Coke-Cap

Table 2 continued

STN	Logger ID	T-fit required	Temperature (ºC)	Nominal Depth (mbsf)	Corrected Depth (mbsf)	Apparent penetration (mbsf)	Location
31	344	no	0.252	0.8	0.8	2.50	Canyon-West
31	216	no	0.254	1.3	1.3	2.50	Canyon-West
31	261	no	0.363	2.3	2.3	2.50	Canyon-West
32	344	no	0.255	0.8	0	1.70	Canyon-West
32	216	no	0.252	1.3	0.5	1.70	Canyon-West
32	261	no	0.371	2.3	1.5	1.70	Canyon-West
33	344	no	0.277	0.8	-0.05	1.65	Canyon-West
33	216	no	0.244	1.3	0.45	1.65	Canyon-West
33	261	no	0.322	2.3	1.45	1.65	Canyon-West
34	493	no	0.336	0.8	0.3	2.00	Canyon-West
34	406	no	0.367	1.3	0.8	2.00	Canyon-West
34	346	no	0.371	1.8	1.3	2.00	Canyon-West
34	407	no	0.399	2.3	1.8	2.00	Canyon-West
35	493	no	0.355	0.8	0.8	2.50	Canyon-West
35	406	no	0.384	1.3	1.3	2.50	Canyon-West
35	346	no	0.386	1.8	1.8	2.50	Canyon-West
35	407	no	0.409	2.3	2.3	2.50	Canyon-West
41	407	no	0.386	0.8	0.5	2.20	420 MV
41	494	no	0.395	1.3	1	2.20	420 MV
41	493	no	0.471	1.8	1.5	2.20	420 MV
41	495	no	0.476	2.05	1.75	2.20	420 MV
41	406	no	0.497	2.3	2	2.20	420 MV
43	261	yes	1.822	0.8	1.35	2.55	420 MV
43	159	yes	2.335	1.3	1.85	2.55	420 MV
43	376	yes	2.554	1.8	2.1	2.55	420 MV
43	344	yes	2.863	2.05	2.35	2.55	420 MV

Table 2 continued

STN	Logger ID	T-fit required	Temperature (ºC)	Nominal Depth (mbsf)	Corrected Depth (mbsf)	Apparent penetration (mbsf)	Location
45	407	yes	1.355	0.8	0.73	2.43	420 MV
45	494	yes	2.626	1.3	1.23	2.43	420 MV
45	493	yes	3.627	1.8	1.73	2.43	420 MV
45	495	yes	4.158	2.05	1.98	2.43	420 MV
45	406	yes	4.764	2.3	2.23	2.43	420 MV
47	203	yes	1.006	1.3	0.8	2.50	420 MV
47	261	yes	1.753	1.8	1.3	2.50	420 MV
47	159	yes	2.321	2.05	1.8	2.50	420 MV
47	376	yes	2.597	2.3	2.05	2.50	420 MV
49	406	no	0.442	0.8	0.43	2.13	420 MV
49	407	no	0.439	1.3	0.93	2.13	420 MV
49	494	no	0.448	1.8	1.43	2.13	420 MV
49	495	no	0.503	2.05	1.68	2.13	420 MV
49	493	no	0.522	2.3	1.93	2.13	420 MV
51	157	no	0.478	0.8	0.75	2.45	420 MV
51	203	no	0.488	1.3	1.25	2.45	420 MV
51	376	no	0.482	1.8	1.75	2.45	420 MV
51	261	no	0.507	2.05	2	2.45	420 MV
51	159	no	0.523	2.3	2.25	2.45	420 MV
56	346	frozen	n/a	n/a	1.2	3.10	Coke-Cap
56	190	T-jump	(3.203)	n/a	1.7	3.10	Coke-Cap
56	261	frozen	n/a	n/a	2.2	3.10	Coke-Cap
56	493	yes	5.720	2.05	2.55	3.10	Coke-Cap
56	157	yes	6.099	2.3	2.9	3.10	Coke-Cap

Table 2 continued

STN	Logger ID	T-fit required	Temperature (ºC)	Nominal Depth (mbsf)	Corrected Depth (mbsf)	Apparent penetration (mbsf)	Location
58	406	yes	2.880	0.8	0.79	2.69	Coke-Cap
58	407	yes	3.479	1.3	1.29	2.69	Coke-Cap
58	376	yes	4.135	1.8	1.79	2.69	Coke-Cap
58	494	yes	4.568	2.05	2.14	2.69	Coke-Cap
58	216	yes	4.933	2.3	2.49	2.69	Coke-Cap
60	346	yes	1.412	0.8	0.9	2.80	Coke-Cap
60	261	yes	2.211	1.8	1.9	2.80	Coke-Cap
60	493	yes	2.542	2.05	2.25	2.80	Coke-Cap
60	157	yes	2.8235	2.3	2.6	2.80	Coke-Cap
62	406	no	0.479	0.6	0.23	2.13	Coke-Cap
62	407	no	0.397	1.1	0.73	2.13	Coke-Cap
62	376	no	0.348	1.6	1.23	2.13	Coke-Cap
62	494	no	0.339	1.95	1.58	2.13	Coke-Cap
62	216	no	0.324	2.3	1.93	2.13	Coke-Cap
64	190	no	0.325	1.1	1	2.40	Coke-Cap
64	261	no	0.301	1.6	1.5	2.40	Coke-Cap
64	493	no	0.320	1.95	1.85	2.40	Coke-Cap
64	157	no	0.316	2.3	2.2	2.40	Coke-Cap
67	407	no	0.088	0.6	0.4	2.30	Canyon-North
67	376	no	0.091	1.1	0.9	2.30	Canyon-North
67	494	no	0.121	1.6	1.4	2.30	Canyon-North
67	216	no	0.129	1.95	1.75	2.30	Canyon-North
67	346	no	0.177	2.3	2.1	2.30	Canyon-North
68	194	no	0.100	0.6	0.5	2.40	Canyon-North
68	493	no	0.136	1.1	1	2.40	Canyon-North

Table 2 continued

STN	Logger ID	T-fit required	Temperature (ºC)	Nominal Depth (mbsf)	Corrected Depth (mbsf)	Apparent penetration (mbsf)	Location
68	406	no	0.168	1.6	1.5	2.40	Canyon-North
68	203	no	0.164	1.95	1.85	2.40	Canyon-North
68	159	no	0.179	2.3	2.2	2.40	Canyon-North
69	407	no	n/a	0.6	0.25	2.15	Canyon-North
69	376	no	0.077	1.1	0.75	2.15	Canyon-North
69	494	no	0.105	1.6	1.25	2.15	Canyon-North
69	216	no	0.111	1.95	1.6	2.15	Canyon-North
69	346	n/a	n/a		1.95	2.15	Canyon-North
70	194	no	0.072	0.6	0.35	2.25	Canyon-North
70	493	no	0.110	1.1	0.85	2.25	Canyon-North
70	406	no	0.141	1.6	1.35	2.25	Canyon-North
70	203	no	0.136	1.95	1.7	2.25	Canyon-North
70	159	no	0.148	2.3	2.05	2.25	Canyon-North
71	407	n/a	n/a	0.6	0	1.90	Canyon-North
71	376	no	0.039	1.1	0.5	1.90	Canyon-North
71	494	no	0.067	1.6	1	1.90	Canyon-North
71	216	no	0.069	1.95	1.35	1.90	Canyon-North
71	495	no	0.141	2.3	1.7	1.90	Canyon-North
75	190	no	n/a	0.6	0.36	2.26	760 MV
75	494	no	0.104	1.1	0.86	2.26	760 MV
75	407	no	0.162	1.6	1.36	2.26	760 MV
75	495	no	0.204	1.95	1.71	2.26	760 MV
75	261	no	0.205	2.3	2.06	2.26	760 MV
76	190	n/a	n/a	0.6	0.17	2.07	760 MV
76	494	no	0.114	1.1	0.67	2.07	760 MV

Table 2 continued

STN	Logger ID	T-fit required	Temperature (ºC)	Nominal Depth (mbsf)	Corrected Depth (mbsf)	Apparent penetration (mbsf)	Location
76	407	no	0.177	1.6	1.17	2.07	760 MV
76	495	no	0.221	1.95	1.52	2.07	760 MV
76	261	T-jump	(-0.031)	2.3	1.87	2.07	760 MV
77	203	no	0.114	1.95	1.33	3.23	760 MV
77	194	no	0.160	1.1	1.83	3.23	760 MV
77	157	no	0.200	1.6	2.33	3.23	760 MV
77	216	no	0.114	0.6	2.68	3.23	760 MV
77	406	no	0.247	2.3	3.03	3.23	760 MV
78	406	yes	0.120	0.6	-0.65	1.25	760 MV
78	194	yes	0.112	1.1	-0.15	1.25	760 MV
78	203	yes	0.174	1.6	0.35	1.25	760 MV
78	216	yes	0.182	1.95	0.7	1.25	760 MV
78	157	yes	0.289	2.3	1.05	1.25	760 MV
79	407	n/a	no data	0.6	-0.83	1.07	760 MV
79	195	n/a	no data	1.1	-0.33	1.07	760 MV
79	376	no	0.149	1.6	0.17	1.07	760 MV
79	494	no	0.200	1.95	0.52	1.07	760 MV
79	159	T-jump	(0.523)	2.3	0.87	1.07	760 MV
80	203	no	0.003	0.6	-0.7	1.20	760 MV
80	157	no	0.091	1.95	-0.2	1.20	760 MV
80	406	no	0.025	1.1	0.3	1.20	760 MV
80	216	no	0.053	1.6	0.65	1.20	760 MV
80	194	no	0.134	2.3	1	1.20	760 MV
81	194	no	0.150	0.6	0.15	2.05	Central Shelf
81	406	no	0.034	0.95	0.65	2.05	Central Shelf

Table 2 continued

STN	Logger ID	T-fit required	Temperature (ºC)	Nominal Depth (mbsf)	Corrected Depth (mbsf)	Apparent penetration (mbsf)	Location
81	216	no	-0.154	1.3	1.15	2.05	Central Shelf
81	203	no	-0.171	1.8	1.5	2.05	Central Shelf
81	157	no	-0.192	2.3	1.85	2.05	Central Shelf
83	159	no	-0.268	0.95	0.14	1.54	Central Shelf
83	376	no	-0.428	1.3	0.64	1.54	Central Shelf
83	190	no	-0.497	1.8	0.99	1.54	Central Shelf
83	494	no	-0.563	2.3	1.34	1.54	Central Shelf
85	406	no	-0.929	0.6	-0.53	1.37	Central Shelf
85	157	no	-0.785	0.95	-0.03	1.37	Central Shelf
85	216	no	-1.070	1.3	0.47	1.37	Central Shelf
85	194	yes	-0.863	1.8	0.82	1.37	Central Shelf
85	203	yes	-0.658	2.3	1.17	1.37	Central Shelf
87	494	no	-0.709	1.3	0.16	2.06	Central Shelf
87	376	no	-0.786	1.8	0.66	2.06	Central Shelf
87	261	no	-0.506	2.3	1.16	2.06	Central Shelf
89	216	no	-0.931	0.6	-0.72	1.18	Central Shelf
89	406	no	-0.826	0.95	-0.22	1.18	Central Shelf
89	194	no	-0.766	1.3	0.28	1.18	Central Shelf
89	203	yes	-0.965	1.8	0.63	1.18	Central Shelf
89	157	yes	-1.068	2.3	0.98	1.18	Central Shelf
91	159	no	-1.010	0.6	-0.03	1.87	Central Shelf
91	261	no	-1.027	0.95	0.47	1.87	Central Shelf
91	376	no	-1.115	1.8	1.32	1.87	Central Shelf

Table 2 continued

STN	Logger ID	T-fit required	Temperature (ºC)	Nominal Depth (mbsf)	Corrected Depth (mbsf)	Apparent penetration (mbsf)	Location
91	494	no	-0.798	2.3	1.67	1.87	Central Shelf
94	494	no	-0.100	0.6	-0.98	0.92	Canyon West
94	261	no	-0.082	0.95	-0.48	0.92	Canyon West
94	376	no	-0.088	1.3	0.02	0.92	Canyon West
94	216	no	-0.076	1.8	0.37	0.92	Canyon West
94	203	no	-0.025	2.3	0.72	0.92	Canyon West
95	493	no	0.001	0.6	0.2	2.10	Canyon West
95	406	no	0.035	0.95	0.7	2.10	Canyon West
95	194	no	0.075	1.8	1.55	2.10	Canyon West
95	157	no	0.101	2.3	1.9	2.10	Canyon West
96	261	yes	4.048	0.6	0.85	2.75	420 MV
96	494	yes	5.625	0.95	1.35	2.75	420 MV
96	216	yes	7.012	1.3	1.85	2.75	420 MV
96	203	yes	8.116	1.8	2.2	2.75	420 MV
96	376	yes	9.147	2.3	2.55	2.75	420 MV
97	346	no	1.368	0.6	1.13	2.53	420 MV
97	157	no	1.719	0.95	1.63	2.53	420 MV
97	406	no	1.954	1.3	1.98	2.53	420 MV
97	493	no	2.225	1.8	2.33	2.53	420 MV
99	216	no	0.630	0.6	0.1	2.00	420 MV
99	494	no	0.902	0.95	0.6	2.00	420 MV
99	376	no	1.169	1.3	1.1	2.00	420 MV
99	261	no	1.355	1.8	1.45	2.00	420 MV
99	203	no	1.548	2.3	1.8	2.00	420 MV

Table 2 continued

STN	Logger ID	T-fit required	Temperature (ºC)	Nominal Depth (mbsf)	Corrected Depth (mbsf)	Apparent penetration (mbsf)	Location
101	190	yes	0.905	0.6	0.24	2.14	420 MV
101	157	yes	1.483	0.95	0.74	2.14	420 MV
101	346	yes	2.032	1.3	1.24	2.14	420 MV
101	406	yes	2.384	1.8	1.59	2.14	420 MV
101	493	yes	2.764	2.3	1.94	2.14	420 MV
103	261	no	0.459	0.6	-0.14	1.76	420 MV
103	376	yes	1.266	0.95	0.36	1.76	420 MV
103	203	yes	2.077	1.3	0.86	1.76	420 MV
103	216	yes	2.487	1.8	1.21	1.76	420 MV
103	494	yes	3.107	2.3	1.56	1.76	420 MV
105	493	yes	1.508	0.6	0.49	2.39	420 MV
105	346	yes	2.479	1.3	0.99	2.39	420 MV
105	157	yes	3.462	1.8	1.49	2.39	420 MV
105	406	yes	4.817	2.3	2.19	2.39	420 MV
105	190	T-jump	4.138	1.95	1.84	2.36	420 MV
111	216	no	-1.462	1.3	0.15	2.05	South of landslide
111	203	no	-1.325	1.8	0.65	2.05	South of landslide
111	261	no	-1.330	2.3	1.15	2.05	South of landslide
113	493	no	-1.425	0.6	-0.26	1.64	South of landslide
113	406	no	-1.369	0.95	0.24	1.64	South of landslide
115	376	yes	-1.465	n/a	-0.53	1.37	South of landslide
117	376	no	-1.389	0.6	0.3	2.20	Gary Knolls
117	261	no	-1.360	0.95	0.8	2.20	Gary Knolls
117	203	no	-1.311	1.8	1.65	2.20	Gary Knolls
117	157	no	-1.285	2.3	2	2.20	Gary Knolls

Table 2 continued

STN	Logger ID	T-fit required	Temperature (ºC)	Nominal Depth (mbsf)	Corrected Depth (mbsf)	Apparent penetration (mbsf)	Location
119	216	yes	-1.435	0.6	-0.1	1.80	Gary Knolls
119	494	yes	-1.364	1.3	0.9	1.80	Gary Knolls
119	406	no	-1.299	1.8	1.25	1.80	Gary Knolls
121	157	no	-1.325	1.3	0.8	1.70	Gary Knolls
121	203	no	-1.346	1.8	1.15	1.70	Gary Knolls
121	376	yes	-1.345	2.3	1.5	1.70	Gary Knolls
123	190	no	n/a	0.6	0.25	2.15	Gary Knolls
123	261	no	-1.400	0.95	0.75	2.15	Gary Knolls
123	494	no	n/a	1.3	1.25	2.15	Gary Knolls
123	406	no	-1.409	1.8	1.6	2.15	Gary Knolls
125	376	no	-1.417	0.95	-0.3	1.10	Gary Knolls
125	159	no	-1.360	1.3	0.2	1.10	Gary Knolls
125	203	no	-1.370	1.8	0.55	1.10	Gary Knolls
125	157	no	-1.356	2.3	0.9	1.10	Gary Knolls
127	216	no	-1.353	1.3	0.6	1.50	Gary Knolls
127	406	yes	-1.304	1.8	0.95	1.50	Gary Knolls
127	261	yes	-1.292	2.3	1.3	1.50	Gary Knolls
129	376	no	-1.362	0.6	0.1	1.00	Gary Knolls
129	159	no	-1.328	0.95	0.45	1.00	Gary Knolls
129	203	no	-1.310	1.3	0.8	1.00	Gary Knolls

Appendix Detailed temperature records and regression analyses

In this appendix, all temperature data are shown from the original deployments. Time of the logger is shown in consecutive seconds, which was set and synchronized with the time of the PC used to read out the data from the MTLs at the start of each deployment site. Absolute time (local time) was also recorded, but is not shown here. In all plots, the time of the MTL deployed in the sediment is shown, together with the portion of the temperature data during lowering and retrieving of the core barrel. Absolute start time (local time) of the individual loggers may vary.

Winch speed was approximately 1 m/s, thus the temperature data recorded through the water column are equivalent to standard oceanographic casts using a conductivity/temperature/depth (CTD) tool. However, the winch speed may not have been always constant and therefore exact transformation of time to meters cannot be made.

For several stations, temperatures have not reached equilibrium by the time the core was pulled out of the sediments. Therefore a linear regression analysis was performed to estimate the in situ temperature. Temperatures for the last 100 – 120 seconds prior to pulling of the core were used in those calculations. The estimate of in situ temperature is made by plotting first the temperature data as function of inverse time (1 / t) and then attempting a linear best-fit to the data. The intercept of the best-fit linear line defines the in situ temperature. These temperature values are used in section 3 of the main report. The resolution of the MTL is 0.001ºC and in the regression analyses we found that this is insufficient for a high-resolution regression, as temperatures did not change over several seconds at a resolution of one-thousands of a degree.

A.1.1 Eastern Shelf Region, Station 3

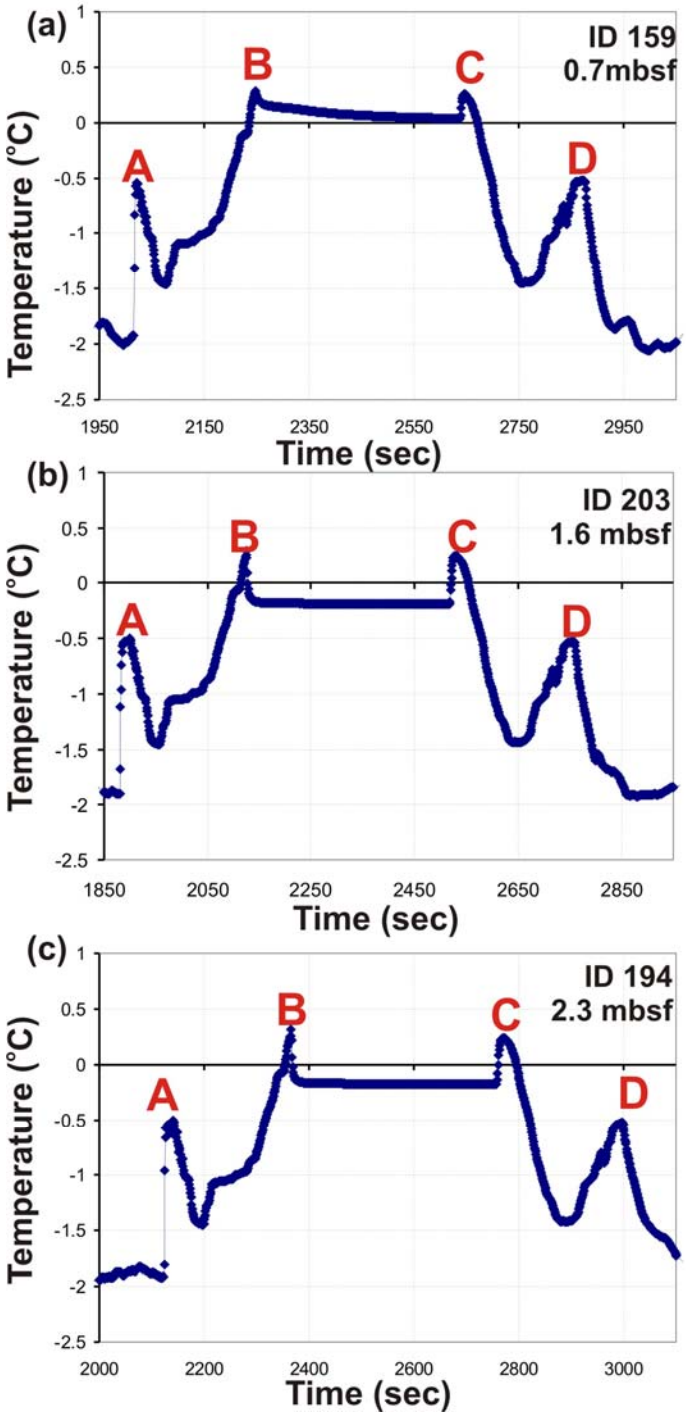

Figure A.1.1 Temperature records at Station 03 for MTL (a) ID 159 at 0.7mbsf, (b) ID 203 at 1.6 mbsf, and (c) ID 194 at 2.3 mbsf. A: Core deployed, B: frictional heating pulse from core entering the sediment, C: frictional heating pulse from core pulled out of sediment, D: core back on deck.

A.1.2 Eastern Shelf Region, Station 5

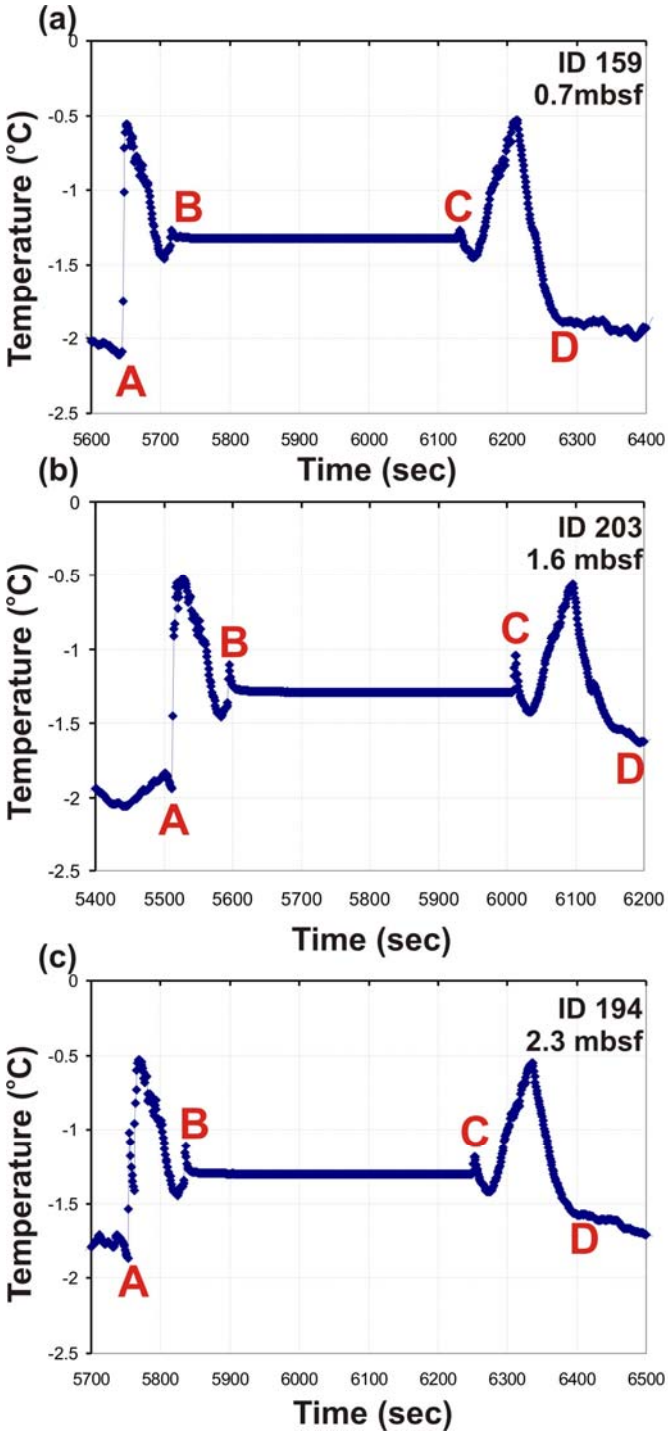

Figure A.1.2 Temperature records at Station 05 for MTL (a) ID 159 at 0.7mbsf, (b) ID 203 at 1.6 mbsf, and (c) ID 194 at 2.3 mbsf. A: Core deployed, B: frictional heating pulse from core entering the sediment, C: frictional heating pulse from core pulled out of sediment, D: core back on deck.

A.1.3 Eastern Shelf Region, Station 7

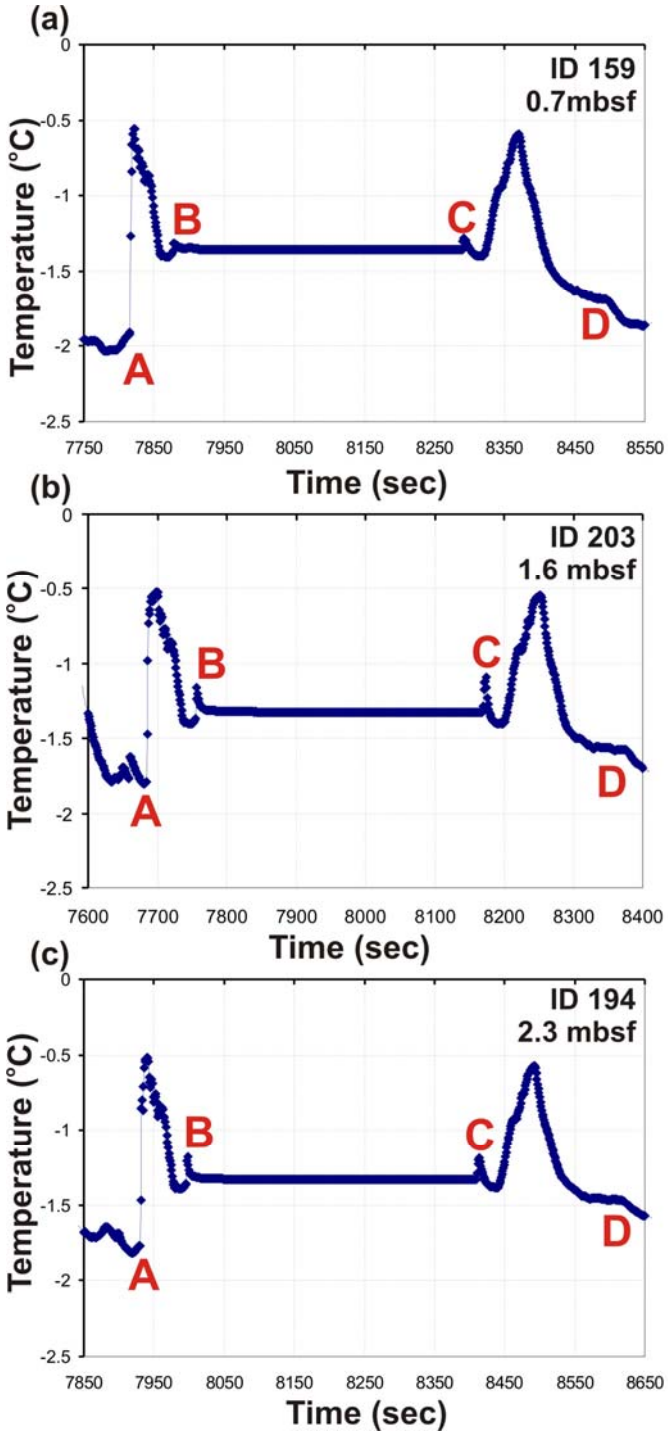

Figure A.1.3 Temperature records at Station 07 for MTL (a) ID 159 at 0.7mbsf, (b) ID 203 at 1.6 mbsf, and (c) ID 194 at 2.3 mbsf. A: Core deployed, B: frictional heating pulse from core entering the sediment, C: frictional heating pulse from core pulled out of sediment, D: core back on deck.

A.1.4 Eastern Shelf Region, Station 9

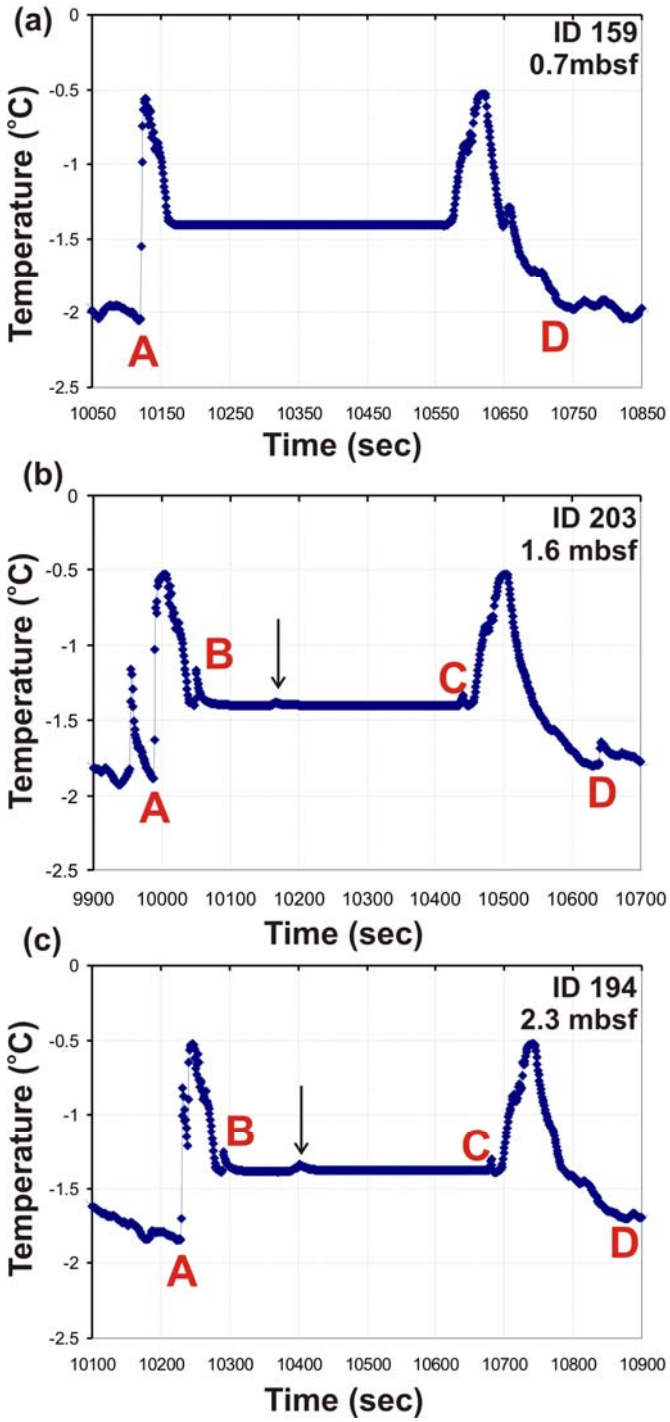

Figure A.1.4 Temperature records at Station 09 for MTL (a) ID 159 at 0.7mbsf, (b) ID 203 at 1.6 mbsf, and (c) ID 194 at 2.3 mbsf. A: Core deployed, B: frictional heating pulse from core entering the sediment, C: frictional heating pulse from core pulled out of sediment, D: core back on deck. MTL at 0.7 mbsf may not have entered sediment due to the absence of a friction heating pulse. A secondary friction pulse occurred (indicated by arrow), but did not influence the final temperature estimation.

A.1.5 Eastern Shelf Region, Station 11

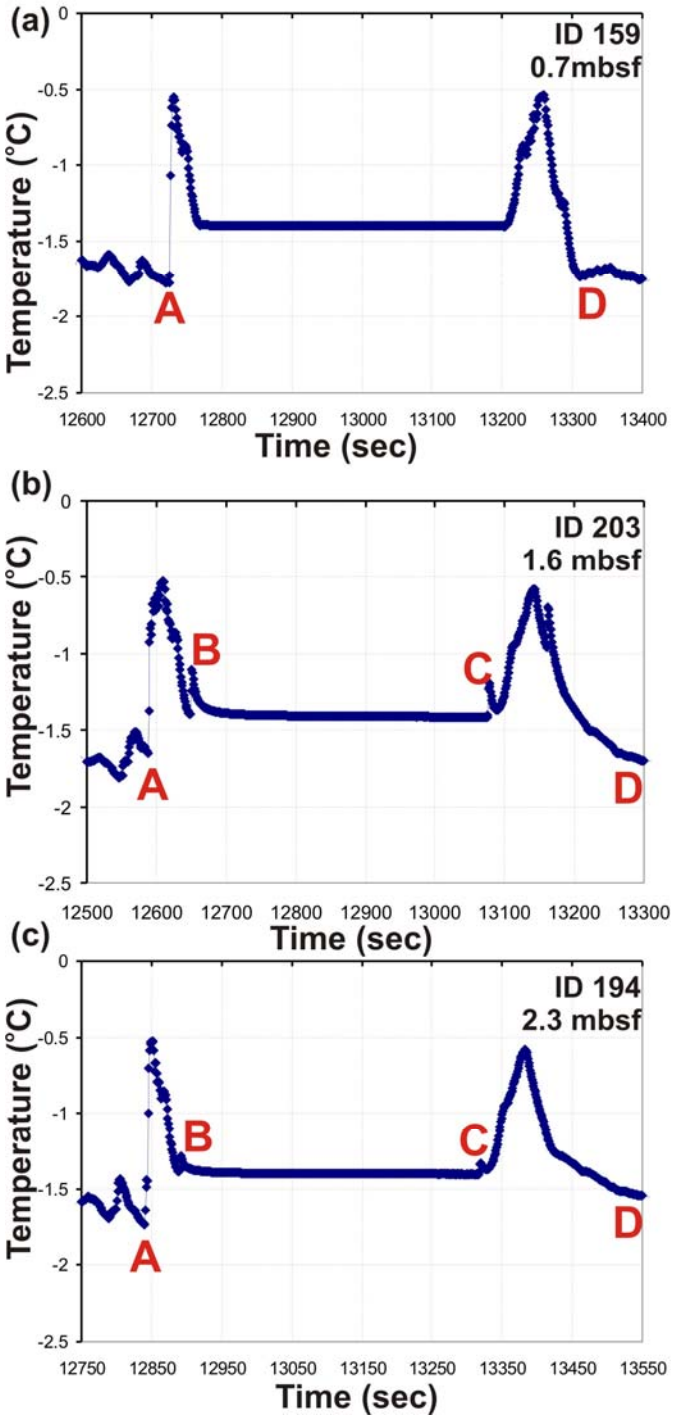

Figure A.1.5 Temperature records at Station 11 for MTL (a) ID 159 at 0.7mbsf, (b) ID 203 at 1.6 mbsf, and (c) ID 194 at 2.3 mbsf. A: Core deployed, B: frictional heating pulse from core entering the sediment, C: frictional heating pulse from core pulled out of sediment, D: core back on deck. MTL at 0.7 mbsf may not have entered sediment due to the absence of a friction heating pulse.

A.1.6 Eastern Shelf Region, Station 13

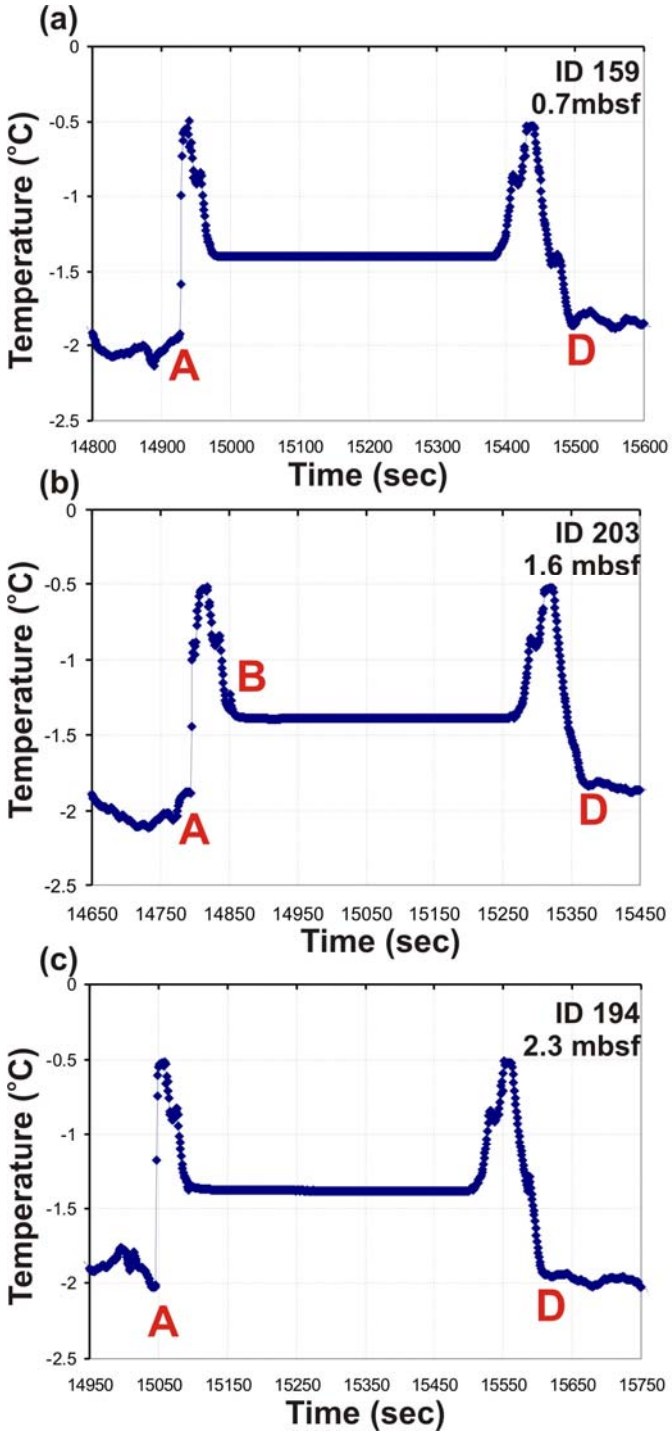

Figure A.1.6 Temperature records at Station 13 for MTL (a) ID 159 at 0.7mbsf, (b) ID 203 at 1.6 mbsf, and (c) ID 194 at 2.3 mbsf. A: Core deployed overboard, B: frictional heating pulse from core entering the sediment, C: frictional heating pulse from core pulled out of sediment, D: core back on deck. Note, that no clear frictional heating pulses are seen in any record, despite an apparent penetration of 1.5mbsf. However, core recovery was only 28cm.

A.2.1 Coke-Cap, Station 17

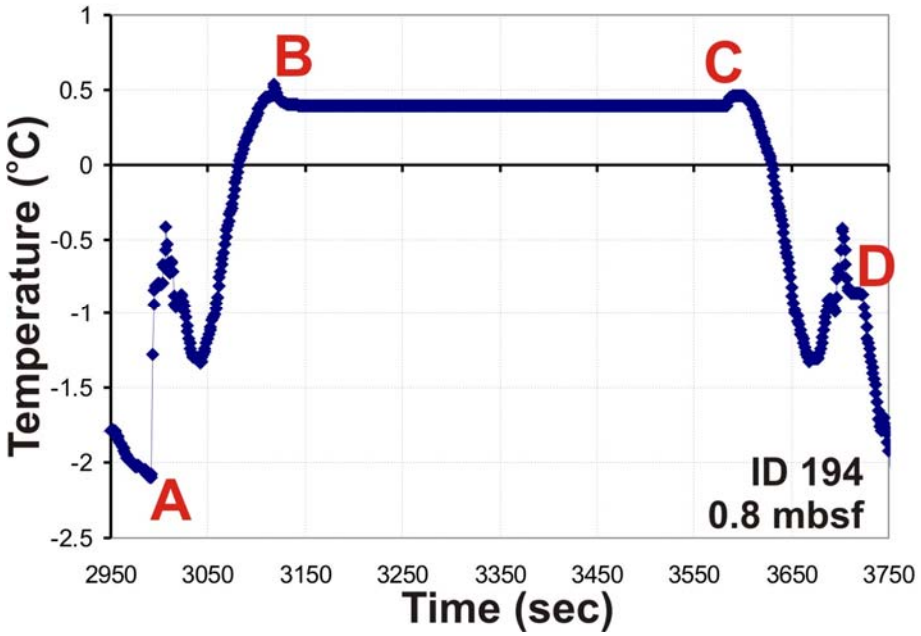

Figure A.2.1 Temperature records at Station 17 for the only MTL ID 194 at 0.8mbsf. A: Core deployed, B: frictional heating pulse from core entering the sediment, C: frictional heating pulse from core pulled out of sediment, D: core back on deck.

A.2.2 Coke-Cap, Station 19

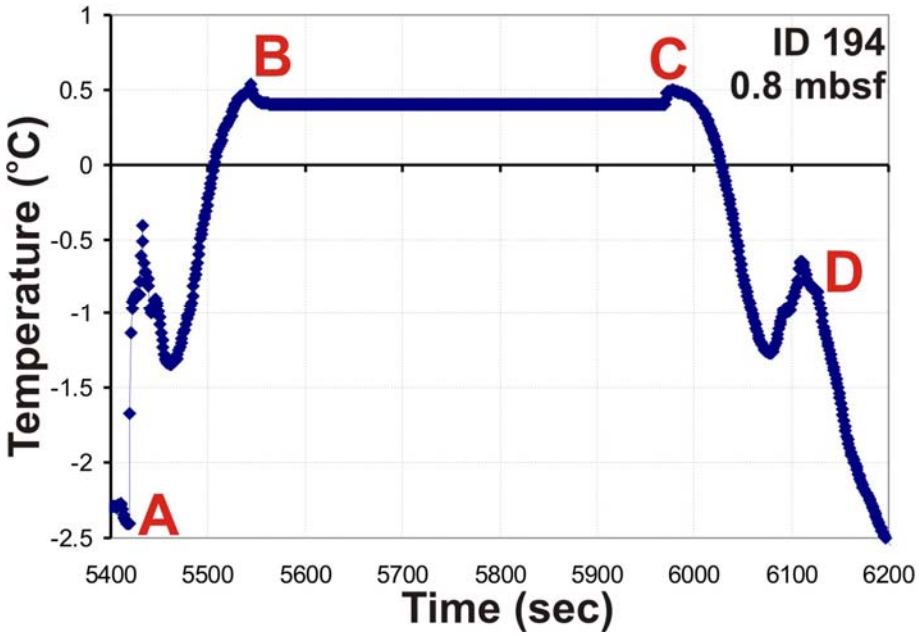

Figure A.2.2 Temperature records at Station 19 for the only MTL ID 194 at 0.8mbsf. A: Core deployed, B: frictional heating pulse from core entering the sediment, C: frictional heating pulse from core pulled out of sediment, D: core back on deck.

A.2.3 Coke-Cap, Station 21

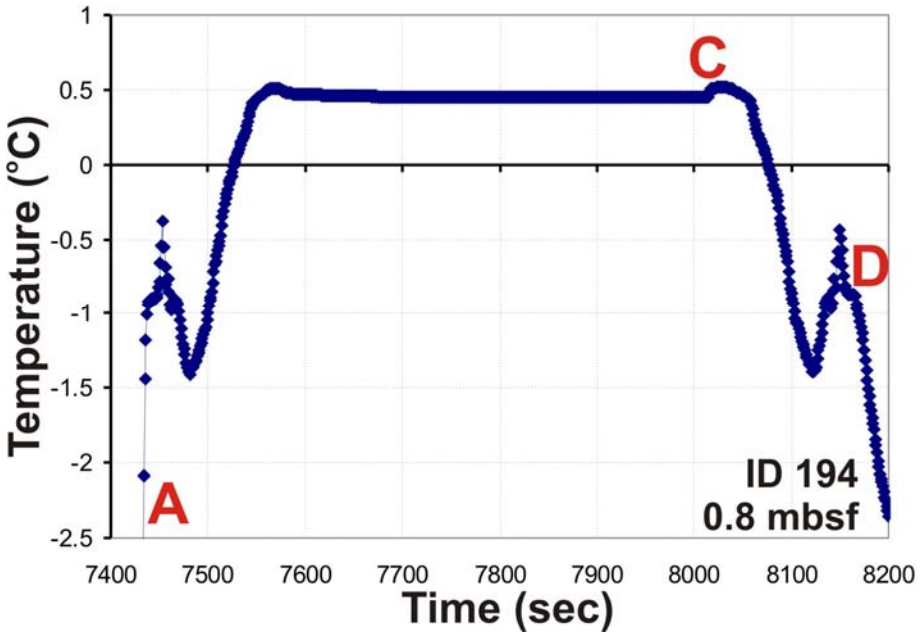

Figure A.2.3 Temperature records at Station 21 for the only MTL ID 194 at 0.8mbsf. A: Core deployed, B: frictional heating pulse from core entering the sediment, C: frictional heating pulse from core pulled out of sediment, D: core back on deck.

A.2.4 Coke-Cap, Station 23

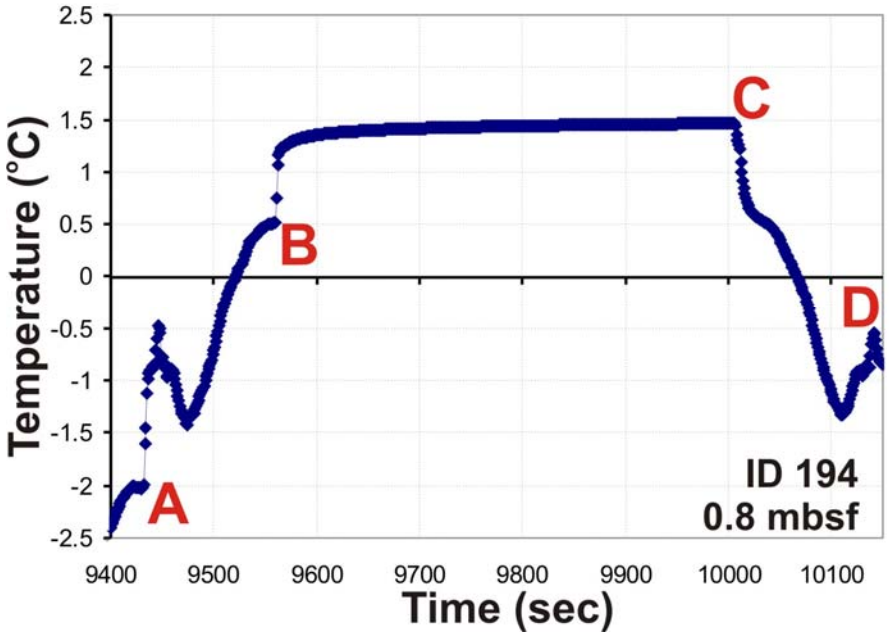

Figure A.2.4.1 Temperature records at Station 23 for the only MTL ID 194 at 0.8mbsf. A: Core deployed, B: frictional heating pulse from core entering the sediment, C: frictional heating pulse from core pulled out of sediment, D: core back on deck.

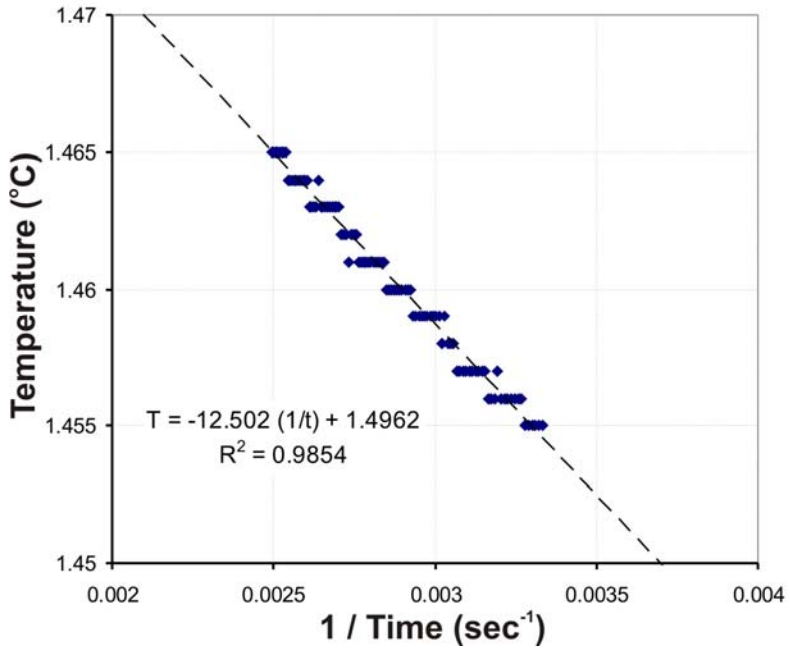

Figure A.2.4.2 Linear regression analysis to estimate equilibrium temperature at Station 23 for the last 100 seconds prior to pulling out of the core.

A.2.5 Coke-Cap, Station 25

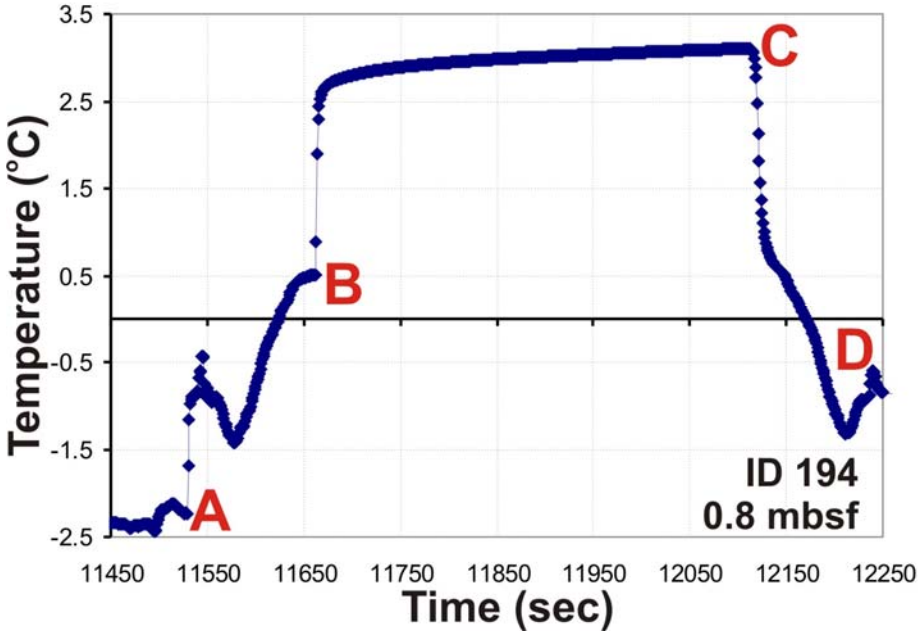

Figure A.2.5.1 Temperature records at Station 25 for the only MTL ID 194 at 0.8mbsf. A: Core deployed, B: frictional heating pulse from core entering the sediment, C: frictional heating pulse from core pulled out of sediment, D: core back on deck.

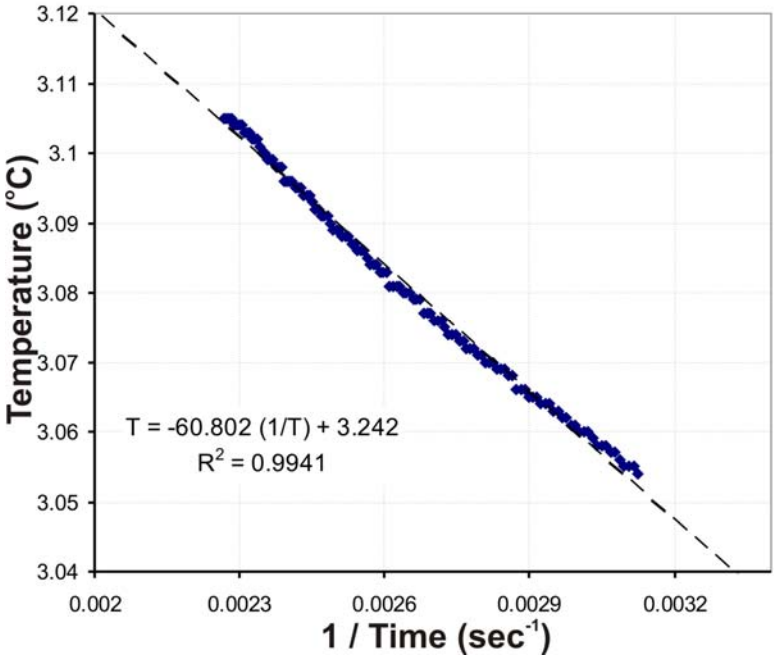

Figure A.2.5.2 Linear regression analysis to estimate equilibrium in situ temperature at Station 25 for the last 120 seconds prior to pulling out of the core.

A.2.6 Coke-Cap, Station 27

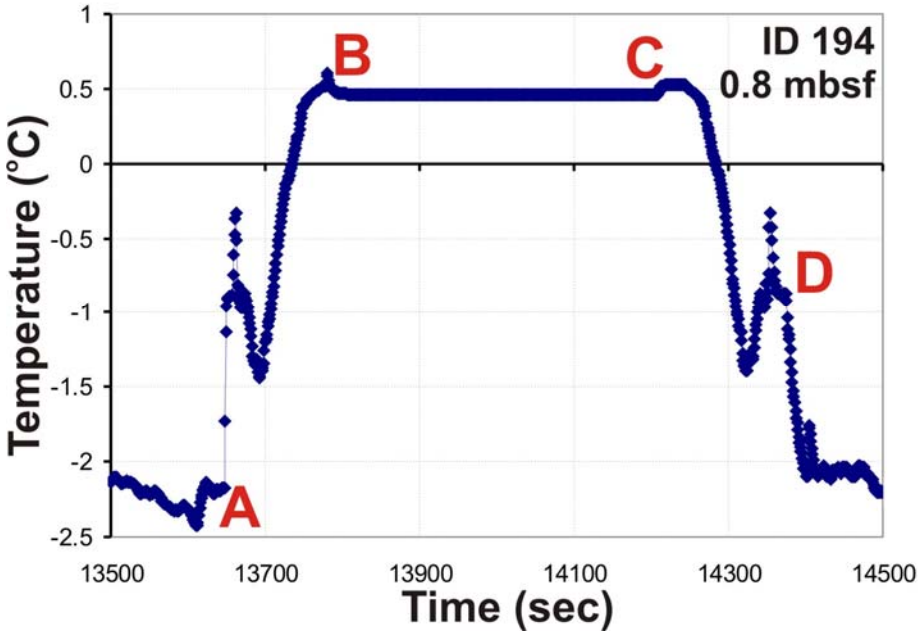

Figure A.2.6 Temperature records at Station 27 for the only MTL ID 194 at 0.8mbsf. A: Core deployed, B: frictional heating pulse from core entering the sediment, C: frictional heating pulse from core pulled out of sediment, D: core back on deck.

A.2.7 Coke-Cap, Station 56

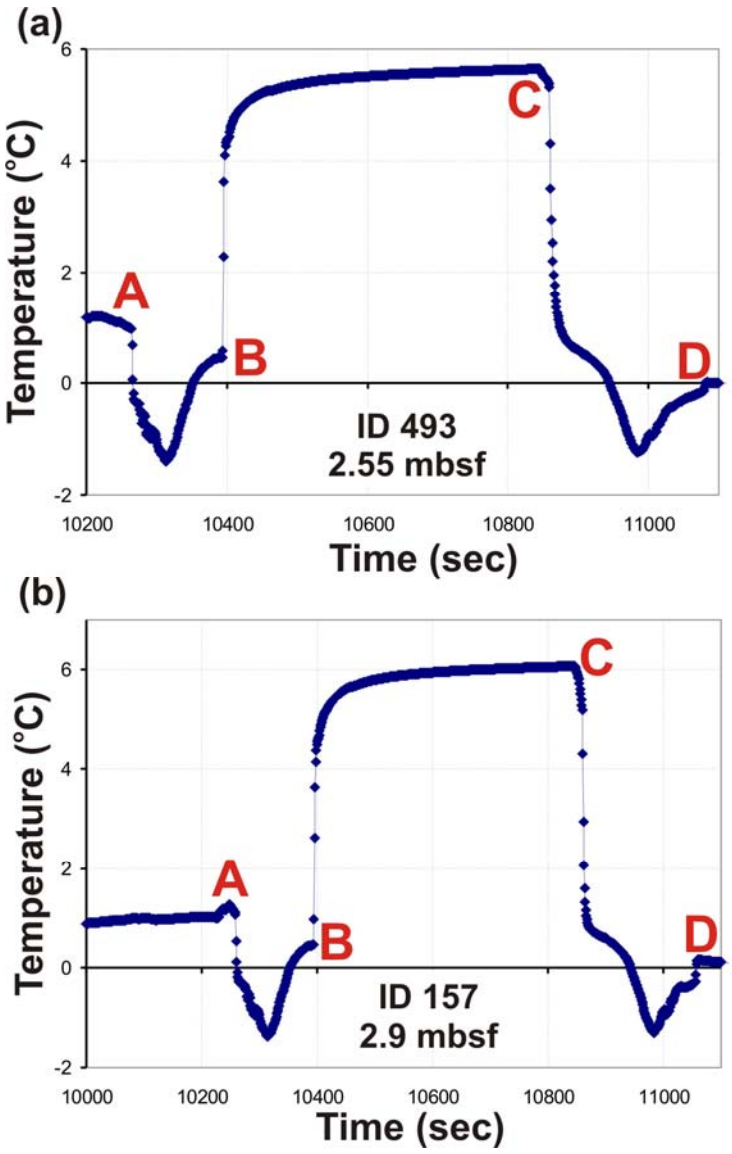

Figure A.2.7.1 Temperature records at Station 56 for MTL (a) ID 493 at 2.55 mbsf, and (b) ID 157 at 2.9 mbsf. A: Core deployed, B: frictional heating pulse from core entering the sediment, C: frictional heating pulse from core pulled out of sediment, D: core back on deck.

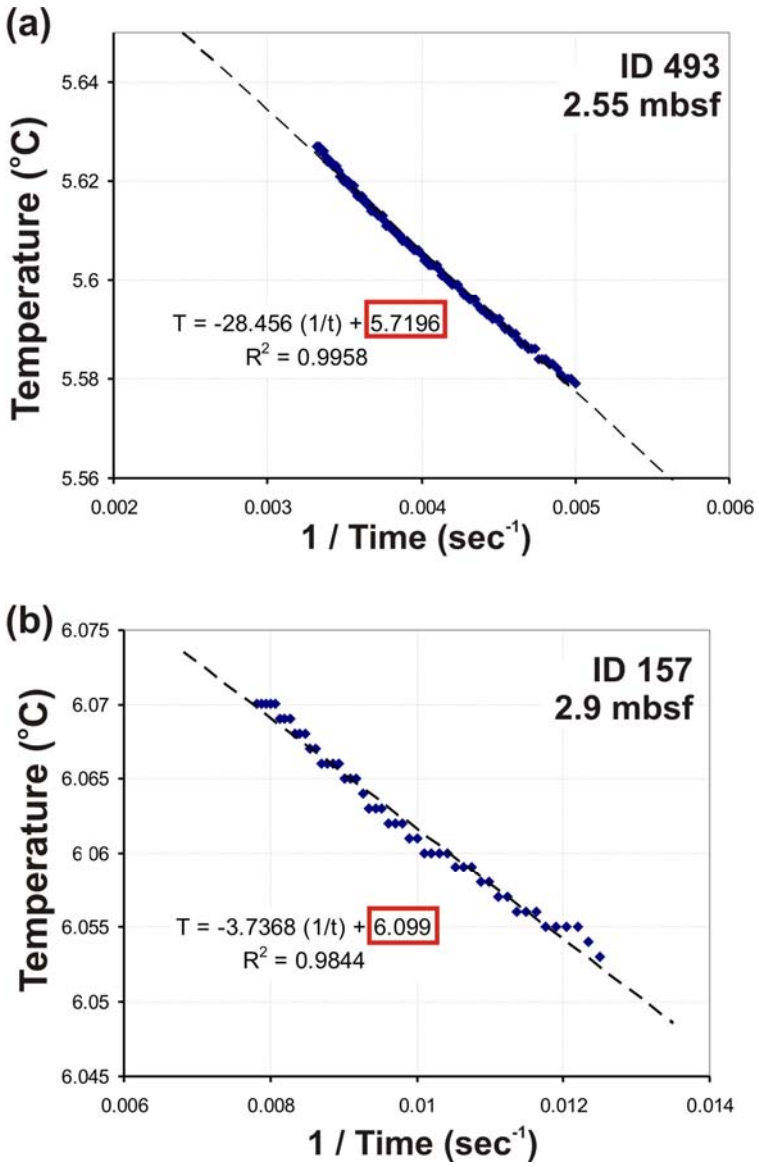

Figure A.2.7.2 Linear regression analysis to estimate equilibrium in situ temperature at Station 56 for the last 120 seconds prior to pulling out of the core for MTL (a) ID 493 at 2.55 mbsf, and (b) ID 157 at 2.9 mbsf.

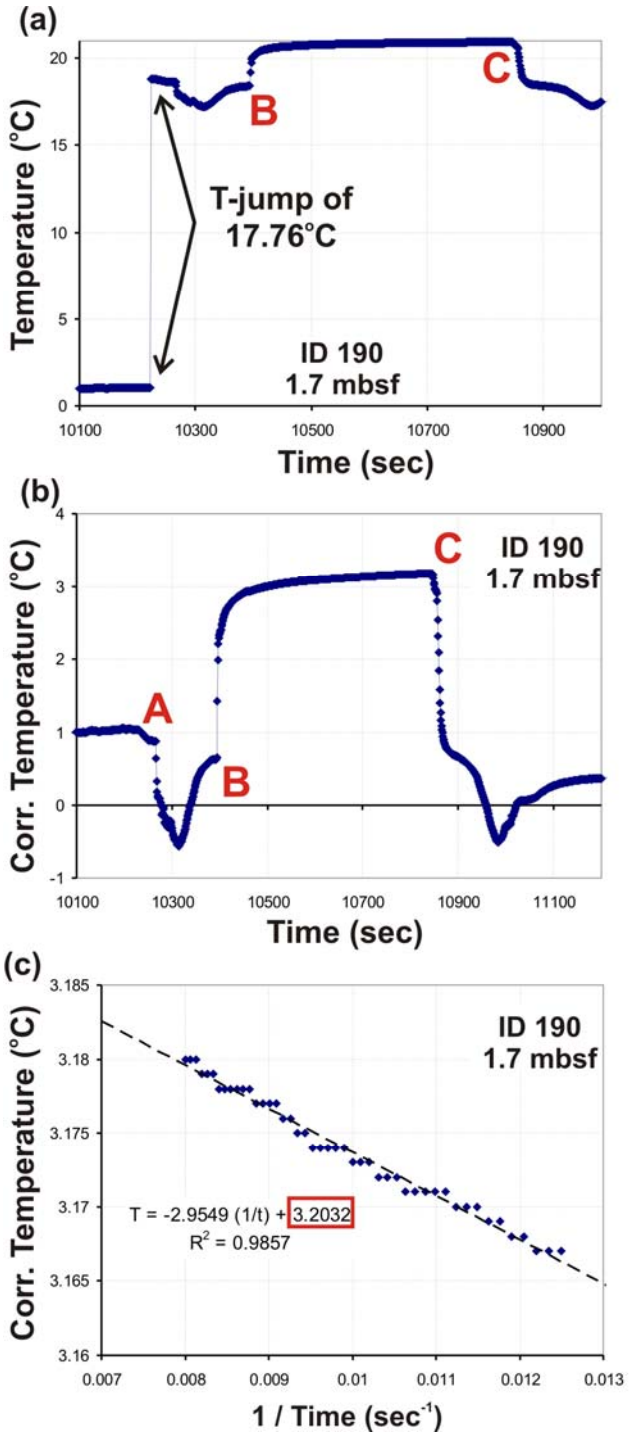

Figure A.2.7.3 Temperature record at Station 56 for MTL ID 190 at 1.7 mbsf with temperature-jump of 17.76ºC, (b) corrected temperature (subtracting 17.76ºC after jump occurred), and (c) subsequent linear regression analysis to estimate equilibrium in situ temperature. A: Core deployed, B: frictional heating pulse from core entering the sediment, C: frictional heating pulse from core pulled out of sediment. Estimated equilibrium temperature from the best-fit linear equation is highlighted in the red box.

A.2.8 Coke-Cap, Station 58

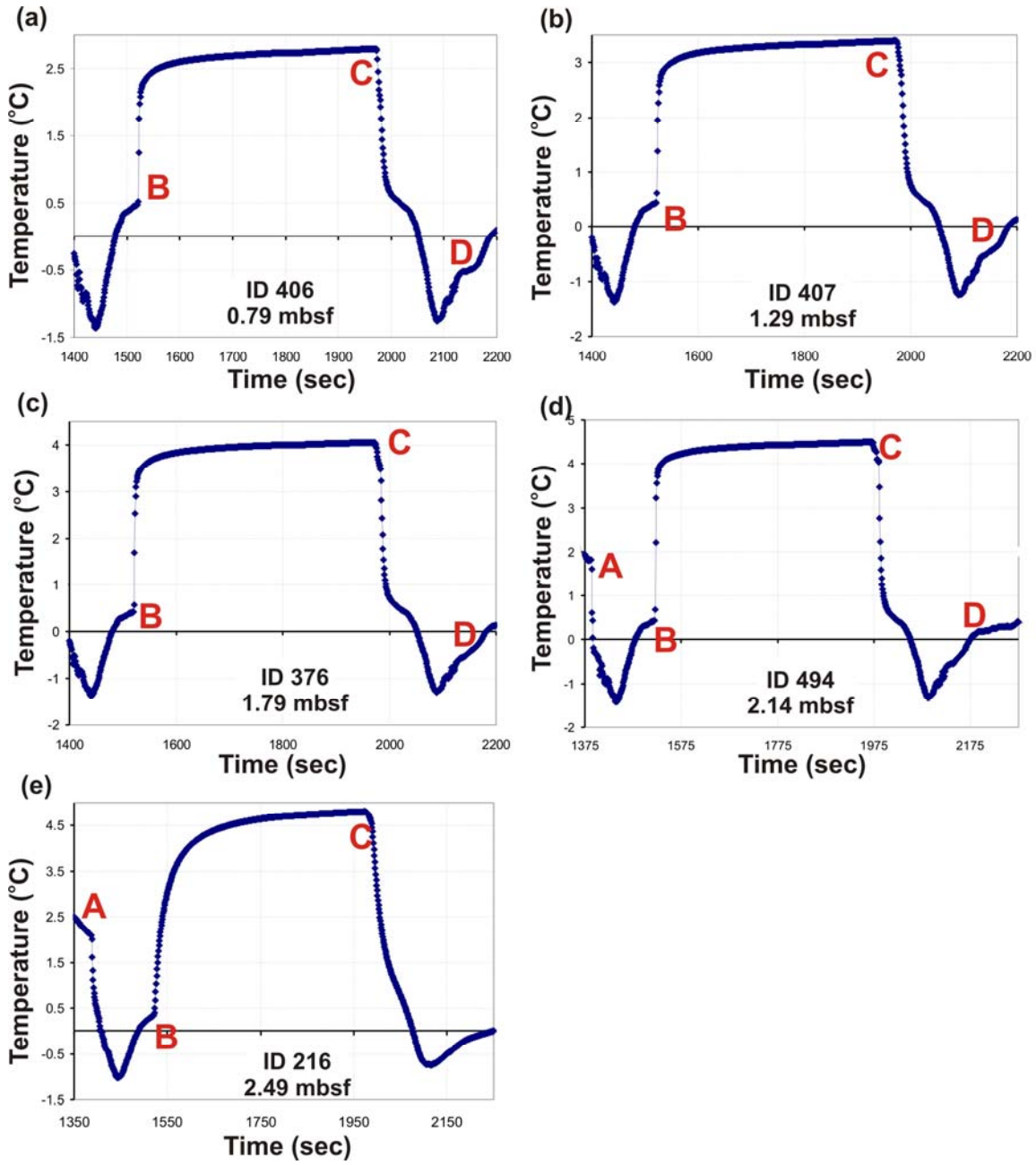

Figure A.2.8.1 Temperature records at Station 58 for MTL (a) ID 406 at 0.79 mbsf, (b) ID 407 at 1.29 mbsf, (c) ID 376 at 1.79 mbsf, (d) ID 494 at 2.14 mbsf, and (e) ID 216 at 2.49 mbsf. A: Core deployed, B: frictional heating pulse from core entering the sediment, C: frictional heating pulse from core pulled out of sediment, D: core back on deck.

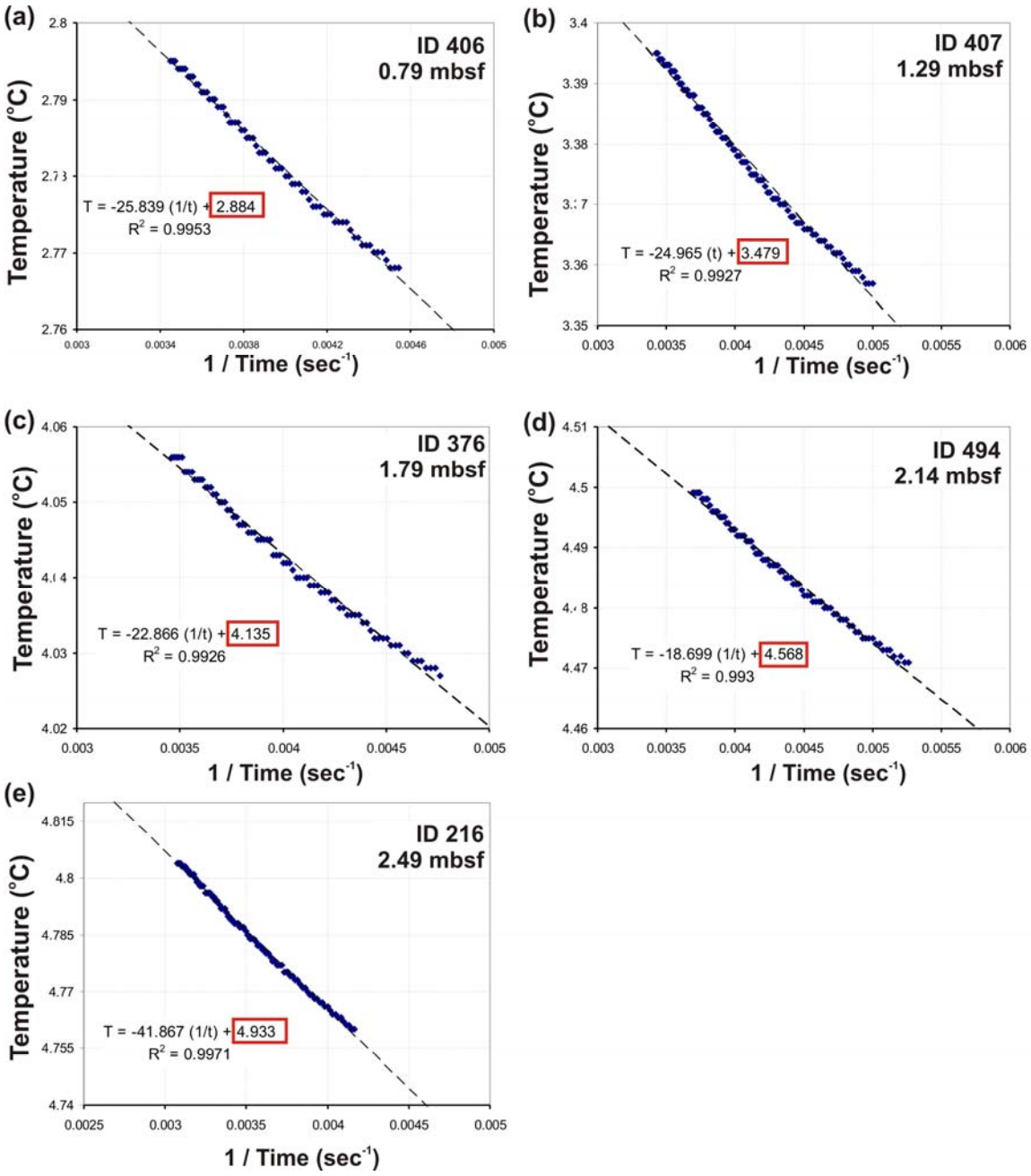

Figure A.2.8.2 Linear regression analysis to estimate equilibrium in situ temperature at Station 58 for the last ~100 seconds prior to pulling out of the core for MTL (a) ID 406 at 0.79 mbsf, (b) ID 407 at 1.29 mbsf, (c) ID 376 at 1.79 mbsf, (d) ID 494 at 2.14 mbsf, and (e) ID 216 at 2.49 mbsf.

A.2.9 Coke-Cap, Station 60

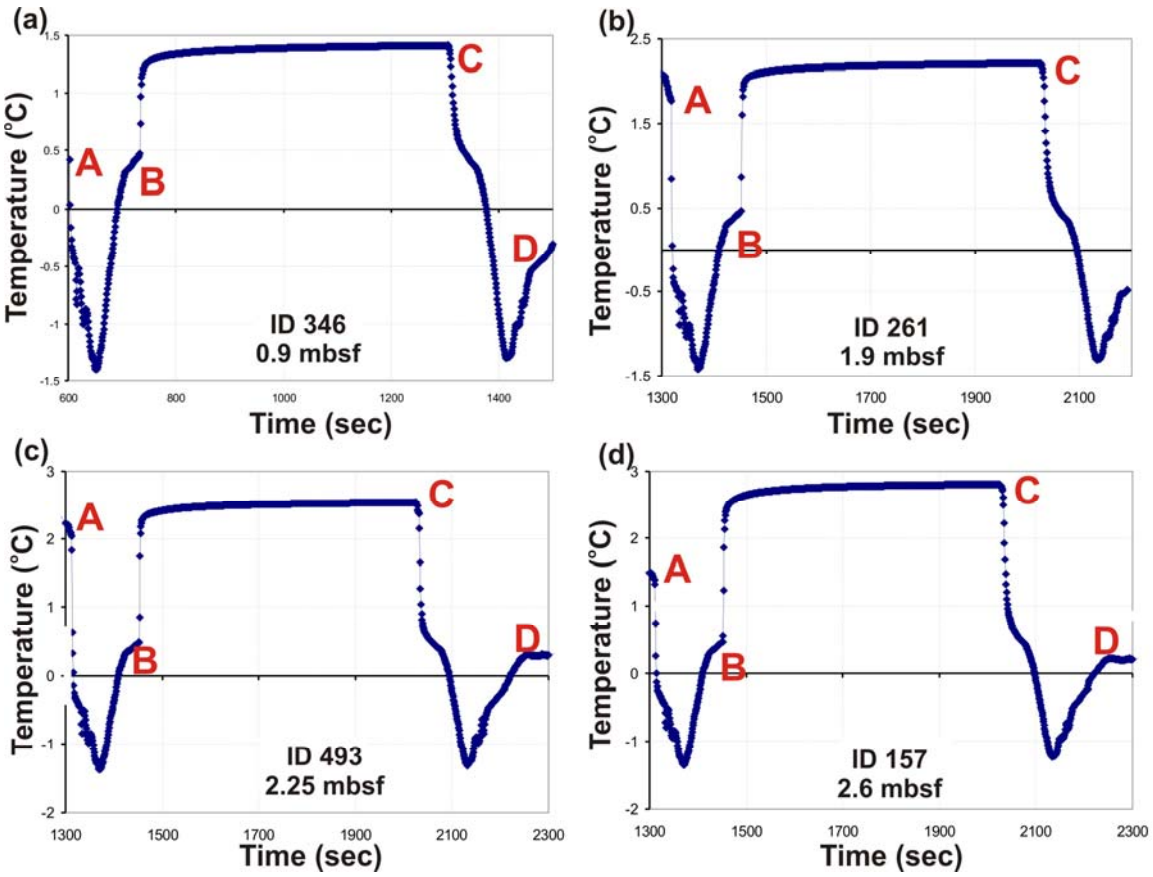

Figure A.2.9.1 Temperature records at Station 60 for MTL (a) ID 346 at 0.9 mbsf, (b) ID 261 at 1.9 mbsf, (c) ID 493 at 2.25 mbsf, and (d) ID 157 at 2.6 mbsf. A: Core deployed, B: frictional heating pulse from core entering the sediment, C: frictional heating pulse from core pulled out of sediment, D: core back on deck.

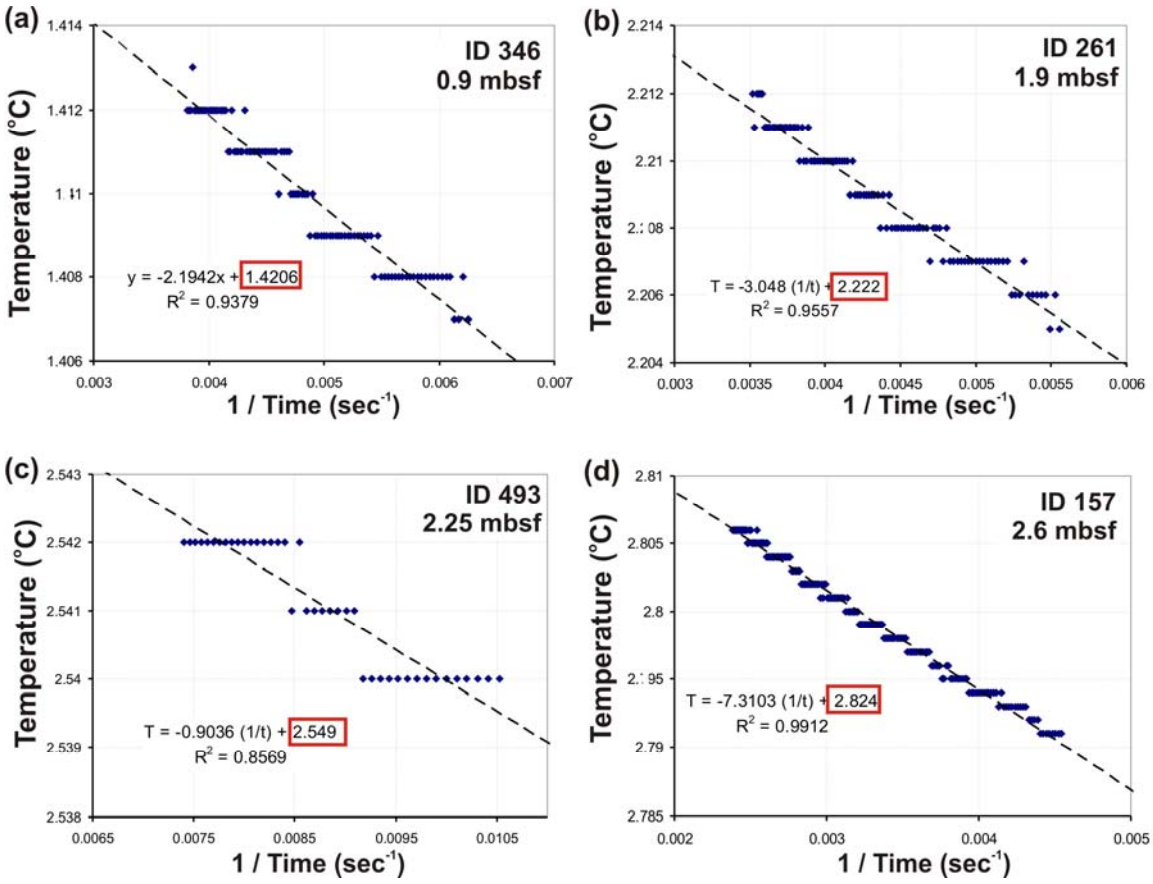

Figure A.2.9.2 Linear regression analysis to estimate equilibrium in situ temperature at Station 60 for the last ~100 seconds prior to pulling out of the core for MTL (a) ID 346 at 0.9 mbsf, (b) ID 261 at 1.9 mbsf, (c) ID 493 at 2.25 mbsf, and (d) ID 157 at 2.6 mbsf.

A.2.10 Coke-Cap, Station 62

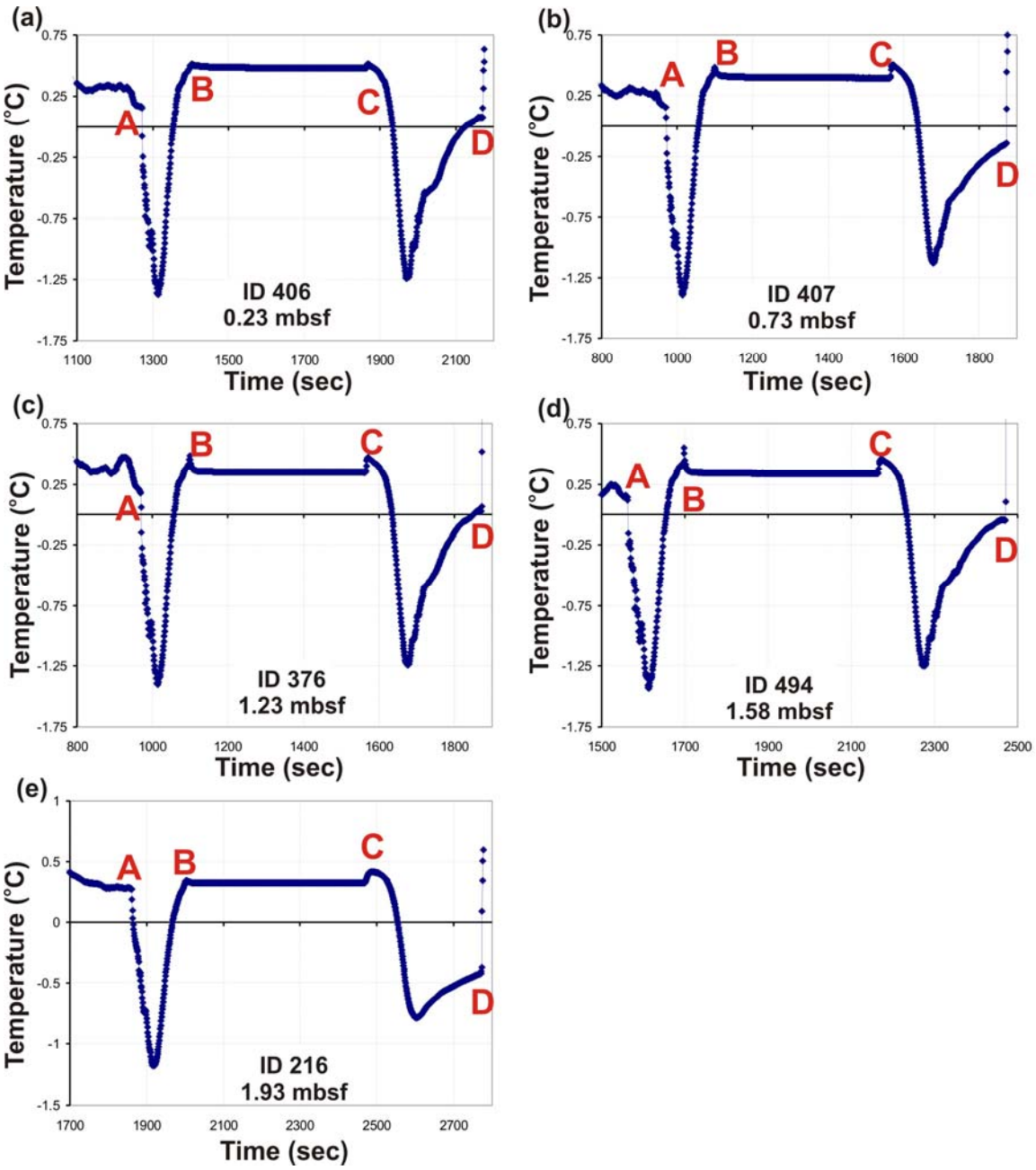

Figure A.2.10 Temperature records at Station 62 for MTL (a) ID 406 at 0.23 mbsf, (b) ID 407 at 0.73 mbsf, (c) ID 376 at 1.23 mbsf, (d) ID 494 at 1.58 mbsf, and (e) ID 216 at 1.93 mbsf. A: Core deployed, B: frictional heating pulse from core entering the sediment, C: frictional heating pulse from core pulled out of sediment, D: core back on deck.

A.2.11 Coke-Cap, Station 64

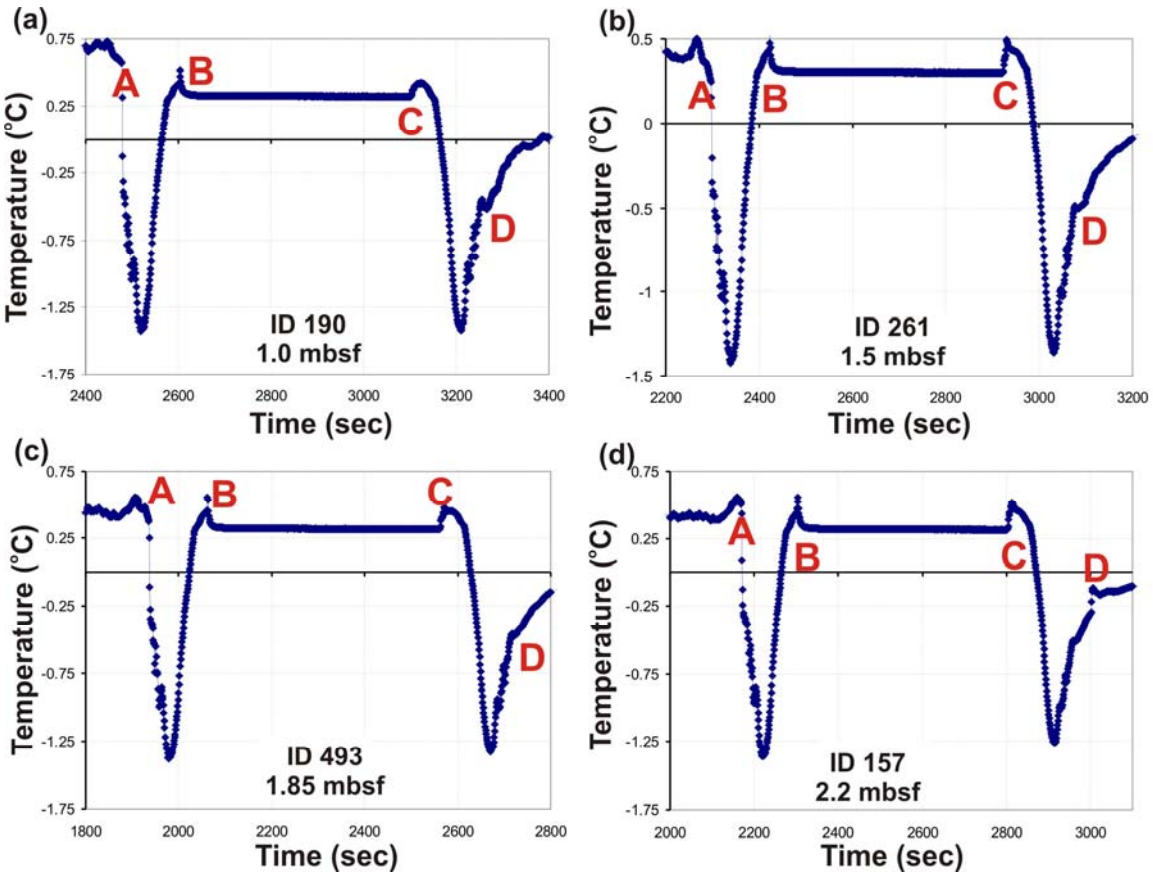

Figure A.2.11 Temperature records at Station 64 for MTL (a) ID 190 at 1.0 mbsf, (b) ID 261 at 1.50 mbsf, (c) ID 493 at 1.85 mbsf, and (d) ID 157 at 2.2 mbsf. A: Core deployed, B: frictional heating pulse from core entering the sediment, C: frictional heating pulse from core pulled out of sediment, D: core back on deck.

A.3.1 420 meter water depth expulsion feature, Station 41

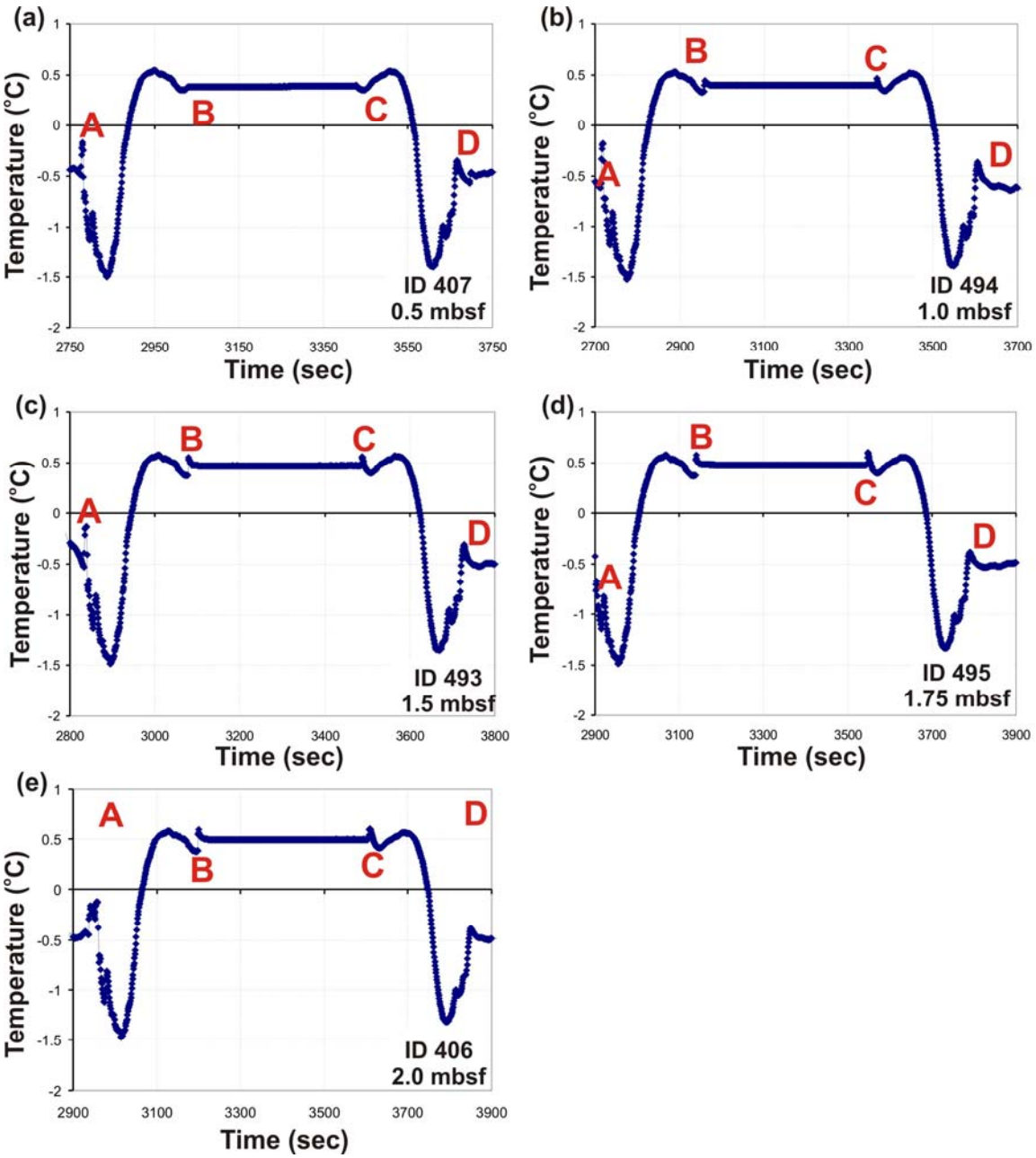

Figure A.3.1 Temperature records at Station 41 for MTL (a) ID 407 at 0.5 mbsf, (b) ID 494 at 1.0 mbsf, (c) ID 493 at 1.5 mbsf, (d) ID 495 at 1.75 mbsf, and (e) ID 406 at 2.0 mbsf. A: Core deployed, B: frictional heating pulse from core entering the sediment, C: frictional heating pulse from core pulled out of sediment, D: core back on deck.

A.3.2 420 meter water depth expulsion feature, Station 43

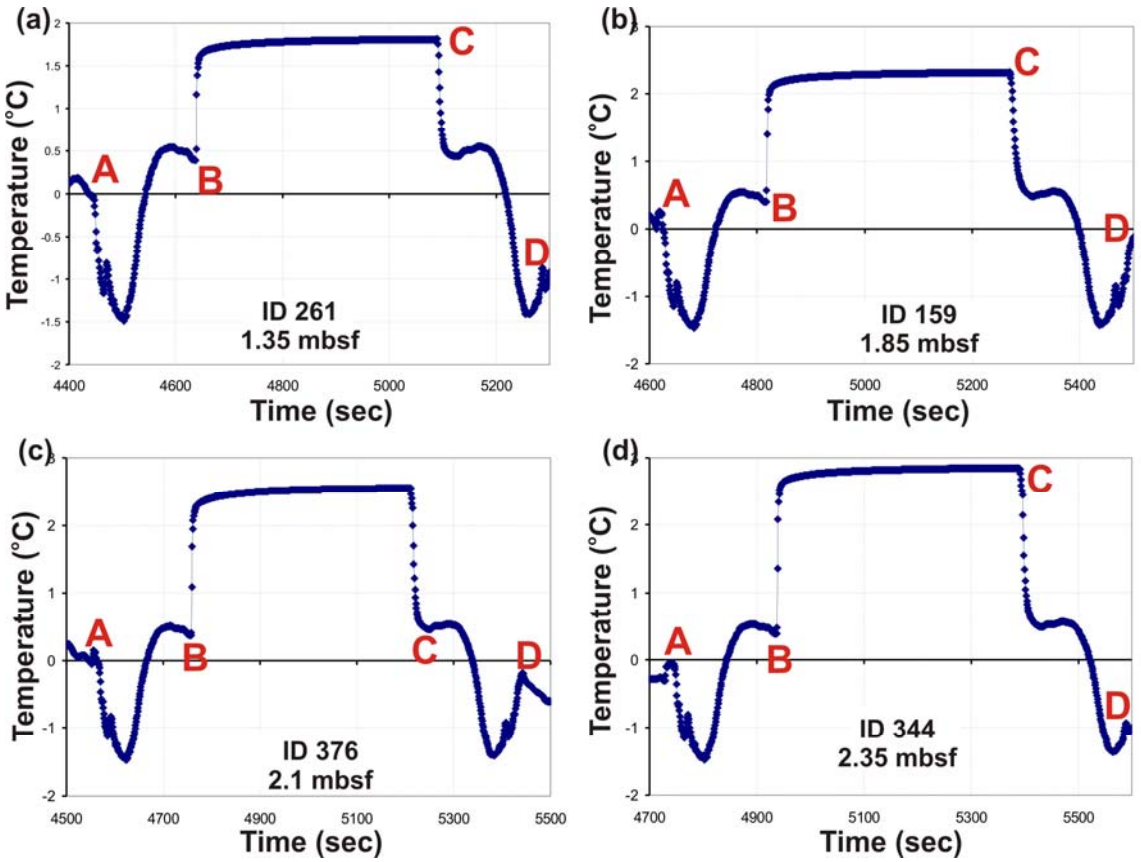

Figure A.3.2.1 Temperature records at Station 43 for MTL (a) ID 261 at 1.35 mbsf, (b) ID 159 at 1.85 mbsf, (c) ID 376 at 2.1 mbsf, and (d) ID 344 at 2.35 mbsf. A: Core deployed, B: frictional heating pulse from core entering the sediment, C: frictional heating pulse from core pulled out of sediment, D: core back on deck.

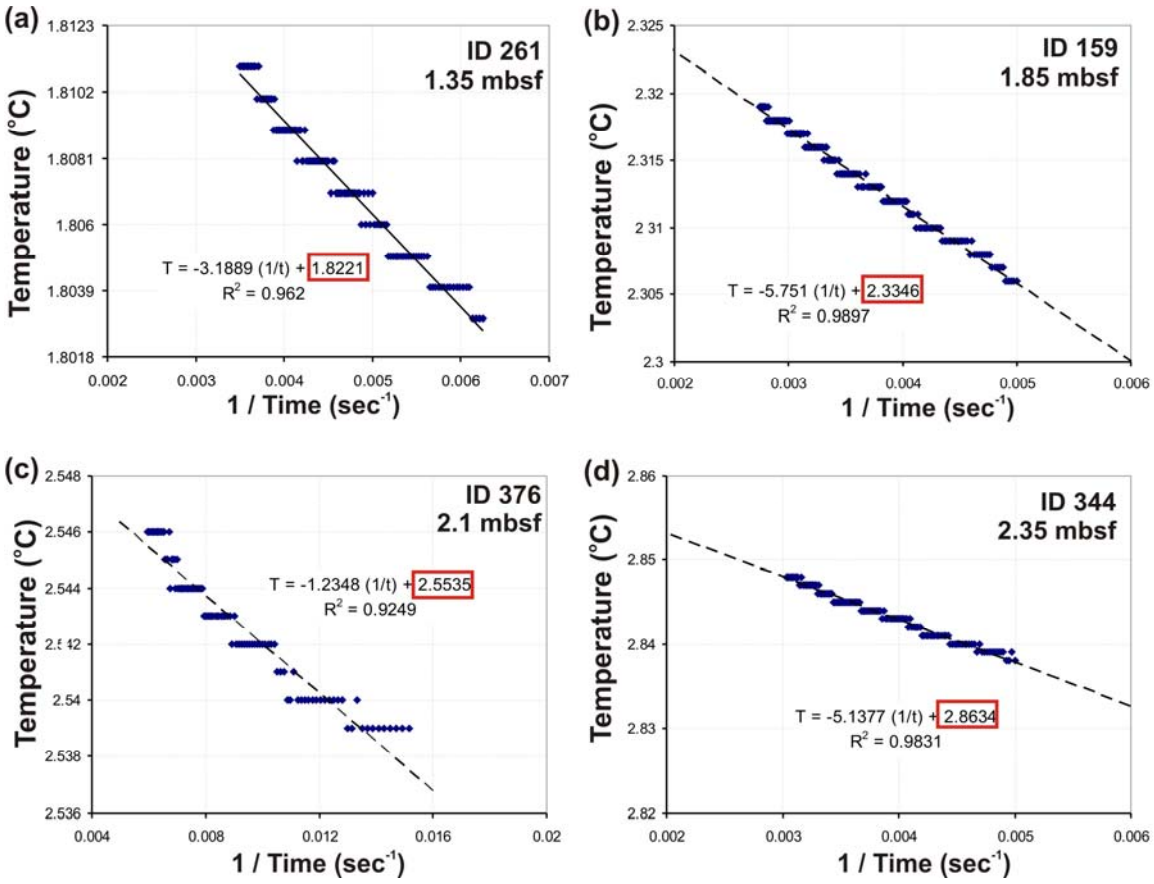

Figure A.3.2.2 Linear regression analysis to estimate equilibrium in situ temperature at Station 43 for the last ~100 seconds prior to pulling out of the core for each MTL: (a) ID 261 at 1.35 mbsf, (b) ID 159 at 1.85 mbsf, (c) ID 376 at 2.1 mbsf, and (d) ID 344 at 2.35 mbsf. Estimated equilibrium temperatures from the best-fit linear equation are highlighted in the red boxes for each MTL.

A.3.3 420 meter water depth expulsion feature, Station 45

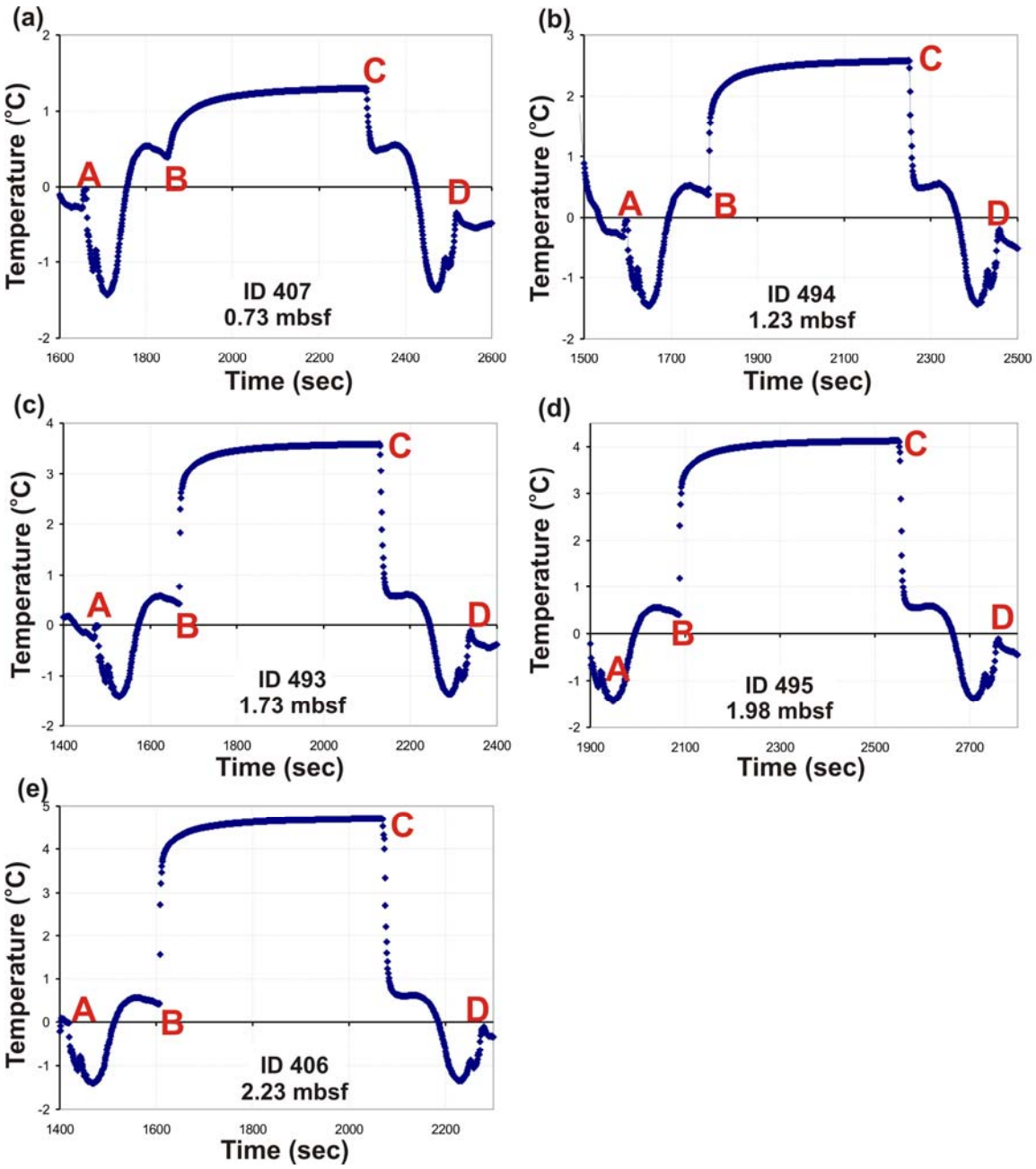

Figure A.3.3.1 Temperature records at Station 45 for MTL (a) ID 407 at 0.73 mbsf, (b) ID 494 at 1.23 mbsf, (c) ID 493 at 1.73 mbsf, (d) ID 495 at 1.98 mbsf, and (e) ID 406 at 2.23 mbsf. A: Core deployed, B: frictional heating pulse from core entering the sediment, C: frictional heating pulse from core pulled out of sediment, D: core back on deck.

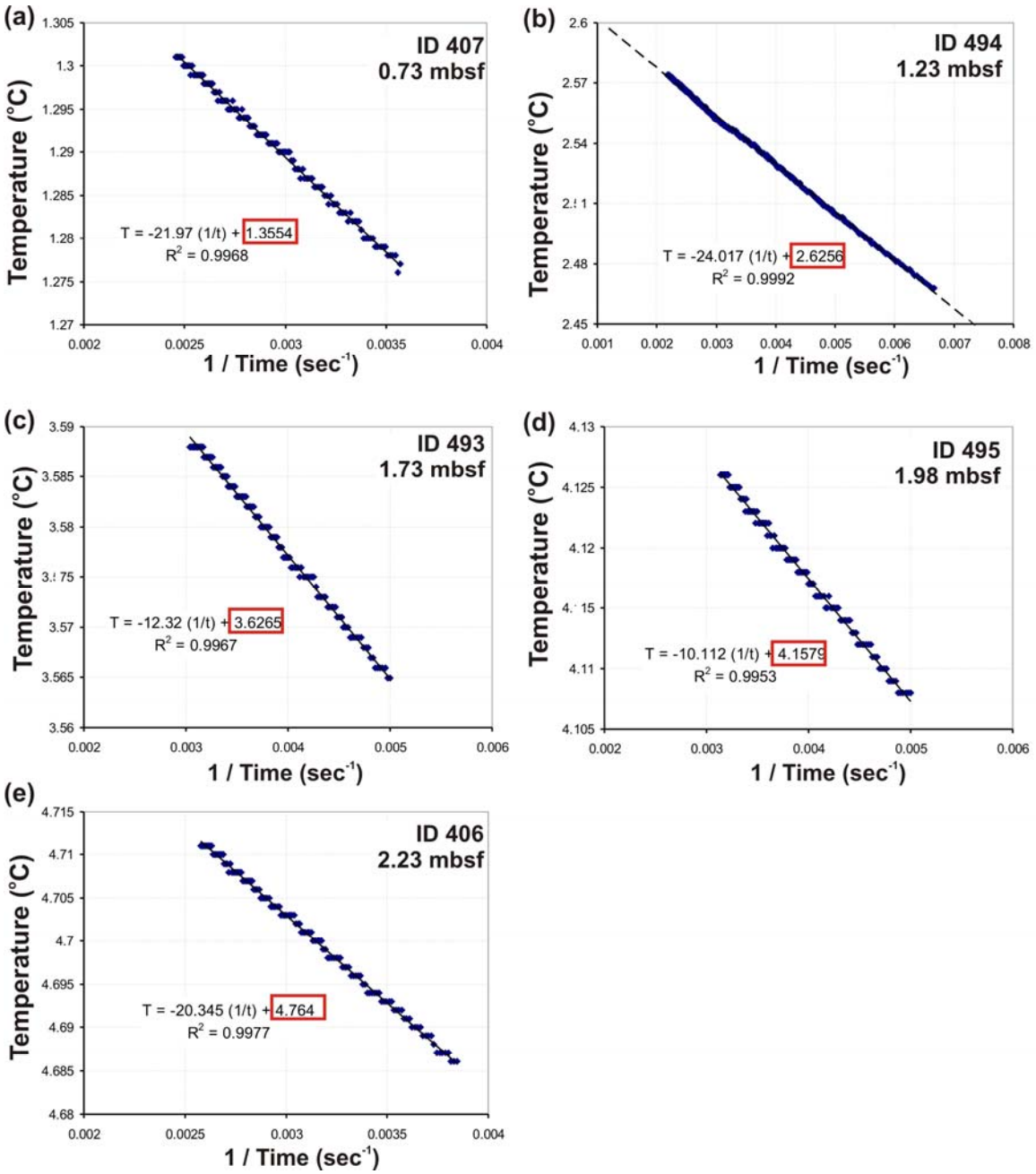

Figure A.3.3.2 Linear regression analysis to estimate equilibrium in situ temperature at Station 45 for the last ~100 seconds prior to pulling out of the core for each MTL: (a) ID 407 at 0.73 mbsf, (b) ID 494 at 1.23 mbsf, (c) ID 493 at 1.73 mbsf, (d) ID 495 at 1.98 mbsf, and (e) ID 406 at 2.23 mbsf. Estimated equilibrium temperatures from the best-fit linear equation are highlighted in the red boxes for each MTL.

A.3.4 420 meter water depth expulsion feature, Station 47

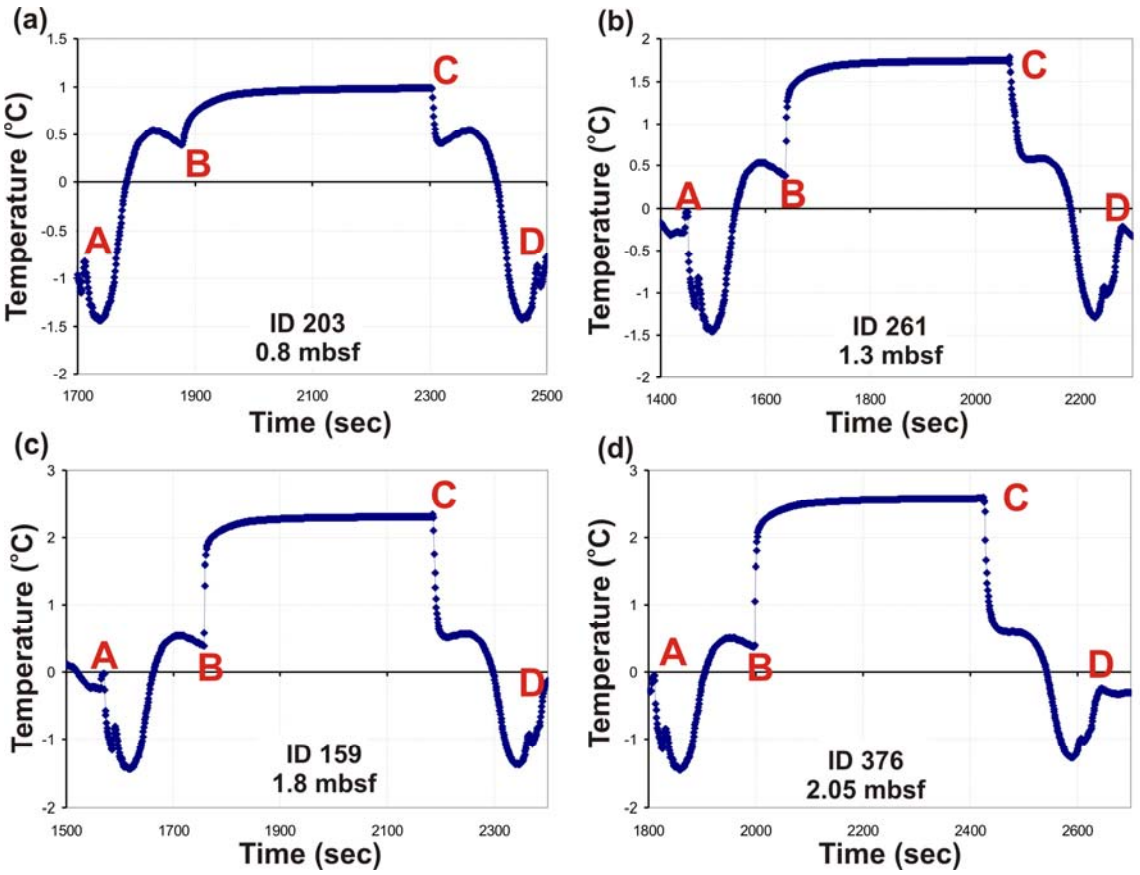

Figure A.3.4.1 Temperature records at Station 47 for MTL (a) ID 203 at 0.8 mbsf, (b) ID 261 at 1.3 mbsf, (c) ID 159 at 1.8 mbsf, and (d) ID 376 at 2.05 mbsf. A: Core deployed, B: frictional heating pulse from core entering the sediment, C: frictional heating pulse from core pulled out of sediment, D: core back on deck.

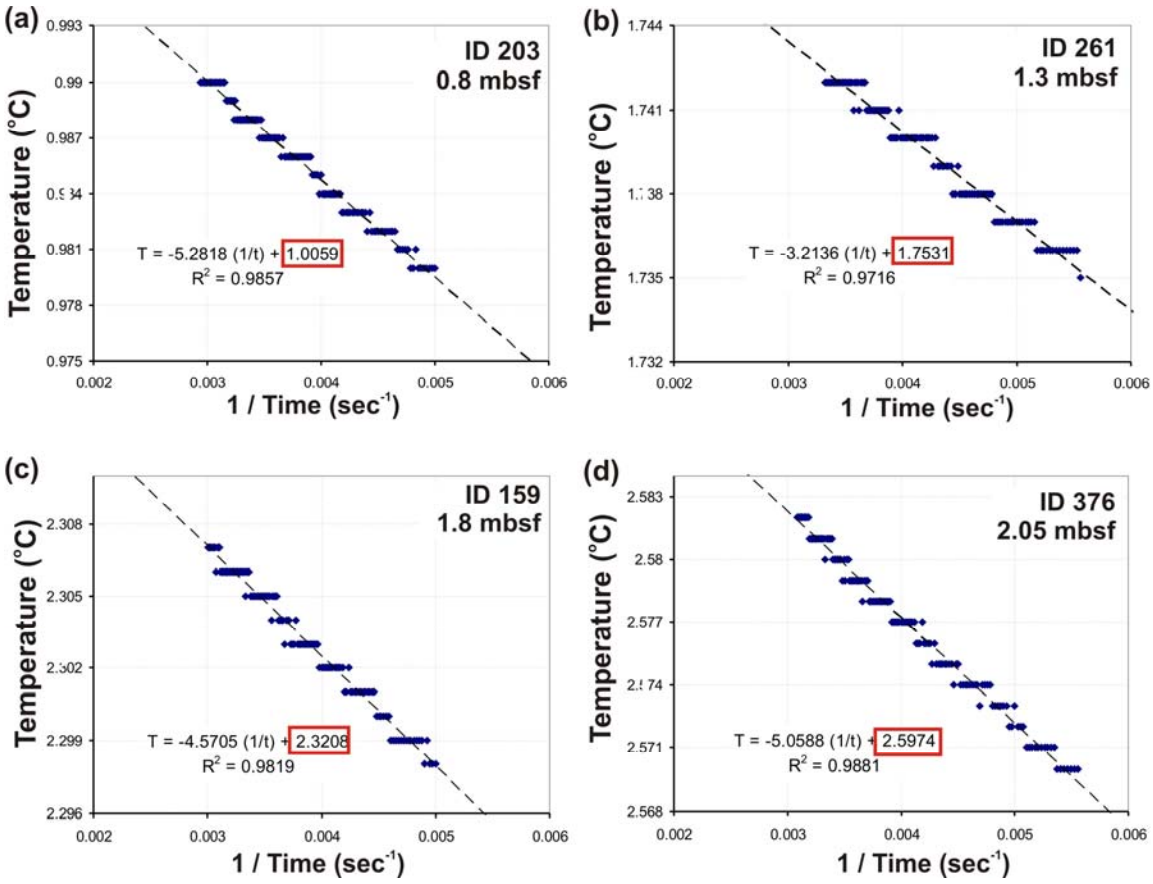

Figure A.3.4.2 Linear regression analysis to estimate equilibrium in situ temperature at Station 47 for the last ~100 seconds prior to pulling out of the core for each MTL: (a) ID 203 at 0.8 mbsf, (b) ID 261 at 1.3 mbsf, (c) ID 159 at 1.8 mbsf, and (d) ID 376 at 2.05 mbsf. Estimated equilibrium temperatures from the best-fit linear equation are highlighted in the red boxes for each MTL.

A.3.5 420 meter water depth expulsion feature, Station 49

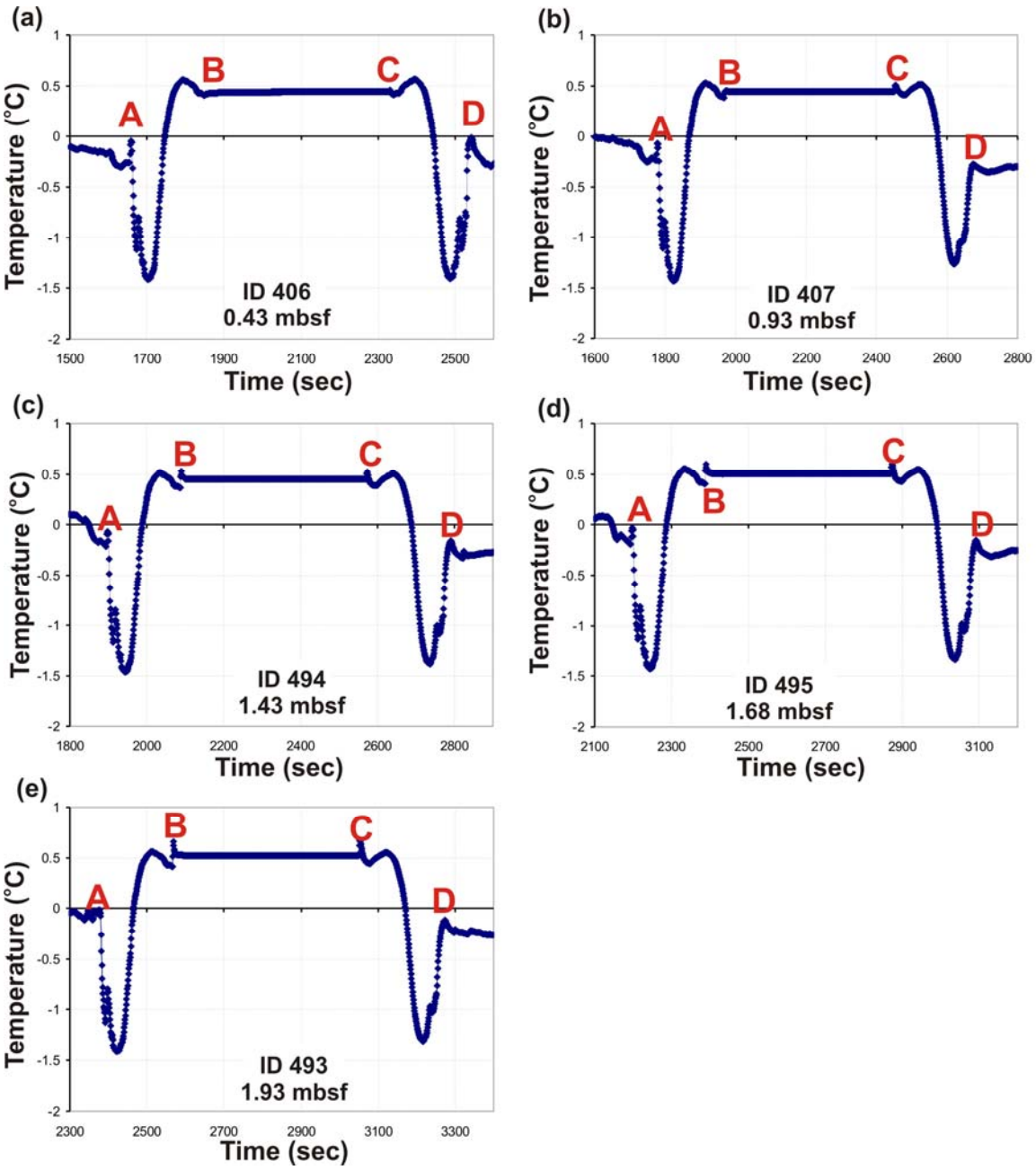

Figure A.3.5 Temperature records at Station 49 for MTL (a) ID 203 at 0.8 mbsf, (b) ID 261 at 1.3 mbsf, (c) ID 159 at 1.8 mbsf, and (d) ID 376 at 2.05 mbsf. A: Core deployed, B: frictional heating pulse from core entering the sediment, C: frictional heating pulse from core pulled out of sediment, D: core back on deck.

A.3.6 420 meter water depth expulsion feature, Station 51

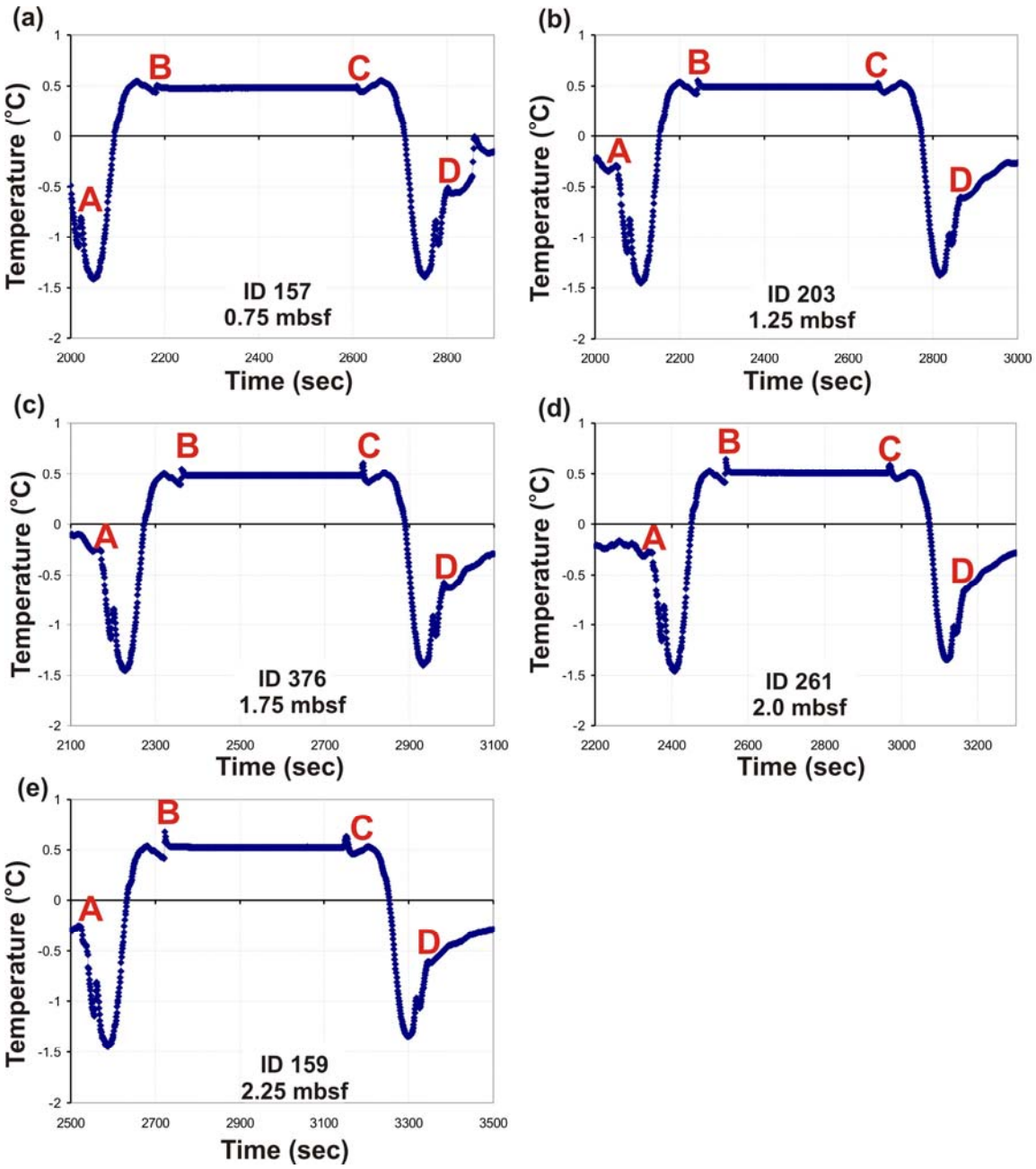

Figure A.3.6 Temperature records at Station 51 for MTL (a) ID 157 at 0.75 mbsf, (b) ID 203 at 1.25 mbsf, (c) ID 376 at 1.75 mbsf, (d) ID 261 at 2.0 mbsf, and (e) ID 159 at 2.25 mbsf. A: Core deployed, B: frictional heating pulse from core entering the sediment, C: frictional heating pulse from core pulled out of sediment, D: core back on deck.

A.3.7 420 meter water depth expulsion feature, Station 96

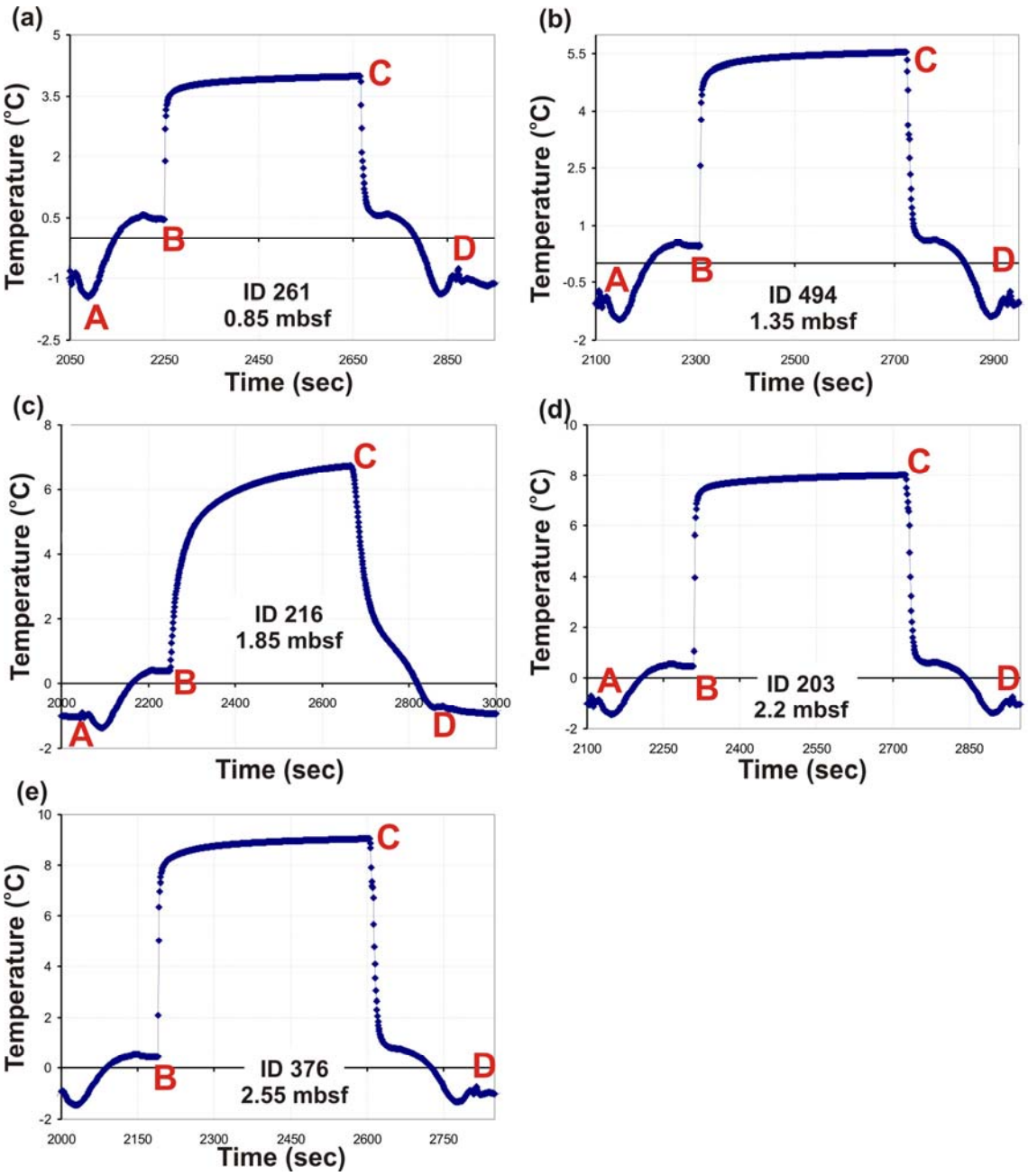

Figure A.3.7.1 Temperature records at Station 96 for MTL (a) ID 261 at 0.85 mbsf, (b) ID 494 at 0.35 mbsf, (c) ID 216 at 1.85 mbsf, (d) ID 203 at 2.2 mbsf, and (e) ID 376 at 2.55 mbsf. A: Core deployed, B: frictional heating pulse from core entering the sediment, C: frictional heating pulse from core pulled out of sediment, D: core back on deck.

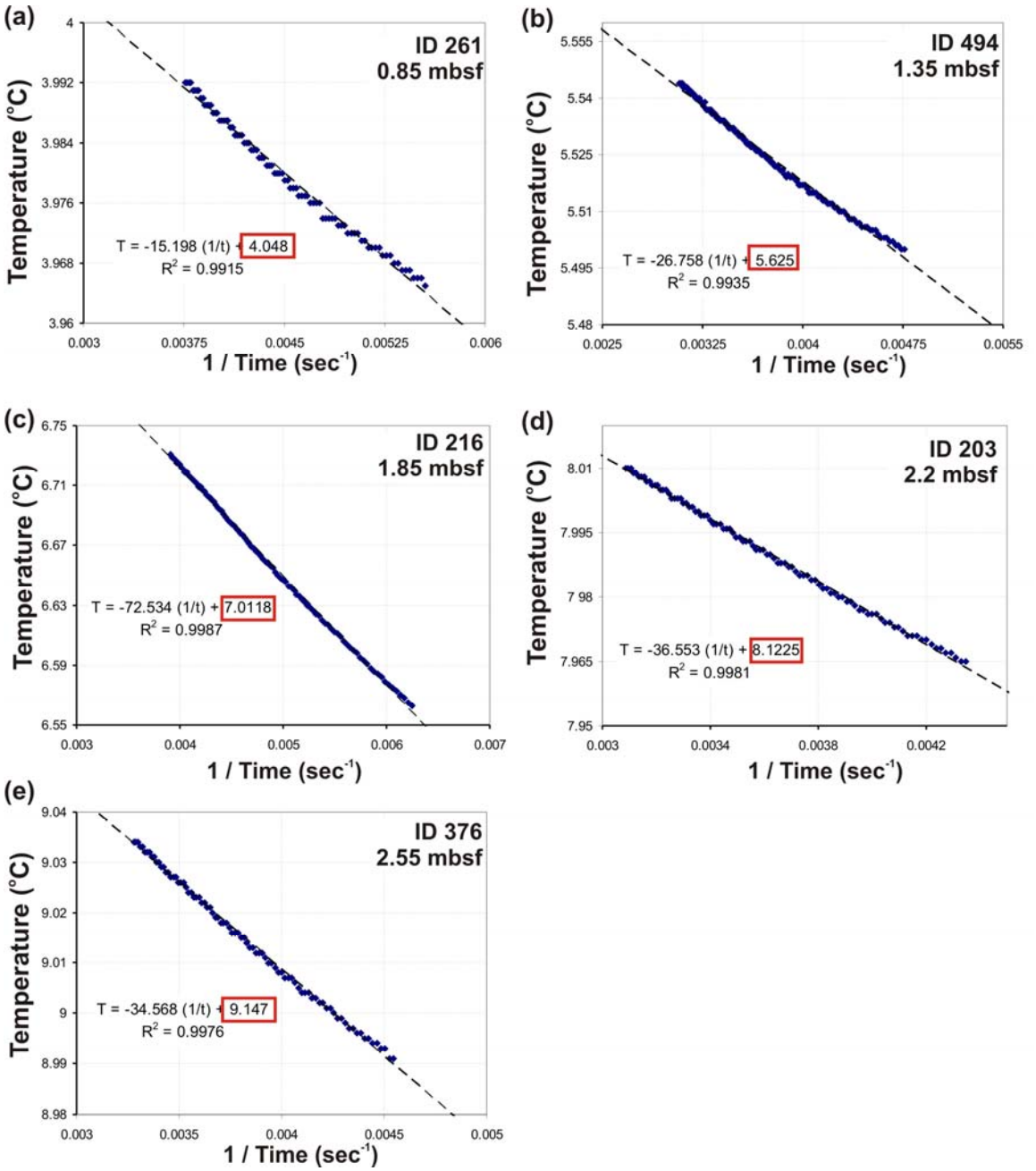

Figure A.3.7.2 Linear regression analysis to estimate equilibrium in situ temperature at Station 96 for the last ~100 seconds prior to pulling out of the core for each MTL: MTL (a) ID 261 at 0.85 mbsf, (b) ID 494 at 0.35 mbsf, (c) ID 216 at 1.85 mbsf, (d) ID 203 at 2.2 mbsf, and (e) ID 376 at 2.55 mbsf. Estimated equilibrium temperatures from the best-fit linear equation are highlighted in the red boxes for each MTL.

A.3.8 420 meter water depth expulsion feature, Station 97

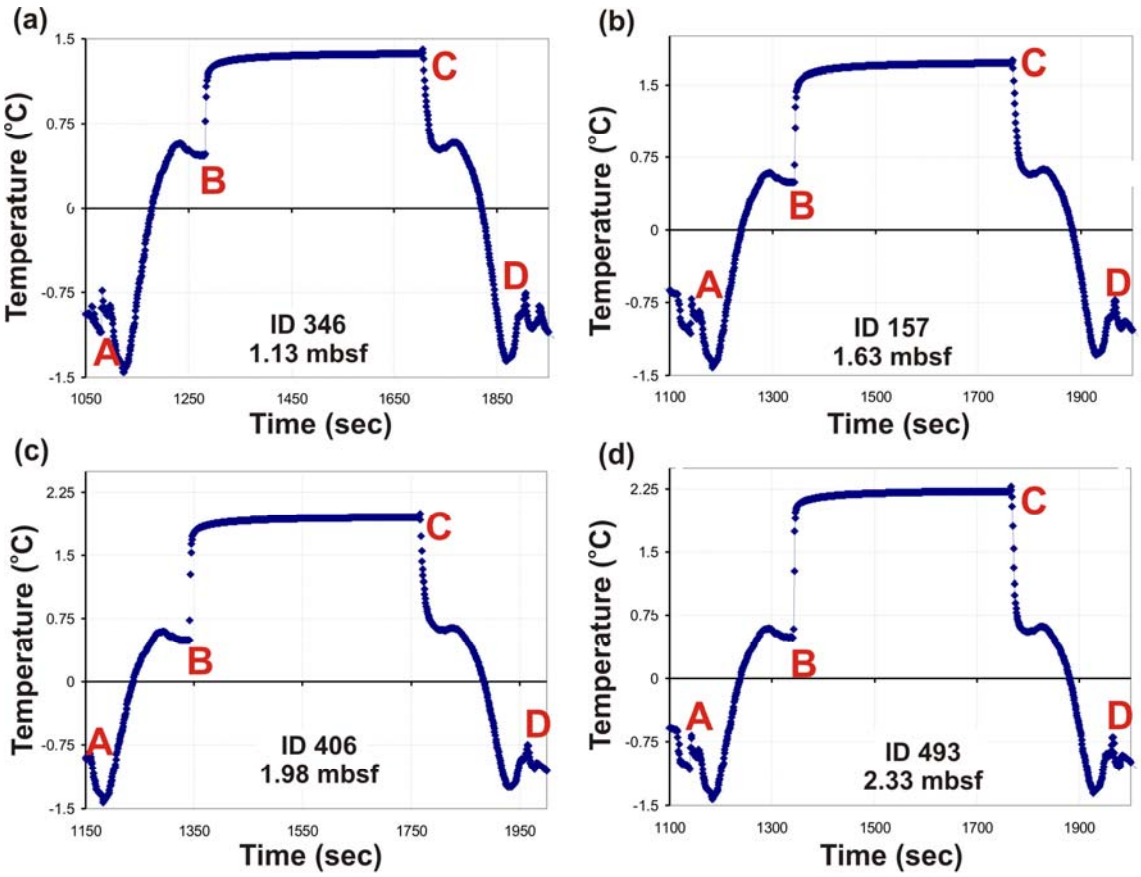

Figure A.3.8 Temperature records at Station 97 for MTL (a) ID 346 at 1.13 mbsf, (b) ID 157 at 1.63 mbsf, (c) ID 406 at 1.98 mbsf, and (d) ID 493 at 2.33 mbsf. A: Core deployed, B: frictional heating pulse from core entering the sediment, C: frictional heating pulse from core pulled out of sediment, D: core back on deck.

A.3.9 420 meter water depth expulsion feature, Station 99

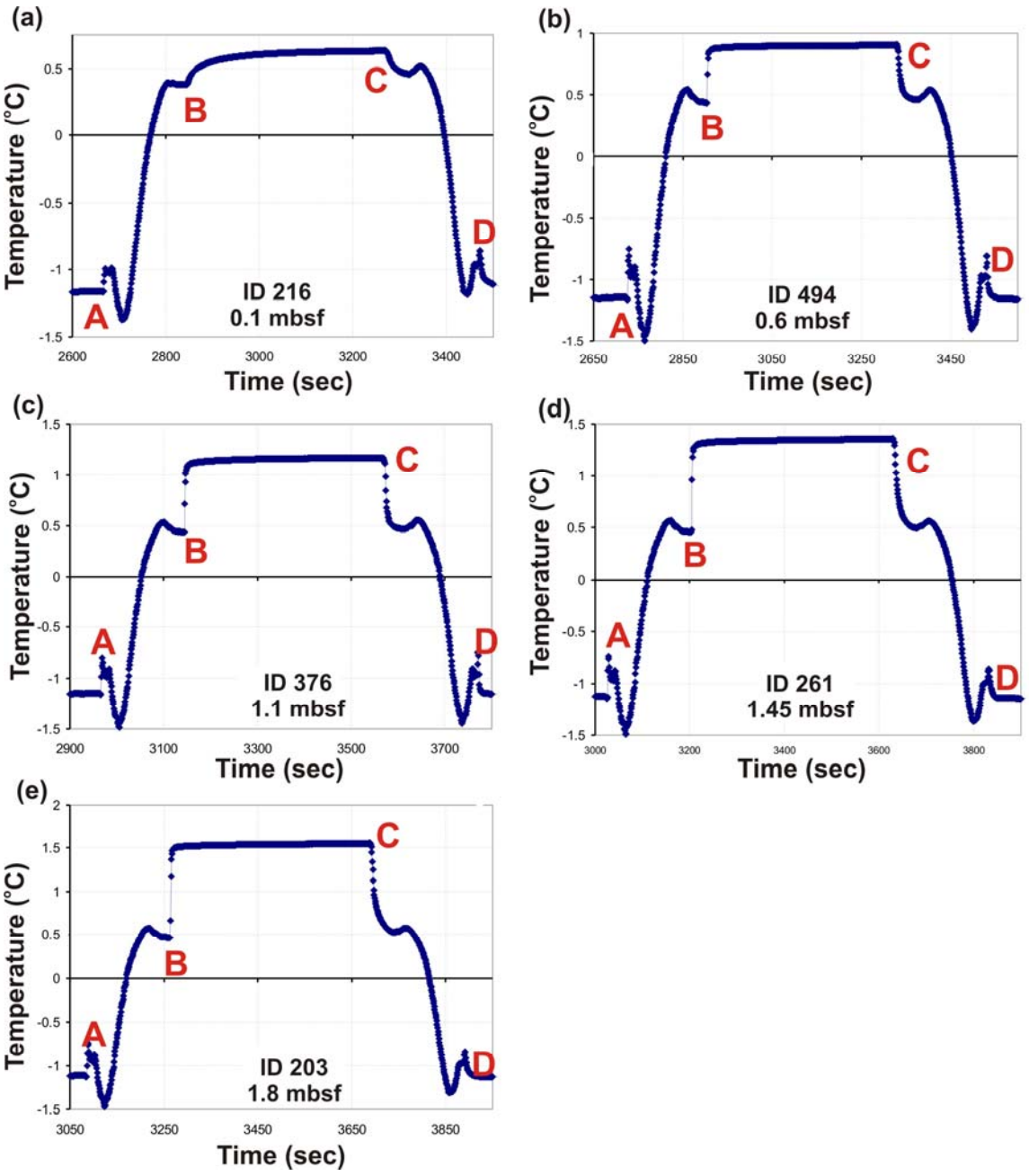

Figure A.3.9 Temperature records at Station 99 for MTL (a) ID 216 at 0.1 mbsf, (b) ID 494 at 0.6 mbsf, (c) ID 376 at 1.1 mbsf, (d) ID 261 at 1.45 mbsf, and (e) ID 203 at 1.8 mbsf. A: Core deployed, B: frictional heating pulse from core entering the sediment, C: frictional heating pulse from core pulled out of sediment, D: core back on deck.

A.3.10 420 meter water depth expulsion feature, Station 101

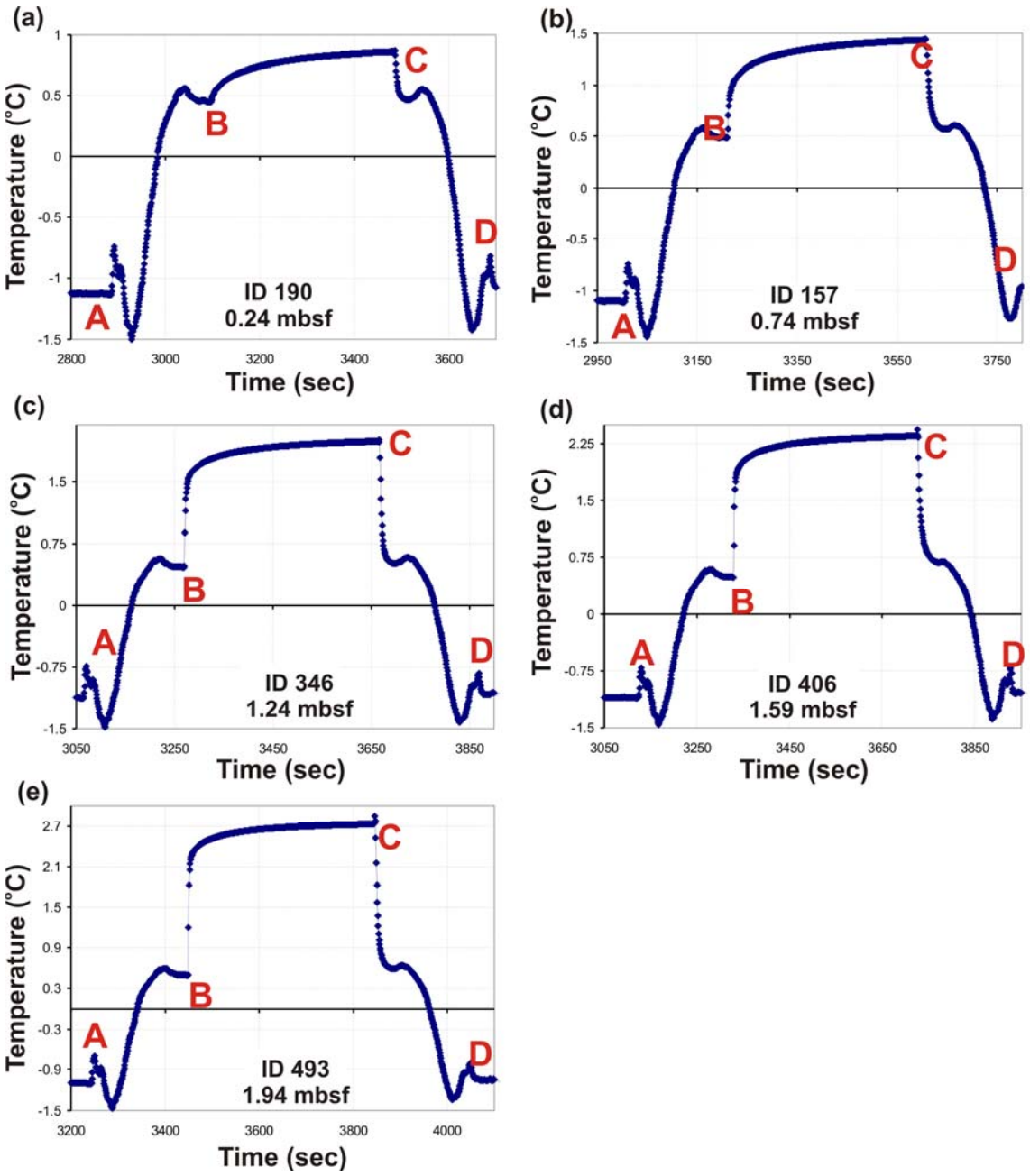

Figure A.3.10.1 Temperature records at Station 101 for MTL (a) ID 190 at 0.24 mbsf, (b) ID 157 at 0.74 mbsf, (c) ID 346 at 1.24 mbsf, (d) ID 406 at 1.59 mbsf, and (e) ID 493 at 1.94 mbsf. A: Core deployed, B: frictional heating pulse from core entering the sediment, C: frictional heating pulse from core pulled out of sediment, D: core back on deck.

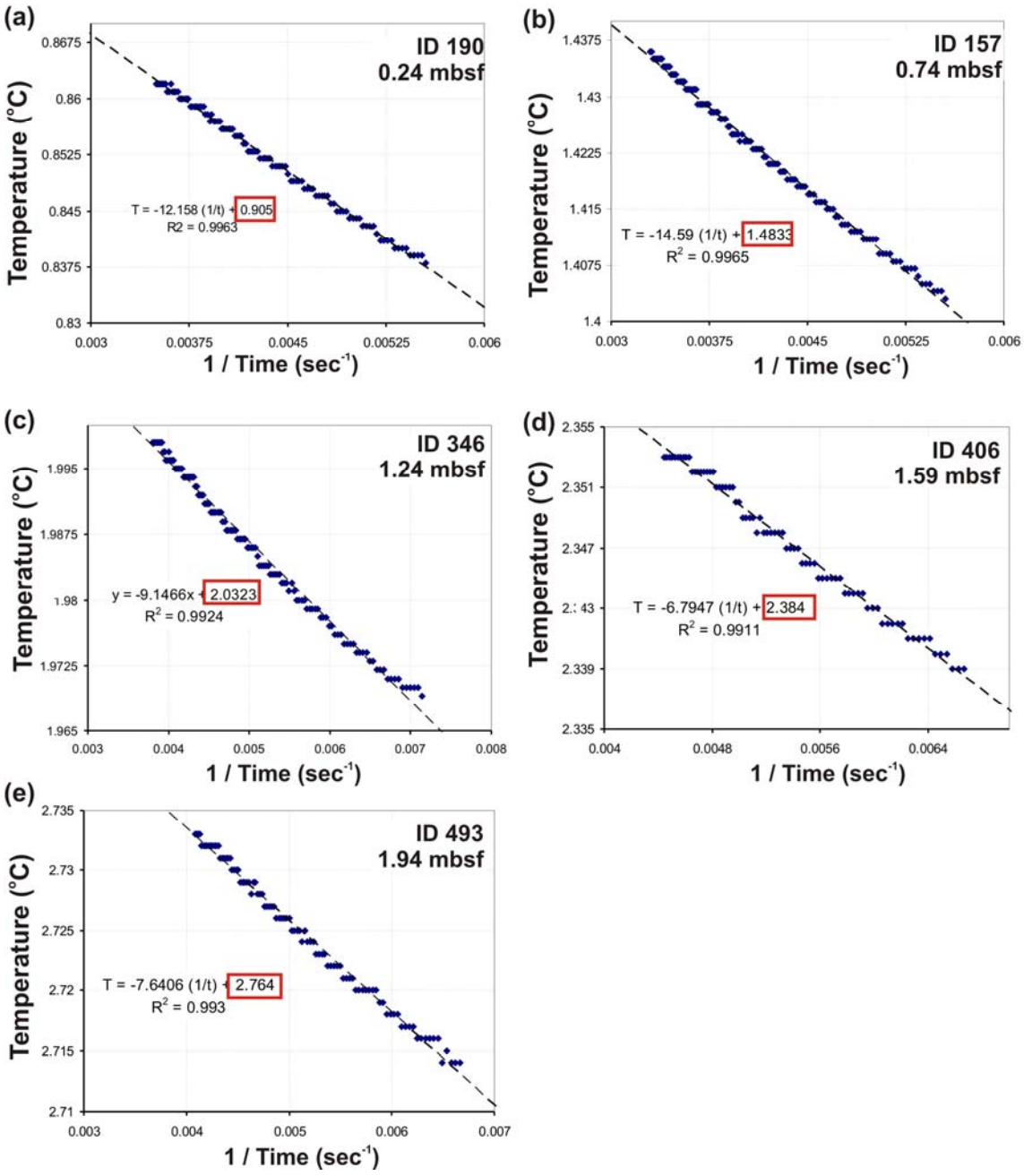

Figure A.3.10.2 Linear regression analysis to estimate equilibrium in situ temperature at Station 101 for the last ~100 seconds prior to pulling out of the core for each MTL: (a) ID 190 at 0.24 mbsf, (b) ID 157 at 0.74 mbsf, (c) ID 346 at 1.24 mbsf, (d) ID 406 at 1.59 mbsf, and (e) ID 493 at 1.94 mbsf. Estimated equilibrium temperatures from the best-fit linear equation are highlighted in the red boxes for each MTL.

A.3.11 420 meter water depth expulsion feature, Station 103

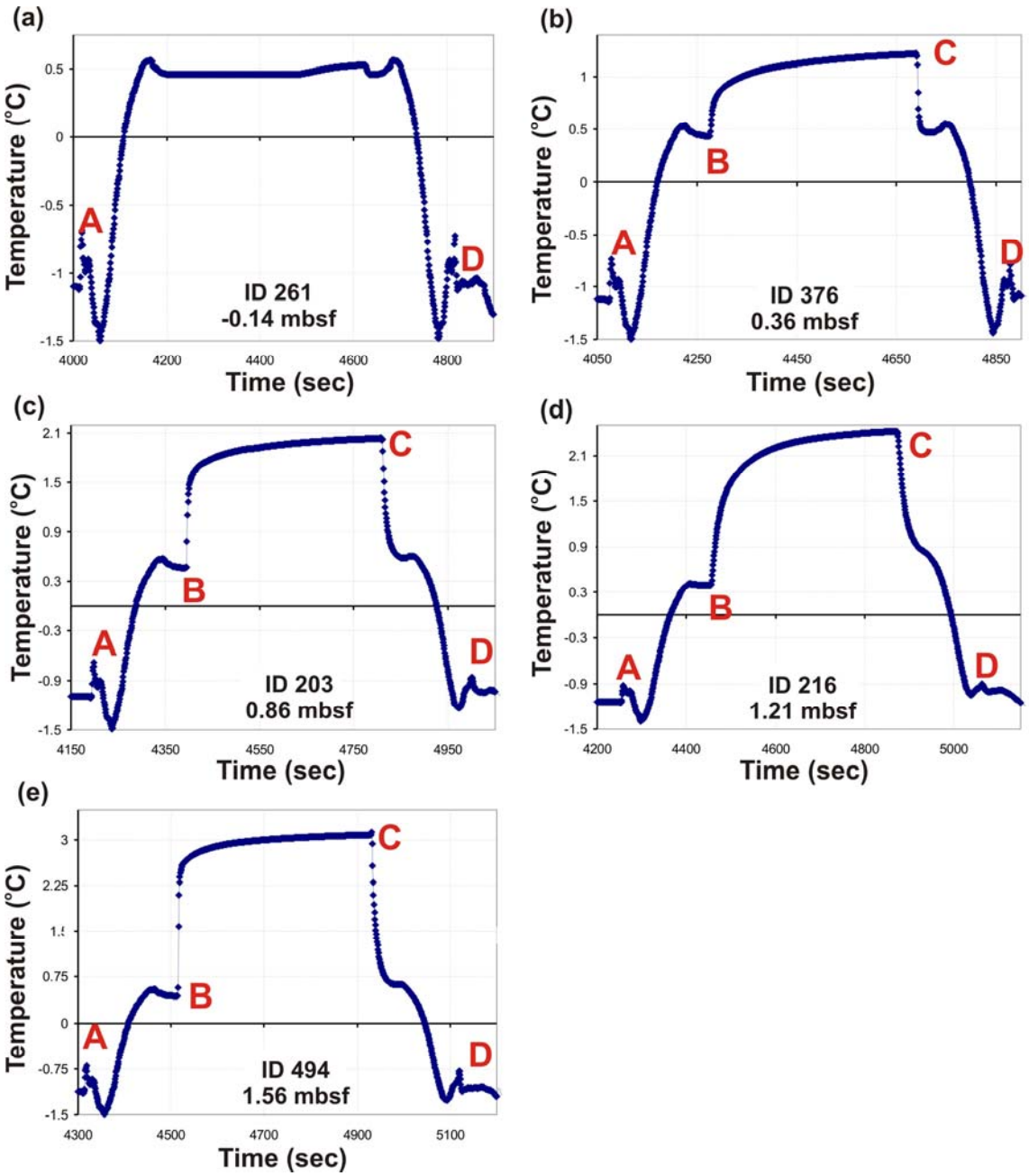

Figure A.3.11.1 Temperature records at Station 103 for MTL (a) ID 261 at -0.14 mbsf, (b) ID 376 at 0.36 mbsf, (c) ID 203 at 0.86 mbsf, (d) ID 216 at 1.21 mbsf, and (e) ID 494 at 1.56 mbsf. A: Core deployed, B: frictional heating pulse from core entering the sediment, C: frictional heating pulse from core pulled out of sediment, D: core back on deck. The top-most logger does not show a frictional heating pulse, which confirms the apparent core penetration that puts this logger above the seafloor.

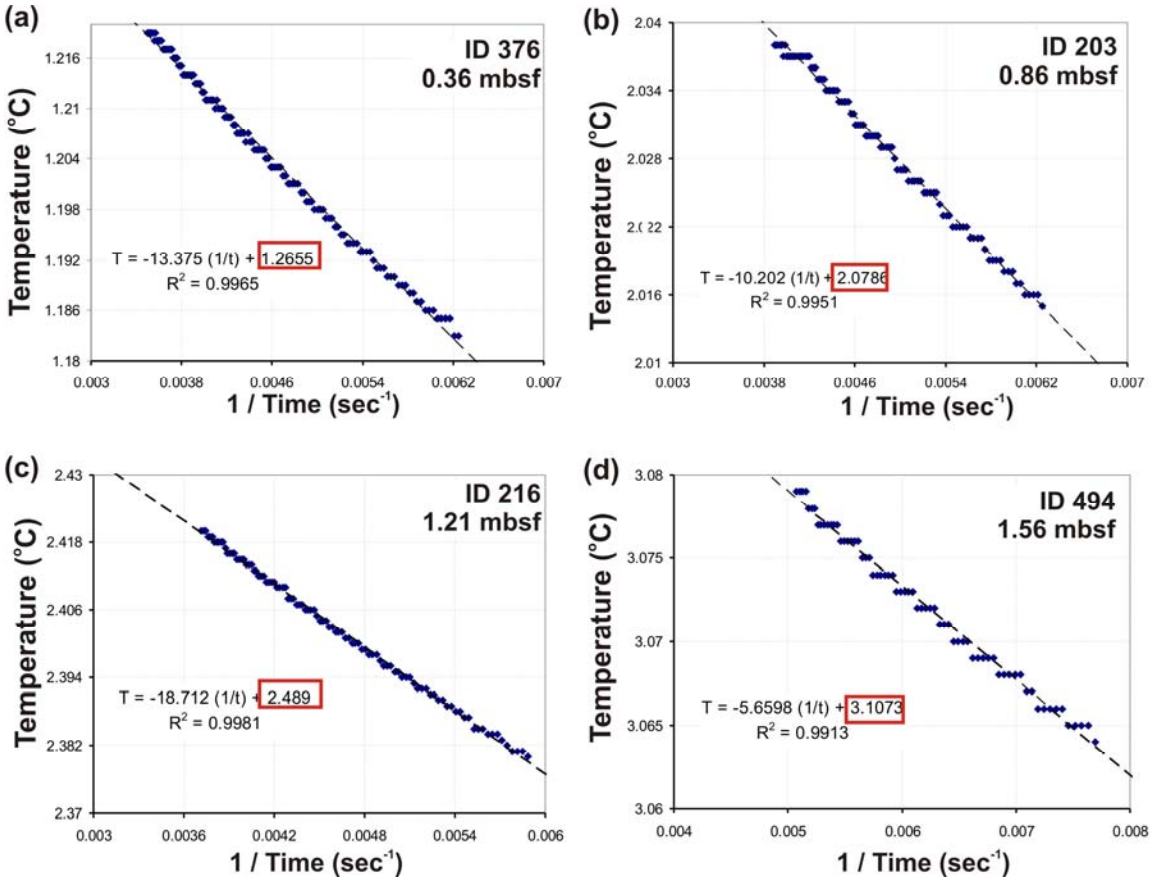

Figure A.3.11.2 Linear regression analysis to estimate equilibrium in situ temperature at Station 103 for the last ~100 seconds prior to pulling out of the core for each MTL: (a) ID 376 at 0.36 mbsf, (b) ID 203 at 0.86 mbsf, (c) ID 216 at 1.21 mbsf, and (d) ID 494 at 1.56 mbsf. Estimated equilibrium temperatures from the best-fit linear equation are highlighted in the red boxes for each MTL.

A.3.12 420 meter water depth expulsion feature, Station 105

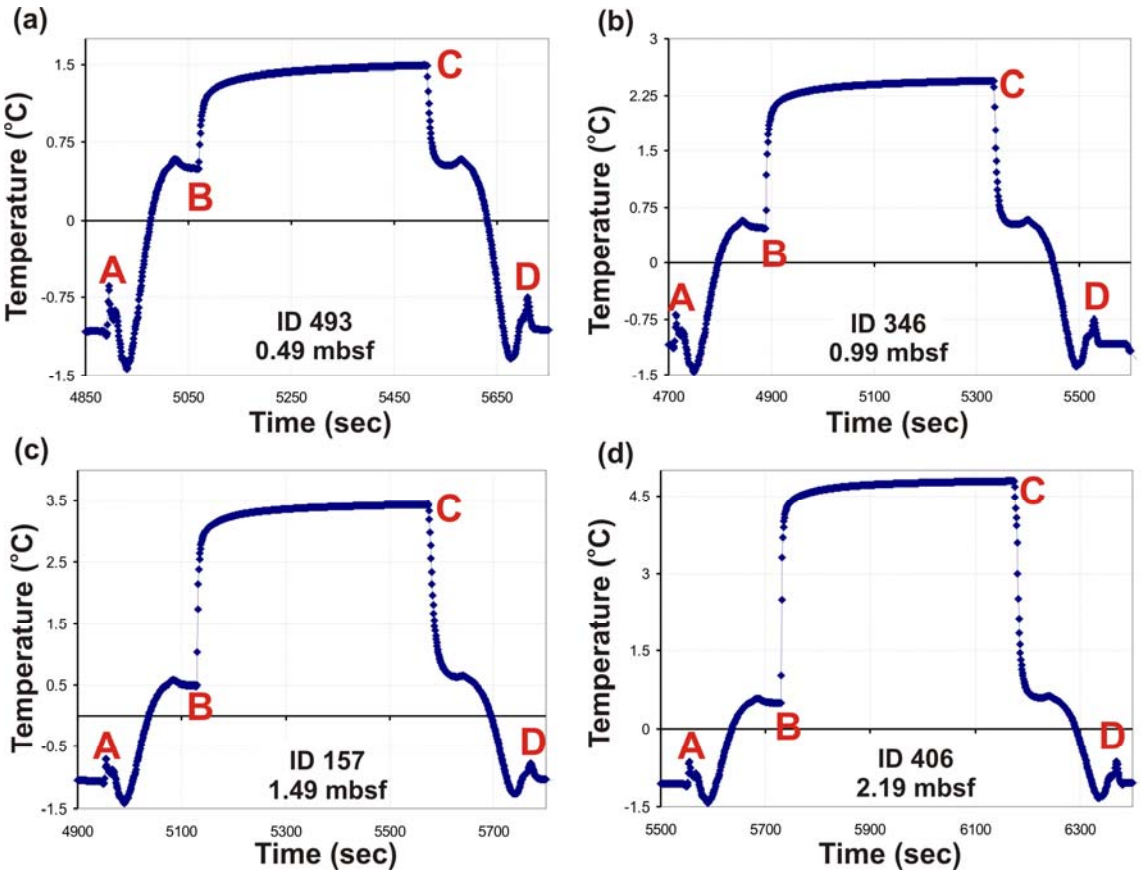

Figure A.3.12.1 Temperature records at Station 105 for MTL (a) ID 493 at 0.49 mbsf, (b) ID 346 at 0.99 mbsf, (c) ID 157 at 1.49 mbsf, and (d) ID 406 at 2.19 mbsf. A: Core deployed, B: frictional heating pulse from core entering the sediment, C: frictional heating pulse from core pulled out of sediment, D: core back on deck.

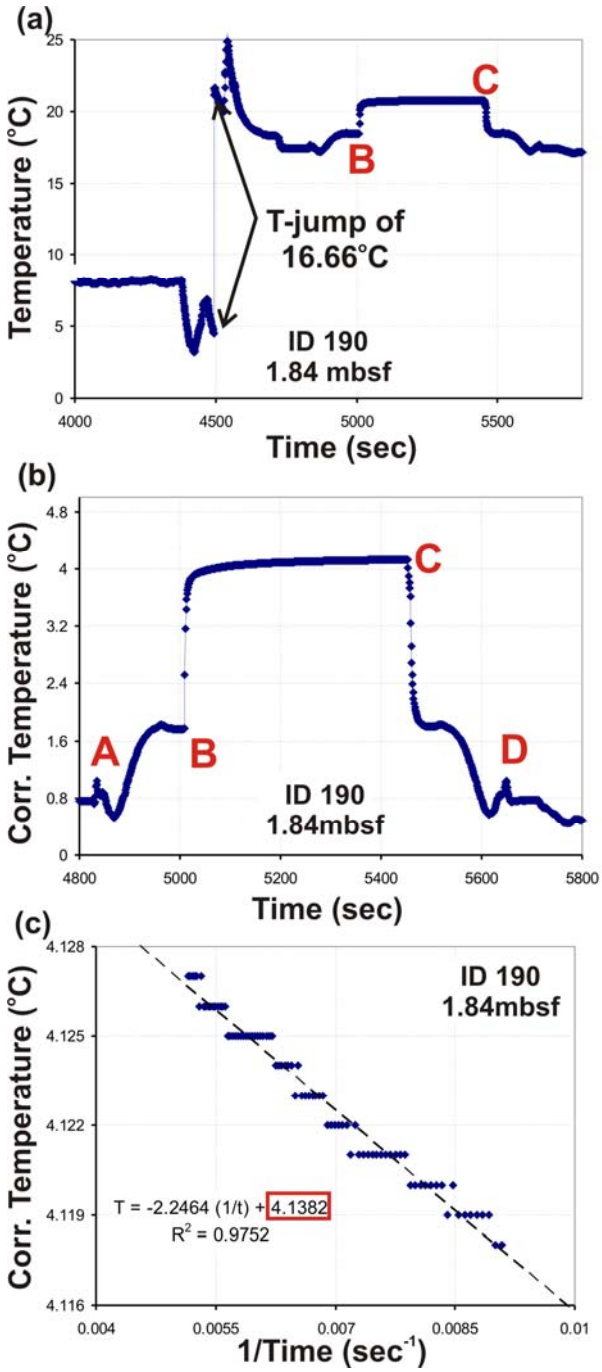

Figure A.3.12.2 Temperature record at Station 105 for (a) MTL ID 190 at 1.84 mbsf with temperature-jump of 16.66ºC, (b) corrected temperature (subtracting 16.66ºC after jump occurred), and (c) subsequent linear regression analysis to estimate equilibrium in situ temperature. B: frictional heating pulse from core entering the sediment, C: frictional heating pulse from core pulled out of sediment. The final temperature after the correction is 4.127ºC (which fits perfectly onto the thermal gradient defined by all other stations, see Figure 16 above).

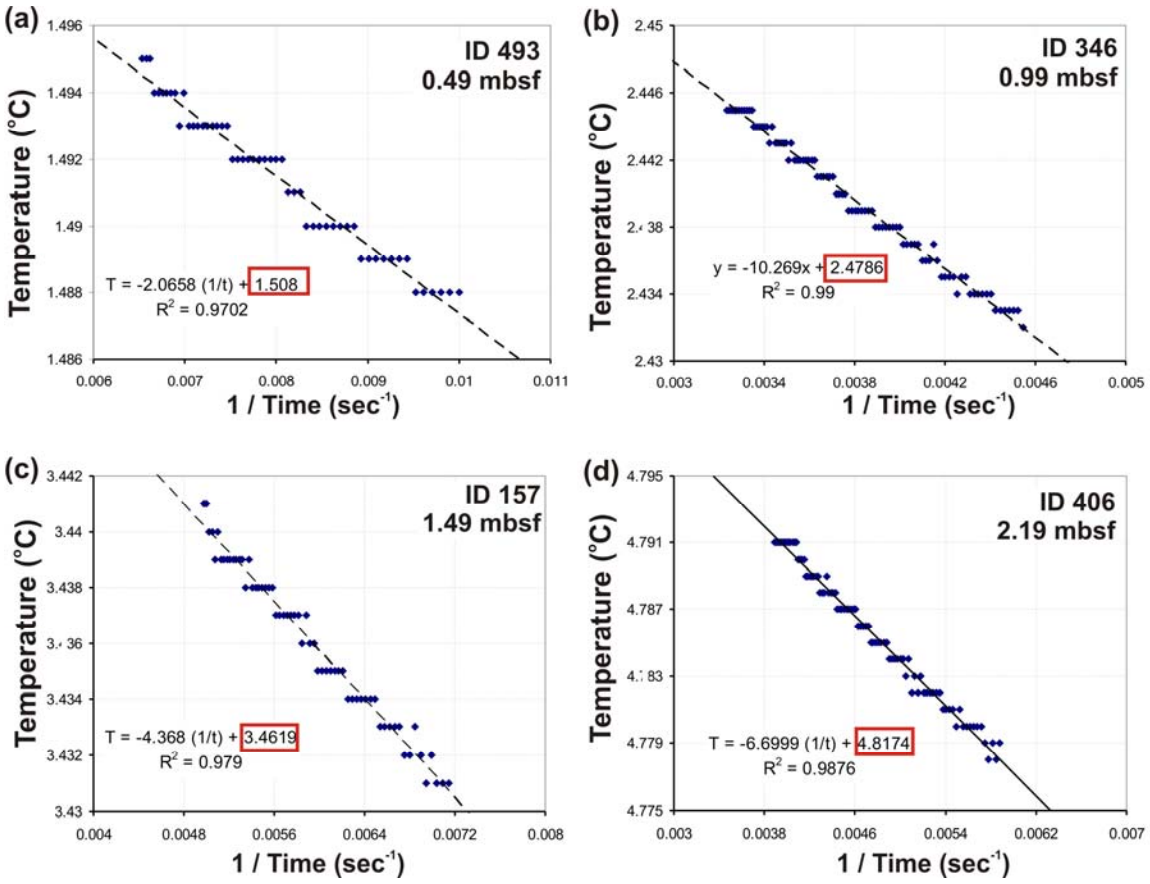

Figure A.3.12.3 Linear regression analysis to estimate equilibrium in situ temperature at Station 105 for the last ~100 seconds prior to pulling out of the core for each MTL: (a) ID 493 at 0.49 mbsf, (b) ID 346 at 0.99 mbsf, (c) ID 157 at 1.49 mbsf, and (d) ID 406 at 2.19 mbsf. Estimated equilibrium temperatures from the best-fit linear equation are highlighted in the red boxes for each MTL.

A.4.1 760 meter water depth expulsion feature, Station 75

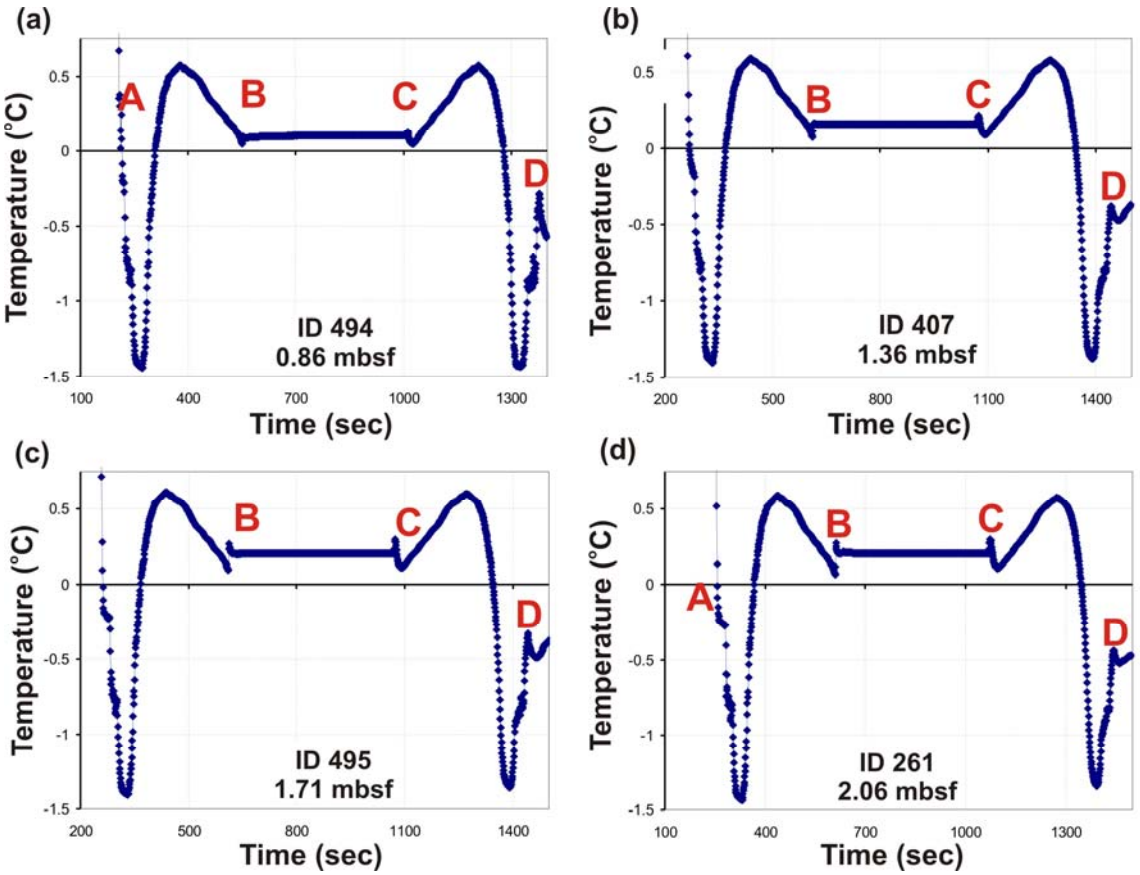

Figure A.4.1 Temperature records at Station 75 for MTL (a) ID 494 at 0.86 mbsf, (b) ID 407 at 1.36 mbsf, (c) ID 495 at 1.71 mbsf, and (d) ID 261 at 2.06 mbsf. A: Core deployed, B: frictional heating pulse from core entering the sediment, C: frictional heating pulse from core pulled out of sediment, D: core back on deck.

A.4.2 760 meter water depth expulsion feature, Station 76

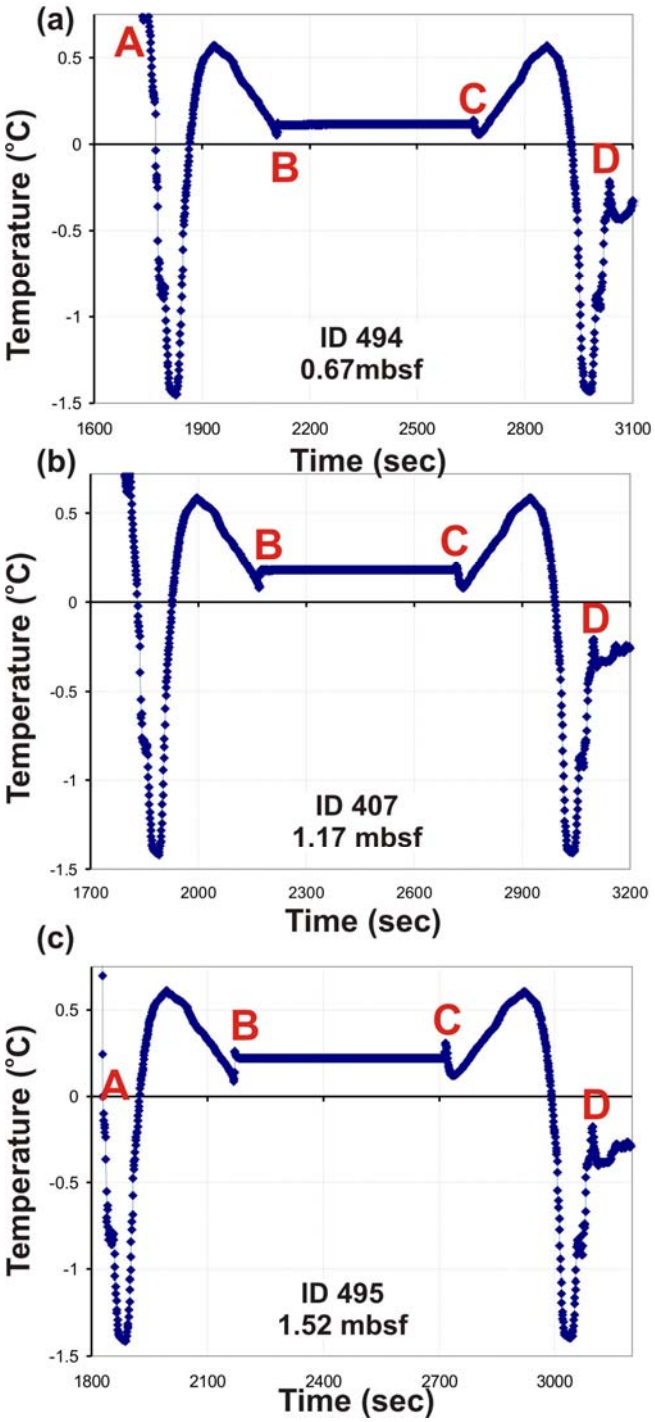

Figure A.4.2.1 Temperature records at Station 76 for MTL (a) ID 494 at 0.67 mbsf, (b) ID 407 at 1.17 mbsf, and (c) ID 495 at 1.52 mbsf. A: Core deployed, B: frictional heating pulse from core entering the sediment, C: frictional heating pulse from core pulled out of sediment, D: core back on deck.

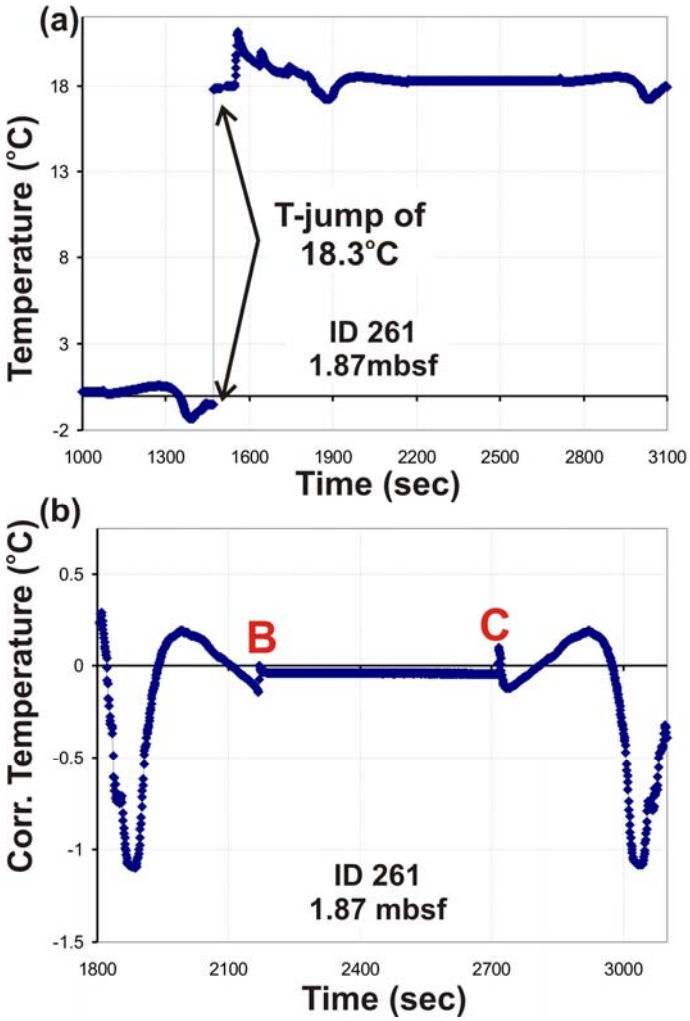

Figure A.4.2.2 Temperature record at Station 76 for (a) MTL ID 261 at 1.87 mbsf with temperature-jump of 18.3ºC, and (b) corrected temperature (subtracting 18.3ºC after jump occurred). B: frictional heating pulse from core entering the sediment, C: frictional heating pulse from core pulled out of sediment. The final temperature after the correction is -0.03ºC.

A.4.3 760 meter water depth expulsion feature, Station 77

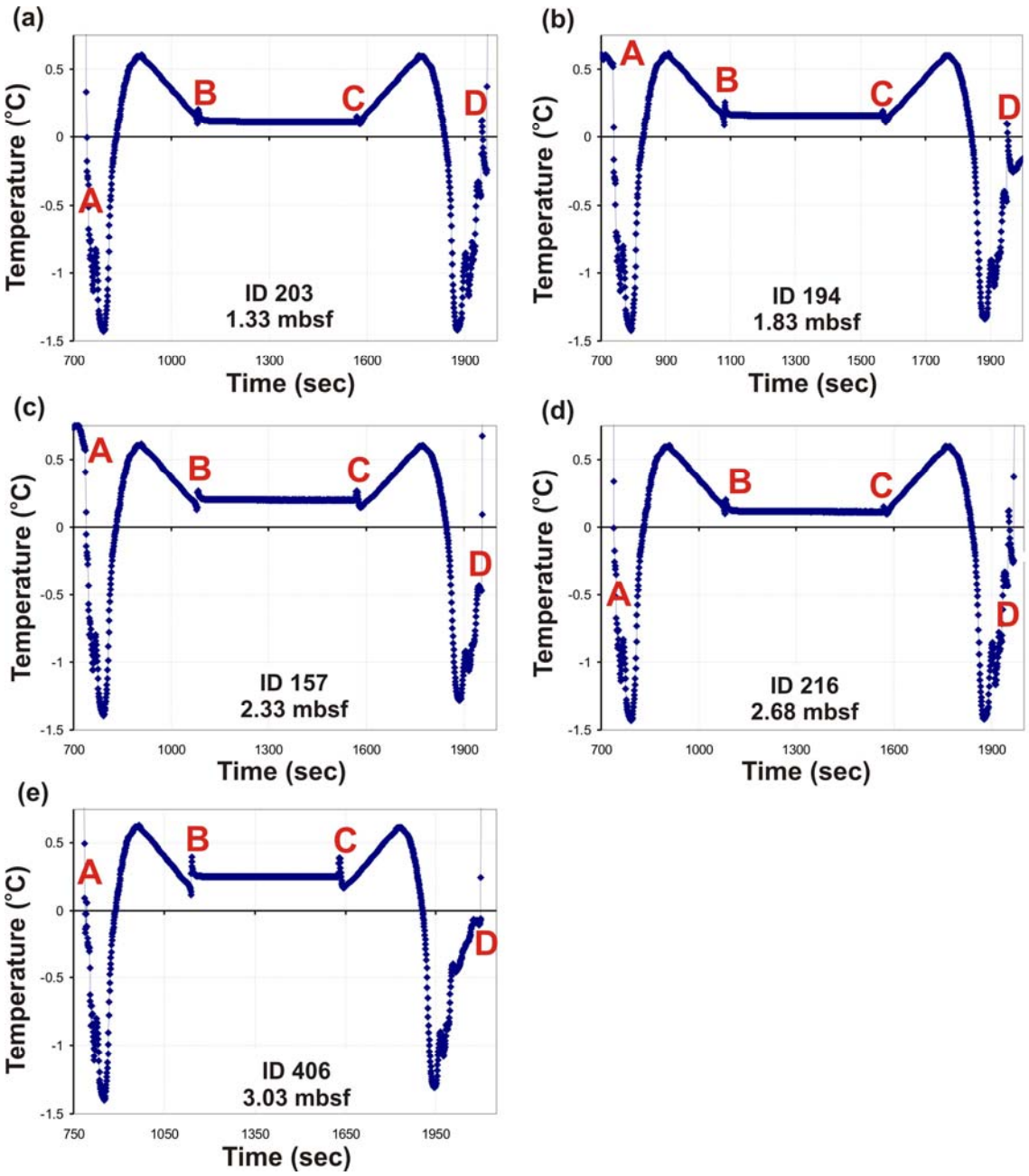

Figure A.4.3 Temperature records at Station 77 for MTL (a) ID 203 at 1.33 mbsf, (b) ID 194 at 1.83 mbsf, (c) ID 157 at 2.33 mbsf, (d) ID 216 at 2.68 mbsf, and (e) ID 406 at 3.03 mbsf. A: Core deployed, B: frictional heating pulse from core entering the sediment, C: frictional heating pulse from core pulled out of sediment, D: core back on deck.

A.4.4 760 meter water depth expulsion feature, Station 78

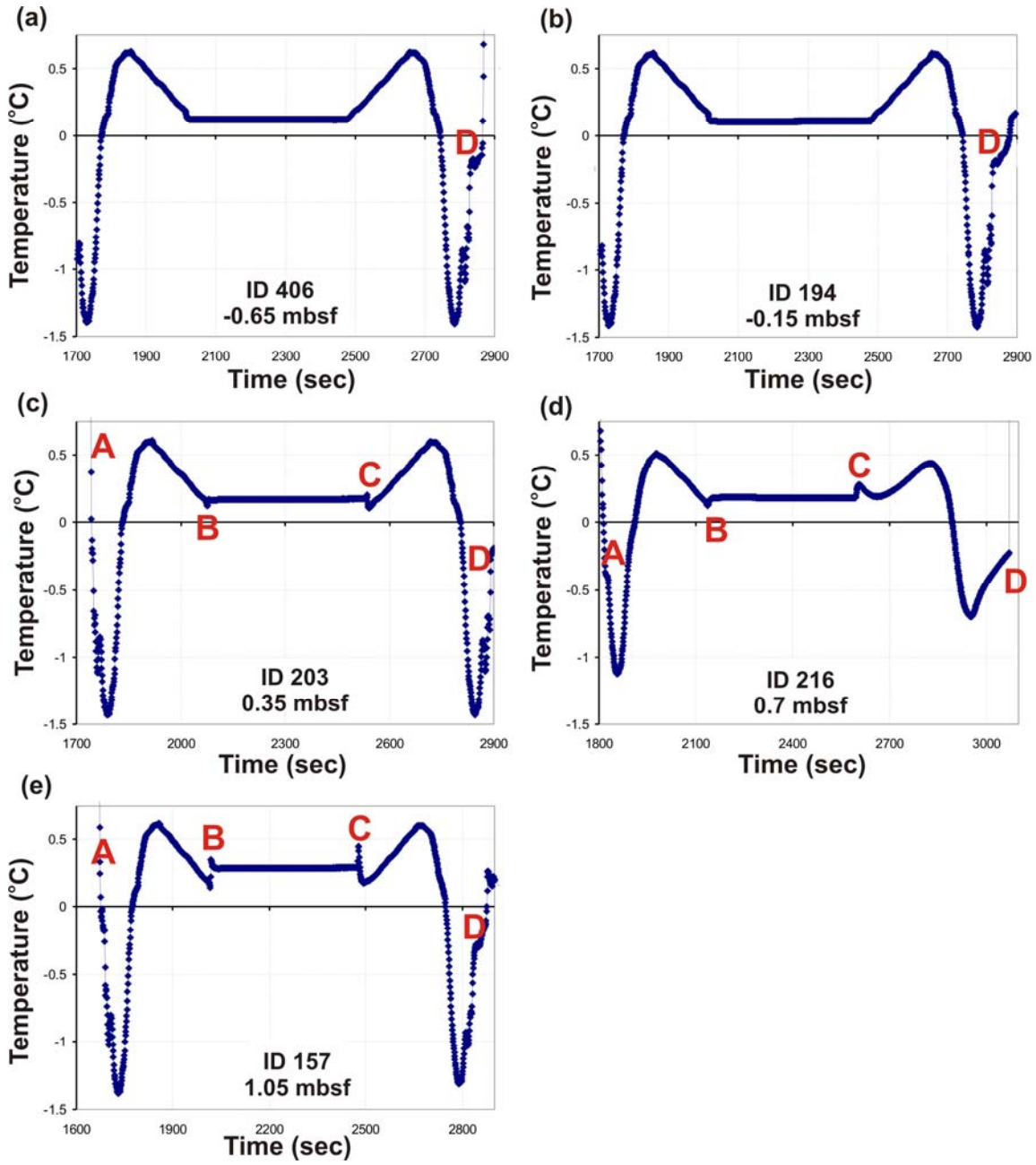

Figure A.4.4 Temperature records at Station 78 for MTL (a) ID 406 at -0.65 mbsf, (b) ID 194 at -0.15 mbsf, (c) ID 203 at 0.35 mbsf, (d) ID 216 at 0.7 mbsf, and (e) ID 157 at 1.05 mbsf. A: Core deployed, B: frictional heating pulse from core entering the sediment, C: frictional heating pulse from core pulled out of sediment, D: core back on deck.

A.4.5 760 meter water depth expulsion feature, Station 79

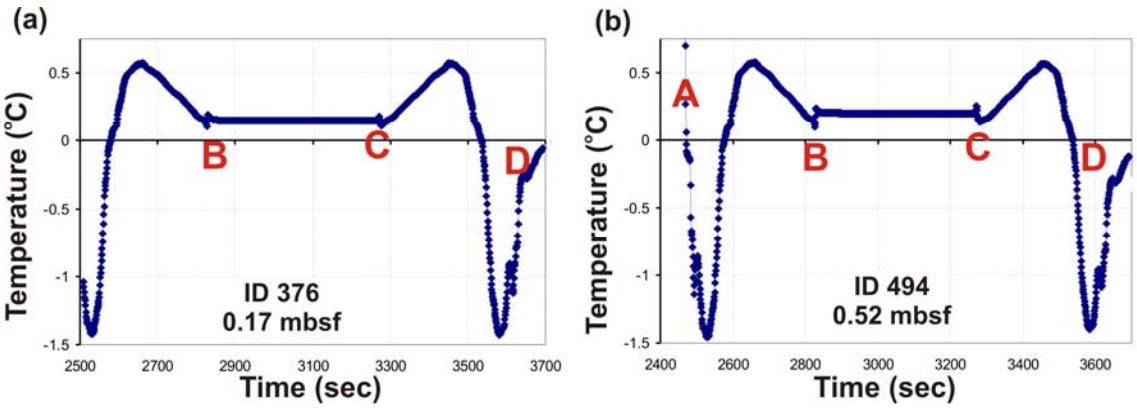

Figure A.4.5.1 Temperature records at Station 79 for MTL (a) ID 376 at 0.17 mbsf, and (b) ID 494 at 0.52 mbsf. A: Core deployed, B: frictional heating pulse from core entering the sediment, C: frictional heating pulse from core pulled out of sediment, D: core back on deck.

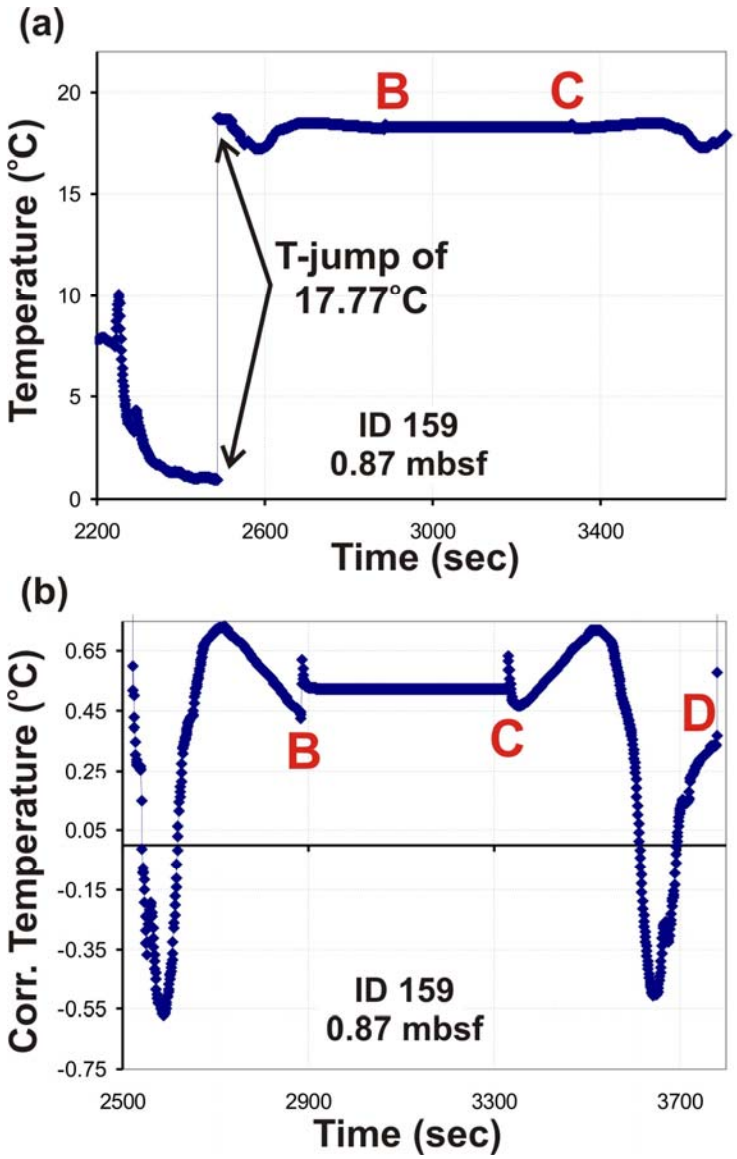

Figure A.4.5.2 Temperature record at Station 79 for (a) MTL ID 159 at 0.87 mbsf with temperature-jump of 17.77ºC, and (b) corrected temperature (subtracting 17.77ºC after jump occurred). B: frictional heating pulse from core entering the sediment, C: frictional heating pulse from core pulled out of sediment. The final temperature after the correction is -0.03ºC.

A.4.6 760 meter water depth expulsion feature, Station 80

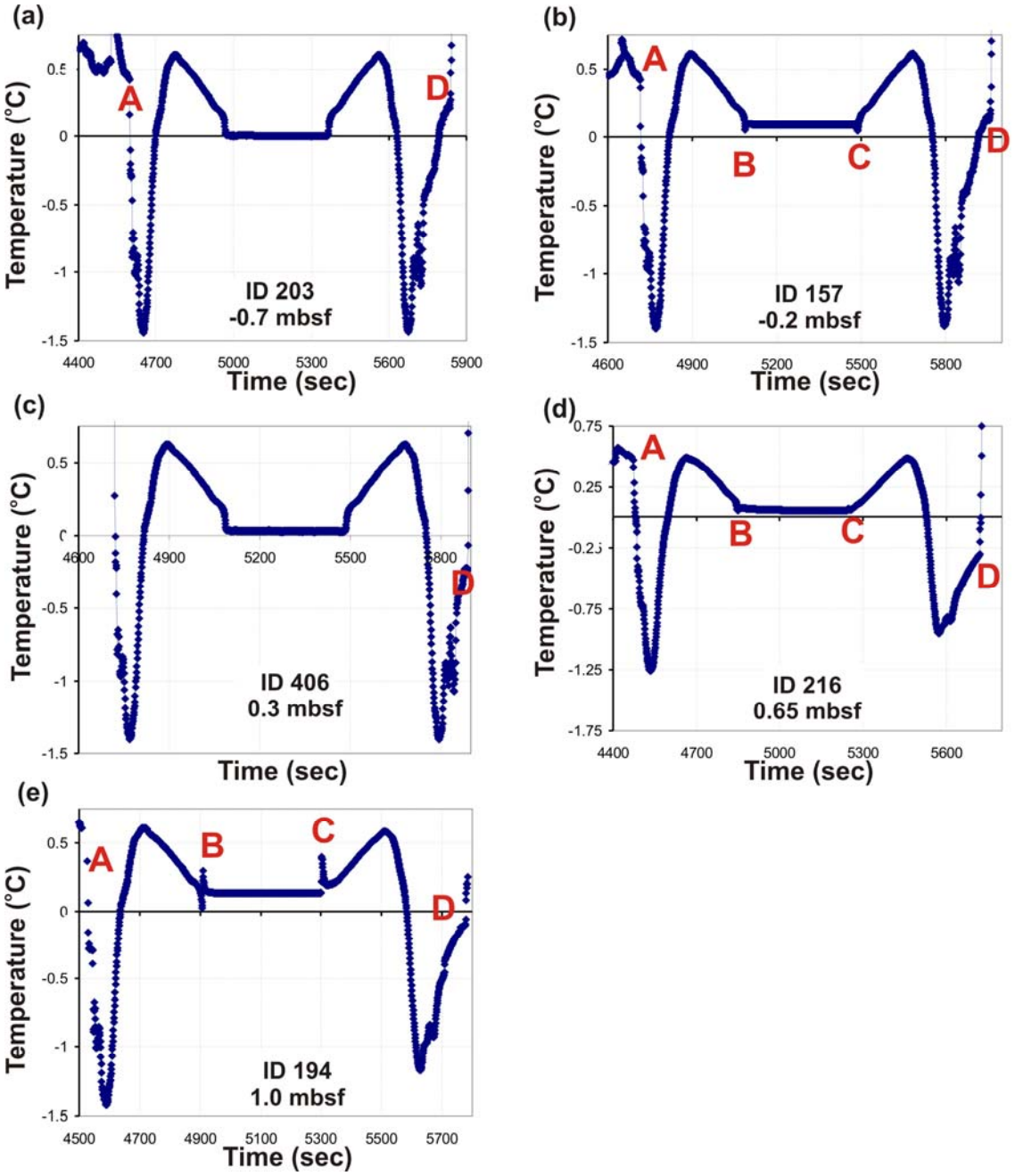

Figure A.4.6 Temperature records at Station 80 for MTL (a) ID 406 at -0.65 mbsf, (b) ID 194 at -0.15 mbsf, (c) ID 203 at 0.35 mbsf, (d) ID 216 at 0.7 mbsf, and (e) ID 157 at 1.05 mbsf. A: Core deployed, B: frictional heating pulse from core entering the sediment, C: frictional heating pulse from core pulled out of sediment, D: core back on deck.
No frictional heating pulses occur at MTLs ID 203 and 406 although ID157 is supposedly "above" the seafloor, but it shows frictional pulses. Field Notes by K. Aßhoff are inconclusive if a switch in logger happened. No corrections to the assigned depths were made, other than adjusting for apparent penetration.

A.5.1 Canyon West, Station 31

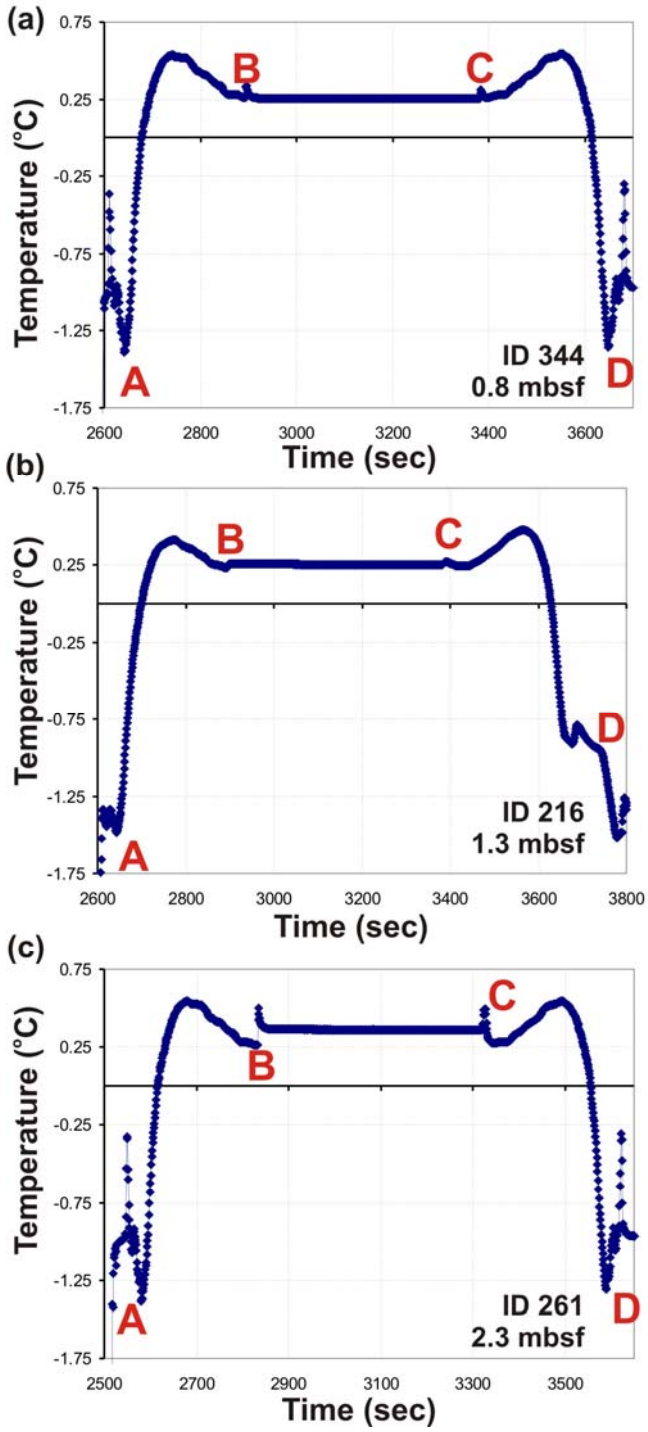

Figure A.5.1 Temperature records at Station 31 for MTL (a) ID 344 at 0.8 mbsf, (b) ID 216 at 1.3 mbsf, and (c) ID 261 at 2.3 mbsf. A: Core deployed, B: frictional heating pulse from core entering the sediment, C: frictional heating pulse from core pulled out of sediment, D: core back on deck.

A.5.2 Canyon West, Station 32

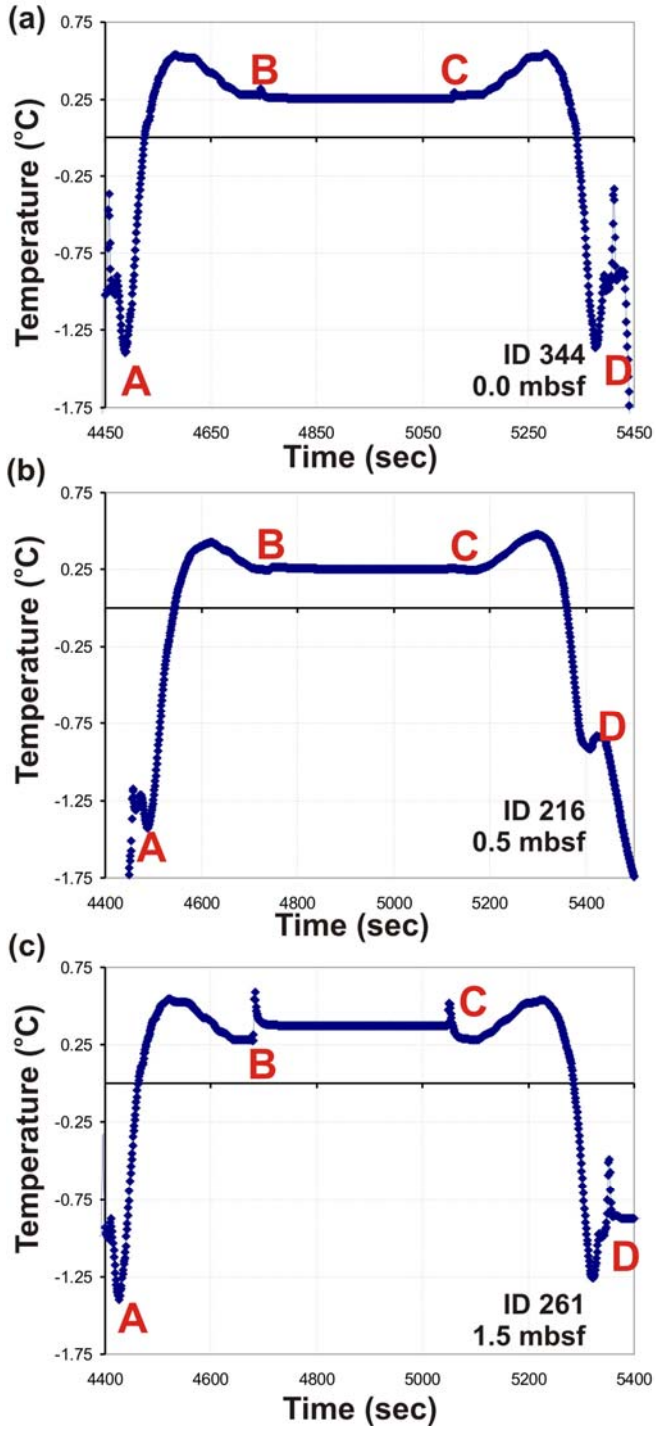

Figure A.5.2 Temperature records at Station 32 for MTL (a) ID 344 at 0.8 mbsf, (b) ID 216 at 1.3 mbsf, and (c) ID 261 at 2.3 mbsf. A: Core deployed, B: frictional heating pulse from core entering the sediment, C: frictional heating pulse from core pulled out of sediment, D: core back on deck.

A.5.3 Canyon West, Station 33

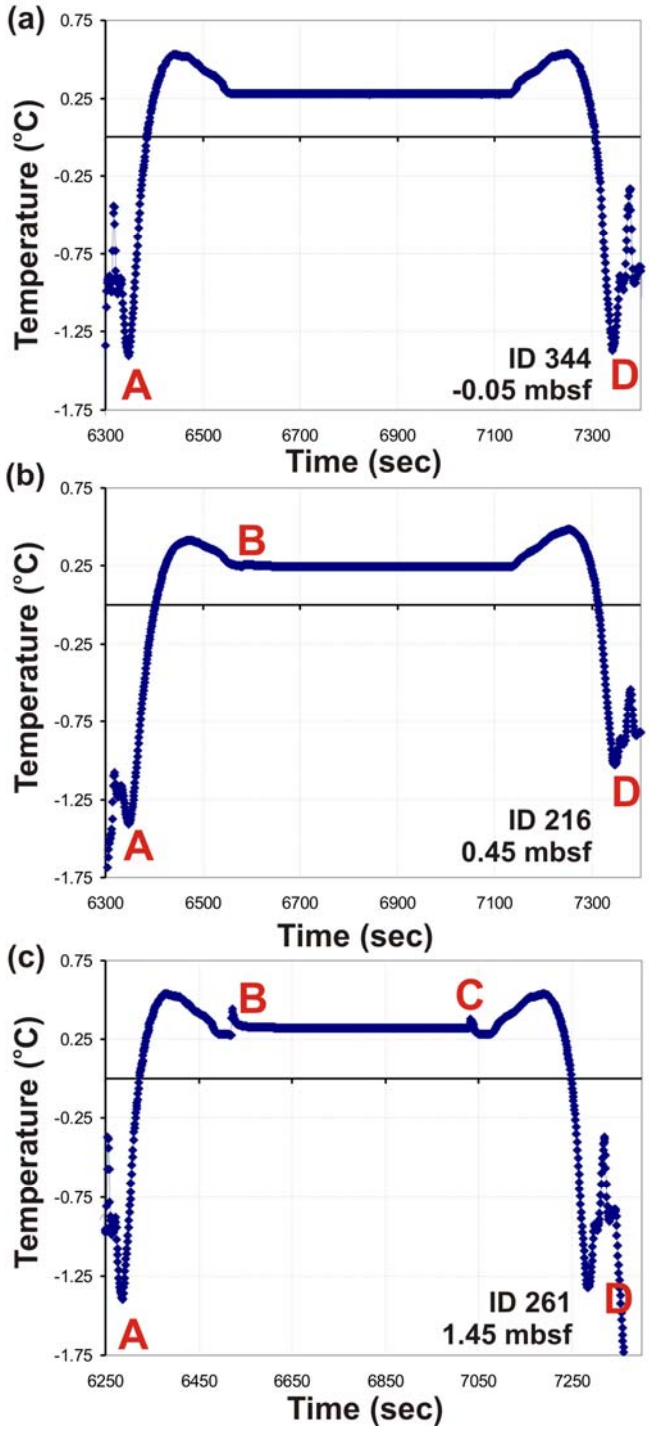

Figure A.5.3 Temperature records at Station 33 for MTL (a) ID 344 at 0.8 mbsf, (b) ID 216 at 1.3 mbsf, and (c) ID 261 at 2.3 mbsf. A: Core deployed, B: frictional heating pulse from core entering the sediment, C: frictional heating pulse from core pulled out of sediment, D: core back on deck.

A.5.4 Canyon West, Station 34

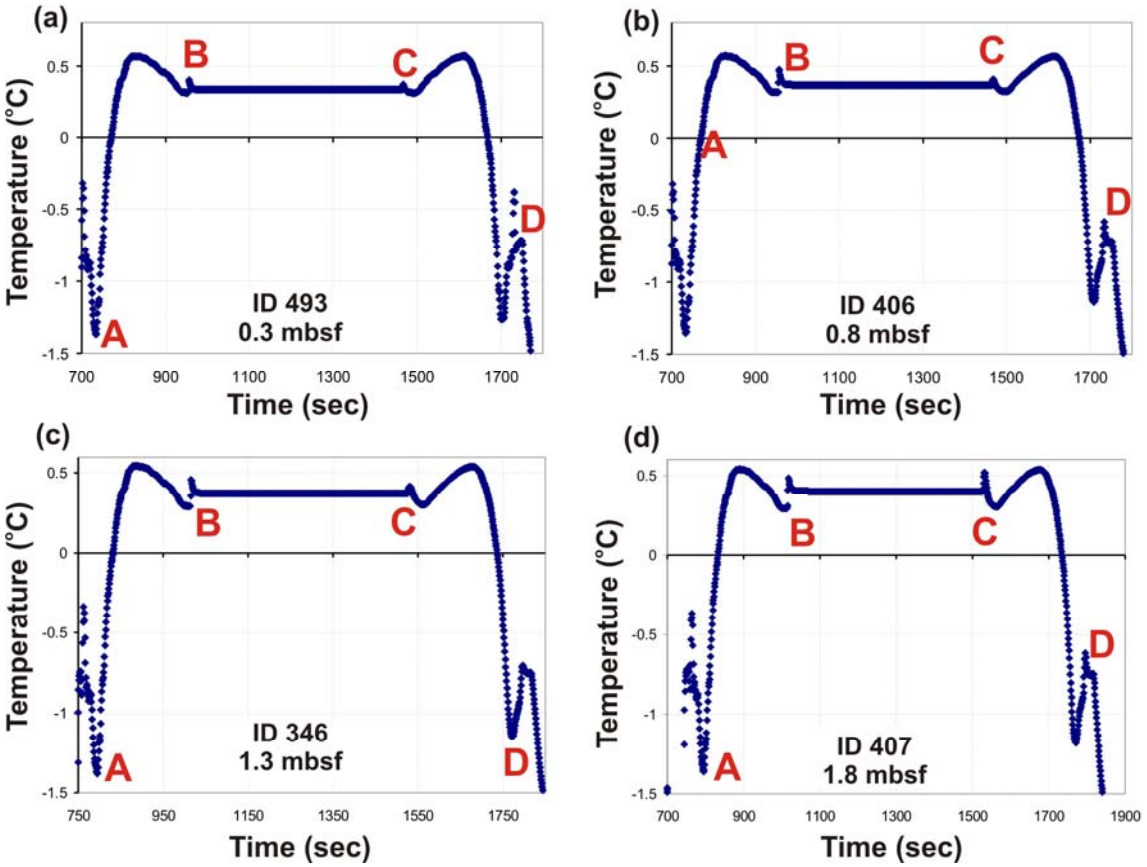

Figure A.5.4 Temperature records at Station 34 for MTL (a) ID 493 at 0.3 mbsf, (b) ID 406 at 0.8 mbsf, (c) ID 346 at 1.3 mbsf, and (d) ID 407 at 1.8 mbsf. A: Core deployed, B: frictional heating pulse from core entering the sediment, C: frictional heating pulse from core pulled out of sediment, D: core back on deck.

A.5.5 Canyon West, Station 35

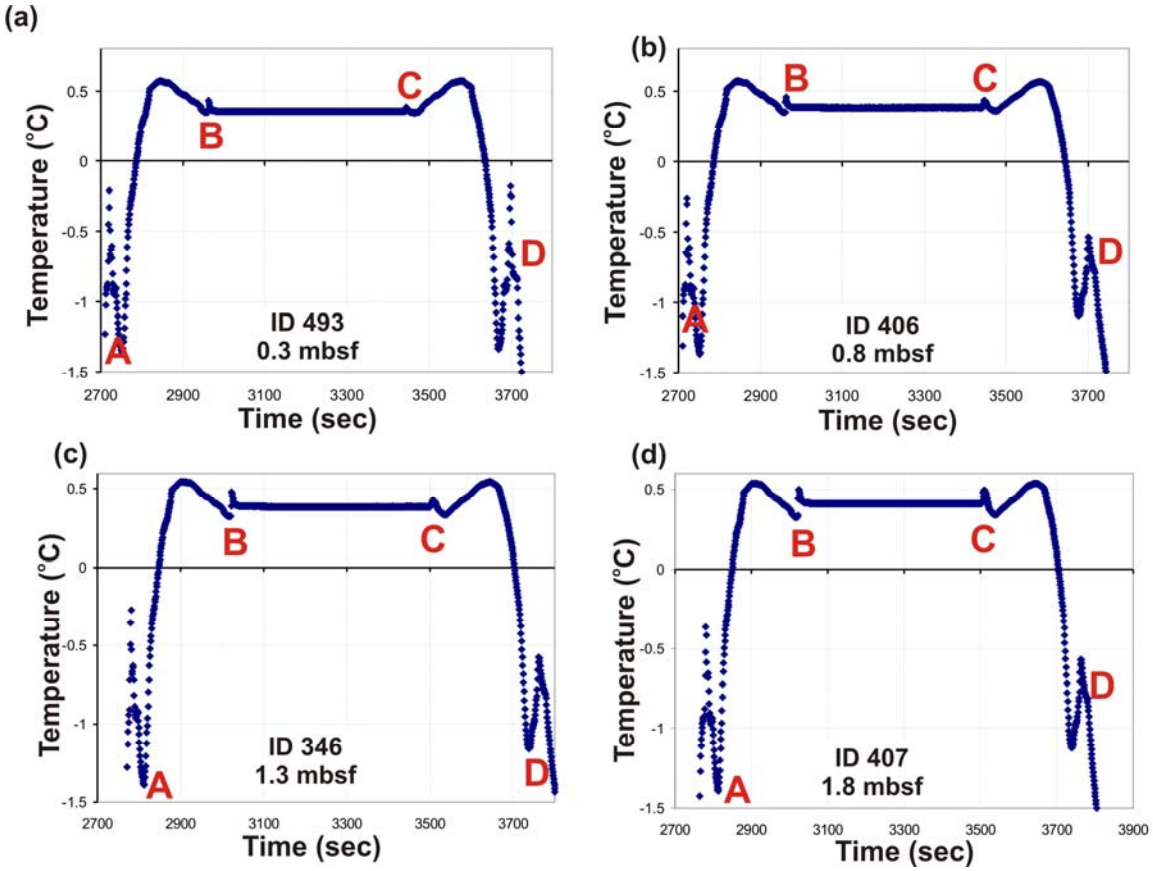

Figure A.5.5 Temperature records at Station 35 for MTL (a) ID 493 at 0.3 mbsf, (b) ID 406 at 0.8 mbsf, (c) ID 346 at 1.3 mbsf, and (d) ID 407 at 1.8 mbsf. A: Core deployed, B: frictional heating pulse from core entering the sediment, C: frictional heating pulse from core pulled out of sediment, D: core back on deck.

A.5.6 Canyon West, Station 94

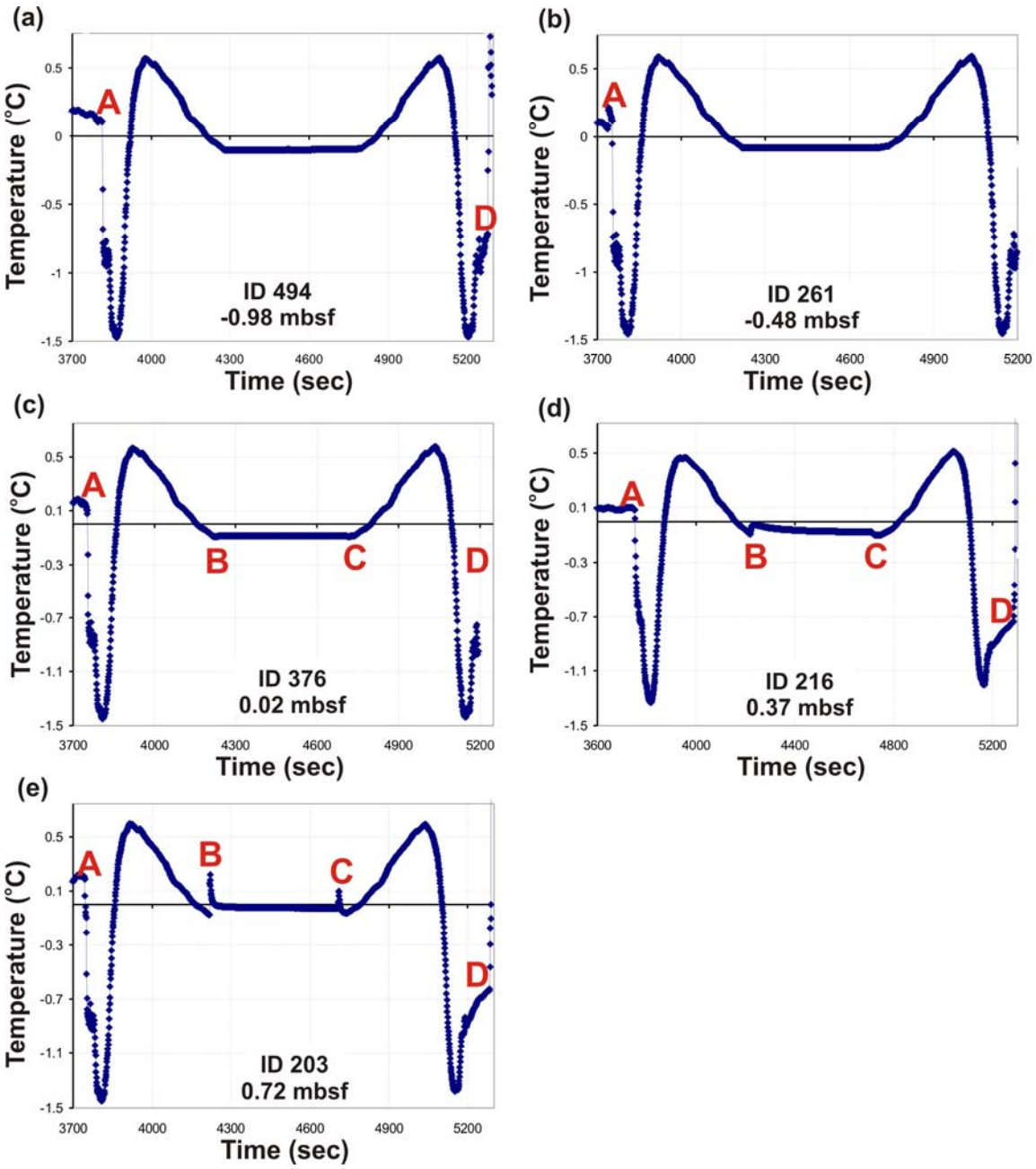

Figure A.5.6 Temperature records at Station 94 for MTL (a) ID 494 at -0.98 mbsf, (b) ID 261 at -0.48 mbsf, (c) ID 376 at 0.02 mbsf, (d) ID 216 at 0.37 mbsf, and (e) ID 203 at 0.72 mbsf. A: Core deployed, B: frictional heating pulse from core entering the sediment, C: frictional heating pulse from core pulled out of sediment, D: core back on deck. The two top-most loggers (ID 494 and ID 261) do not show any frictional heating pulse, confirming the low apparent core penetration that puts these loggers above the seafloor.

A.5.7 Canyon West, Station 95

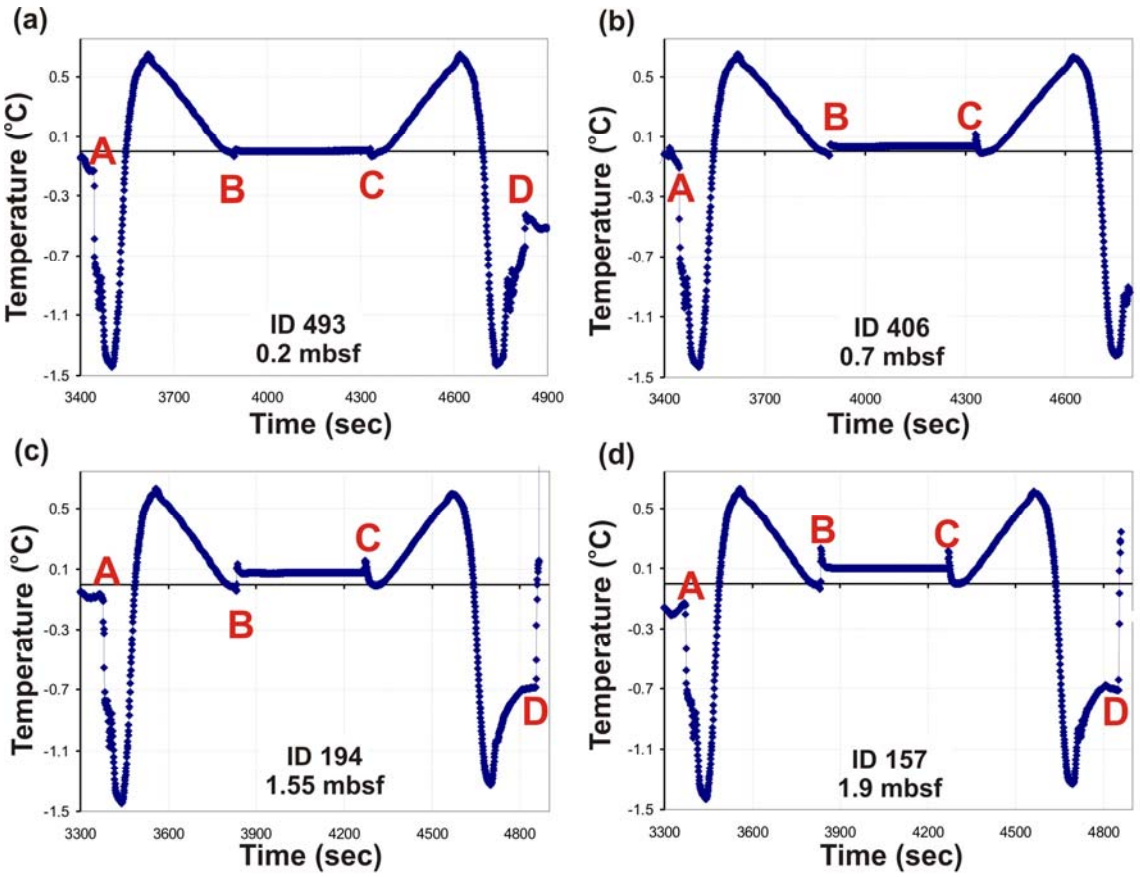

Figure A.5.7 Temperature records at Station 95 for MTL (a) ID 493 at 0.2 mbsf, (b) ID 406 at 0.7 mbsf, (c) ID 194 at 1.55 mbsf, and (d) ID 157 at 1.9 mbsf. A: Core deployed, B: frictional heating pulse from core entering the sediment, C: frictional heating pulse from core pulled out of sediment, D: core back on deck.

A.6.1 Canyon North, Station 67

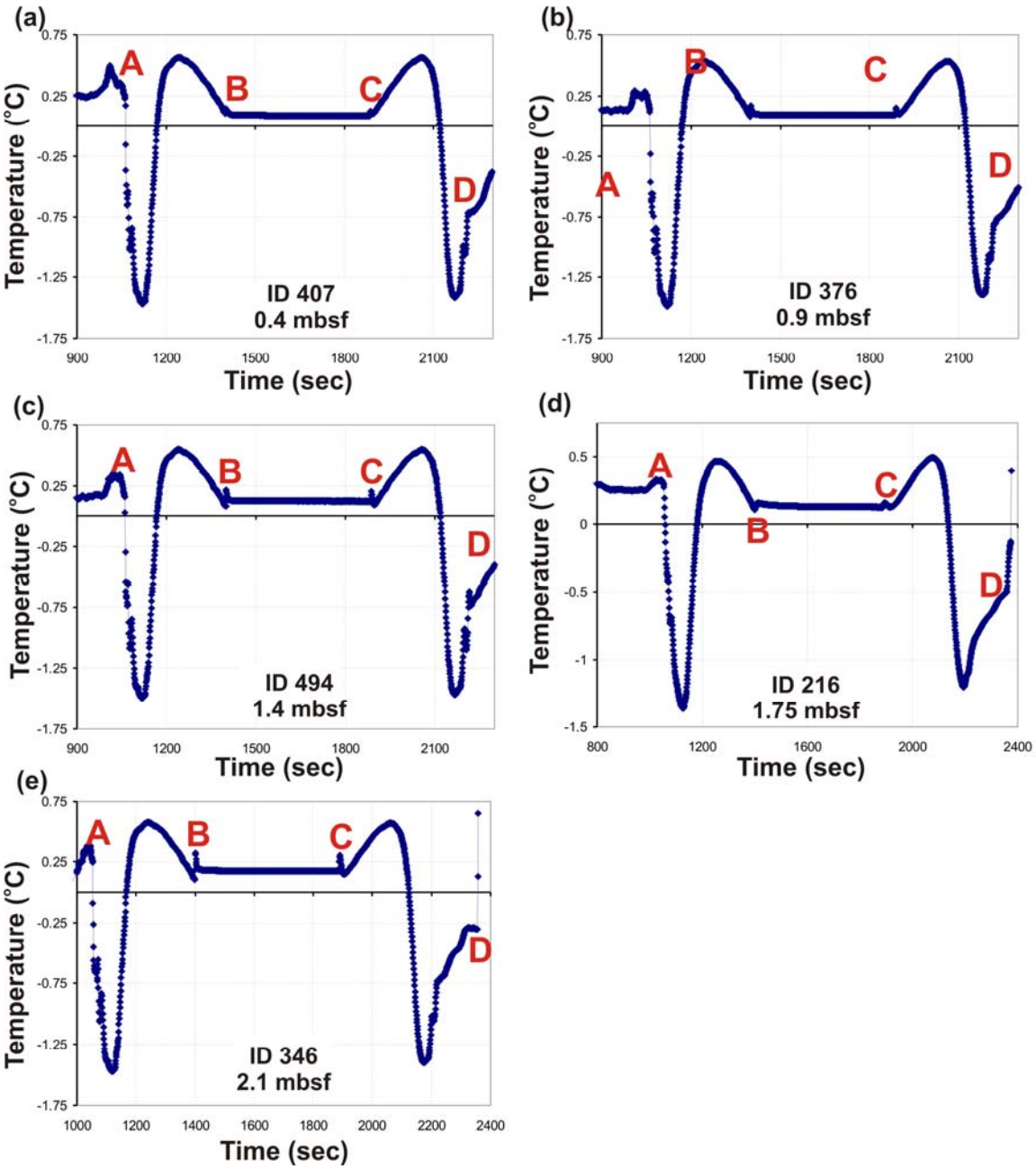

Figure A.6.1 Temperature records at Station 67 for MTL (a) ID 407 at 0.4 mbsf, (b) ID 376 at 0.9 mbsf, (c) ID 494 at 1.4 mbsf, (d) ID 216 at 1.75 mbsf, and (e) ID 346 at 2.1 mbsf. A: Core deployed, B: frictional heating pulse from core entering the sediment, C: frictional heating pulse from core pulled out of sediment, D: core back on deck.

A.6.2 Canyon North, Station 68

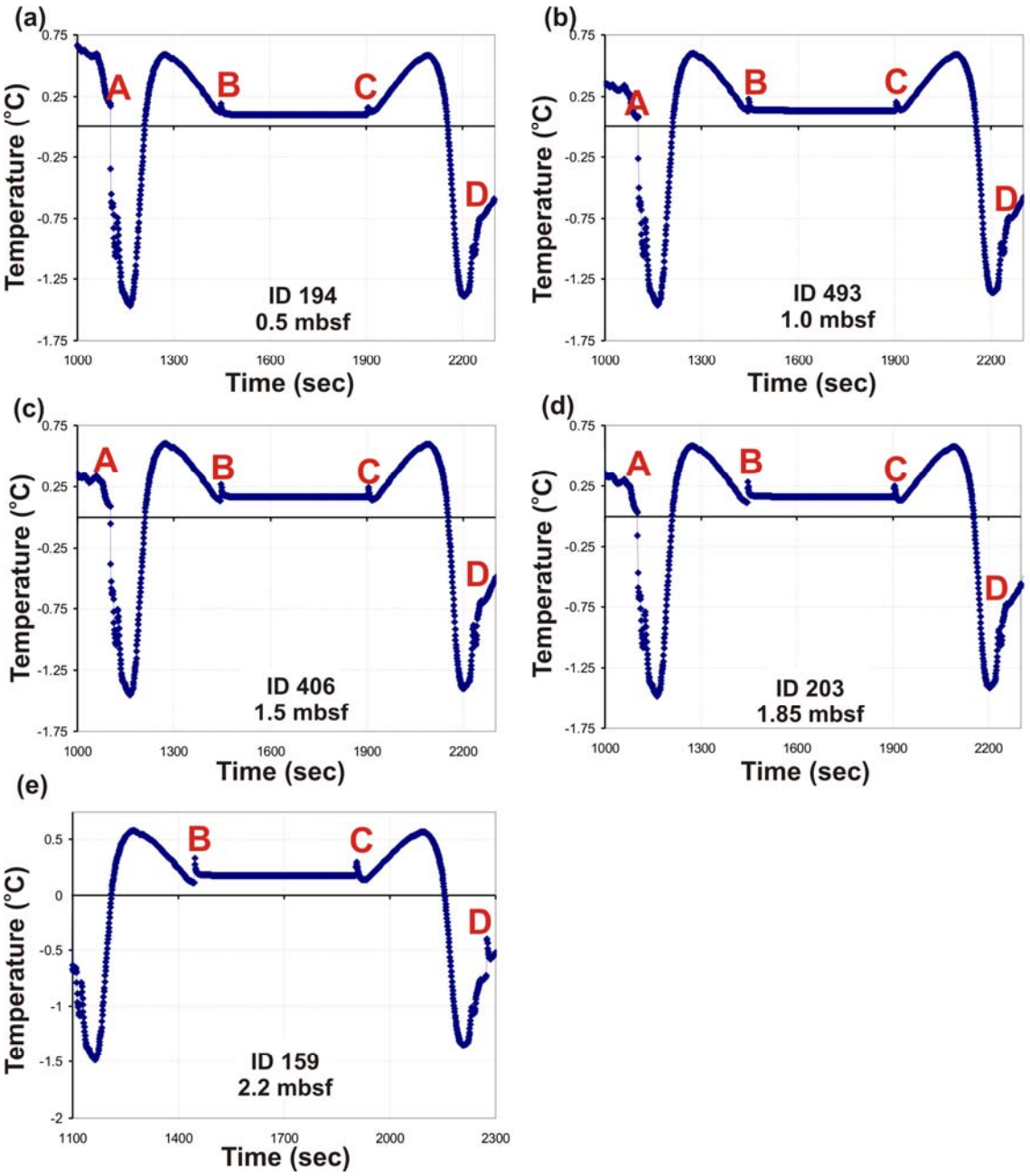

Figure A.6.2 Temperature records at Station 68 for MTL (a) ID 197 at 0.5 mbsf, (b) ID 493 at 1.0 mbsf, (c) ID 406 at 1.5 mbsf, (d) ID 203 at 1.85 mbsf, and (e) ID 159 at 2.2 mbsf. A: Core deployed, B: frictional heating pulse from core entering the sediment, C: frictional heating pulse from core pulled out of sediment, D: core back on deck.

A.6.3 Canyon North, Station 69

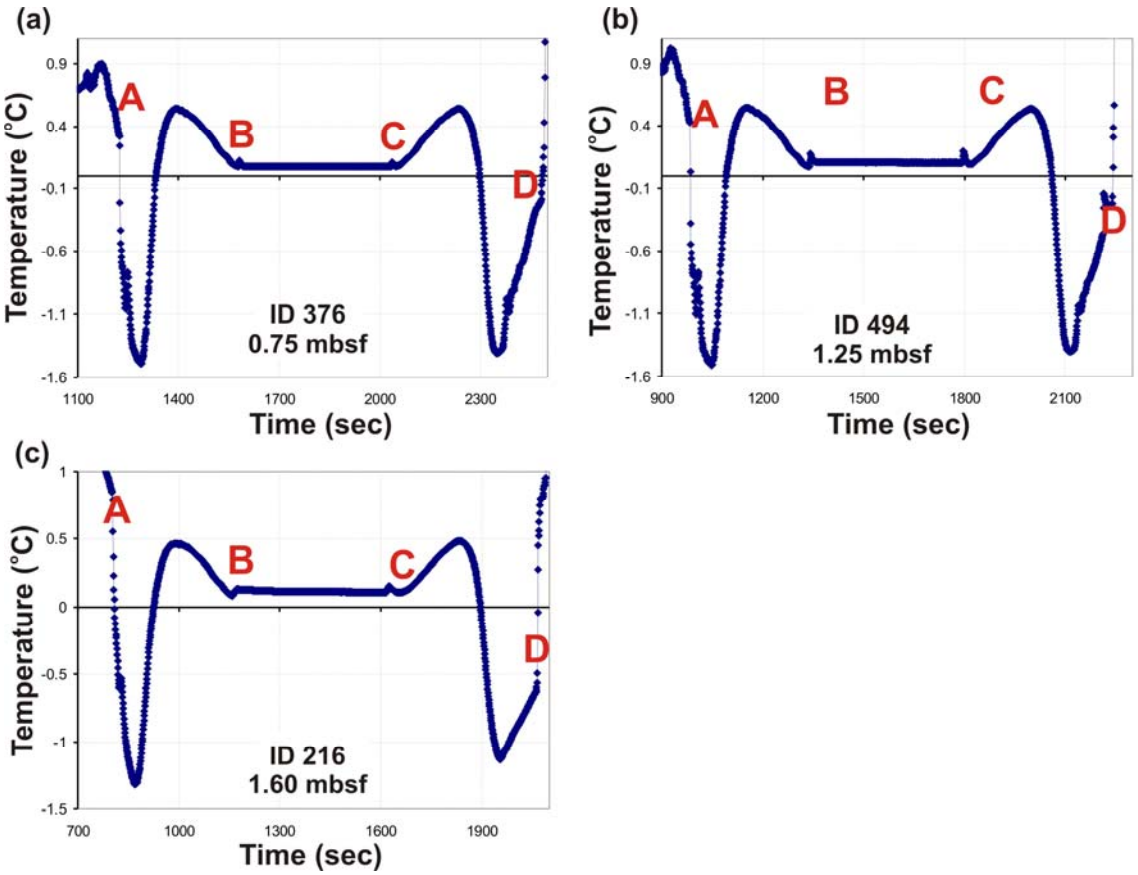

Figure A.6.3 Temperature records at Station 69 for MTL (a) ID 407 at 0.25 mbsf, (b) ID 376 at 0.75 mbsf, (c) ID 494 at 1.25 mbsf, (d) ID 216 at 1.68 mbsf, and (e) ID 346 at 1.95 mbsf. A: Core deployed, B: frictional heating pulse from core entering the sediment, C: frictional heating pulse from core pulled out of sediment, D: core back on deck.

A.6.4 Canyon North, Station 70

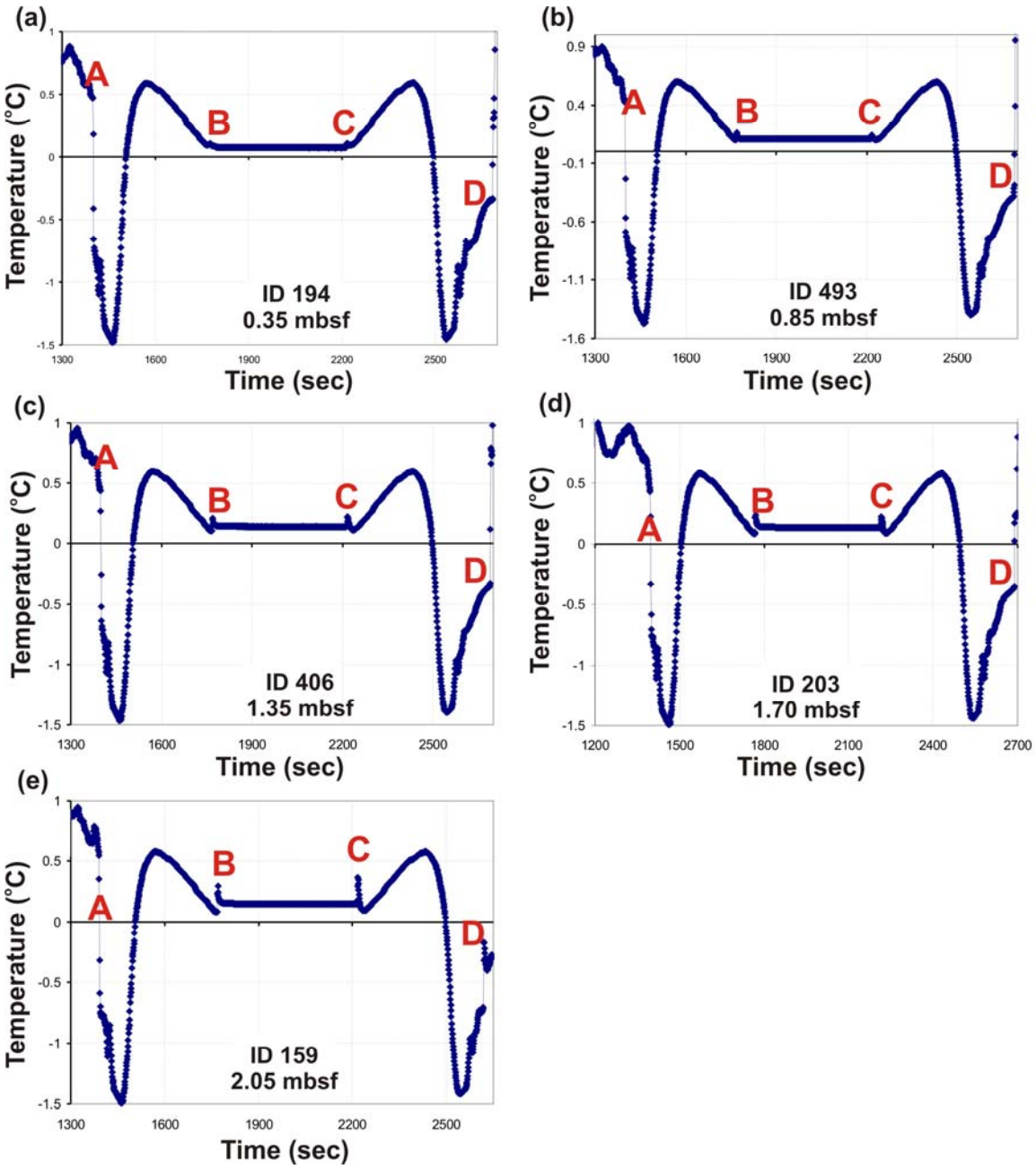

Figure A.6.4 Temperature records at Station 70 for MTL (a) ID 493 at 0.3 mbsf, (b) ID 406 at 0.8 mbsf, (c) ID 346 at 1.3 mbsf, and (d) ID 407 at 1.8 mbsf. A: Core deployed, B: frictional heating pulse from core entering the sediment, C: frictional heating pulse from core pulled out of sediment, D: core back on deck.

A.6.5 Canyon North, Station 71

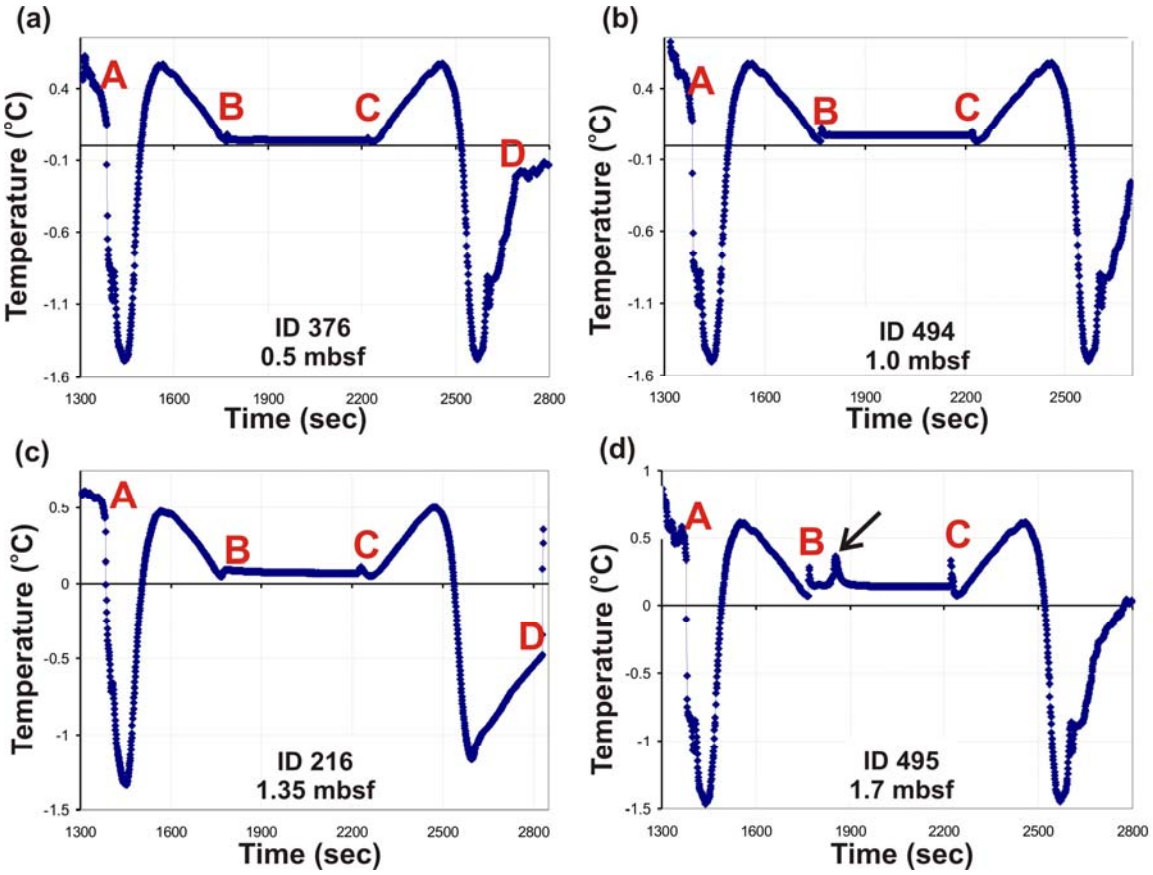

Figure A.6.5 Temperature records at Station 71 for MTL (a) ID 376 at 0.5 mbsf, (b) ID 494 at 1.0 mbsf, (c) ID 216 at 1.35 mbsf, and (d) ID 495 at 1.7 mbsf. A: Core deployed, B: frictional heating pulse from core entering the sediment, C: frictional heating pulse from core pulled out of sediment, D: core back on deck. A secondary friction pulse occurred at the bottom-most MTL ID 495 (indicated by the arrow at ~1840 seconds, about 70 seconds after the core initially penetrated into the sediments).

A.7.1 South of Landslide, Station 111

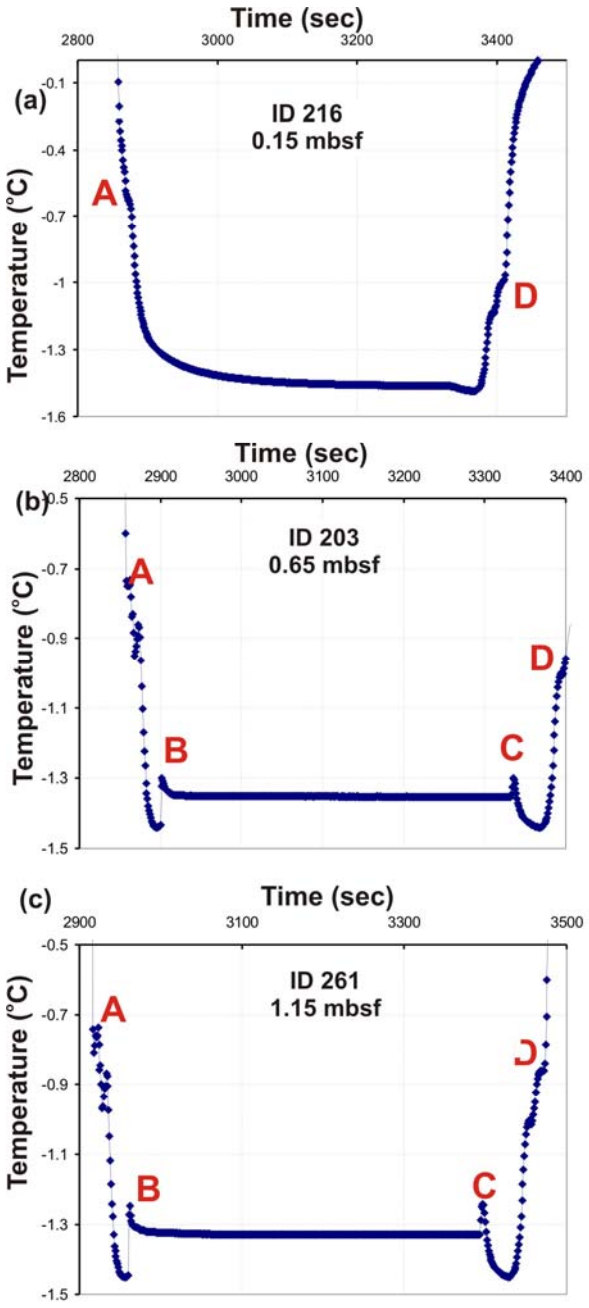

Figure A.7.1 Temperature records at Station 111 for MTL (a) ID 216 at 0.15 mbsf, (b) ID 203 at 0.65 mbsf, and (c) ID 261 at 1.15 mbsf. A: Core deployed, B: frictional heating pulse from core entering the sediment, C: frictional heating pulse from core pulled out of sediment, D: core back on deck. The top-most logger ID 216 does not show any frictional heating pulse, which confirms the low apparent core penetration that put this logger close to the seafloor.

A.7.2 South of Landslide, Station 113

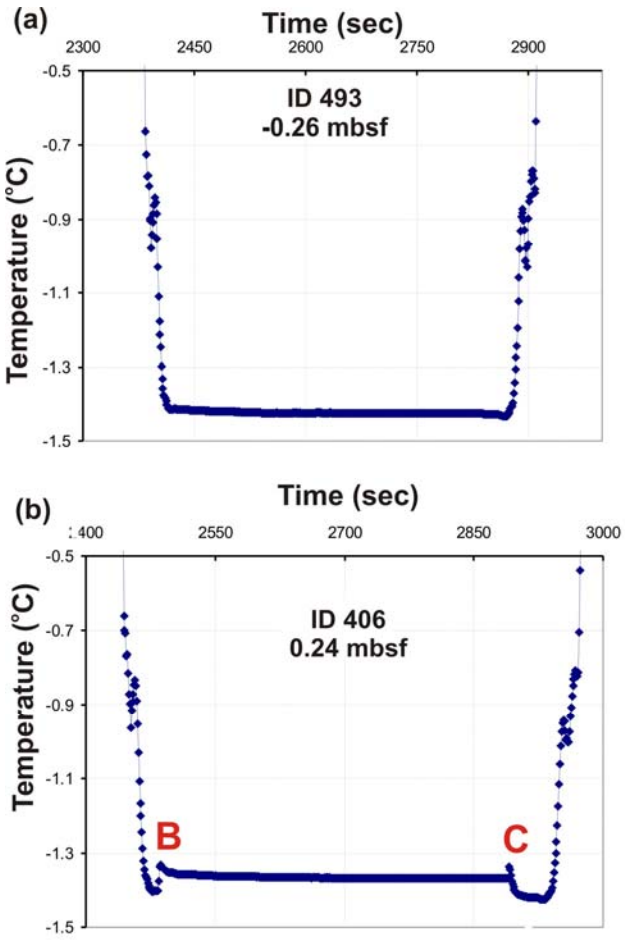

Figure A.7.2 Temperature records at Station 113 for MTL (a) ID 493 at -0.26 mbsf, (b) ID 406 at 0.24 mbsf. B: frictional heating pulse from core entering the sediment, C: frictional heating pulse from core pulled out of sediment. The top-most logger ID 493 does not show any frictional heating pulse, which confirms the low apparent core penetration that put this logger above the seafloor.

A.7.3 South of Landslide, Station 115

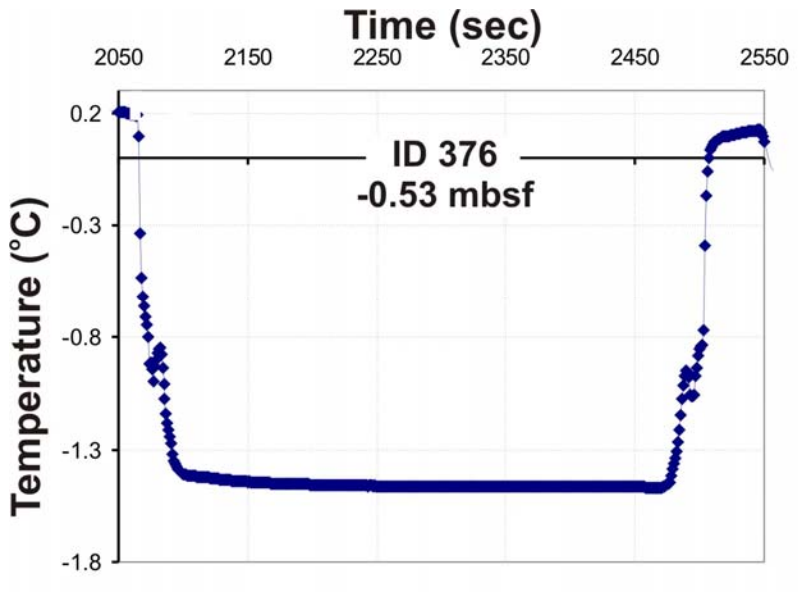

Figure A.7.3 Temperature records at Station 115 for MTL ID 376 at -0.53 mbsf. The logger does not show any frictional heating pulse, which confirms the low apparent core penetration that put this logger above the seafloor.

A.8.1 Central shelf transect, Station 81

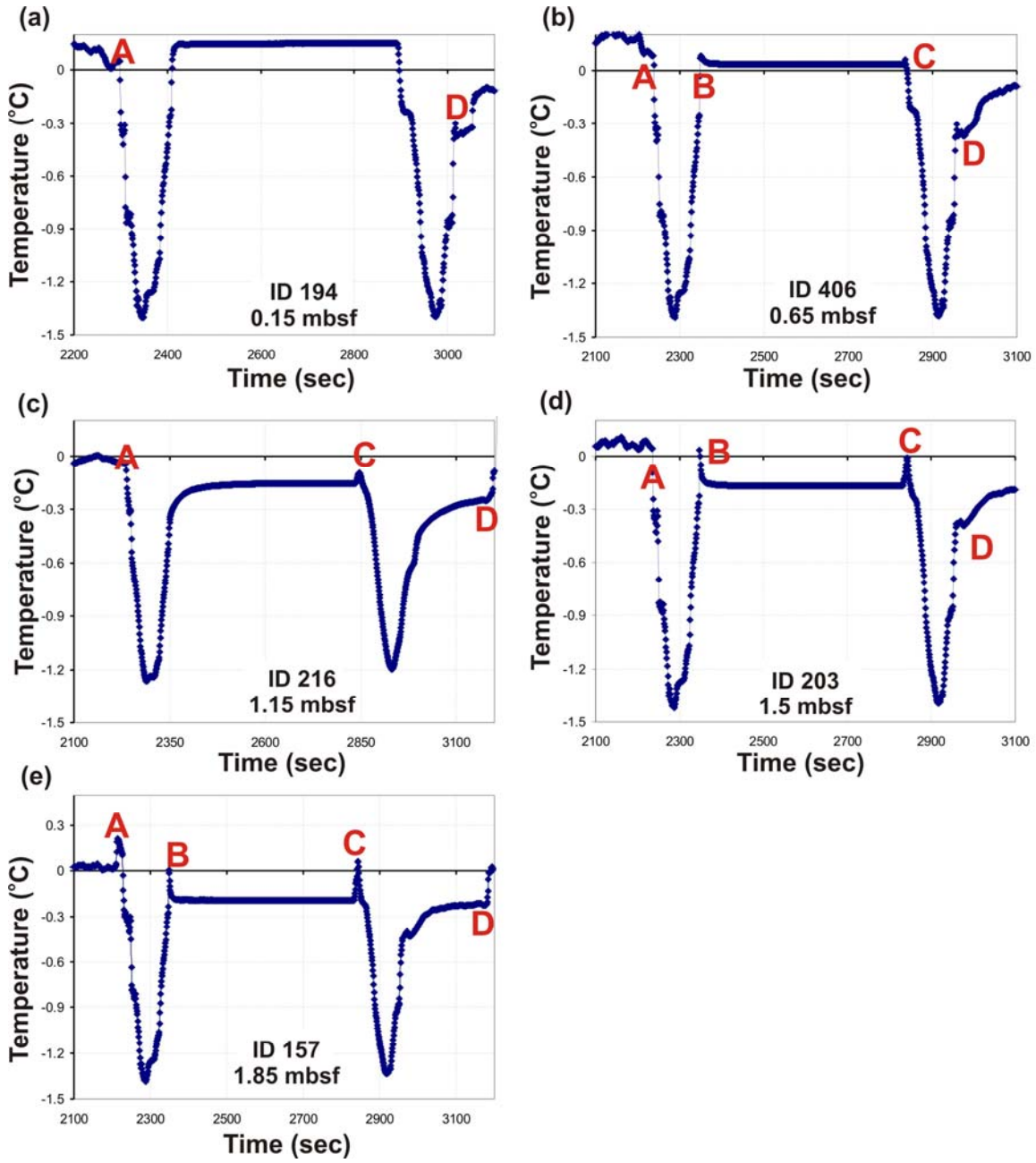

Figure A.8.1 Temperature records at Station 81 for MTL (a) ID 194 at 0.15 mbsf, (b) ID 406 at 0.65 mbsf, (c) ID 216 at 1.15 mbsf, (d) ID 203 at 1.5 mbsf, and (e) ID 157 at 1.85 mbsf. A: Core deployed, B: frictional heating pulse from core entering the sediment, C: frictional heating pulse from core pulled out of sediment, D: core back on deck. The top-most logger ID 194 does not show any frictional heating pulse, which confirms the low apparent core penetration that put this logger close to the seafloor.

A.8.2 Central shelf transect, Station 83

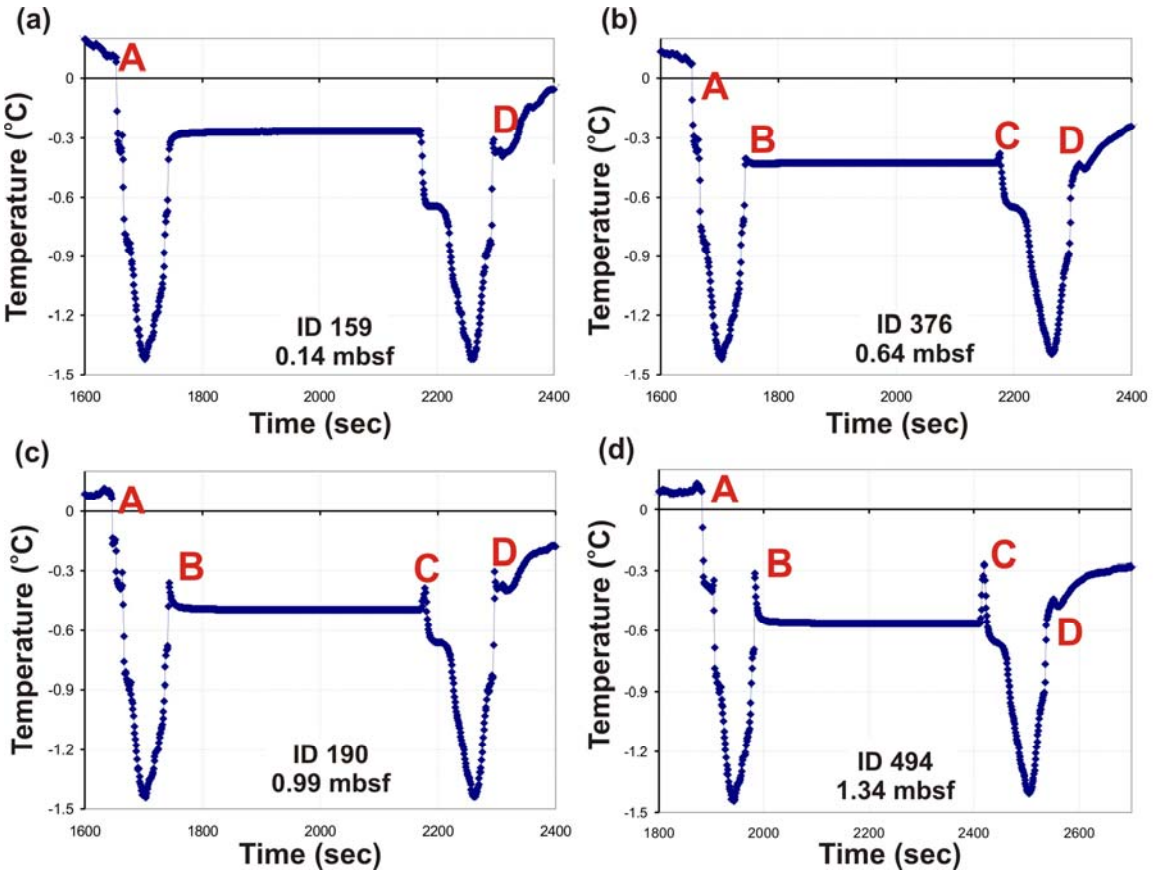

Figure A.8.2 Temperature records at Station 83 for MTL (a) ID 159 at 0.14 mbsf, (b) ID 376 at 0.64 mbsf, (c) ID 190 at 0.99 mbsf, and (d) ID 494 at 1.34 mbsf. A: Core deployed, B: frictional heating pulse from core entering the sediment, C: frictional heating pulse from core pulled out of sediment, D: core back on deck. The top-most logger ID 159 does not show any frictional heating pulse, which confirms the low apparent core penetration that put this logger close to the seafloor.

A.8.3 Central shelf transect, Station 85

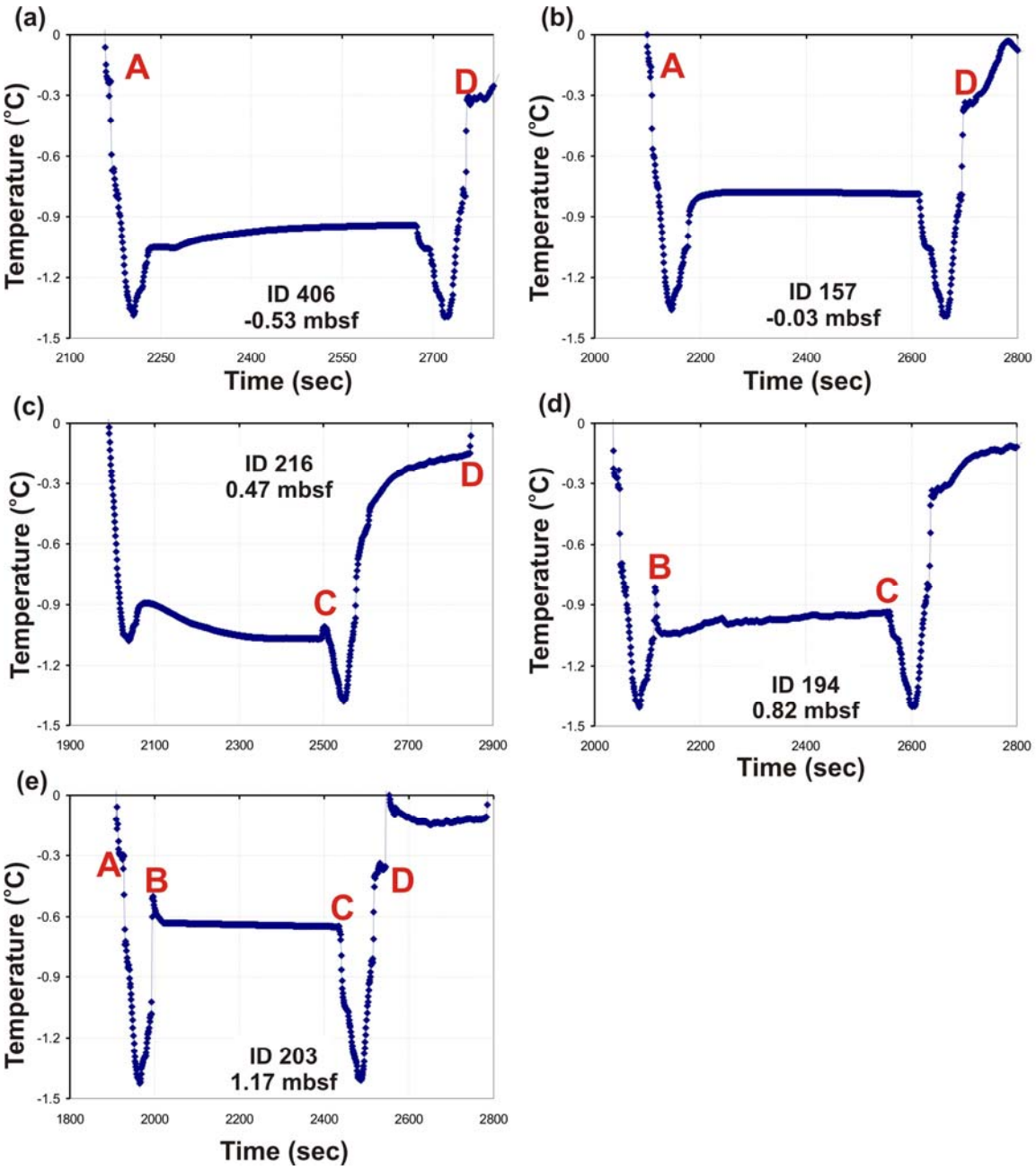

Figure A.8.3.1 Temperature records at Station 85 for MTL (a) ID 159 at 0.14 mbsf, (b) ID 376 at 0.64 mbsf, (c) ID 190 at 0.99 mbsf, and (d) ID 494 at 1.34 mbsf. A: Core deployed, B: frictional heating pulse from core entering the sediment, C: frictional heating pulse from core pulled out of sediment, D: core back on deck. The two top-most loggers (ID 406 and ID 157) do not show frictional heating pulses, which confirm the low apparent core penetration that put these loggers above the seafloor.

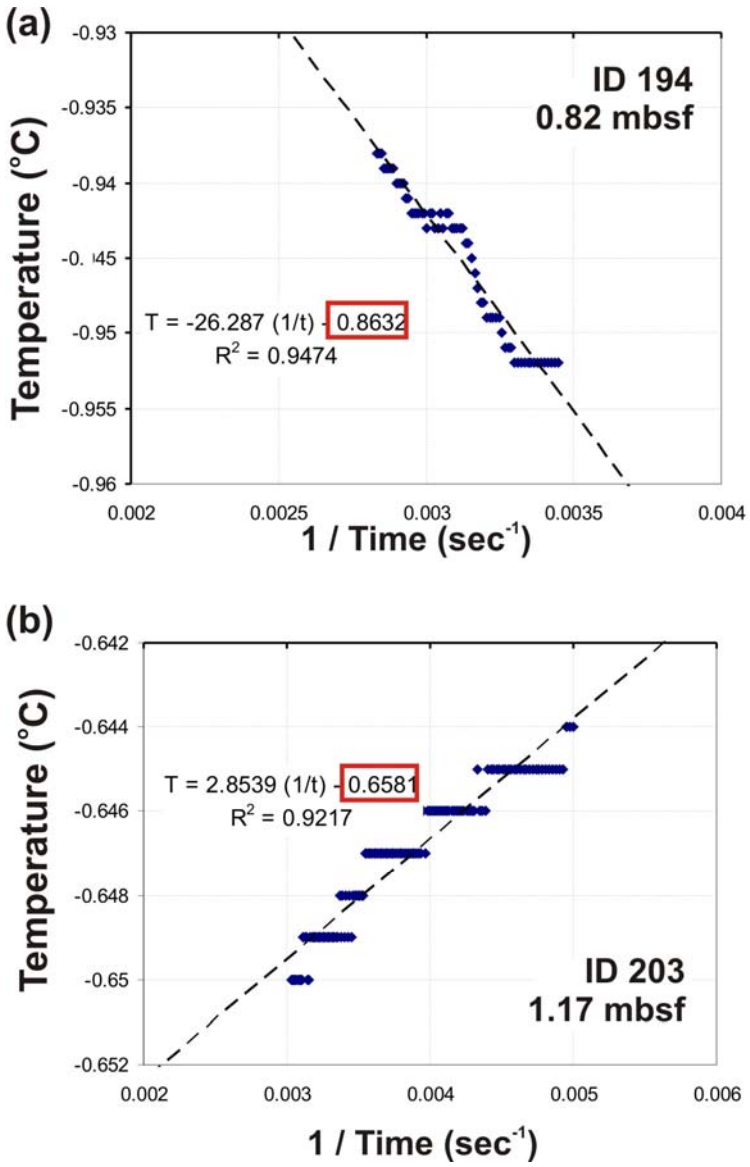

Figure A.8.3.2 Linear regression analysis to estimate equilibrium in situ temperature at Station 85 for the last ~100 seconds prior to pulling out of the core for MTL (a) ID 194 at 0.82 mbsf and (b) ID 203 at 1.17 mbsf. Estimated equilibrium temperatures from the best-fit equation are highlighted in the red boxes for each MTL.

A.8.4 Central shelf transect, Station 87

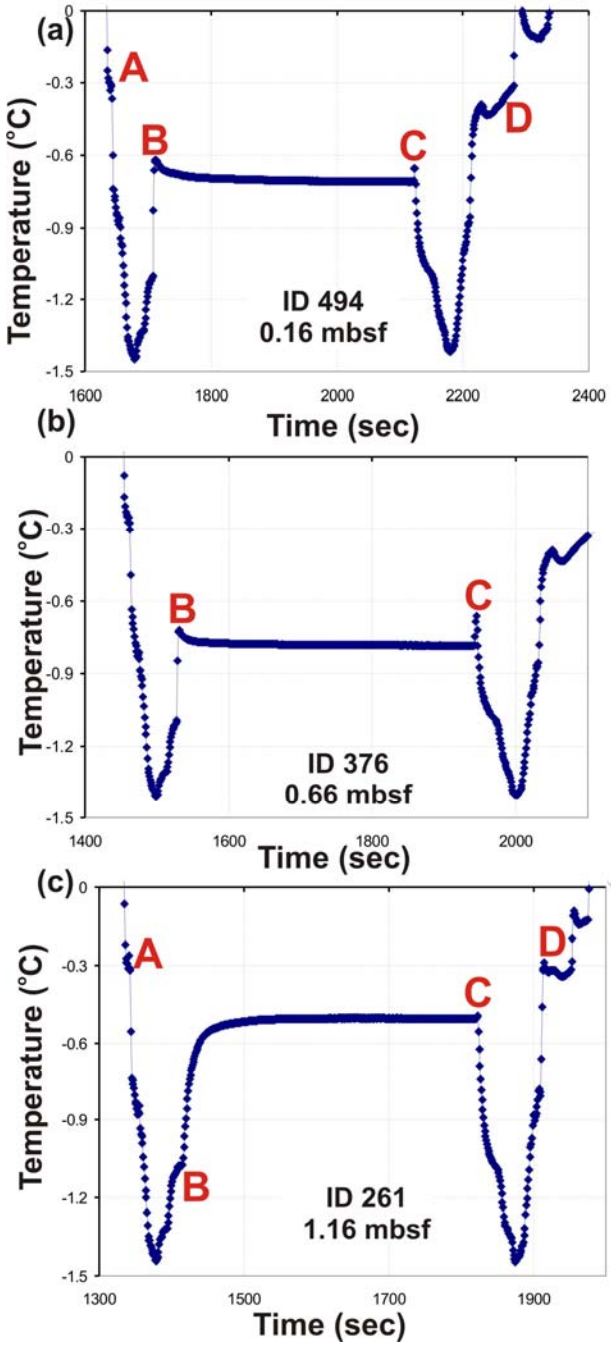

Figure A.8.4.1 Temperature records at Station 87 for MTL (a) ID 494 at 0.16 mbsf, (b) ID 376 at 0.66 mbsf, (c) ID 261 at 1.16 mbsf. A: Core deployed, B: frictional heating pulse from core entering the sediment, C: frictional heating pulse from core pulled out of sediment, D: core back on deck.

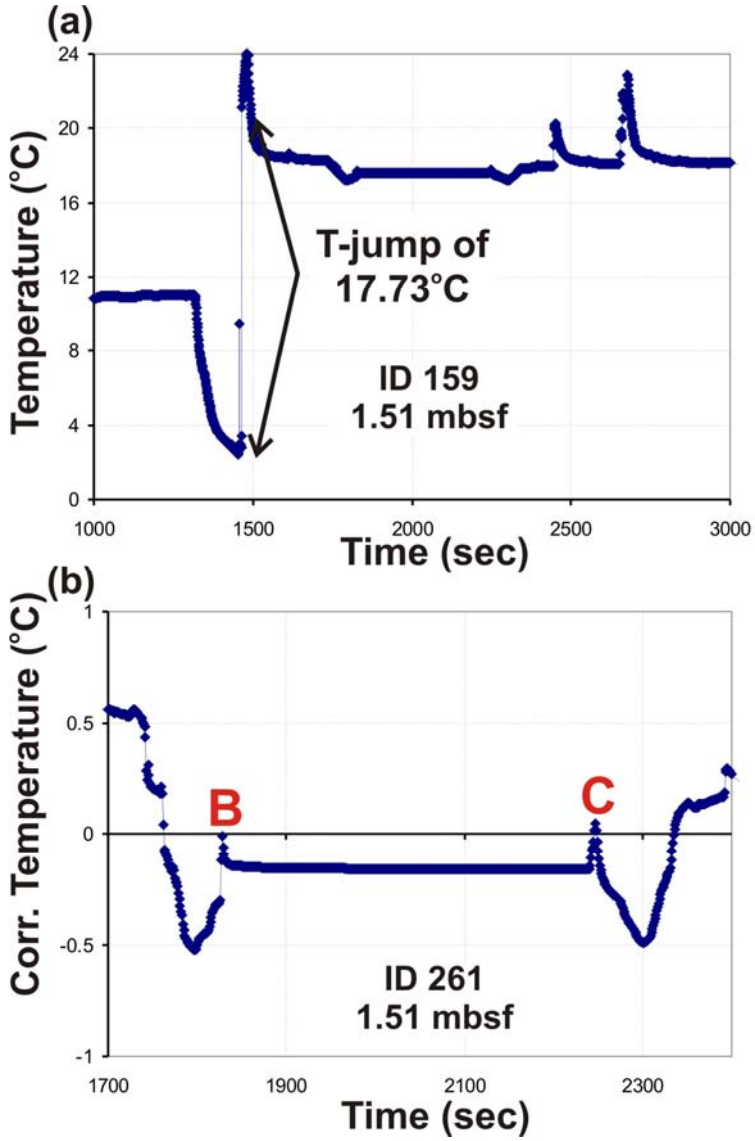

Figure A.8.4.2 Temperature record at Station 87 for MTL ID 159 at 1.51 mbsf with temperature-jump of 17.73ºC, and (b) corrected temperature (subtracting 17.73ºC after jump occurred). B: frictional heating pulse from core entering the sediment, C: frictional heating pulse from core pulled out of sediment. The final temperature after the correction is -0.162ºC.

A.8.5 Central shelf transect, Station 89

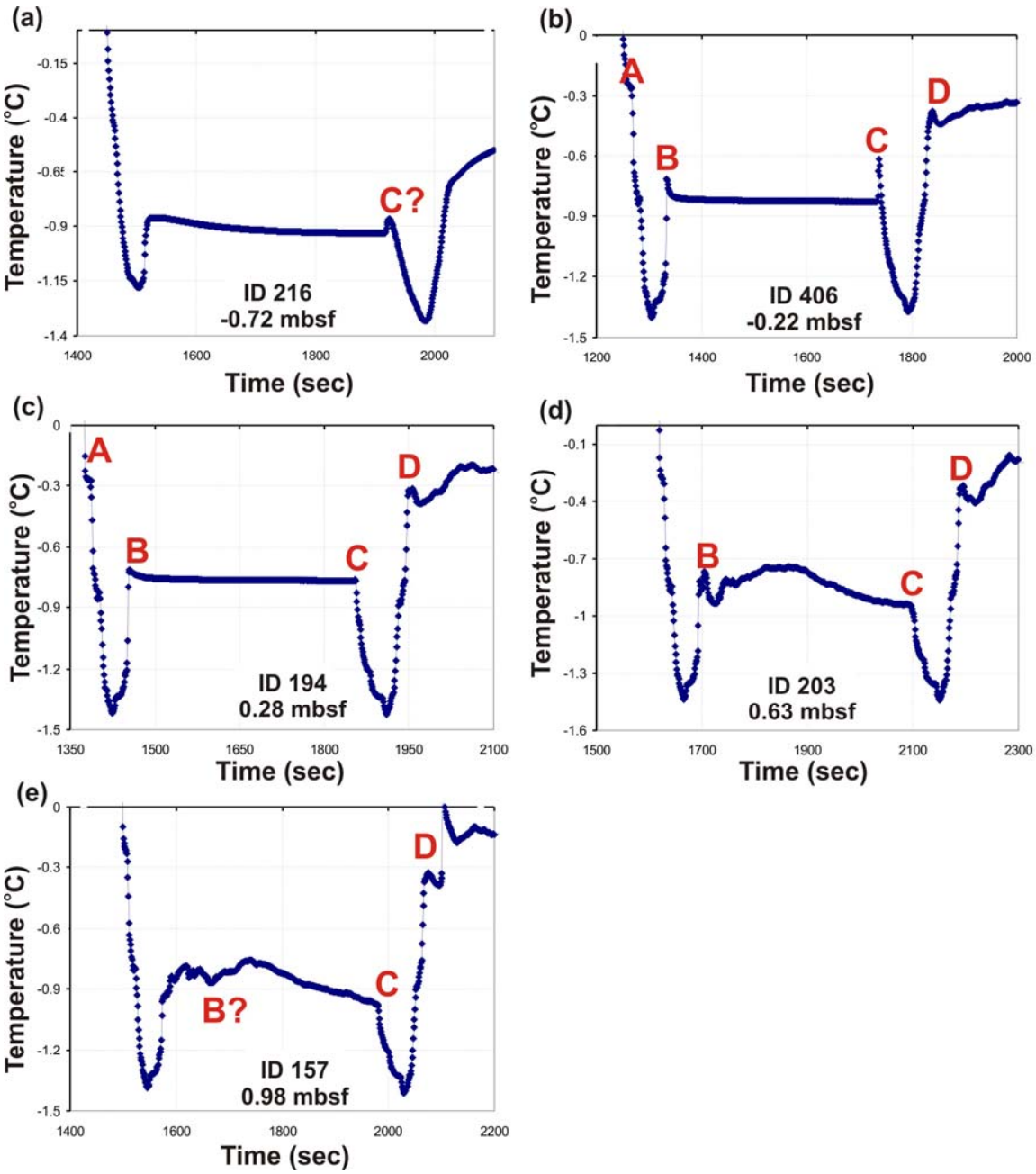

Figure A.8.5.1 Temperature records at Station 89 for MTL (a) ID 216 at -0.72 mbsf, (b) ID 406 at -0.22 mbsf, (c) ID 194 at 0.28 mbsf, (d) ID 203 at 0.63 mbsf, and (e) ID 157 at 0.98 mbsf. A: Core deployed, B: frictional heating pulse from core entering the sediment, C: frictional heating pulse from core pulled out of sediment, D: core back on deck. The top-most logger (ID 216) does not show frictional heating pulses, which confirms the low apparent core penetration that put this logger above the seafloor. However, logger ID 406, supposedly also above seafloor, does show some frictional heating.

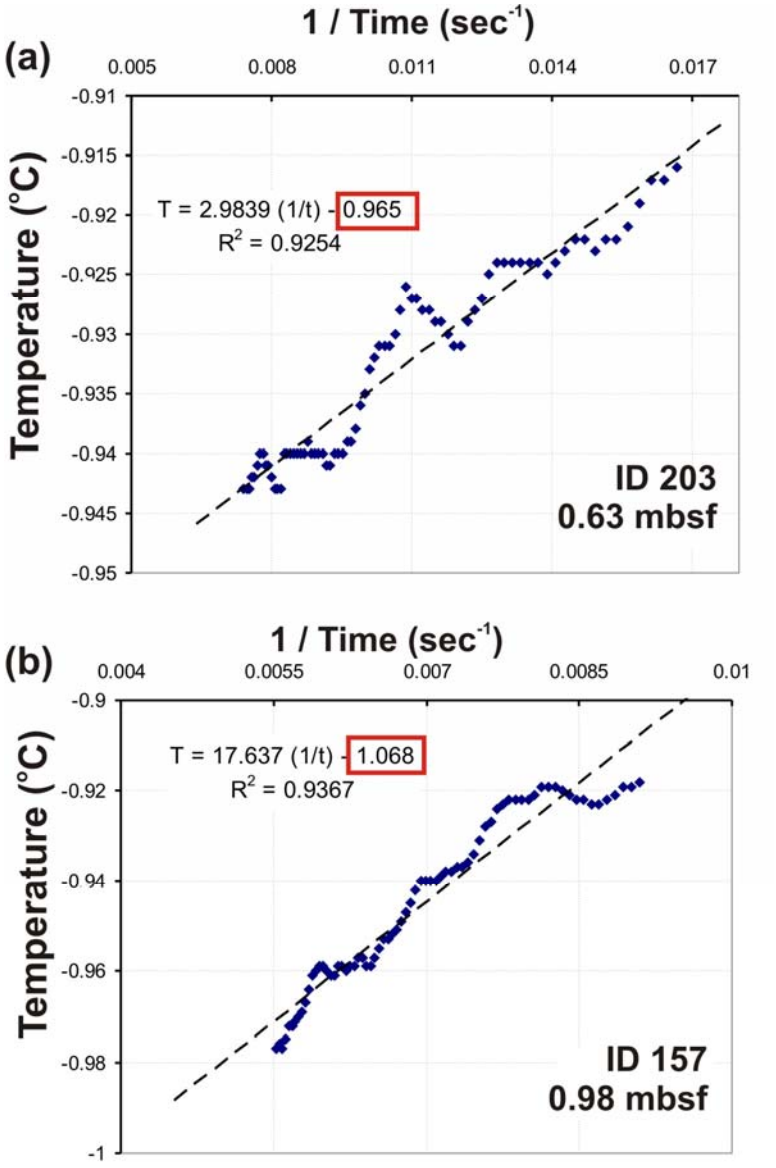

Figure A.8.5.2 Linear regression analysis to estimate equilibrium in situ temperature at Station 89 for the last ~100 seconds prior to pulling out of the core for MTL (a) ID 203 at 0.63 mbsf and (b) ID 157 at 0.98 mbsf. Estimated equilibrium temperatures from the best-fit equation are highlighted in the red boxes for each MTL.

A.8.6 Central shelf transect, Station 91

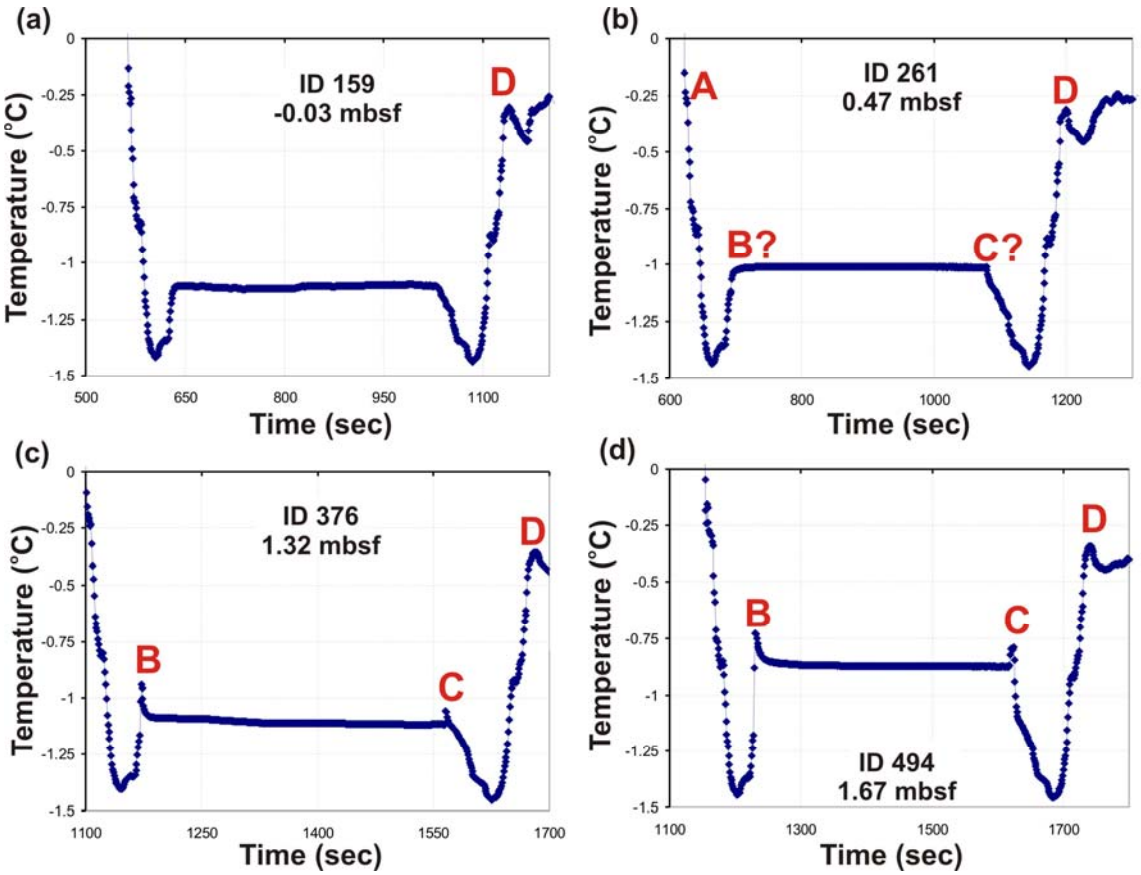

Figure A.8.6 Temperature records at Station 91 for MTL (a) ID 159 at -0.03 mbsf, (b) ID 261 at -0.47 mbsf, (c) ID 376 at 1.32 mbsf, and (d) ID 494 at 1.67 mbsf. A: Core deployed, B: frictional heating pulse from core entering the sediment, C: frictional heating pulse from core pulled out of sediment, D: core back on deck. The two top-most loggers (ID 159 and ID 261) do not show frictional heating pulses, which confirms the low apparent core penetration that put at least logger ID 159 above the seafloor.

A.9.1 Gary Knolls, Station 119

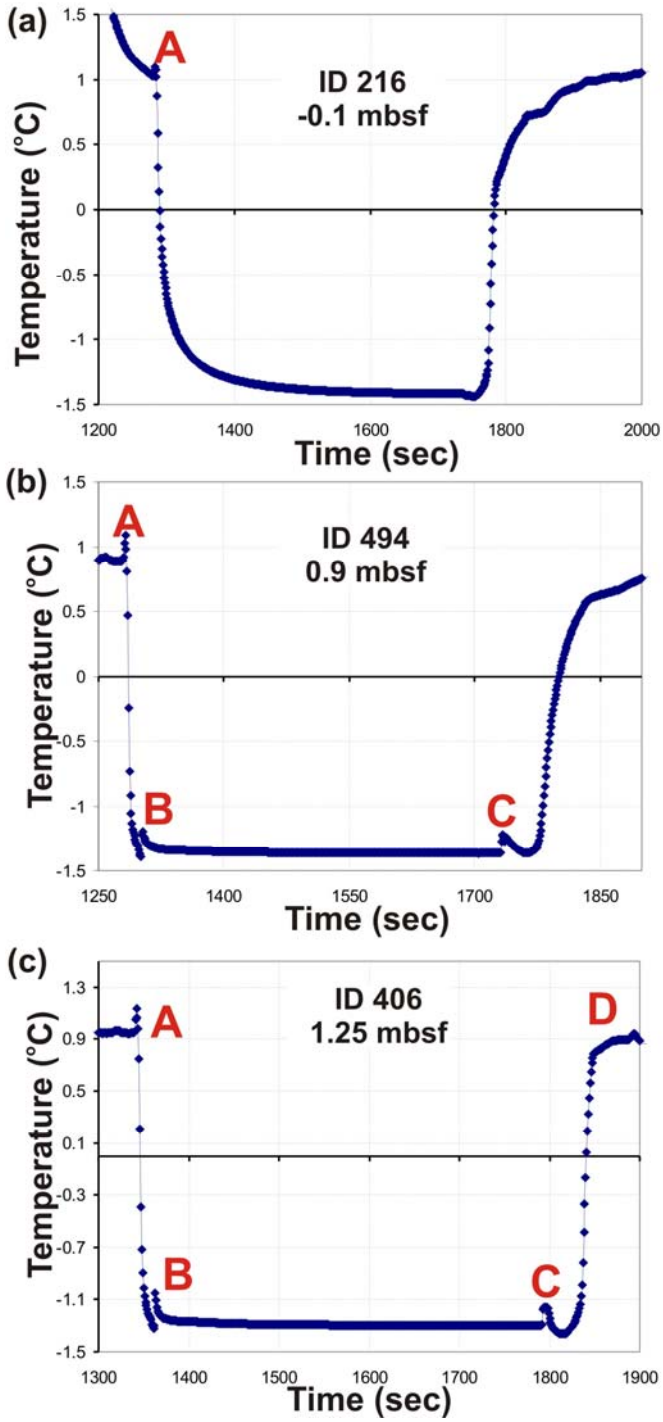

Figure A.9.1 Temperature records at Station 119 for MTL (a) ID 216 at -0.1 mbsf, (b) ID 494 at 0.9 mbsf, (c) ID 406 at 1.25 mbsf. A: Core deployed, B: frictional heating pulse from core entering the sediment, C: frictional heating pulse from core pulled out of sediment, D: core back on deck. The top-most logger (ID 216) does not show frictional heating pulses, which confirms the low apparent core penetration that put this logger above the seafloor.

A.9.2 Gary Knolls, Station 121

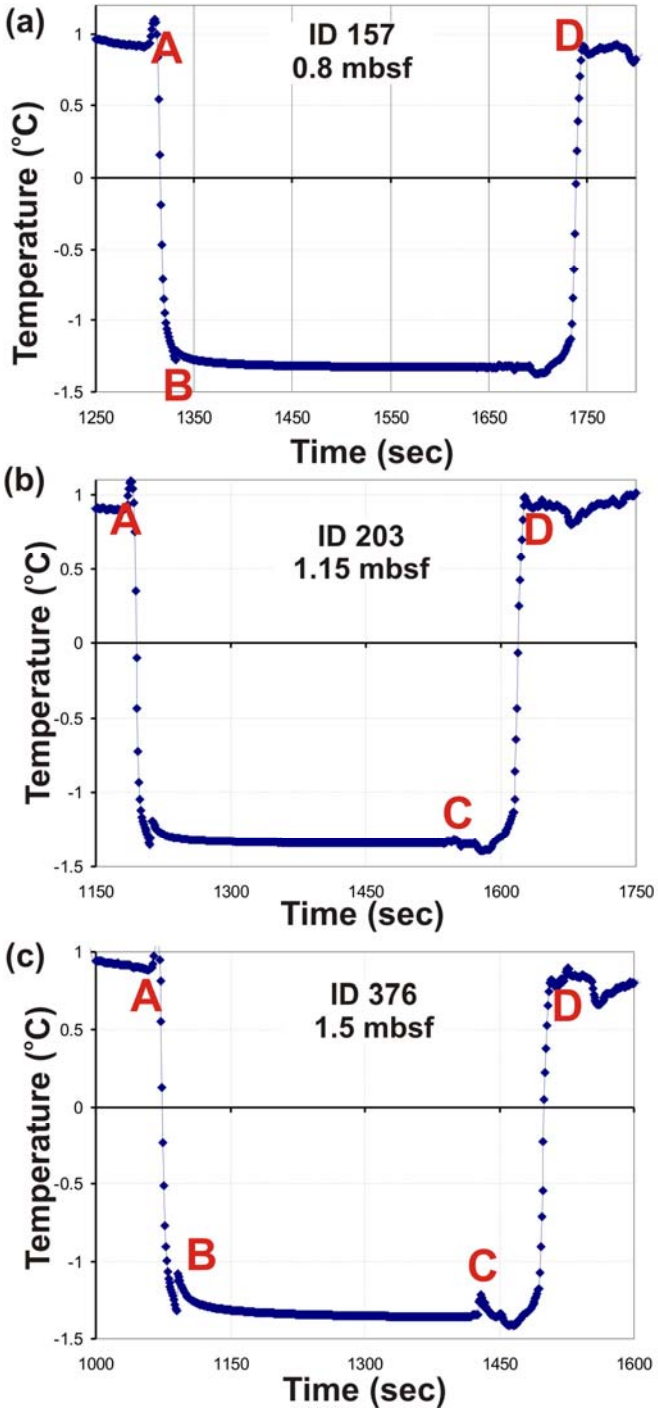

Figure A.9.2 Temperature records at Station 121 for MTL (a) ID 157 at 0.8 mbsf, (b) ID 203 at 1.15 mbsf, and (c) ID 376 at 1.5 mbsf. A: Core deployed, B: frictional heating pulse from core entering the sediment, C: frictional heating pulse from core pulled out of sediment, D: core back on deck.

A.9.3 Gary Knolls, Station 123

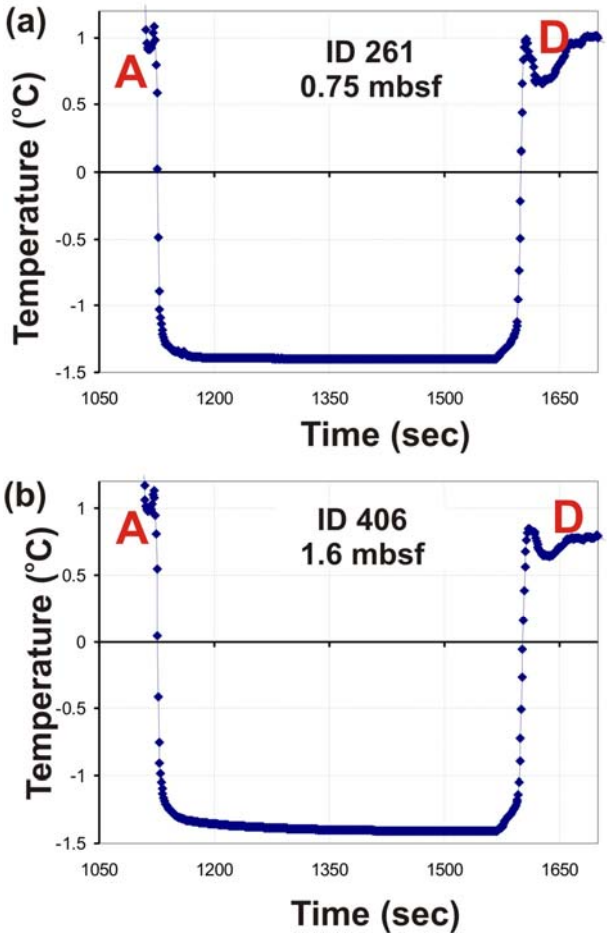

Figure A.9.3 Temperature records at Station 123 for MTL (a) ID 261 at 0.75 mbsf, and (b) ID 406 at 1.6 mbsf. A: Core deployed, D: core back on deck. None of the loggers show any frictional heating pulses. Although apparent core penetration was noted as 2.15 mbsf, only 30cm of core were recovered. The temperature data suggest a lower core penetration, more in line with the small recovery. Mud on the outside of the core barrel may have come from the core falling over as it hit the hard bottom. However, this cannot be confirmed.

A.9.4 Gary Knolls, Station 125

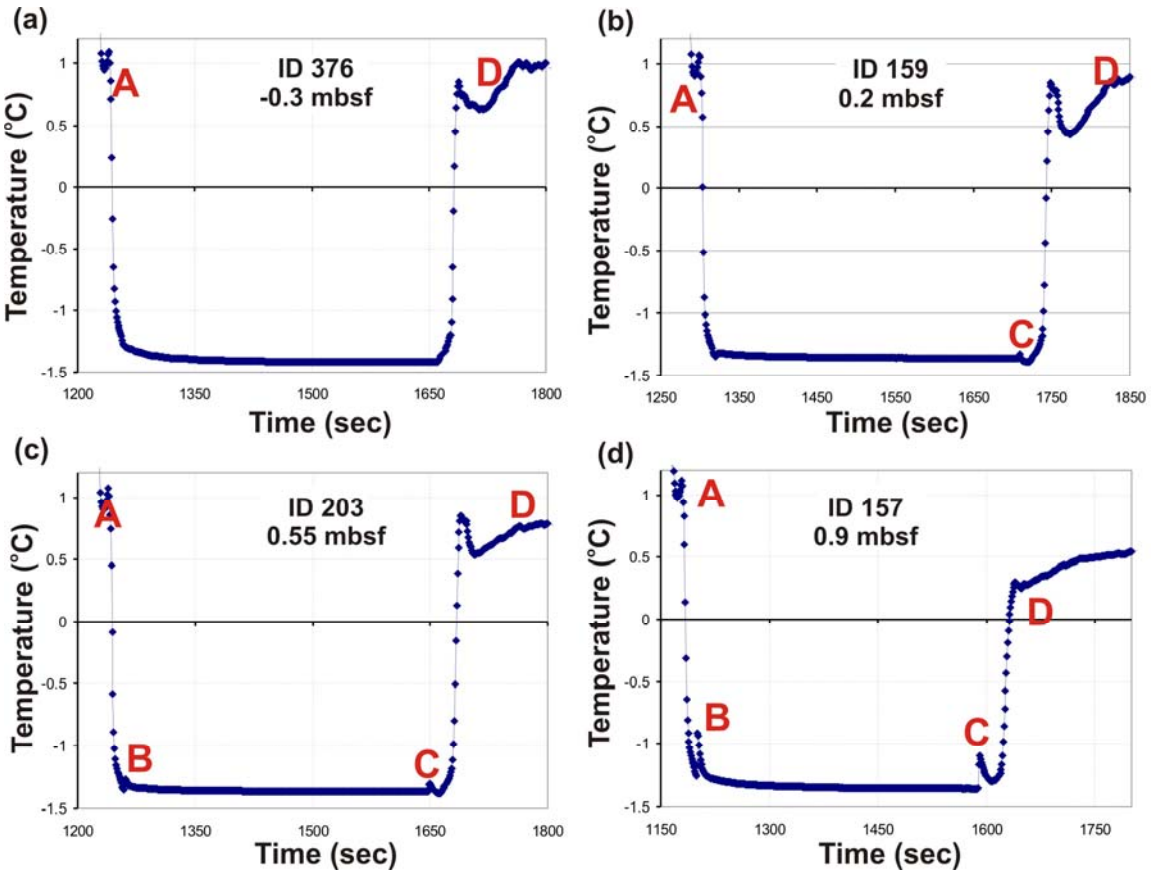

Figure A.9.4 Temperature records at Station 125 for MTL (a) ID 376 at -0.3 mbsf, (b) ID 159 at 0.2 mbsf, (c) ID 203 at 0.55 mbsf, and (d) ID 157 at 0.9 mbsf. A: Core deployed, D: core back on deck. The top-most logger (ID 376) does not show any frictional heating pulses confirming, which confirms the low apparent core penetration that put this logger above the seafloor.

A.9.5 Gary Knolls, Station 127

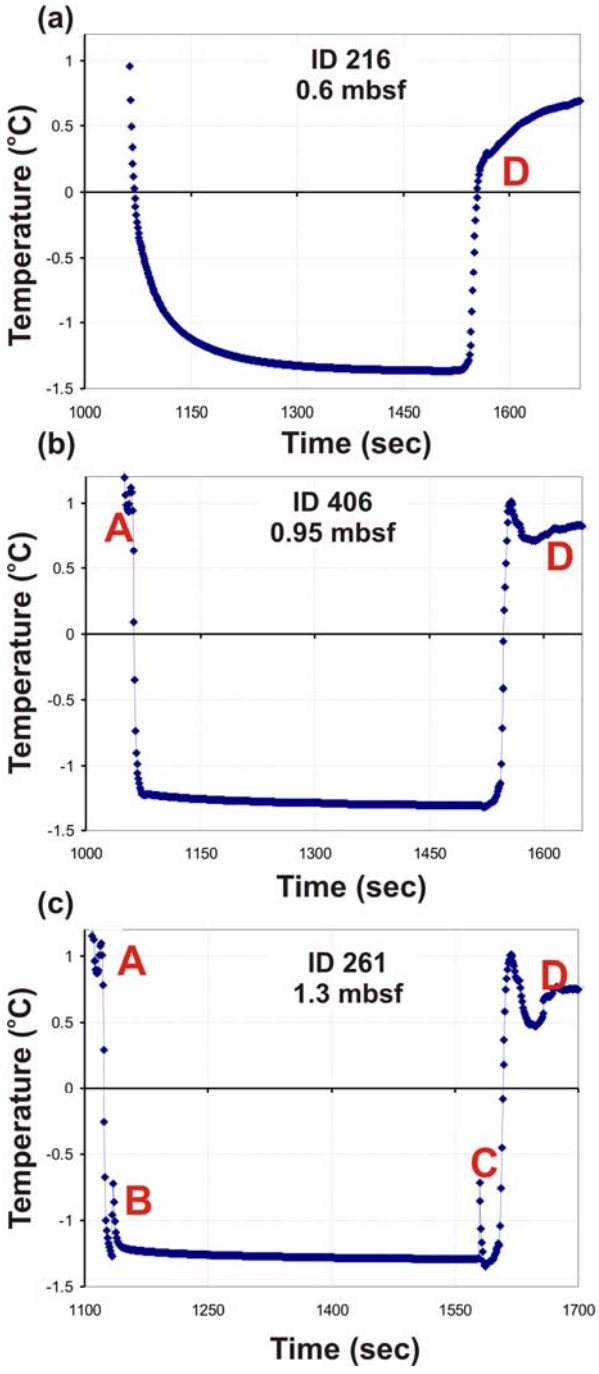

Figure A.9.5 Temperature records at Station 127 for MTL (a) ID 216 at 0.6 mbsf, (b) ID 406 at 0.95 mbsf, and (c) ID 261 at 1.3 mbsf. A: Core deployed, D: core back on deck. The top-most two loggers do not show any frictional heating pulses. The already noted low apparent core penetration may have been even lower and puts both loggers above the seafloor.

A.9.6 Gary Knolls, Station 129

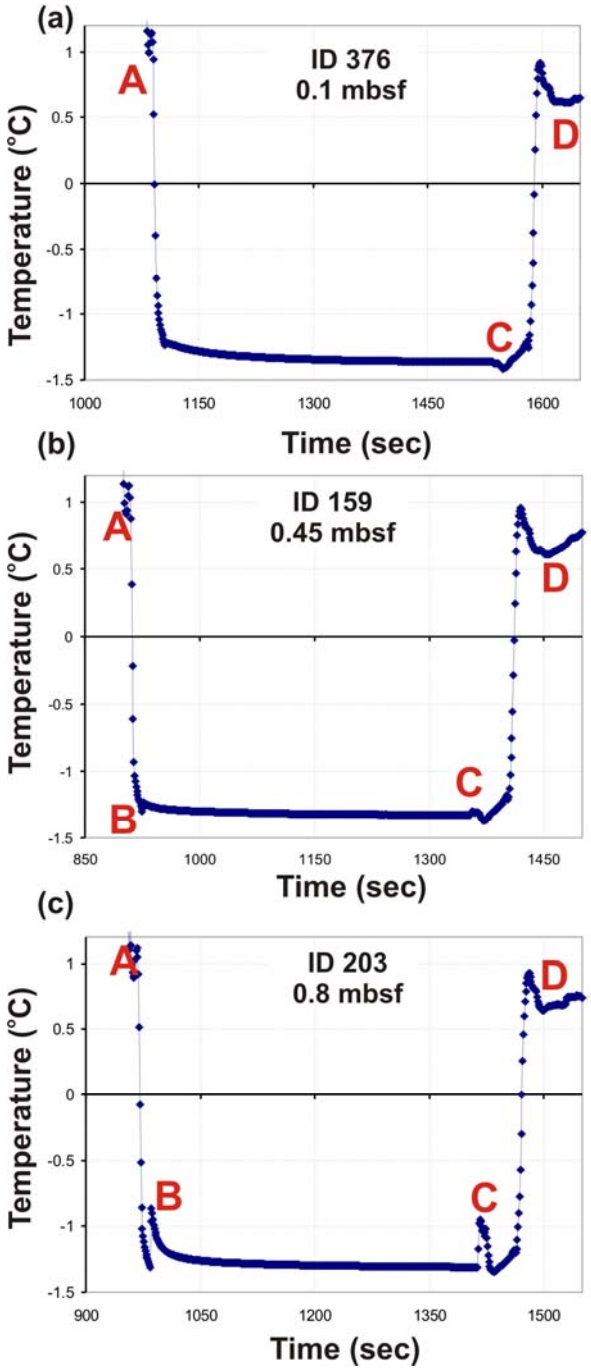

Figure A.9.6 Temperature records at Station 129 for MTL (a) ID 376 at 0.1 mbsf, (b) ID 159 at 0.45 mbsf, and (c) ID 203 at 0.8 mbsf. A: Core deployed, D: core back on deck. The top-most logger does not show a clear frictional heating pulse upon sediment-penetration. The already noted low apparent core penetration may have been even lower and puts this logger above the seafloor.